

**Dissertation zur Erlangung des Doktorgrades der Fakultät für  
Chemie und Pharmazie der Ludwig-Maximilians-Universität  
München**

**The dual roles of  
betacellulin and the ERBB receptors  
in acute pancreatitis & pancreatic ductal  
adenocarcinoma – a mouse study**

**Kathrin Verena Hedegger**

**aus**

**Frankfurt am Main**

**2019**

## **Erklärung**

Diese Dissertation wurde im Sinne von § 7 der Promotionsordnung vom 28. November 2011 von Herrn Prof. Dr. Eckhard Wolf betreut und von Herrn PD Dr. Dietmar Martin von der Fakultät für Chemie und Pharmazie vertreten.

## **Eidesstattliche Versicherung**

Diese Dissertation wurde eigenständig und ohne unerlaubte Hilfe erarbeitet.

München, 02.08.2019, Kathrin Verena Hedegger

---

<b>Dissertation eingereicht am:</b>	<b>02.08.2019</b>
<b>1. Gutachter:</b>	<b>PD Dr. Dietmar Martin</b>
<b>2. Gutachter:</b>	<b>Prof. Dr. Eckhard Wolf</b>
<b>Mündliche Prüfung am:</b>	<b>13.09.2019</b>

***THE DUAL ROLES OF BETACELLULIN AND THE ERBB  
RECEPTORS IN ACUTE PANCREATITIS & PANCREATIC  
DUCTAL ADENOCARCINOMA – A MOUSE STUDY***

## DANKSAGUNG

Ein kleines Dankeschön an alle, die sowohl direkt, als auch indirekt an dieser Arbeit mitgewirkt haben.

Mein Dank geht zunächst an meinen Doktorvater PD. Dr. Dietmar Martin für die Bereitschaft meine Dissertation an der Fakultät Chemie und Pharmazie zu betreuen, für die gute Zusammenarbeit und seine Ratschläge. Herrn Prof. Dr. Eckhard Wolf möchte ich für die Übernahme des Zweitgutachtens danken, sowie für die Bereitstellung seines Labors und für die zahlreichen Diskussionen und Anregungen.

Mein Dank gilt außerdem Herrn PD Dr. Dietmar Martin, Herrn Prof. Dr. Eckhard Wolf, Herrn PD Dr. Maik Dahlhoff, Herrn Prof. Dr. Klaus Förstemann, Herrn Prof. Dr. Julian Stingle und Herrn Prof. Dr. Karl-Peter Hopfner für die Bereitschaft mein Prüfungskomitee zu bilden.

PD Dr. Maik Dahlhoff möchte ich ganz herzlich für die Betreuung meiner Doktorarbeit danken, zunächst für die Auswahl der Projekte, vor allem aber für seine Unterstützung über all die Jahre. In zahlreichen Diskussionen habe ich stets konstruktive Kritik und viel Anregung bekommen, ohne die diese Arbeit nicht möglich gewesen wäre. Auch für das Ermöglichen der vielen Kongressreisen bin ich sehr dankbar, sowie für seine Ruhe und Geduld und die motivierenden Worte: „Das wird super!“

Ebenfalls nicht möglich wären all die Jahre ohne meine Kollegin (soon to be known as Dr. rer. nat. Pingu Star) Christine Hösl gewesen. Nicht jeder kann behaupten, eine der engsten Freunde als Lab-Mate an seiner Seite zu haben, und das auch mal gerne 24/7. Das ist wohl einer der Gründe, wieso wir uns manchmal am Genzentrum „wie zuhause“ fühlen (Du weißt, was ich damit meine). Es war schön zu wissen, dass ich jederzeit Gehör bei Dir finde für Gefühls-Ausbrüche jeglicher Art, sei es Freude, Trauer oder Ärger. Ja, es gab auch Momente der puren Verzweiflung in diesen (ja, ok, fast 5) Jahren, für die man in Worten keine Lösung fand. Am Ende des Tages jedoch machte das Leben immer wieder Gin. Zusammen geht einfach vieles leichter. Tausend Dank auch für Deine Zeit zum Korrekturlesen!

Ich möchte mich außerdem bei dem gesamten Wolf-Labor, insbesondere bei Franziska Kreß, Sepp Millauer, Max Marschall, Tamara Holy und Nicole Wegmann für die tolle und respektvolle Zusammenarbeit und Unterstützung bei sämtlichen Projekten bedanken und bei Sylvia Hornig für die Organisation der gesamten Administration. Außerdem wart Ihr alle im Labor maßgeblich am Spaß an meiner Arbeit beteiligt. Die täglichen Meetings mit

Diskussionen über den (Weißwurst-) Kreuz-Schnitt und, ob es wohl eine Welt außerhalb von Bayern gibt, waren immer sehr aufschlussreich. Auch Petra Renner, Dr. Ingrid Renner-Müller und den restlichen Mitarbeitern des Maus-Hauses möchte ich für die ausgezeichnete und aufopferungsvolle Tierhaltung und -Pflege bedanken.

Ein herzliches Dankeschön gilt auch meinen ehemaligen Bacheloranden, bzw. Praktikanten Caroline Lindner und Michelle Plummer. Durch Euch habe ich sehr viel lernen können.

Ein weiterer Dank geht an unsere Kooperationspartner. Vielen Dank für die tolle Zusammenarbeit an das gesamte Labor von Dr. Helmut Blum am Genzentrum und das Labor von Prof. Dr. Hana Algül am Klinikum rechts der Isar.

Dem gesamten Team des Genzentrums, vor allem der Ver- und Entsorgungs- und IT-Abteilung möchte ich ganz herzlich danken.

Außerdem: ein großes Dankeschön an Dr. Bianca Schulte und Dr. Barbara Stiller für das anteilige Korrekturlesen meiner Arbeit. Auch fünf Jahre nach unserer schönen Zeit in New York kann ich immer wieder auf Euch zählen.

Wer hätte gedacht, dass Senioren in München so fetzen können? Euch allen gilt ein riesengroßer Dank!! Ihr habt die letzten elf Jahre dafür gesorgt, dass München mein zweites zu Hause wurde! Ihr versteht mich, obwohl ich aus Hessen komme (und damit meine ich nicht den Dialekt, den ich nicht habe). Ihr nehmt mich ernster als ich mich selbst und Ihr habt mich immer wieder darauf besinnt, was wirklich zählt, oder Euch einfach zusammen mit mir in den Ärger reingesteigert, das Ganze dann zusammen ausgeGessen oder (als wir noch knackiger waren) beim Abhotten in den guten alten Münchner Tanzlokalen. Das waren noch Zeiten. Danke, dass es Euch gibt! #ohneEuch = #ohneBrot.

Ein besonderes Dankeschön möchte ich meinem quasi-Roomie aussprechen. Danke, Jana für die spontanen Butterbrote auf dem Balkon und den ein oder anderen Spritz, immer, wenn es nötig ist.

Danke an meine treueste Slurp-Freundin für die vielen Suppen, die wir zusammen gegessen haben. Suppe hilft!

Danke meinen Mädels zu Hause in Frankfurt (Ja ok, und dem Felix)! Ihr begleitet mich nun weitaus länger als dieses Studium gedauert hat und Ihr zeigt mir immer wieder aufs Neue, was wahre Freundschaft bedeutet. Ihr gebt mir immer ein gutes Gefühl, wenn ich nach Hause komme und oft bringt Ihr dieses Zu Hause mit nach München. Ohne Euch wäre ich wohl durchgedreht (na gut, noch öfter durchgedreht). Danke!

Du hast mich besonders die letzten (und ich würde meinen, damit auch schwierigsten) Jahren begleitet. Ein Wochenende mit Dir fühlt sich an wie Urlaub, und damit gibst Du mir immer Energie für jede weitere Woche, auch wenn ich Montage noch weniger leiden kann, seit es Dich gibt. Du gibst mir Ruhe und Du erinnerst mich immer wieder daran, mehr an mich selbst zu glauben. Danke für Dein Vertrauen in mich und Deine Unterstützung, Spatz!

Der größte Dank geht an meine Familie. Ohne Euch, Mama und Papa, wäre diese Arbeit niemals möglich gewesen. Ihr unterstützt mich bedingungslos in jeglicher Hinsicht, seid in jeder Situation und Lebenslage da und steht mir immer beratend zur Seite. Mama, Du bist unermüdlich im Trost spenden, auch wenn das Telefon ein paar Mal öfter in der Woche klingelt. Auch Dir, Jenny, und Deiner lieben Familie möchte ich danken. Die Besuche bei Euch oder Eure Besuche hier im München sind immer eine tolle Ablenkung und geben mir immer wieder neue Energie. Filip, Du hast mir unglaublich viel Freude bereitet während meiner gesamten Doktoranden-Zeit und natürlich auch größeres Heimweh. Danke auch der ständigen Nachfrage, wie es meinen Mäusen so geht und für die schönen Namensvorschläge. Danke, dass Ihr an mich glaubt und ich immer auf Euch zählen kann! Das bedeutet mir unglaublich viel! Ab jetzt komme ich Euch auch wieder öfter besuchen.

## SUMMARY

The erythroblastic leukemia viral oncogene homolog (ERBB) system consists of the four receptor tyrosine kinases (RTKs) epidermal growth factor receptor (EGFR), ERBB2 (HER2, neu), ERBB3 (HER3) and ERBB4 (HER4). The receptor family has eleven ligands causing receptor homo- or hetero-dimerization, and transphosphorylation of mainly tyrosine residues in the cytosolic receptor domains. Thus, numerous signaling cascades are induced, which associate the ERBB receptors with functions in development, tissue homeostasis and diseases. Betacellulin (BTC) is an ERBB ligand with binding affinities for EGFR and ERBB4. It was first identified in murine pancreatic insulinoma-derived cell lines and apparently plays a role in many tissues, e.g. in pancreatic islets of Langerhans, in the stomach and in the mammary gland, as well as in tumors, e.g. in sarcoma, in breast cancer and many others. BTC is synthesized as a single-transmembrane precursor, which requires cleavage by A disintegrin and metalloproteinase 10 (ADAM10), in order to induce paracrine or autocrine signaling with the soluble extracellular domain. Membrane-bound BTC can also induce juxtacrine signaling. Additionally, BTC is able to differentiate many different cell types and it acts as a potent mitogen in epithelial and smooth muscle cells. Furthermore, BTC was associated with resistance to EGFR therapy in breast cancer cells. Despite its abundance and multiple functions, the ubiquitous depletion of BTC in mice showed no overt phenotype. On the contrary, its ubiquitous overexpression results in numerous phenotypes, and it was shown, that BTC transgenic mice were protected against experimental induced acute pancreatitis (AP).

AP is an inflammatory disease of the pancreas, induced by gall stones or alcohol abuse. Digestive enzymes are activated prematurely and released into the interstitium of the pancreas, where they auto-digest the membranes of different cell types constituting the pancreas. This is accompanied by an inflammatory reaction, which manifests as severe pain, signs of inflammatory response syndrome (SIRS) and frequently multi-organ failure and death.

Regarding the ERBB receptor network, EGFR and its ligand EGF were associated with an ameliorated course of AP, previously, but follow-up studies were missing. The remaining ERBB family members have not been investigated until our group revealed that BTC overexpression has a protective effect in AP, which was shown not to be mediated by EGFR but associated with increased SAPK activity. However, the mechanisms behind this finding were revealed in the following study.

In the first study of this thesis '*The protective effect of betacellulin against acute pancreatitis is ERBB4-dependent*', ERBB4 was characterized as the transmitting receptor of BTC-mediated protection against AP. Here, the ERBB4 receptor was deleted in *Btc* transgenic (*Btc* tg) mice specifically in the pancreas under the promoter *Pancreas associated transcription factor 1A*

(*Ptf1a*) using the Cre-loxP system (*ErbB4<sup>fl/fl</sup>;Ptf1a<sup>Cre/+</sup>;Btc<sup>tg/+</sup>*). Also, *Btc* tg mice were crossed into a kinase-dead *Egfr* background (*Egfr<sup>Wa5/+</sup>;Btc<sup>tg/+</sup>*). *ErbB4<sup>fl/fl</sup>;Ptf1a<sup>Cre/+</sup>;Btc<sup>tg/+</sup>* mice and *Egfr<sup>Wa5/+</sup>;Btc<sup>tg/+</sup>* mice were subjected to caerulein- and L-arginine induced AP. Serum lipase and serum amylase levels and histological parameters, such as pancreatic apoptosis, necrosis and edema were determined to grade the AP. *Btc* tg mice were protected from AP. While *Egfr<sup>Wa5/+</sup>;Btc<sup>tg/+</sup>* mice presented like *Btc* tg mice in all parameters, the loss of *ErbB4* inhibited the BTC-mediated phenotype with *ErbB4<sup>fl/fl</sup>;Ptf1a<sup>Cre/+</sup>;Btc<sup>tg/+</sup>* mice presenting with parameters like their wildtype littermates. *Btc* tg mice showed less fibrosis upon AP induction compared to wildtype animals. Microarray and Western blot analyses revealed the enhanced expression of the extracellular matrix (ECM)-regulating proteins matrix metalloproteinase 2 (MMP2), MMP3, periostin (POSTN), and matrix-gla protein (MGP) in BTC transgenic mice and in *Egfr<sup>Wa5/+</sup>;Btc<sup>tg/+</sup>* littermates but not in *ErbB4<sup>fl/fl</sup>;Ptf1a<sup>Cre/+</sup>;Btc<sup>tg/+</sup>* animals upon AP induction. BTC induced the regulated intramembrane proteolysis (RIP) of ERBB4, which was associated with trafficking of the intracellular domain (ICD) of ERBB4 into the cytosol and nucleus, where it is known to act as transcriptional co-activator. This suggests that the ERBB4 ICD enhances the expression of ECM-proteins and -modifiers as a transcriptional regulator, in order to remodel the pancreatic microenvironment. Furthermore, BTC enhanced SAPK signaling via ERBB4, which could be associated with increased apoptosis rates. In summary, we suggest that BTC induces a dual mechanism in order to prevent AP development in mice, comprising tissue remodeling and increasing apoptosis. These data strongly recommend an inclusion of BTC in the development of novel therapeutic strategies or at least to investigate further mechanisms of the ERBB4-BTC signaling axis to uncover more suitable targets for AP treatment.

The second study '*Unraveling the ERBB network upon betacellulin signaling in pancreatic ductal adenocarcinoma in mice*' shows that a high BTC expression is not always beneficial for pancreatic diseases. High BTC levels in pancreatic cancer have been reported previously and being a growth factor, it is not surprising that BTC also functions as a mitogen in pancreatic cancer cell lines. Pancreatic ductal adenocarcinoma (PDAC) is a deadly disease which is only treated using resection and toxic chemotherapy, and it remains the cancer with the lowest survival rate (5-year survival: 8%). The only targeted therapy affects EGFR, albeit with marginal clinical relevance and the frequent development of resistance.

The aim of the study was to reveal the role of BTC in PDAC and to investigate, which ERBB receptors are involved. To address these questions, an established mouse model was used. We used mice expressing constitutively active KRAS under the pancreas-specific promoter *Ptf1a* (*Ptf1a<sup>Cre/+</sup>;Kras<sup>G12D/+</sup>*, herein referred to as KC mice). These mice mimic human PDAC development, yet, showing a slow progression and incomplete penetrance of invasive carcinoma. However, the development of premalignant lesions, called pancreatic intraepithelial metaplasia (PanIN) and their subsequent progression into pancreatic cancer imitates the

human condition very well. Prior to PanIN development, induced by the activating mutation *KRAS*<sup>G12D</sup>, acinar cells transdifferentiate to duct cells (acinar-ductal metaplasia, ADM). Some ERBB ligands have been implicated in PDAC development, the role of BTC as a ligand of EGFR and ERBB4 was however unknown before we performed our study.

In this study, we found BTC expression in human PDAC specimen, human pancreatic cancer cell lines and in pancreatic premalignant lesions of KC mice. Upon the deletion of BTC in KC mice by CRISPR/Cas9 (*Btc*<sup>-/-</sup>; *Ptf1a*<sup>Cre/+</sup>; *Kras*<sup>G12D/+</sup>), PDAC development and progression were decelerated, which might be associated with the decreased EGFR expression and phosphorylation, we observed. Concordant with this observation, the overexpression of BTC in KC mice (*Btc*<sup>tg/+</sup>; *Ptf1a*<sup>Cre/+</sup>; *Kras*<sup>G12D/+</sup>, herein referred to as BKC mice) accelerated PDAC development and progression and led to the decrease of the median survival by approximately nine months compared to KC mice. In BKC mice, not only EGFR was activated, but also ERBB4 and ERBB2 (the latter at least by hetero-dimerization with EGFR). BTC enhanced RAS activity very early, which was exclusively mediated by EGFR, shown by the pancreas-specific deletion of the designated receptors, using the *Cre-loxP* system (*Btc*<sup>tg/+</sup>; *Ptf1a*<sup>Cre/+</sup>; *Kras*<sup>G12D/+</sup>; *Egfr*<sup>fl/fl</sup> (EGFR KO;BKC), *Btc*<sup>tg/+</sup>; *Ptf1a*<sup>Cre/+</sup>; *Kras*<sup>G12D/+</sup>; *ErbB2*<sup>fl/fl</sup> (ERBB2 KO;BKC), *Btc*<sup>tg/+</sup>; *Ptf1a*<sup>Cre/+</sup>; *Kras*<sup>G12D/+</sup>; *ErbB4*<sup>fl/fl</sup> (ERBB4 KO;BKC)). Beyond RAS activation, BTC induced ADM in isolated murine acinar cell clusters in 3-D cell culture. The deletion of *ErbB2* and *ErbB4* in BKC mice resulted in a drastically prolonged survival. This finding fitted to the observation that PDAC development was decelerated in ERBB2 KO;BKC mice, while the lack of ERBB4 showed no overt difference when compared to the histopathology of BKC mice. The deficiency of each receptor led to a decreased EGFR activation, and the loss of ERBB4 resulted in concomitantly decreased ERBB2, MAPK and SAPK activation. Interestingly, the depletion of EGFR rescued the BKC phenotype to an almost normal appearing pancreas, which was associated with prolonged survival, but the development of sporadic ADM could not be prevented. These ADM lesions were immuno-positive for ERBB2, ERBB3 and ERBB4, but Western blot analysis revealed that the same receptors were down-regulated in expression and activity. However, increased ERBB4 ICD signaling could be detected in the pancreas of EGFR KO;BKC mice, indicating a compensatory mechanism by ERBB4 upon the loss of EGFR.

These data are in line with the common view of the PDAC research community that EGFR is a crucial player in PDAC development. However, we could show that ERBB2 and ERBB4 are significantly involved in the survival of BKC mice and should be considered in further studies to reveal the mechanisms. Importantly, the loss of EGFR also decreased the impact of ERBB2 and ERBB3, which shows that targeting EGFR is the right way for treatment since EGFR inhibition is accompanied by the inhibition of further oncogenic receptors. However, we provide evidence that upon the loss of EGFR, a compensatory induction of the

ERBB4 ICD occurs which suggests ERBB4 to be involved in the development of resistances in EGFR-targeted therapies. This study strongly indicates that instead of targeting EGFR only, the complete ERBB family should be considered for inhibition in PDAC therapies.

The projects presented in this thesis reveal novel aspects of the spectrum of BTC signaling. Being beneficial on the one hand, it can cause detrimental effects on the other hand. Furthermore, we confirm that ERBB4 signaling has two faces, as well. In one setting, BTC-mediated ERBB4 signaling is beneficial to the outcome of disease, as observed in AP. In a different setting, the activation of ERBB4 by the same ligand has dreadful consequences for the course of the disease, as observed in pancreatic cancer. Moreover, we showed that BTC prefers ERBB4- over EGFR-binding in AP, whereas in PDAC, BTC activates three out of four of the available ERBB receptors, revealing the predominant participation of EGFR signaling. This indicates that, regarding the ERBB family, the key to the outcome of diseases might be determined by receptor involvement after ligand binding. The bias in ligand-receptor interactions within the ERBB system needs to be further investigated. This is the point where the therapeutic benefit of BTC becomes questionable and must be qualified. BTC might be beneficial in AP, however, as soon as it encounters a cell with oncogenic KRAS, it has a detrimental effect, potentially enhancing RAS activity and causing ADM, thereby providing the basic component of PDAC development. Importantly, future studies of the ERBB receptor system should be regarded in a context-dependent manner and should implicitly consider the whole ERBB family.

## ZUSAMMENFASSUNG

Das ERBB (*erythroblastic leukemia viral oncogene homologs*) System besteht aus vier Rezeptor-Tyrosinkinase (RTKs): *epidermal growth factor receptor* (EGFR), ERBB2- (HER2, neu), ERBB3- (HER3) und ERBB4-Rezeptor (HER4). Die Rezeptoren der ERBB-Familie können von elf Liganden gebunden werden, was zu einer Homo- oder Hetero-Dimerisierung der Rezeptoren führt, sowie zu einer anschließenden Transphosphorylierung, hauptsächlich von Tyrosin-Resten in der zytosolischen Rezeptordomäne. Die ERBB-Rezeptoren induzieren zahlreiche Signalkaskaden, die bei der Embryonalentwicklung, Gewebemöiostase und auch bei der Entstehung von Krankheiten beteiligt sind. *Betacellulin* (BTC) ist einer der ERBB-Liganden mit Bindungsaffinitäten für EGFR und ERBB4. Er wurde erstmals in einer murinen Pankreas-Insulinom-Zelllinie identifiziert, spielt aber in zahlreichen Geweben und Organen, z.B. in den Langerhans-Inseln des Pankreas, in der Brustdrüse, dem Magen, im Gehirn, aber auch in Tumoren, z.B. im Sarkom, in Brustkrebs und vielen anderen Krebsarten eine bedeutende Rolle. BTC wird als membrangebundenes Vorläuferprotein synthetisiert, und durch das Enzym *a disintegrin and matrix 10* (ADAM10) gespalten, um freigesetzt als Wachstumsfaktor parakrin oder autokrin zu wirken. Membrangebundenes BTC kann auch juxtakrin mit Nachbarzellen kommunizieren. BTC ist in der Lage, verschiedenste Zellen zu differenzieren und es fungiert als potentes Mitogen in Epithel- und in glatten Muskelzellen. In Brustkrebszellen wird die BTC-Expression mit der Resistenzbildung in der EGFR-Therapie assoziiert. Der Knockout (KO) von BTC zeigte in Mäusen keinen offensichtlichen Phänotyp. Hingegen kommt es bei einer ubiquitären Überexpression von BTC zu einem ausgeprägten Phänotyp der transgenen Mäuse. BTC transgene (tg) Mäuse sind z.B. vor experimentell induzierter akuter Pankreatitis (AP) geschützt.

AP ist eine entzündliche Erkrankung der Bauchspeicheldrüse (Pankreas), die durch Gallensteine oder Alkoholmissbrauch verursacht wird. Verdauungsenzyme werden vorzeitig aktiviert und in das Interstitium des Pankreas freigesetzt, wo sie die Membranen verschiedenster Pankreas-bildender Zelltypen verdauen (Auto-Digestion). Begleitet wird dies von einer Entzündungsreaktion, die sich als heftiger Schmerz äußert und häufig zum *signs of inflammatory response syndrome* (SIRS), Multiorganversagen und zum Tod führt.

Es konnte bereits gezeigt werden, dass EGFR und die Applikation seines Liganden *epidermal growth factor* (EGF) zu einer Verbesserung der AP führten, jedoch wurden die zugrundeliegenden Mechanismen nicht untersucht. Die übrigen ERBB-Familienmitglieder wurden erst untersucht, als unsere Gruppe zeigen konnte, dass BTC die Entwicklung einer AP verhinderte. Dieser Schutzmechanismus wird aber nicht durch den EGFR vermittelt, allerdings wurde eine erhöhte SAPK-Aktivität im Zusammenhang mit dem BTC vermittelten Schutz

festgestellt. Die zugrundeliegenden Mechanismen wurden erst in dieser Doktorarbeit untersucht.

In der ersten Studie dieser Arbeit „*The protective effect of betacellulin against acute pancreatitis is ERBB4-dependent*“, wurde ERBB4 als entscheidender Vermittler des BTC-induzierten Schutzes vor AP identifiziert. Dazu wurde der ERBB4-Rezeptor in BTC tg Mäusen spezifisch im Pankreas unter dem Promotor *pancreas-associated transcription factor 1A* (*Ptf1a*) mit Hilfe des Cre-loxP-Systems (*ErbB4<sup>fl/fl</sup>;Ptf1a<sup>Cre/+</sup>;Btc<sup>tg/+</sup>*) ausgeschaltet. Zusätzlich wurden die *Btc* tg Mäuse in ein Knockdown Mausmodell für den EGFR eingekreuzt (*Egfr<sup>Wa5</sup>;Btc<sup>tg/+</sup>*). *ErbB4<sup>fl/fl</sup>;Ptf1a<sup>Cre/+</sup>;Btc*-Mäusen und *Egfr<sup>Wa5</sup>;Btc<sup>tg/+</sup>*-Mäusen wurde mittels Caerulein oder L-Arginin eine AP induziert. Um die Schwere der AP zu bestimmen, wurden klinische Parameter wie Lipase- und Amylase-Spiegel im Serum, sowie histologische Parameter wie Apoptose, Nekrose und Ödem im Pankreas bestimmt. *Btc* tg Mäuse blieben von der AP-Induktion unbeeinflusst. Während sich die *Egfr<sup>Wa5</sup>;Btc<sup>tg/+</sup>* Mäuse in sämtlichen Parametern wie *Btc* tg Mäuse verhielten, verhielten sich die *ErbB4<sup>fl/fl</sup>;Ptf1a<sup>Cre/+</sup>;Btc<sup>tg/+</sup>* Mäuse wie Wildtyp-Tiere. Zusätzlich zeigten *Btc* tg Mäuse nach AP-Induktion weniger Fibrose im Vergleich zu Wildtyp-Tieren. Microarray- und Western-Blot-Analysen ergaben eine erhöhte Expression der extrazellulären Matrix-(ECM)-Proteine *matrix-metalloproteinase 2* (MMP2), MMP3, *periostin* (POSTN) und *matrix-gla-protein* (MGP) in *Btc* tg Mäusen und in *Egfr<sup>Wa5/+</sup>;Btc<sup>tg/+</sup>* Kontrollen, aber nicht in *ErbB4<sup>fl/fl</sup>;Ptf1a<sup>Cre/+</sup>;Btc<sup>tg/+</sup>*-Tieren nach AP-Induktion. BTC verursachte die regulierte intramembran-Proteolyse von ERBB4 mit anschließendem Transport der intrazellulären Domäne (ICD) von ERBB4 in das Zytosol und den Zellkern, wo diese bekanntlich als Co-Aktivator der Transkription wirkt. Dies deutet darauf hin, dass die ICD von ERBB4 die Expression von ECM-Proteinen und -Modulatoren auf transkriptioneller Ebene reguliert, um die Mikroumgebung des Pankreas positiv zu beeinflussen. Die zuvor beobachtete Erhöhung von BTC-induziertem SAPK-Signaling war ebenfalls ERBB4 vermittelt und korrelierte mit einer erhöhten Apoptose-Rate. Zusammenfassend vermuten wir, dass BTC einen zweifachen Mechanismus induziert, bestehend aus dem Umbau des umliegenden Gewebes und einer erhöhten Apoptose-Rate, um die AP-Entwicklung bei Mäusen zu verhindern. Diese Daten legen nahe, BTC zukünftig als neues Medikament in der AP-Therapie einzusetzen. Ebenfalls könnte es therapeutisch sinnvoll sein den ERBB4-Rezeptor zu aktivieren, um die Behandlung der AP zu unterstützen.

Die zweite Studie "*Unraveling the ERBB network upon betacellulin signaling in pancreatic ductal adenocarcinoma in mice*" zeigt, dass sich eine hohe BTC-Expression nicht nur vorteilhaft auf Erkrankungen des Pankreas auswirkt. Es ist bekannt, dass BTC im Pankreaskarzinom exprimiert wird, was nicht verwunderlich ist, da BTC stark mitogen wirkt. Allerdings wurde die Rolle dieses Liganden im Pankreaskarzinom nicht näher charakterisiert. Das duktales Adenokarzinom des Pankreas (PDAC) ist eine Erkrankung mit einer sehr hohen

Mortalität, die nur durch Chemotherapie und Resektion behandelt wird, und nach wie vor ist PDAC der Tumor mit der niedrigsten Überlebensrate (5-Jahres-Überlebensrate: 8%). Die einzige gezielte Therapie involviert EGFR, wenn auch nur mit geringer klinischer Relevanz und häufiger Resistenzentwicklung.

Ziel dieser Studie war es, die Rolle von BTC im PDAC aufzuklären und zu untersuchen, welche Rezeptoren an der BTC-Aktivierung beteiligt sind. Um diese Fragen zu beantworten, wurde ein etabliertes PDAC-Mausmodell verwendet. Wir haben Mäuse verwendet, die unter dem pankreas-spezifischen Promotor *Ptf1a* konstitutiv aktives KRAS exprimieren (*Ptf1a<sup>Cre/+</sup>;Kras<sup>G12D/+</sup>*, im Weiteren als KC-Mäuse bezeichnet). Diese Mäuse tragen die gleiche Mutation, wie sie auch hauptsächlich beim humanen PDAC vorkommt, jedoch schreitet die Erkrankung langsamer fort und die Penetranz des invasiven Karzinoms ist unvollständiger als beim humanen PDAC. Die Entwicklung prämaligener Läsionen, der so genannten *pancreatic intraepithelial metaplasia* (PanIN), und ihr anschließendes Fortschreiten in das Pankreas-Karzinom, imitiert jedoch sehr gut den pathophysiologischen Verlauf, wie er in PDAC-Patienten zu beobachten ist. Vor der PanIN-Entwicklung transdifferenzieren Azinus-Zellen in Duct-Zellen (acinar-ductal metaplasia, ADM), die sich durch die initial aktivierende Mutation KRAS<sup>G12D</sup> in Pankreas-Zellen entwickelt. Einige ERBB-Liganden wurden bereits mit der PDAC-Entwicklung assoziiert, allerdings ist noch nichts über die Funktion von BTC in PDAC bekannt. In dieser Studie konnten wir die BTC-Expression in humanen PDAC-Proben, in humanen PDAC-Zelllinien und in prämaligen Läsionen des Pankreas von KC-Mäusen nachweisen. Nach der Deletion von BTC in KC-Mäusen durch CRISPR/Cas9 (*Btc<sup>-/-</sup>;Ptf1a<sup>Cre/+</sup>;Kras<sup>G12D/+</sup>*) wurden sowohl die PDAC-Entwicklung, als auch die PDAC-Progression verzögert, was mit einer verminderten EGFR-Expression und Phosphorylierung einherging. In Übereinstimmung mit dieser Beobachtung beschleunigte die Überexpression von BTC bei KC-Mäusen (*Btc<sup>tg/+</sup>;Ptf1a<sup>Cre/+</sup>;Kras<sup>G12D/+</sup>*, weiterhin als BKC-Mäuse bezeichnet) die Entwicklung und Progression von PDAC und führte zu einer Abnahme der mittleren Überlebensrate um etwa neun Monate im Vergleich zu KC-Mäusen. In BKC-Mäusen wurde nicht nur EGFR aktiviert, sondern auch ERBB4 und ERBB2 (letzteres zumindest durch die Hetero-Dimerisierung mit EGFR). BTC erhöhte die RAS-Aktivität, was ausschließlich über EGFR vermittelt wurde. Dies konnte mittels pankreasspezifischer Deletion der jeweiligen Rezeptoren unter Verwendung des Cre-loxP-Systems gezeigt werden (*Btc<sup>tg/+</sup>;Ptf1a<sup>Cre/+</sup>;Kras<sup>G12D/+</sup>;Egfr<sup>fl/fl</sup>* (EGFR KO;BKC), *Btc<sup>tg/+</sup>;Ptf1a<sup>Cre/+</sup>;Kras<sup>G12D/+</sup>;Erb2<sup>fl/fl</sup>* (ERBB2 KO;BKC), *Btc<sup>tg/+</sup>;Ptf1a<sup>Cre/+</sup>;Kras<sup>G12D/+</sup>;Erb4<sup>fl/fl</sup>* (ERBB4 KO;BKC)). Neben der RAS-Aktivierung induzierte BTC ADM in isolierten murinen Azinus-Zell-Clustern in der 3-D-Zellkultur. Die Deletion von *Erb2* bzw. *Erb4* in BKC-Mäusen führte zu einer stark verlängerten Überlebensrate der jeweiligen KO-Mäuse. Dieser Befund passte zu der Beobachtung, dass die PDAC-Entwicklung bei ERBB2 KO;BKC-Mäusen verlangsamt war,

während der Verlust von ERBB4 in der Histopathologie keinen offensichtlichen Unterschied im Vergleich zu BKC-Mäusen zeigte. Der Verlust beider Rezeptoren führte zu einer verminderten EGFR-Aktivierung. Der Verlust von ERBB4 führte zusätzlich zu einer Verminderung der ERBB2, MAPK- und SAPK-Aktivierung. Interessanterweise hat die Deletion von EGFR den BKC-Phänotyp fast komplett kompensiert, was mit einer verlängerten Überlebensrate verbunden war, jedoch konnte die Entwicklung von sporadischer ADM nicht verhindert werden. Diese ADM-Läsionen waren positiv für ERBB2, ERBB3 und ERBB4, aber die Western-Blot-Analyse ergab, dass sowohl die Expression, als auch die Aktivität dieser Rezeptoren herunterreguliert waren. Allerdings konnte eine erhöhte Phosphorylierung der ERBB4 ICD im Pankreas von EGFR KO;BKC-Mäusen detektiert werden, was darauf hinweist dass ERBB4 beim Verlust von EGFR eine kompensatorische Rolle einnimmt.

Diese Daten stehen im Einklang mit der gängigen Meinung in der PDAC-Forschungsgemeinschaft, dass EGFR ein entscheidender Akteur in der PDAC-Entwicklung ist. Wir konnten jedoch zeigen, dass die Bedeutung von ERBB2 und ERBB4 nicht unterschätzt werden darf, da sie maßgeblich an der Überlebensrate von BKC-Mäusen beteiligt sind, allerdings müssen deren Mechanismen noch genauer untersucht werden. Bemerkenswert ist, dass der Verlust von EGFR die Aktivität von ERBB2 und ERBB3 verringert, was zeigt, dass EGFR auch weiterhin ein wichtiges *Target* in der PDAC-Therapie sein sollte. Die kompensatorische Induktion der ERBB4-ICD in EGFR KO-Mäusen weist darauf hin, dass ERBB4 an der Entwicklung von Resistenzen in EGFR-gezielten Therapien beteiligt ist. Diese Studie zeigt deutlich, dass die Hemmung der kompletten ERBB-Familie bei PDAC-Therapien berücksichtigt werden sollte.

Die in dieser Arbeit vorgestellten Projekte zeigen neue Aspekte des Spektrums des BTC-Signaling. Einerseits hat BTC eine vorteilhafte Wirkung, wie in der AP beobachtet, andererseits kann es großen Schaden anrichten, indem es die PDAC-Entwicklung stark beschleunigt. Darüber hinaus bestätigen wir, dass ERBB4-Signaling ebenfalls zwei Seiten hat. In AP ist eine BTC-vermittelte ERBB4-Aktivierung vorteilhaft, in der Tumorgenese des Pankreaskarzinoms hat die Aktivierung von ERBB4 durch denselben Liganden gravierende Folgen für den Verlauf der Erkrankung. Darüber hinaus haben wir gezeigt, dass BTC die Bindung von ERBB4 gegenüber des EGFR in AP bevorzugt, während BTC im PDAC drei von vier der verfügbaren ERBB-Rezeptoren aktiviert, was mit einer hohen Beteiligung des EGFR einhergeht. Dies deutet darauf hin, dass die Auswirkungen des Signaling des ERBB-Netzwerks auf den Verlauf von Krankheiten dadurch bestimmt werden, welche Rezeptor-Beteiligungen der jeweiligen Liganden induziert werden. Was ERBB-Liganden beeinflusst, welche Liganden-Rezeptor- und Rezeptor-Rezeptor-Interaktionen innerhalb des ERBB-Systems bevorzugt werden, ist noch nicht genau verstanden. An diesem Punkt wird der therapeutische Nutzen von BTC fragwürdig und muss qualifiziert werden. BTC-Behandlung könnte in AP vorteilhaft sein, aber sobald der

Ligand auf eine Zelle mit onkogenem KRAS trifft, dreht sich seine Wirkung in das Gegenteil um, da es dort wahrscheinlich die RAS-Aktivität erhöht, somit ADM verursacht und den Grundbaustein für die PDAC-Entwicklung legt. Wichtig ist, dass zukünftige Studien des ERBB-Rezeptorsystems kontext-abhängig betrachtet werden sollten und unbedingt die ERBB-Familie in ihrer Gesamtheit untersucht werden sollte.

## PRESENTATIONS AND GRANTS

### PODIUM TALKS

- SEPTEMBER, 2016                    **EUROPEAN ASSOCIATION FOR THE STUDIES OF DIABETES (EASD)**,  
Munich, Germany. *'Maternal and paternal pre-conceptual  
overweight results in different sex-specific transcriptome changes  
of blastocysts and spermatozoa sncRNAs'*.
- DECEMBER, 2016                    **BIOSYSNET, ABSCHLUSS SEMINAR, MÜNCHEN** *'Maternal  
and paternal pre-conceptual overweight results in different  
sex-specific transcriptome changes of blastocysts and  
spermatozoa sncRNAs'*
- FEBRUARY, 2017                    **50. JAHRESTAGUNG PHYSIOLOGIE U. PATHOLOGIE  
DER FORTPFLANZUNG**, Munich, Germany. *'Peri-conceptual  
overweight in male and female mice causes sex-specific  
transcriptome changes in blastocysts which could result from  
differentially expressed sncRNA in spermatozoa of obese males'*.
- AUGUST, 2018                    **CSHL MEETING: MECHANISMS & MODELS OF CANCER**, Cold Spring  
Harbor, New York, USA. *'Unraveling the ERBB network upon  
betacellulin signaling in pancreatic ductal adenocarcinoma in  
mice'*.

### POSTER PRESENTATIONS

- JUNE, 2016                    **81ST COLD SPRING HARBOR LABORATORY SYMPOSIUM  
ON QUANTITATIVE BIOLOGY TARGETING CANCER**, Cold Spring  
Harbor, New York, USA. *'A high betacellulin expression  
accelerates the development of pancreatic ductal adenocarcinoma  
in mice'*.
- FEBRUARY, 2019                    **39. JAHRESTAGUNG DES DEUTSCHEN PANKREASCLUBS  
E.V.**, Göttingen, Germany. *'Uncovering the role of ERBB receptors  
in pancreatic ductal adenocarcinoma upon betacellulin-induced  
signaling in mice'*. (Poster-Talk)

### GRANTS

- AUGUST, 2018                    **DAAD STIPENDIUM**  
  
To support the congress trip *'CSHL Meeting: Mechanisms &  
Models of Cancer'* in Cold Spring Harbor, New York, USA

## PROLOGUE

This thesis consists of two research projects, which both investigate the ERBB receptor system in pancreatic diseases as acute pancreatitis and pancreatic cancer. Chapter 2 comprises the manuscript '*The protective effect of betacellulin against acute pancreatitis is ERBB4-dependent*', which has been re-submitted after major revisions to '*Journal of Gastroenterology*' in July, 2019 (*addendum*: The manuscript has been accepted and published in '*Journal of Gastroenterology*' in August, 2019.). Chapter 3 comprises the manuscript '*Unraveling the ERBB network upon betacellulin signaling in pancreatic ductal adenocarcinoma in mice*', which is in the process of submission. Both chapters include a separate introduction referring to the disease, the state of literature on ERBB network involvement in the disease, an aim and the study. A summary with the major conclusions and outlook on the whole chapter is provided afterwards. The thesis starts with an extensive introduction about the ERBB receptor system.

A further project, which I was involved in during my PhD studies, can be found under chapter 4. This comprises the manuscript '*Sex-specific programming effects of parental obesity in pre-implantation embryonic development*', which has been re-submitted after major revisions to '*International Journal of Obesity*' in July, 2019 (*addendum*: The manuscript has been accepted for publication in '*International Journal of Obesity*' in October, 2019.). A summary of the manuscript prefaces chapter 4.

## TABLE OF CONTENTS

<b>DANKSAGUNG</b>	<b>I</b>
<b>SUMMARY</b>	<b>IV</b>
<b>ZUSAMMENFASSUNG</b>	<b>VIII</b>
<b>PRESENTATIONS AND GRANTS</b>	<b>XIII</b>
<b>PROLOGUE</b>	<b>XIV</b>
<b>TABLE OF CONTENTS</b> <b>LIST OF FIGURES</b>	<b>XV</b>
<b>LIST OF FIGURES</b>	<b>XVII</b>
<b>ABBREVIATIONS</b>	<b>XVIII</b>
<b>1 INTRODUCTION</b>	<b>1</b>
<b>1.1 ERBB NETWORK</b>	<b>1</b>
1.1.1 THE RECEPTORS	1
1.1.2 ERBB4	2
1.1.3 CANONICAL SIGNALING OF THE ERBB FAMILY	5
1.1.4 SILENCING THE ERBBS	5
1.1.5 THE LIGANDS	6
<b>2 BTC IN ACUTE PANCREATITIS</b>	<b>9</b>
<b>2.1 INTRODUCTION</b>	<b>9</b>
2.1.1 ACUTE PANCREATITIS	9
2.1.2 THE ERBB FAMILY IN ACUTE PANCREATITIS	12
<b>2.2 AIM OF THE STUDY</b>	<b>14</b>
<b>2.3 STUDY: THE PROTECTIVE EFFECT OF BETACELLULIN AGAINST ACUTE PANCREATITIS IS ERBB4-DEPENDENT</b>	<b>14</b>
2.3.1 ABSTRACT	15
2.3.2 INTRODUCTION	16
2.3.3 METHODS	17
2.3.4 RESULTS	21
2.3.5 DISCUSSION	29
2.3.6 SUPPLEMENTARY FIGURES	31
2.3.7 SUPPLEMENTARY TABLES	33
<b>2.4 CONCLUSIONS &amp; OUTLOOK</b>	<b>36</b>
<b>2.5 BRIDGE</b>	<b>38</b>

<b>3</b>	<b><i>BTC IN PANCREATIC CANCER</i></b>	<b>39</b>
<b>3.1</b>	<b>INTRODUCTION</b>	<b>39</b>
3.1.1	PANCREATIC CANCER	39
3.1.2	THE ERBB FAMILY IN PANCREATIC CANCER	44
<b>3.2</b>	<b>AIM OF THE STUDY</b>	<b>49</b>
<b>3.3</b>	<b>STUDY: UNRAVELING THE ERBB NETWORK UPON BETACELLULIN SIGNALING IN PANCREATIC DUCTAL ADENOCARCINOMA IN MICE</b>	<b>50</b>
3.3.1	ABSTRACT	51
3.3.2	INTRODUCTION	52
3.3.3	METHODS	53
3.3.4	RESULTS	58
3.3.5	DISCUSSION	67
3.3.6	SUPPLEMENTARY FIGURES	71
3.3.7	SUPPLEMENTARY TABLES	73
<b>3.4</b>	<b>CONCLUSIONS &amp; OUTLOOK</b>	<b>76</b>
<b>4</b>	<b><i>SUPPLEMENTARY PROJECT</i></b>	<b>79</b>
<b>4.1</b>	<b>CONCLUSIONS</b>	<b>79</b>
<b>4.2</b>	<b>SEX-SPECIFIC PROGRAMMING EFFECTS OF PARENTAL OBESITY IN PRE-IMPLANTATION EMBRYONIC DEVELOPMENT</b>	<b>81</b>
4.2.1	ABSTRACT	81
4.2.2	INTRODUCTION	82
4.2.3	MATERIALS AND METHODS	82
4.2.4	SUPPLEMENTARY MATERIALS AND METHODS	83
4.2.5	RESULTS	89
4.2.6	DISCUSSION	93
4.2.7	SUPPLEMENTARY FIGURES	94
4.2.8	SUPPLEMENTARY TABLES	96
<b>5</b>	<b><i>REFERENCES</i></b>	<b>100</b>
<b>6</b>	<b><i>APPENDIX</i></b>	<b>116</b>

## LIST OF FIGURES

<b>FIGURE 1.1:</b> SCHEME OF ERBB RECEPTORS	2
<b>FIGURE 1.2:</b> REGULATED INTRAMEMBRANE PROTEOLYSIS	3
<b>FIGURE 2.1:</b> INVESTIGATION OF WA5+BTC MICE DURING CAERULEIN-INDUCED AP	22
<b>FIGURE 2.2:</b> INVESTIGATION OF ERBB4 <sup>DEL</sup> +BTC MICE DURING CAERULEIN INDUCED AP	23
<b>FIGURE 2.3:</b> THE PROTECTIVE EFFECT OF BTC IS ALSO LOST IN ERBB4 <sup>DEL</sup> +BTC MICE DURING L- ARGININE PANCREATITIS	25
<b>FIGURE 2.4:</b> ANALYSIS OF ECM	26
<b>FIGURE 2.5:</b> BTC TRANSGENIC ANIMALS REVEALED INCREASED LEVELS OF THE ERBB4-ICD	28
<b>FIGURE 3.1:</b> DEVELOPMENT AND PROGRESSION OF (PRE)NEOPLASTIC LESIONS PRIOR TO PDAC DEVELOPMENT	40
<b>FIGURE 3.2:</b> CHARACTERIZATION OF B <sup>-/-</sup> KC MICE	59
<b>FIGURE 3.3:</b> BTC IS EXPRESSED IN HUMAN PDAC SAMPLES, IN HUMAN PDAC CELL LINES AND IN PANCREATA OF KC MICE.	60
<b>FIGURE 3.4:</b> BTC INDUCES ADVERSE EVENTS IN KC MICE	61
<b>FIGURE 3.5:</b> BTC ACTIVATES THE ERBB RECEPTORS, ENHANCES RAS ACTIVITY AND INDUCES ADM	63
<b>FIGURE 3.6:</b> ERBB2 AND ERBB4 AFFECT THE TUMOR BURDEN IN BKC MICE	65
<b>FIGURE 3.7:</b> THE LACK OF EGFR IN BKC MICE REVEALED MAJOR CHANGES IN BODY WEIGHT, HISTOLOGY AND IN ERBB SIGNALING	66
<b>FIGURE 4.1:</b> MICROARRAY ANALYSIS OF MALE AND FEMALE BLASTOCYSTS FROM DIFFERENT MALE (M <sub>Ob</sub> ) AND FEMALE (F <sub>Ob</sub> ) OBESE PARENTS	90
<b>FIGURE 4.2:</b> DIFFERENTIAL ABUNDANCE OF SMALL RNAs IN THE SPERM OF OBESE (M <sub>Ob</sub> ) COMPARED WITH LEAN CONTROL MALES (M <sub>Co</sub> )	92

## ABBREVIATIONS

ACTA	Alpha-smooth muscle actin
ADAM	A disintegrin and metalloproteinase
ADM	Acinar to ductal metaplasia
AKT	Protein Kinase B
AP	Acute pancreatitis
AREG	Amphiregulin
ATP	Adenosine tri-phosphate
bp	Base pair
BTC	Betacellulin
CDKN2A	Cyclin-dependent kinase inhibitor 2A
co	Control
CP	Chronic pancreatitis
CYT	Intracellular cytoplasm domain
DAT	Differentially abundant transcripts
DMEM	Dulbecco's Modified Eagle Medium
DPC4	Deleted in pancreatic cancer-locus 4
ECM	Extra cellular matrix
EGF	Epidermal growth factor
EGFR	Epidermal growth factor receptor
EPGN	Epigen
ER	Endoplasmic reticulum
ERBB	Avian erythroblastosis oncogene B homologue
EREG	Epiregulin
FBS	Fetal bovine serum
GAP	GTPase activating protein
GAPDH	Glyceraldehyde-3-phosphate dehydrogenase
GEMM	Genetically engineered mouse model
GRB	Growth factor receptor bound protein
h	Hour
H&E	Haemotoxylin and eosin
HBEGF	Heparin-binding EGF
HER	Human epidermal growth factor receptor
ICD	Intracellular domain
IPMN	Intraductal papillary mucinous neoplasm
JM	Juxtamembrane
KO	Knockout
KRAS	K-rat sarcoma
Lys	Lysine
MAPK	Mitogen-activated protein kinase
MCN	Mucinouscystic neoplasm
MDM2	Mouse double minute 2 homolog
MGP	Matrix gla protein
min	Minute
MMP	Metalloproteinase

mRNA	Messenger ribonucleic acid
NGS	Next generation sequencing
NRG	Neuregulin
PAGE	Polyacrylamide gel electrophoresis
PanIN	Pancreatic intraepithelial neoplasia
PBS	Phosphate-buffered saline
PCR	Polymerase chain reaction
PDAC	Pancreatic ductal adenocarcinoma
PDX	Patient-derived xenograft
PI3K	Phosphoinositol-3-Kinase
PLC	Phospholipase C
POSTN	Periostin
PSC	Pancreatic stellate cell
PTB	Phospho-tyrosine binding domain
PTF1A	Pancreatic transcription factor 1 alpha
PVDF	Polyvinylidenfluorid
RIP	Regulated intramembrane proteolysis
RIP	Regualted intramembrane proteolysis
RPMI	Roswell Park Memorial Institute
RTK	Receptor tyrosine kinase
RT-PCR	Reverse transcriptase polymerase chain reaction
SAPK	Stress activated protein kinases
Ser	Serine
SerpinA6	Serine peptidase inhibitor A6
SH	Src Homology
SHC	Src homolog 2 domain-containing
SIRS	signs of inflammatory response syndrome
SMAD4	Mothers against decapentaplegic homolog 4
Src	Sarcoma
STAT	Signal transducers and activators of transcription
TACE	Tumour necrosis factor a converting enzyme
TACE	Tumor necrosis factor-alpha converting enzyme
TBS	Tris buffered saline
tg	Transgenic
Thr	Threonine
TKI	Tyrosine kinase inhibitor
TP53	Tumorsuppressor protein 53
Tyr	Tyrosine
UPR	Unfolded protein response
Wa5	Waved 5
wt	Wildtype
YAP1	Yes-associated protein 1

# 1 INTRODUCTION

## 1.1 ERBB NETWORK

The erythroblastic leukemia viral oncogene homolog (ERBB) network, a highly complex signaling system, transmitting extracellular stimuli into the cell, encompasses a family of four receptors, as well as eleven ligands. The receptors epidermal growth factor receptor (EGFR, ERBB1, HER1), ERBB2 (HER2; neu), ERBB3 (HER3) and ERBB4 (HER4) are controlled by the ligands: epidermal growth factor (EGF), transforming growth factor alpha (TGFA), amphiregulin (AREG), epigen (EPGN), epiregulin (EREG), heparin-like epidermal growth factor (HBEGF), betacellulin (BTC), and the neuregulins1-4 (NRG1-4).

### 1.1.1 THE RECEPTORS

The ERBB receptors of the EGFR family are essential RTKs for the mammalian body. The ubiquitous deletion of only one of the receptors is lethal in mice. EGFR loss in mice results in either peri-implantational, mid-gestational or postnatal lethality (depending on the genetic background) due to epithelial dysfunction<sup>1-3</sup>. Mice lacking ERBB2, ERBB3 or ERBB4 die during mid-gestation due to severe defects in neuronal and cardiac development<sup>4-6</sup>.

All family members are type I transmembrane proteins containing a highly glycosylated extracellular ligand binding domain, a short single transmembrane region and a large cytoplasmic part containing the tyrosine kinase domain which is flanked by a tyrosine-rich tail. Ligand binding induces a conformational change in the receptors which enables them to dimerize. This event is required for the activation of the tyrosine kinase domain and for the subsequent induction of the reciprocal transphosphorylation of mainly tyrosine (Tyr) residues of the C-terminal tail<sup>7</sup>. This process leads to the exposure of docking sites which then provide a platform for the interaction of the receptor with signaling molecules as SRC proto-oncogene non-receptor tyrosine kinase (scr)-homology (SH2) or phospho-Tyr binding (PTB) domains, such as phosphatidylinositol 3-kinase (PI3K), signal transducers and activators of transcription (STAT) or adapter molecules which forward signals phosphorylation-independently, *e.g.* growth factor receptor bound protein (GRB)<sup>8</sup> (Figure 1.1). These signaling molecules, in turn, induce various cascades, thereby mediating intracellular responses which are involved in cell division, migration, apoptosis, differentiation and adhesion<sup>9</sup>. Hence, the ERBB receptors play an essential role in embryonic development and adult homeostasis, as well as in pathological processes, such as carcinogenesis<sup>7</sup>. Receptor dimerization includes homo- and hetero-dimerization of 28 possible combinations. However, the affinity between the family members varies. The preferred dimerization partner of all receptors is ERBB2<sup>10,11</sup>. ERBB3 lacks the intrinsic kinase activity<sup>12</sup>, which prevents the initiation of Tyr-phosphorylation. Thus,

for proper activation ERBB3 requires a hetero-dimerization partner. ERBB2 activation also depends on receptor hetero-dimerization due to the lack of ERBB2-specific ligands<sup>9,13</sup>. These features make the ERBB2/ERBB3 dimer a perfect couple because they compensate each other's disabilities. Indeed, the hetero-dimer is frequently involved in carcinogenesis being a very potent oncogenic dimer<sup>14-17</sup>. Nevertheless, ligand-independent ERBB2 signaling also occurs: Upon ERBB2 overexpression, predominantly as a consequence of *ERBB2* gene amplification, it can build homo-dimers and signal autonomously, an event frequently observed in breast cancer. This led to the development of the ERBB2 specific antibody trastuzumab which is successfully used in breast cancer therapy<sup>18-21</sup>. The choice of the ligand, as well as the composition of the receptor-dimer determines which signaling cascade will be initiated<sup>22,23</sup>. EGFR and ERBB4 have a variety of cytosolic interaction partners, while ERBB2 has the fewest of all members and ERBB3 predominantly acts through PI3K signaling. All receptors share binding motifs for GRB2 and SHC<sup>8</sup>. A common downstream target of all members of the ERBB family is the RAS/RAF/MAPK signaling pathway as well as phospholipase C (PLC) signaling<sup>24</sup>. Another very important player in the ERBB network is the PI3K/activated protein kinase B (PKB/AKT) pathway, either through direct or indirect interaction of PI3K with the receptors<sup>24,25</sup>.

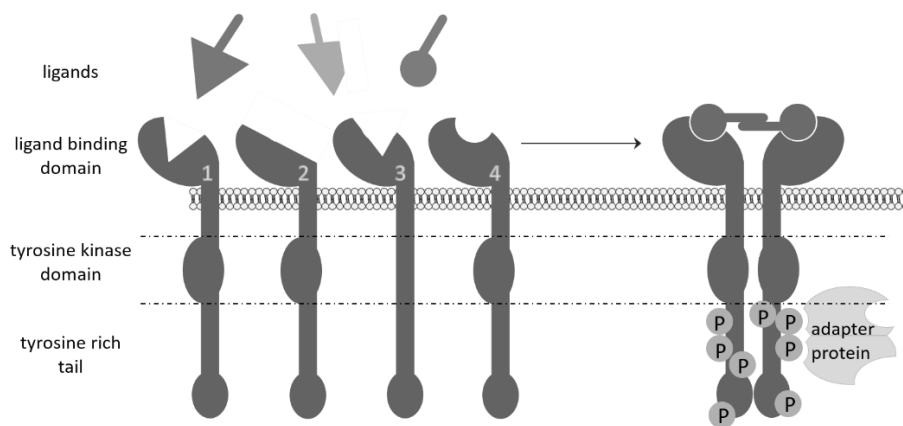


**Figure 1.1: Scheme of ERBB receptors**

EGFR (1) and ERBB4 (4) are fully functional receptors. ERBB2 (2) has no known ligand and ERBB3 (3) has no intracellular Tyr-kinase domain. Upon ligand binding, ERBB receptors dimerize and auto-phosphorylate the Tyr-rich cytosolic domain of their dimerization partner. Phospho-Tyrosines (P) serve as docking sites for adapter proteins.

## 1.1.2 ERBB4

### 1.1.2.1 BINDING SITES

Like all family members ERBB4 is a 180 kDa glycoprotein consisting of a single transmembrane domain which separates the glycosylated extracellular ligand-binding domain from the intracellular domain (ICD)<sup>26</sup>. ERBB4 is an autonomous RTK, able to either operate as a homo-dimer or to serve as a binding partner for each of its relatives in order to form hetero-dimers. BTC<sup>27,28</sup>, EREG<sup>29,30</sup>, HBEGF<sup>10,28,31</sup> and the neuregulins NRG1<sup>32-35</sup>, NRG2<sup>35-38</sup>,

NRG3<sup>39,40</sup> and NRG4<sup>41</sup> activate the receptor. Along with all other family members it provides binding sites for SHC and GRB2<sup>8</sup>, adapter proteins which, when bound to RTKs, induce the activation of the RAS signaling cascade, which results in a mitogenic cell response. Like EGFR and ERBB2, ERBB4 provides a binding site for the cytosolic tyrosine phosphatases SH1 and SH2 (PTP-2c)<sup>8</sup>. In common with ERBB3 is the ability of ERBB4 to associate with PI3K<sup>31,42</sup>, which links the AKT/PKB pathway to ERBB4 signaling, thereby implicating a role for ERBB4 in the regulation of cell growth and survival. As EGFR, ERBB4 provides a binding site for STAT5 enabling it to bind this transcription factor<sup>8,43,44</sup>, and thereby associating ERBB4 to gene expression regulation. Moreover, it also affects gene expression regulation in a direct manner by acting as a transcriptional co-activator<sup>44-49</sup>.

### 1.1.2.2 REGULATED INTRAMEMBRANE PROTEOLYSIS

After undergoing regulated intramembrane proteolysis (RIP), ERBB4 can send its intracellular domain (ICD) into the nucleus. Through binding of NRG or the induction of 12-O-tetradecanoylphorbol-13-acetate (TPA), RIP is initiated. In a first step, a disintegrin and metalloproteinase domain-containing protein 17 (ADAM17) cleaves off the 120 kDa extracellular fragment (ECD) of ERBB4 and leaves the remaining part of the receptor associated to the cell membrane<sup>50,51</sup>. At the cytosolic juxtamembrane region, the ICD is subsequently cleaved by gamma secretase and released into the cytosol as a soluble fragment of 80 kDa (ICD) (Figure 1.2). The ICD is also able to interact with other transcription factors or transcriptional regulators and translocate into the nucleus where it activates the transcription of a variety of target genes<sup>44-49</sup>. All other members of the ERBB family have also been found in the nuclei of cells<sup>52-57</sup>, however, RIP has only been observed to occur in ERBB4.

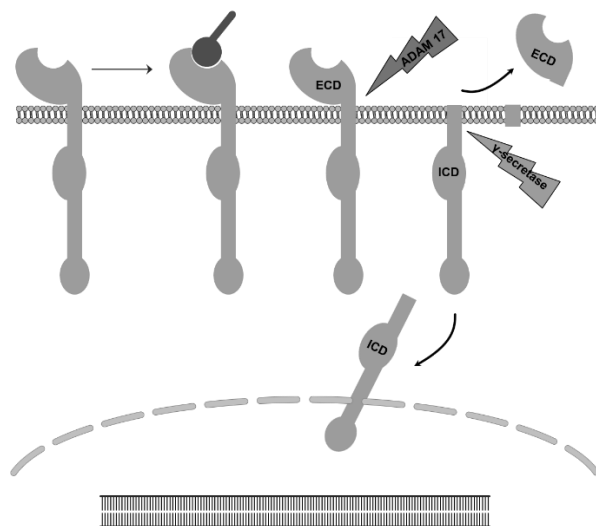


**Figure 1.2: Regulated intramembrane proteolysis**

After RIP induction, ADAM17 cleaves off the extracellular domain (ECD) of ERBB4. Subsequently, gamma secretase cleaves off the intracellular domain (ICD) of ERBB4, enabling it to enter the nucleus.

### **1.1.2.3 ALTERNATIVE SPLICING**

ERBB4 possesses another unique feature. It can undergo alternative mRNA splicing, thereby producing four functionally distinct isoforms. The first isoforms were found to differ in their juxtamembrane (JM) region where exon 16, encoding for 23 amino acids (JM-a), is replaced by exon 15b, encoding for 13 alternative amino acids (JM-b). The two mutually exclusive isoforms have distinct expression patterns in the mouse. Since ERBB4 JM-b lacks the proteolytic cleavage site for ADAM17, it is protected from RIP and lacks ICD signaling<sup>58</sup>. Elenius *et al.* also discovered a cytosolic splice form which was unable to bind and thus, also to activate PI3K due to a lack of exon 26, which encodes for a sequence of 16 amino acids. They called this functional isoform CYT-2, compared to the full-length cytosolic domain CYT-1 and found it to be predominantly expressed in neural tissues of the mouse<sup>59</sup>. In summary, there are four functionally different isoforms: CYT-1 JM-a, CYT-1 JM-b, CYT-2 JM-a, CYT-2 JM-b.

### **1.1.2.4 FUNCTIONAL CONSEQUENCES OF ERBB4 SINGULARITY**

While the JM isoforms promote different cellular responses, the cytosolic isoforms also activate different signaling pathways and differ in their stability. *In vitro* experiments revealed that the expression of CYT-2 JM-a led to the survival of fibroblasts, while the expression of CYT-2 JM-b promoted cell death of the same cell type, indicating opposing effects of the same gene<sup>60</sup>. Furthermore, also the cytosolic variants were revealed to function oppositely: While the expression of CYT-2 was found to result in hyperplasia of the mammary epithelium *in vivo*, the expression of CYT-1 rather resulted in the differentiation of the same<sup>61</sup>. These were only two examples of the contradictory face of ERBB4, owing to its splice isoforms. This and its capability of independent ICD signaling might be the reason for the contradictory face of ERBB4 in different types of cancer. In bladder cancer, increased levels of ERBB4 correlated with a better prognosis<sup>62</sup> and in colitis-associated cancer, Ni *et al.* reported a protective role of ERBB4 by negatively regulating the cholesterol metabolic pathway<sup>63</sup>. And while ERBB4 acts as a tumor suppressor in the development of hepatocellular carcinoma<sup>64</sup>, its activation in glioblastoma was associated with a poor prognosis<sup>65</sup>. ERBB4 is frequently mutated in metastatic melanoma and provides a promising target in developing novel melanoma drug therapies<sup>66,67</sup>. The CYT-1 isoform was revealed to be an independent prognostic factor on the time to progression in malignant melanoma, while total ERBB4 or CYT-2 had no influence on the time to progression<sup>68</sup>. A multivariate analysis demonstrated that the cytosolic ICD of ERBB4 is a positive prognostic factor in lymph-node negative invasive breast cancer patients<sup>69</sup>. In another study, high overall ERBB4 levels correlated with a significantly longer survival in estrogen-positive breast cancer patients, while the exclusive nuclear ICD immunostaining was associated with a shorter survival than membrane-bound ERBB4 staining<sup>70</sup>. The Janus face of ERBB4 is especially prominent in breast cancer, which is probably attributed to the great

research interest in ERBB4 in this field, while it is neglected in a variety of other diseases. Many studies attribute ERBB4 an oncogenic role in breast cancer<sup>71-74</sup>, however, as many publications match ERBB4 a rather favorable role<sup>75-78</sup>.

These examples show that investigations on ERBB4 must be carried out very thoughtfully. Alternative splicing and the question whether ICD signaling occurs biases ERBB4-mediated responses.

### **1.1.3 CANONICAL SIGNALING OF THE ERBB FAMILY**

A typical MAPK activation cascade is illustrated as follows: BTC binds to EGFR and ERBB4, thereby inducing receptor dimerization and autophosphorylation. P-Tyr-1068 of EGFR serves as a docking site for GRB2, which is in complex with and thereby recruits the intracellular adapter molecule son of sevenless homolog 1 (SOS1) to the receptor dimer via its SH3 domain and concomitantly, it brings SOS1 into close proximity to membrane-bound RAS. SOS1 is a GEF which promotes GDP/GTP exchange in the RAS molecule, thereby inducing a conformational change and activating it<sup>79,80</sup>. Active RAS, in turn, binds RAF, thereby transforming it into an active state. RAF is a Serine/Threonine (Ser/Thr) kinase which positively regulates mitogen-activated protein kinase kinase 1 (MAPKK/MEK1) by the phosphorylation of Ser residues in its catalytic domain. MEK is a Tyr- and Ser/Thr-dual specific kinase, which, in turn, phosphorylates mitogen-activated protein kinase (MAPK/ERK), enabling it to enter the nucleus in order to activate numerous transcription factors by Ser- or Thr-phosphorylation resulting in the regulation of proliferation, differentiation and apoptosis<sup>81</sup>.

### **1.1.4 SILENCING THE ERBBs**

There are several ways to down-regulate the ERBB signal. Since phosphorylation is the major way to start the cascade and to keep it running, dephosphorylation of Tyr, Ser and Thr is one way to stop the cascade. Phosphatases can hydrolyze phosphates either from receptors or signaling molecules in the cytosol. Another way to turn off the signal is the removal of the receptor from the cell surface, called internalization. After internalization, the receptor can either undergo recycling or degradation. The exact mechanism how internalization is initialized is not revealed yet. However, in the case of EGFR, endocytosis is promoted by mono- and polyubiquitination of lysines (Lys) in the kinase domain of the receptor, mediated by GRB2 and the E3 ubiquitin ligase CBL. This highly complex process depends on many other factors. After endocytosis, the receptor is sorted in the early endosome and will either be transported to the lysosome in order to be degraded according to its ubiquitination pattern or it will be recycled back to the cell surface, while the latter is the default pathway for EGFR. The ligand occupancy is crucial to determine EGFR internalization towards recycling or degradation. At the

dominating pH in the endosome, EGF binding to the receptor is stable, whereas TGFA dissociates from EGFR very fast. Since continuous ubiquitination is believed to depend on persistent ligand binding, EGF signaling predisposes the receptor to degradation, while TGFA stimulation results in fast receptor recycling, thereby maintaining a steady signal. ERBB2, ERBB3 and ERBB4 are impaired to endocytic downregulation, however, little is known about the differences in their susceptibilities to ligand-induced internalization compared to the EGF receptor<sup>82</sup>.

## **1.1.5 THE LIGANDS**

### **1.1.5.1 AN OVERVIEW**

In the absence of any ligand, all ERBB members are present in a tethered conformation preventing them from dimerization. Upon ligand binding, the receptors undergo a conformational change, exposing the dimerization arm in order to interact with another family member<sup>83</sup>. The ERBB family recognizes several structurally similar growth factors including EGF, HBEGF, TGFA, AREG, BTC, EPGN, EREG, as well as NRG1-4<sup>7</sup>. All ligands are transmembrane proteins, which share a conserved EGF-like motif and are synthesized as large precursors. They are activated upon the proteolytic cleavage by ADAM10 and 17, resulting in the release of their ectodomain<sup>84,85</sup>. This soluble extracellular domain can diffuse over a short distance and act in a paracrine way, affecting nearby cells. It can also act in a juxtacrine manner, affecting neighboring cells or in an autocrine manner, impacting the cell it originated from<sup>24</sup>. The ligands have different binding specificities and affinities for the ERBB receptors, *i.e.* all ligands, except for the NRGs, bind EGFR and all NRGs bind the ERBB4 receptor but not EGFR. ERBB growth factors are ambivalent, but for ERBB2 no ligand exists<sup>7</sup>. According to their receptor specificity, it is common practice to categorize them into groups: Group I is built by the EGFR specific ligands: EGF, TGFA, AREG and EPGN; group II consists of ligands which recognize EGFR and ERBB4: HBEGF, EREG and BTC; group III is formed by growth factors which bind to ERBB3 and ERBB4: NRG1 and NRG2; and group IV consists of NRG3 and NRG4 with affinities for ERBB4 only<sup>86</sup>. Interestingly, although triggering the same receptor, group I ligands induce different responses in the cell. The mechanisms for this phenomenon are not understood. One solution might be, in part, that the EGF receptor chooses different dimerization partners with different kinetics in a ligand-dependent manner thereby providing binding sites for different signaling molecules, thus, ending in different signaling cascades. A study revealed that EGF and TGFA biased EGFR to rather dimerize with ERBB2 than with another EGFR monomer, while BTC and AREG produced equal amounts of EGFR homo-dimers and hetero-dimers with ERBB2. AREG was only able to produce half as many dimers compared to all other EGFR ligands, independent of the dimer-type<sup>87</sup>. These results suggest that the choice of the dimerization partner and the corresponding

kinetics are the keys to the question which answer is favorably given by the cell. Possibly, this is achieved by conformational or steric changes in the receptor. Also important is the fact that ERBB ligands can cross- and auto-induce further ERBB ligands. BTC, AREG, EREG and EPGN are often co-expressed due to their spatial proximity on the chromosome locus, which makes the signaling network even more complex and also difficult to investigate<sup>23</sup>.

### **1.1.5.2 BTC – THE LIGAND OF INTEREST**

#### *CHARACTERISTICS OF BTC*

BTC is synthesized as a precursor protein, consisting of 178 amino acids with an extracellular region, comprising an EGF-like domain, a transmembrane region, and a cytoplasmic tail<sup>101</sup>. In addition to the three di-sulphide bridges in the EGF-like domain, BTC is the only EGFR ligand possessing an extra cystein-cystein (Cys) bond in its extracellular part, which does not affect EGFR binding affinity, but of which the function remains to be solved<sup>102</sup>. Its ectodomain is predominantly cleaved by ADAM10<sup>85</sup>, ready to induce paracrine or autocrine signaling via EGFR or ERBB4. Thus, BTC is able to mediate signals through every member of the ERBB family by receptor hetero-dimerization. Also, unshed BTC can interact with adjacent cells in a juxtacrine manner<sup>103</sup>. Together with HBEGF, BTC has the biggest potential among all EGFR ligands to induce receptor internalization and degradation. This is due to the ability of BTC to resist low pH levels, thereby, ensuring steady ubiquitination of the receptor after internalization. Compared to its relatives, BTC and HBEGF rarely induce EGFR recycling back to the cell surface, indicating a rather fast shut down of the induced signal than signal amplification<sup>104</sup>. This points to an internalization mechanism that is different from the canonical pathway and which might not end in receptor degradation<sup>105</sup>.

BTC was identified in the conditioned medium of murine pancreatic insulinoma derived cell lines. *Btc* mRNA was expressed in mouse sarcoma cell lines, but also in many other tissues, including murine pancreatic islets of the pancreas. Additionally, human *BTC* mRNA was found to be detected in the breast cancer cell line MCF-7. Early, BTC was found to be a potent mitogen for retinal pigment epithelium and vascular smooth muscle cells<sup>100</sup>. BTC can convert exocrine cells of the rat pancreas into insulin-producing cells when combined with activin A<sup>106</sup>. It also converts murine glucagon producing alpha-cells<sup>107</sup>, rat intestinal crypt-like cells<sup>108</sup>, human hepatoma cells<sup>109</sup>, and rat mesenchymal stem cells<sup>110</sup> into insulin producing beta-cells, strongly indicating a role for the growth factor in differentiation, thus providing a great therapeutic potential in diabetes research. BTC acts mitogenic on undifferentiated human pancreatic epithelial cells<sup>111</sup> and on rat insulinoma cells<sup>112</sup>, as well as on fetal rat pancreatic ductal epithelial cells, which correlates with high EGFR expression<sup>113</sup>. BTC plays a role in human hepatocellular carcinoma, endometrial adenocarcinoma, head and neck squamous

cell carcinoma and prostate cancer metastasis<sup>103</sup>. In one breast cancer study, BTC expression was found to be associated with a poor clinical outcome, whereas the effect was even worse, when HBEGF was overexpressed concomitantly<sup>114</sup>. Furthermore, BTC was associated with resistance to EGFR treatment in breast cancer cell lines. The treatment with tyrosine kinase inhibitors (TKI) led to the acute expression of BTC, induction of ERBB2/ERBB4 dimers and ERBB4 cleavage, thereby evading EGFR inhibition and reactivation of EGFR mediated signaling cascades<sup>115</sup>. This mechanism could also be important in other tumors.

#### *BTC OVEREXPRESSION IN MICE*

While the BTC KO in mice revealed no apparent phenotype with mice being viable and fertile<sup>116</sup>, the overexpression of BTC bares numerous alterations. BTC transgenic (tg) mice display stunted growth, pulmonary haemorrhage syndrome, defects in the eyes and high post-natal mortality<sup>117</sup>. BTC is required for female reproduction and its ubiquitous overexpression in mice lead to delayed blastocyst implantation into the uterus due to impaired fertilization, resulting in a reduced litter size<sup>118</sup>. Interestingly, the relative weight of the vast majority of organs was increased in BTC tg mice, except for the pancreas. Although BTC has a proliferative effect on beta-cells, the pancreas weight in BTC tg mice was significantly decreased, indicating an adverse effect of BTC on the exocrine part<sup>117</sup>. However, BTC tg pancreata displayed increased proliferation rates, but also increased apoptosis rates, suggesting an increased turnover of pancreatic cells upon BTC signaling. It was revealed that the retarded growth of the pancreas in BTC tg mice was mediated by ERBB4, while all other BTC-related organ weight changes were dependent on the EGF receptor. Another very intriguing feature of BTC, revealed by our group, is its protective effect in acute pancreatitis (AP) upon overexpression suggesting increased apoptosis and decreased necrosis rates possibly induced by enhanced SAPK signaling and thereby ameliorating the AP clinical course<sup>119</sup>.

Apparently, there are many levels in the complex ERBB hierarchical structure - from receptor activation via the signaling cascade and the final response of the cell to the fate of the receptor - that provide a platform for aberrant signal transduction allowing them functions in pathological processes. The impact of the ERBB receptors and their ligands on pancreatic cancer and acute pancreatitis will be reviewed in this work.

## **2 BTC IN ACUTE PANCREATITIS**

### **2.1 INTRODUCTION**

#### **2.1.1 ACUTE PANCREATITIS**

##### **2.1.1.1 DEVELOPMENT AND INCIDENCE**

AP is an inflammatory disease with many causes. In principal, pancreatic duct obstruction or acinar cell injury lead to the release of active digestive enzymes into the interstitial space, instead of into the lumen of the pancreatic ducts in order to be transported to the duodenum. This deregulation results in the protease-induced damage of cell membranes (auto-digestion) of the pancreas, which, in turn, causes an inflammatory response within the pancreatic parenchyma<sup>120</sup>. Gall stones and alcohol abuse are the main causes of pancreatitis (70-80%), followed by uncommon causes, e.g. infections, abdominal trauma, drug-induced adverse reactions, pancreatic tumors (10-15%) and idiopathic causes (10-20%)<sup>121</sup>. With an annual incidence of 13-45/100.000 in the U.S. and Europe, AP is one of the most common gastrointestinal causes for contacting the emergency services and for hospitalization and incidences are increasing<sup>122,123</sup>. 25% of all AP patients develop insufficiency of the exocrine pancreas<sup>124</sup> and up to 40% develop pre-diabetes or diabetes after the first episode of AP<sup>125</sup>. Recurrence occurs in 18% of AP patients and 8% of the patients develop chronic pancreatitis (CP), which coincides with a drastic decrease in the quality of life<sup>126</sup>. Symptoms of AP include persistent abdominal epigastric pain and nausea. The diagnosis is made, if at least two of the following criteria are fulfilled: severe abdominal pain radiating to the back, enhanced serum lipase (or amylase) activity, at least three-fold compared to normal serum, and hallmarks of AP in computer tomography or magnetic resonance imaging<sup>120</sup>.

##### **2.1.1.2 CLASSIFICATION**

The severity of the disease is represented by the mortality rates that are as high as 36-50% in high grade AP (severe AP), which is characterized by persistent (>48 hours) single or multiple organ failure. Mortality is declining with the decrease of AP severity. Moderately severe AP is accompanied by transient (<48 hours) organ failure and/or local or systemic complications, while mild AP shows no signs of complications or the involvement of other organs. The determinant of the risk of developing organ failure is the immune response of the host to local pancreatic injury during the first week of AP. This immune response results in the increase of heart and respiration rate, a deregulated body temperature and an unbalanced white blood count. These symptoms are all summarized in the term "Signs of systemic inflammatory response syndrome" (SIRS). Persistence of SIRS in the early phase of AP increases the risk of developing organ failure and severe AP<sup>127</sup>. While these parameters classify the clinical severity of AP, the distinction between interstitial or edematous pancreatitis and necrotizing

AP (NAP) defines the morphological severity, with the former being the milder type of AP. NAP affects 5-10% of all patients<sup>127</sup>. It is further sub-divided into three groups: NAP with necrosis affecting exclusively the pancreatic parenchym (very rare), NAP with necrosis affecting peri-pancreatic tissues only and NAP affecting both compartments, representing the most common type of NAP<sup>121</sup>.

### **2.1.1.3 THERAPY**

Analgesic therapy is administered in the first place. The administration of opiates is often inevitable, although opiates enhance the paralytic ileus, which frequently accompanies AP. However, opiates are an appropriate analgesic for AP, since they affect the clinical outcome of AP as bad as other analgesics, however, they also reduce the need for supplementary pain treatment<sup>128</sup>. In order to increase the chance of preserving as much tissue as possible, patients receive fluid replacement, of which the volume and rate are crucial. The right balance must be found and the patient requires constant monitoring. In this way, optimal organ perfusion can be ensured and typically fast developing hypovolemia can be prevented<sup>129</sup>. It is discussed controversially, whether enteral or parenteral nutrition ameliorates the outcome of the AP course. Food or fluid ingestion leads to an intensification of pain, classifying nutrition therapy as pain management. The current consensus is that nutrition support should only be provided in severe AP or when required, and that enteral nutrition should be preferred over parenteral nutrition<sup>130</sup>. While it is discussed controversially whether early endoscopic retrograde cholangiopancreatography (ERCP) affects mortality and complications of AP, an overview of randomized controlled trials revealed no adverse effect of ERCP on the course of AP. However, the common sense is that indication for ERCP is given in patients with coexisting cholangitis or biliary obstruction or when remaining pancreatic or bile duct obstructions are expected<sup>131</sup>. NAP is also predominantly treated in a conservative manner, being effective in two thirds of the patients. Approximately one third of the patients develops infectious necrosis, making them subject to surgery or endoscopic drainage techniques in order to target the necrotic tissue. Due to high mortality rates of 11-39%, open necrosectomy has been replaced by minimally invasive approaches<sup>132</sup>. In summary, AP treatment only consists of symptomatic treatment. No therapies exist affecting the physiopathology of the disease.

### **2.1.1.4 PATHOGENESIS**

The two most common types of AP differ in their pathological mechanism. While gall stones and the exposure of duct cells to bile acid lead to ductal obstruction and associated pressure on the tissue, the exposure of acinar cells to ethanol and bile acids is toxic. These events, independent of the cause, result in the deregulation of trypsinogen activation, mitochondrial function, calcium signaling and endoplasmic reticulum (ER) stress<sup>126</sup>.

#### *PREMATURE TRYPSINOGEN ACTIVATION*

In the acinar cell of a normal pancreas, chymotrypsin and trypsin are stored as inactive precursors (zymogens) in granules. Upon a physiological stimulus, zymogens are secreted into the lumen of the pancreatic duct and transported to the duodenum, where enteropeptidases cleave off N-terminal amino acids in order to activate trypsin. Active trypsin, in turn, cleaves and thus, activates chymotrypsinogen<sup>133</sup>.

Pancreatic ductal obstruction blocks the apical release of zymogen granules (containing the inactive precursors chymotrypsinogen and trypsinogen) into the lumen, leading to the fusion of such granules with acinar lysosomes. Products of this fusion are autophagic vacuoles, where lysosomal cathepsin B activates the proteolysis of trypsinogen to trypsin. This event starts a cascade of zymogen activation with the subsequent release of active digestion enzymes into the interstitial space where they damage cellular membranes by auto-digestion. Intracellular proteases also break down the lysosomal membrane, thereby triggering mitochondrial cytochrome c release and inducing Caspase 3-mediated apoptosis<sup>126</sup>.

#### *ER STRESS*

The ER is the organelle within the eukaryotic cell where protein modification takes place and where the delivery of these proteins to their target sites is determined. In the ER, proper protein folding and post-translational modification is carried out in order to send the correctly folded protein to the Golgi apparatus.

Incomplete or improper folding results in the retention of the protein in the ER in order to repair the misfolded protein or to target it for degradation. A deregulation of any of these processes is called ER stress and induces the unfolded protein response (UPR)<sup>134</sup>. UPR is initially activated to adapt to the altered environment and to restore physiological ER function by changing the transcriptome in favor of enhanced protein folding and degradation capacity of the ER<sup>135</sup>. Since acinar cells produce an enormous amount of protein, they are particularly sensitive to ER stress. In AP, toxins like ethanol induce an increased need of acinar cell products, thereby stressing the ER. The UPR enhances the transcription of ER chaperone and factors required for ER expansion and ER-dependent protein degradation. Also, autophagy is induced for the removal of incorrectly folded proteins. However, if the UPR is overwhelmed, it induces cell death as the last response<sup>126</sup>.

#### *DISTURBED $Ca^{2+}$ SIGNALING*

With a concentration of 5 mM, the ER is also the major deposit of Calcium ions ( $Ca^{2+}$ ) in the cell (compared to 0.1  $\mu$ M in the cytosol). Upon physiological triggers,  $Ca^{2+}$  is released into the cytosol for a transient cytosolic  $Ca^{2+}$  increase, and is then transported back into the ER or out

of the cell by two adenosine triphosphate (ATP)-dependent  $\text{Ca}^{2+}$  channels. Disturbed  $\text{Ca}^{2+}$  signaling is a major incident during AP<sup>126</sup>.

In normal acinar cells,  $\text{Ca}^{2+}$  influx induces zymogen exocytosis and stimulates ATP production in the mitochondria. Ethanol, bile acids and cholecystokinin disturb the physiological  $\text{Ca}^{2+}$  cycle in acinar cells, initially, by the induction of inositol 1,4,5- trisphosphate receptor signaling. This further results in the potentiation of cytosolic  $\text{Ca}^{2+}$  by the activation of the  $\text{Ca}^{2+}$ -dependent  $\text{Ca}^{2+}$ -influx into the cell from the outside, leading to permanently high cytosolic  $\text{Ca}^{2+}$  concentrations which causes mitochondrial membrane permeability and the loss of the mitochondrial membrane potential to generate ATP. The resulting ATP depletion even potentiates the cytosolic  $\text{Ca}^{2+}$  increase due to the ATP-dependence of channels which are responsible for transporting  $\text{Ca}^{2+}$  back into the ER or outside of the cell. Constitutive  $\text{Ca}^{2+}$  elevation results in mitochondrial dysfunction and necrosis, as well as in premature zymogen activation. Premature zymogen activation due to disturbed  $\text{Ca}^{2+}$  signaling is also the mechanism that underlies the experimental mouse model, that was used for this work. Caerulein is an analogue of cholecystokinin. It triggers the increase of cytosolic  $\text{Ca}^{2+}$  and the release of active zymogens into the interstitial space, thereby inducing AP<sup>136</sup>.

### **2.1.2 THE ERBB FAMILY IN ACUTE PANCREATITIS**

The EGFR ligand EGF was early found to be implicated in AP. More than 20 years ago, the exogenic administration of human recombinant EGF in caerulein-inducible AP in rats did not alter gross or histologic morphology of the pancreas, but it ameliorated septic complications by protecting the intestinal mucosa from damage, thereby preventing rats from secondary infections in acute necrotizing pancreatitis<sup>137</sup>. Also in rats, exogenous EGF decreased the severity of caerulein-induced AP by possibly increasing the pancreatic blood flow and cell proliferation and by decreasing the activation of the immune response<sup>138</sup>. Another role was attributed to EGF only shortly after, when Dembinski *et al.* demonstrated accelerated recovery of pancreatic cells during AP regeneration, which they also associated with an improved pancreatic blood flow<sup>139</sup>. However, despite all of these promising characteristics of EGF, it was never tested in clinical trials to treat AP.

Also, for its designated receptor EGFR, similar findings were made a few years later. EGFR was associated with the protection against necrosis upon exogenous regenerating protein 4 (Reg4) administration in mice. Reg4 enhanced the expression of the anti-apoptotic proteins B-cell lymphoma 2 (Bcl-2) and B-cell lymphoma extra-large (Bcl-xL), which, in turn, stimulated EGFR-induced AKT signaling and which was inversely correlated with necrosis<sup>140</sup>. However, caerulein-induced AP in mice with EGFR-depleted acinar cells showed no signs of altered severity in AP, indicating that EGFR plays no overt role in AP<sup>141</sup>. A more recent study evaluated

data obtained from a gene expression database and found EGFR to be upregulated in AP samples of caerulein-treated mice. The consequences of increased EGFR levels were not evaluated<sup>142</sup>. These data indicate that EGFR does not play a role in the development of AP, but might be abundantly expressed as a reaction of AP development to exert a protecting role.

A study from a time, when the presence of ERBB4, the last member of the ERBB family, was not revealed, yet, found differential expression pattern of the remaining ERBB receptors in AP, compared to normal tissue, indicating a role for the ERBB system in this disease<sup>143</sup>.

AP is associated with fibrosis early in disease development<sup>144,145</sup>. The ERBB ligands TGFA and HBEGF were found to induce fibrosis, when overexpressed in the pancreas of mice<sup>146-148</sup>, while the overexpression of AREG did not<sup>149</sup>. Thus, the generation of fibrosis in the pancreas is ligand-specific and possibly, also receptor-specific, since HBEGF has affinities for EGFR and ERBB4. Indeed, for HBEGF, it was shown that it mediates its fibrosis-promoting effect through EGFR. However, pancreatic fibrosis of HBEGF transgenic mice was not completely abrogated in all mice (only in 38%) after crossing them into mice with an EGFR hypomorphic *Wa<sup>2</sup>* background. This suggests either remaining EGFR activity<sup>150</sup>, or the involvement of ERBB4 as the second binding partner of HBEGF.

The most striking finding about ERBB receptor family involvement was discovered by our group. We revealed that BTC transgenic mice were protected from AP in caerulein- and L-arginine-inducible pancreatitis models of AP. The overexpression of BTC led to a significant reduction of pancreatic weights, which was limited to the exocrine pancreas, possibly mediated by an enhanced cell-turnover in BTC transgenic mice. The crossing of BTC transgenic mice with mice expressing a kinase-dead EGFR did not rescue the pancreatic weight indicating no EGFR involvement in regard to the pancreas weight. Upon AP induction, BTC transgenic mice presented with significantly reduced serum lipase and amylase levels, decreased necrosis, edema and inflammation which was possibly due to increased SAPK activity, resulting in enhanced apoptosis and proliferation rates<sup>119</sup>. But not only prevented BTC from developing AP, it was also possible to treat mice suffering from AP with intraperitoneally administered BTC.

## **2.2 AIM OF THE STUDY**

AP is a common disease with rising incidences, which is frequently life-threatening to patients in the severe disease stage. Once overcome, AP frequently results in secondary diseases, e.g. insufficiency of the exocrine pancreas, chronic pancreatitis or *diabetes mellitus*. Thus, the quality of life often decreases drastically. The current treatment is only symptomatic and aims to decrease the pain, to save pancreatic tissue and prevent hypovolemia. However, these standard therapies still need optimization. Although clinical trials are performed testing therapeutics, e.g. targeting Ca<sup>2+</sup> trafficking, there is an urgent need to find better targets amenable to therapy, and also to find biomarkers to diagnose the disease in pre-clinical stages. There is increasing evidence that the ERBB system is involved in AP development and might carry out a protective role, but the mechanisms underlying this protection remain to be revealed. Since BTC, among all ERBB ligands, appears to have the most protective effect on the course of AP, we aimed to study the role of BTC in AP pathophysiology in more detail, including the identification of the ERBB receptors involved. This is particularly important for the development of therapeutic agents against AP and the reduction of possible side-effects.

## **2.3 STUDY: THE PROTECTIVE EFFECT OF BETACELLULIN AGAINST ACUTE PANCREATITIS IS ERBB4-DEPENDENT**

Kathrin Hedegger,<sup>1</sup> Franziska Stumpf,<sup>1</sup> Helmut Blum,<sup>3</sup> Alexander Graf,<sup>3</sup> Roland M. Schmid,<sup>2</sup> Marina Lesina,<sup>2</sup> Hana Algül,<sup>2</sup> Marlon R. Schneider,<sup>1</sup> and Maik Dahlhoff<sup>1\*</sup>

<sup>1</sup>Institute of Molecular Animal Breeding and Biotechnology, Gene Center of the LMU Munich, Germany

<sup>2</sup>Second Department of Internal Medicine, Klinikum rechts der Isar, Technical University of Munich, Germany

<sup>3</sup>Laboratory for Functional Genome Analysis (LAFUGA), Gene Center of the LMU Munich, Germany

*Addendum:* This manuscript has been accepted and published in 'Journal of Gastroenterology' in August, 2019.

### 2.3.1 ABSTRACT

#### Background

The EGFR ligand betacellulin (BTC) has been previously shown to protect mice against experimentally-induced acute pancreatitis (AP). BTC binds both autonomous ERBB receptors EGFR and ERBB4. In this study, we evaluated the mechanism underlying the protection from AP-associated inflammation in detail.

#### Methods

AP was induced with caerulein or L-arginine and investigated in a pancreas-specific ERBB4 knockout and in an EGFR knockdown mouse model (*Egfr<sup>Wa5/+</sup>*). Pancreatitis was evaluated by scoring inflammation, necrosis, and edema, while microarrays were performed to analyze alterations in the transcriptome between mice with AP and animals which were protected against AP. The intracellular domain (ICD) of ERBB4 was analyzed in different cell compartments.

#### Results

While the pancreas of BTC transgenic mice in the background of *Egfr<sup>Wa5/+</sup>* is still protected against AP, the BTC-mediated protection is no longer present in the absence of ERBB4. We further demonstrate that BTC activates the ICD of ERBB4, and increases the expression of the extracellular matrix (ECM) proteins periostin and matrix gla protein as well as the ECM modulator matrix metalloproteinases 2 and 3, but only in the presence of ERBB4. Notably, the increased expression of these proteins is not accompanied by increased ECM amount.

#### Conclusions

These findings suggest that BTC derivatives, as a drug, or the ERBB4 receptor, as a druggable target protein, could play an important role in modulating the course of AP and even prevent AP in humans.

### 2.3.2 INTRODUCTION

Acute pancreatitis (AP), a frequent inflammatory disease of the exocrine pancreas, is often caused by gallstone migration into the bile duct or alcohol abuse. Patients develop a severe, extremely painful inflammatory disease with multisystem organ failure<sup>151</sup>. During AP pancreatic acinar cells activate digestive enzymes like trypsinogen and chymotrypsinogen, resulting in autodigestion followed by interstitial edema, inflammation and acinar necrosis<sup>152</sup>. In spite of intense research, the etiology and the progress of this potentially lethal disease remain poorly understood.

Growth factors are important regulators of gene transcription, and transcriptome alterations are a powerful cell answer to environmental changes, challenges, or to diseases like inflammation or cancer. One of the most potent signaling systems in eukaryotic cells is the tyrosine kinase epidermal growth factor receptor (EGFR, ERBB1, HER1) and its family members ERBB2 (HER2, NEU), ERBB3 (HER3), and ERBB4 (HER4). All four receptors are expressed in the exocrine pancreas and play important roles in pancreatic homeostasis and during pancreatic tumorigenesis, as pancreatic ductal adenocarcinoma (PDAC)<sup>153,154</sup>. EGFR is a main receptor for initiating PDAC<sup>155,156</sup>, and several EGFR ligands have been implicated in neoplastic changes of the pancreas: overexpression of transforming growth factor alpha (TGFA)<sup>157</sup> in mice induces acinar-to-ductal metaplasia; amphiregulin (AREG)<sup>158</sup> overexpression increases proliferation of duct cells; and overexpression of heparin-binding epidermal growth factor-like growth factor (HBEGF) leads to proliferation of metaplastic duct epithelium and fibrosis<sup>159</sup>. Our previous studies revealed that mice overexpressing the EGFR and ERBB4 ligand betacellulin (BTC) are protected against caerulein- and L-arginine induced AP<sup>160</sup>. Although it is known that EGFR, ERBB2<sup>161</sup>, and ERBB3<sup>162</sup> are involved in PDAC or AP, potential roles of ERBB4 in the exocrine pancreas and its associated diseases remain unknown.

The autonomous ERBB4 receptor can be expressed in four different isoforms. Alternative splicing results in the JM-b isoform lacking the juxtamembrane cleavage site for regulated intramembrane proteolysis (RIP), which is present in the predominantly expressed JM-a isoform<sup>163</sup>. Additionally, exon skipping results in the deletion of the PI3K binding site (CYT-2), compared to the full length and functionally fully active cytoplasmic CYT-1 form<sup>164</sup>. Furthermore, ERBB4 is able to undergo gamma-secretase-dependent regulated intramembrane proteolysis (RIP), releasing its intracellular domain (ICD) to the cytosol, or to the nucleus<sup>165,166</sup>. The ICD is able to interact with other proteins and migrate into the nucleus and then act as a transcriptional co-factor/regulator<sup>167,168</sup>. These different possibilities result in

an ambiguous function of ERBB4, depending on isoform expression and/or intramembrane proteolysis.

In our current study, we investigated in detail how BTC protects the pancreas against inflammation and which receptor mediates this effect. Therefore, we deleted ERBB4 specifically in the pancreas of BTC transgenic mice (*Btc*) or crossed *Btc* mice with a mouse line carrying a dominant negative EGFR (*Egfr<sup>Wa5/+</sup>*).

### 2.3.3 METHODS

#### 2.3.3.1 ANIMALS

Transgenic mouse lines overexpressing BTC ubiquitously under the control of the chicken-beta-actin gene promoter have been described previously<sup>169</sup>. *Egfr<sup>Wa5/+</sup>* (*Wa5*) mice expressing an antimorphic *Egfr* allele<sup>170</sup> were donated by the Medical Research Council (Oxfordshire, UK) via Dr. David Threadgill (University of North Carolina, NC, USA). *B6;129-ErbB4<sup>tm1Fej/Mmucd</sup>* (*ErbB4<sup>fl/fl</sup>*) mice<sup>171</sup> were purchased from the Jackson Laboratory (Bar Harbor, ME, US), and *Ptf1a<sup>tm1(cre)Hnak</sup>* transgenic mice expressing cre recombinase under the control of the pancreas specific transcription factor 1 alpha (*Ptf1a<sup>Cre/+</sup>*)<sup>172</sup> have been described previously. We generated *ErbB4<sup>fl/fl</sup>; Ptf1a<sup>Cre/+</sup>* mice to delete the *ErbB4* gene pancreas-specific by using the Cre-loxP-system. All mice were maintained in the C57BL/6N background and housed under specific pathogen-free conditions in the closed barrier facility of the Gene Center Munich at 23°C, 50% humidity and with a 12-h light/dark cycle (lights on at 7 AM), and had free access to a standard rodent diet (V1534, Ssniff, Soest, Germany) and water. All animal experiments were approved by the author's institutional committee on animal care and carried out in accordance with the German Animal Protection Law with permission from the responsible veterinary authority.

#### 2.3.3.2 CAERULEIN-INDUCED PANCREATITIS IN TRANSGENIC MICE

Pancreatitis experiments were performed as previously described<sup>160</sup>. Briefly, after fasting for 18 h, all animals received hourly intraperitoneal applications (*i.p.*) of 50 µg/kg body weight caerulein (Merck, Darmstadt, Germany) in saline. One experimental group of mice was killed 3 h after the first injection. A second group received eight consecutive caerulein injections and animals were killed 24 h after the first application. Blood samples were centrifuged at 4°C at 1000xg, and serum was stored at -80°C for further studies. The pancreas was removed and samples were either frozen on dry ice and stored at -80°C for expression analysis or fixed in 4% PFA for histological studies. One pancreas sample was immediately homogenized in RLT buffer (Qiagen, Hilden, Germany) buffer supplemented with 1% beta-mercaptoethanol and snap frozen in liquid nitrogen for RNA analysis.

### **2.3.3.3 L-ARGININE INDUCED PANCREATITIS**

The L-arginine model of pancreatitis in non-fasted mice was induced by *i.p.* application of 4 g/kg L-arginine as described previously<sup>160</sup>. In brief, a sterile solution of L-arginine hydrochloride (8%) (Merck) was prepared in normal saline and the pH was adjusted to 7.0. Mice received two hourly injections of L-arginine (4 g/kg), while controls were administered saline. 24, 48, 72 hours after the first injection mice were sacrificed. Tissue and blood samples were removed and processed as described above.

### **2.3.3.4 PANCREAS PREPARATION AND IMMUNOHISTOCHEMISTRY**

Immunohistochemistry was employed for determining apoptosis, proliferation and the ERBB4 receptor in formalin-fixed, paraffin-embedded pancreatic tissue. Anesthetized mice were killed by exsanguination and blood was collected. The pancreas was removed immediately, carefully trimmed free of adjacent tissues, weighed to the nearest mg, fixed in 4% paraformaldehyde (in phosphate-buffered saline, PBS, pH 7.4), and embedded in paraffin. Antibodies and dilutions are listed in Suppl. Table S 2.1. For the immunostaining of ERBB4 and Ki67 the slides were sub-boiled in a water bath for 20 min at 97°C in 10 mM sodium citrate buffer pH 6.0 and for cl. Caspase 3 the slides were boiled in a pressure cooker for 30 min. The primary antibody was incubated over night at 4°C. After washing the slides three times in PBS the sections were incubated with an appropriate secondary antibody for one hour at room temperature. Diaminobenzidine (Merck) was used as the chromogen in all immunohistochemical experiments and the immunolabeled sections were counterstained with hematoxylin.

### **2.3.3.5 DETERMINATION OF PROLIFERATION AND APOPTOSIS RATES**

All immunostained cell nuclei present in the pancreas sections from one individual were counted. The numerical area density of immunostained exocrine pancreas cell nuclei was obtained by dividing the total number of immunostained cell nuclei by the cross-sectional area of the exocrine pancreas. The proportion of immunostained exocrine cell nuclei was obtained by dividing the numerical area density of immunostained cell nuclei by the numerical area density of exocrine cell nuclei. For determination of the numerical area density of exocrine cell nuclei, every 25<sup>th</sup> visual field covering exocrine pancreas tissue was selected for counting of cell nuclei using an unbiased counting frame<sup>173</sup>. Cell proliferation and apoptosis indices were defined as the number of immunolabeled cell nuclei divided by the number of cell nuclei counted, and expressed as the number of immunolabeled cell nuclei per 10<sup>5</sup> cell nuclei.

### **2.3.3.6 DETERMINATION OF THE NECROTIC AREA IN PERCENT**

Every 25<sup>th</sup> visual field covering exocrine pancreas tissue was selected for determining the total area and the necrotic area using an unbiased counting frame<sup>173</sup>.

### **2.3.3.7 SERUM AMYLASE AND LIPASE CONCENTRATIONS**

Serum was diluted 1:10 in sterile water to a volume of 100µl. Amylase and lipase were measured by Modular-P + ISE (Roche, Mannheim, Germany) at the Institut für Klinische Chemie, Klinikum rechts der Isar, Munich, Germany.

### **2.3.3.8 HISTOPATHOLOGICAL SCORE**

Coded, H&E-stained histological sections were graded according to the severity of pancreatitis using a scoring criteria described previously<sup>173</sup>. The connective tissue score was performed on Masson's Trichrome stained paraffin sections of paraformaldehyde-fixed (4%) pancreas using a scoring criteria described previously<sup>173</sup>. Lung histopathology score were performed on H&E stainings as described previously<sup>174</sup>.

### **2.3.3.9 WESTERN BLOT ANALYSIS**

Protein was prepared from mouse pancreas by homogenization in extraction buffer as described previously<sup>175</sup>. Protein samples with equal concentrations were electrophoresed on 12% polyacrylamide-sodium dodecyl sulfate gels and then blotted to PVDF-membranes (GE Healthcare, Munich, Germany). Incubation with primary antibodies was carried out overnight at 4°C. Antibodies and dilutions (either in 5% dry milk or in 5% BSA) are listed in Suppl. Table S 2.1. Afterwards the membranes were incubated with an appropriate horseradish peroxidase-conjugated secondary antibody. Immunoreactive bands were visualized by chemiluminescence with ECL kit (GE Healthcare).

### **2.3.3.10 FRACTIONATION OF PANCREATIC CELLS**

To fractionate pancreatic cells into nucleus, membrane, and cytosol, the QIAGEN Qproteome® Cell Compartment Kit was used according to the manufacturer's instructions. To verify the purity of each fraction, a Western blot experiment was performed. ERBB2 was chosen as a specific membrane protein marker, GAPDH as a marker of the cytosol fraction and histone H3 as a specific protein marker for the nucleus fraction. Western blot experiments were performed as described previously.

### **2.3.3.11 REAL-TIME-PCR**

RNA was extracted from shock-frozen pancreatic tissues with RNeasy kit (Qiagen, Hilden, Germany) and cDNA was synthesized with RevertAid reverse transcriptase (Thermo Scientific, Schwerte, Germany) according to the manufacturer's instructions. For qualitative mRNA expression of *ErbB4*, reverse transcription-PCR (RT-PCR) was performed by using reagents from Qiagen. The final reaction volume was 20 µl, and cycle conditions were 94°C for 5 min followed by 35 cycles of 94°C for 1 min, 60°C for 1 min, and 72°C for 1 min. The primers employed are listed in Suppl. Table S 2.2.

Quantitative mRNA expression analysis was performed by real-time quantitative RT-PCR (qRT-PCR) using the LightCycler-480-system and the LightCycler-480-Probes-Master (Roche, Mannheim, Germany) as described previously<sup>176</sup>. Primers (Thermo Fisher Scientific) and probes (Roche) for the evaluated transcripts are listed in Suppl. Table S 2.2.

#### **2.3.3.12 STATISTICS**

Results are expressed as means+SEM and the significance of differences between two groups was tested using the two-tailed unpaired Student's *t*-test and, in the case of more than two groups by analysis of variance (ANOVA) and Tukey's multiple comparison test. The qRT-PCR values were related to the mean of the control group, data were presented as box plots with medians and analyzed with two-tailed Mann-Whitney *U*-test. All data were analyzed with GraphPad Prism (GraphPad Prism version 5.0 for Windows, GraphPad Software, San Diego, CA, USA). *P*-values below 0.05 were considered statistically significant.

## 2.3.4 RESULTS

### 2.3.4.1 PROTECTION AGAINST AP IS NOT MEDIATED BY EGFR

First, BTC expression in the exocrine pancreas was evaluated. BTC was detected by immunofluorescence and Western blot in the exocrine pancreas of control mice, with increased levels in *Btc* transgenic animals (Suppl. Fig. S 2.1 A,D,F). All four ERBB receptors were expressed and phosphorylated during AP with the exception that ERBB3 was not phosphorylated (Suppl. Fig. S 2.1 D). BTC, as a ligand of EGFR and ERBB4, showed significantly increased ERBB phosphorylation levels in *Btc* mice with 3h-AP compared with control animals (Suppl. Fig. S 2.1 D,F). To determine whether the protective effect of BTC is EGFR-dependent, we crossed *Btc* transgenic mice in the *Wa5* mice background. *Wa5* mice have an antimorphic *Egfr* allele with a dead kinase activity, and they represent a well-accepted EGFR knockdown mouse model. With this mouse model we performed a caerulein-induced AP and sacrificed the animals 24 hours after caerulein injection. The histological severity score demonstrated significantly reduced inflammation, necrosis, and edema in *Btc* mice, and this effect was still present in *Wa5+Btc* double mutant mice compared to *Wa5* and control mice (Figure 2.1 A-D). Additionally, *Wa5* mice and control littermates showed significantly increased serum amylase and lipase levels compared with *Btc* mice and *Wa5+Btc* animals (Figure 2.1 E,F). A significantly higher apoptosis-rate was identified in the exocrine pancreas of *Btc* mice and double mutants compared to control littermates and *Wa5* mice (Figure 2.1 G).

### 2.3.4.2 ERBB4 IS DISPENSABLE FOR PANCREAS DEVELOPMENT AND HOMEOSTASIS

To analyze its potential function, we deleted ERBB4 in the pancreas using a genetic approach. For this purpose, we crossed animals carrying a floxed *ErbB4* allele with transgenic mice expressing cre recombinase under the control of the pancreas-specific transcription factor 1 alpha (*Ptf1a<sup>Cre/+</sup>*) promoter. Recombination of the *ErbB4* allele and the resulting pancreas-specific loss of ERBB4, with unchanged receptor levels in the remaining organs were confirmed by RT-PCR (Suppl. Fig. S 2.1 E) and immunohistochemistry (Suppl. Fig. S 2.1 B), respectively. *ErbB4<sup>fl/fl</sup>; Ptf1a<sup>Cre/+</sup>* mice were viable and showed no macroscopic phenotype. H&E-stained sections of *ErbB4<sup>fl/fl</sup>; Ptf1a<sup>Cre/+</sup>* exocrine pancreata (Suppl. Fig. S 2.1 C) showed unchanged histological structure and normal islets of Langerhans (data not shown). Body weight of male and female mice evaluated up to 12 weeks was unchanged in *ErbB4<sup>fl/fl</sup>; Ptf1a<sup>Cre/+</sup>* mice compared with control littermates (data not shown). Absolute and relative pancreas weights of female (Suppl. Fig. S 2.1 G,H) and male (Suppl. Fig. S 2.1 I,J) mice were not altered.

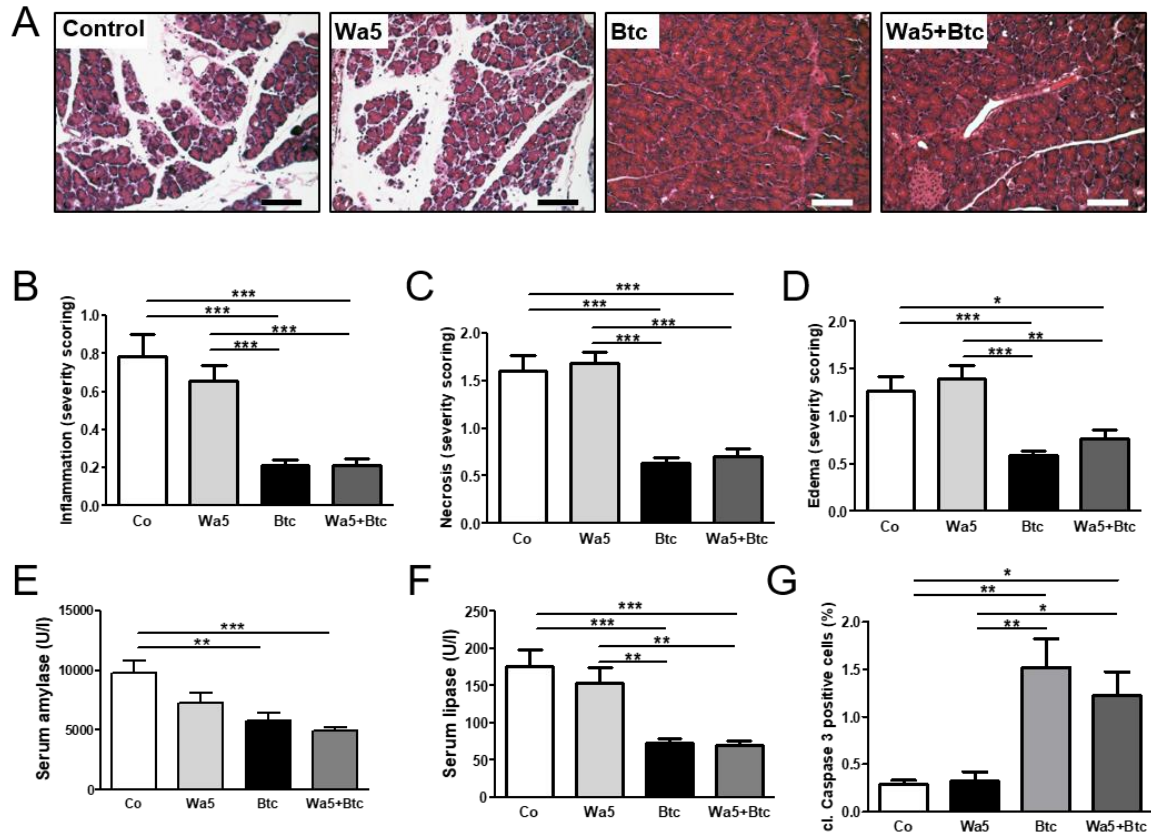


**Figure 2.1: Investigation of Wa5+BTC mice during caerulein-induced AP**

A Representative H&E staining of 24-h-lasting AP in 12 weeks old male mice. BTC and Wa5+BTC mice show less severe B inflammation, C necrosis, and D edema histological scores 24 hours after caerulein injection compared to control and Wa5 mice. During 24 h caerulein-AP E serum amylase and F lipase levels were significantly reduced in BTC and Wa5+BTC mice compared to control and Wa5 animals. G Quantitative evaluation revealed a significantly higher number of cleaved caspase 3-positive cells in the pancreas of BTC and Wa5+BTC animals compared to control and Wa5 mice. Controls n=7, Wa5 n=7, Btc n=8, and Wa5+BTC n=8. Scale bars in a represent 200  $\mu$ m. Data in B-G are presented as mean+SEM (standard error of the mean), and were analyzed by ANOVA followed by Tukey's post hoc test. \* $P$ <0.05; \*\* $P$ <0.01, \*\*\* $P$ <0.001.

### 2.3.4.3 PROTECTION AGAINST AP IS ERBB4-DEPENDENT

As BTC is also able to bind and activate ERBB4, we next performed a caerulein-induced 24h AP experiment in Btc mice with a pancreas-specific deletion of ERBB4 (*ErbB4<sup>fl/fl</sup>;Ptf1a<sup>Cre/+</sup>;Btc<sup>tg/+</sup>*). A histological score revealed no difference in the severity of pancreatitis between *ErbB4<sup>fl/fl</sup>;Ptf1a<sup>Cre/+</sup>* mice, *ErbB4<sup>fl/fl</sup>;Ptf1a<sup>Cre/+</sup>;Btc<sup>tg/+</sup>* mice, and control littermates regarding necrosis, inflammation, and edema; only Btc animals showed significantly reduced scoring values (Figure 2.2 A-D). Serum amylase and lipase levels were also significantly reduced only in Btc mice compared with *ErbB4<sup>fl/fl</sup>;Ptf1a<sup>Cre/+</sup>;Btc<sup>tg/+</sup>* mice, control mice, and *ErbB4<sup>fl/fl</sup>;Ptf1a<sup>Cre/+</sup>* mice (Figure 2.2 E,F). Because apoptosis plays a crucial role in pancreatitis, we investigated apoptotic cells in *ErbB4<sup>fl/fl</sup>;Ptf1a<sup>Cre/+</sup>;Btc<sup>tg/+</sup>* animals 3h after caerulein-induced AP. While cleaved caspase-3-positive cells were only sporadically visible in the pancreas of *ErbB4<sup>fl/fl</sup>;Ptf1a<sup>Cre/+</sup>;Btc<sup>tg/+</sup>* mice and the other control groups, a large number of apoptotic cells were detectable in the pancreas of Btc animals (data not shown). Quantitative evaluation confirmed a significantly higher number of apoptotic cells in the exocrine pancreas

of Btc animals as compared to control groups (Figure 2.2 G). Western blots for stress activated protein kinase (SAPK) (Figure 2.2 H) revealed that SAPK, a pro-apoptotic kinase, was significantly stronger phosphorylated in Btc mice compared with the control groups (Figure 2.2 I).

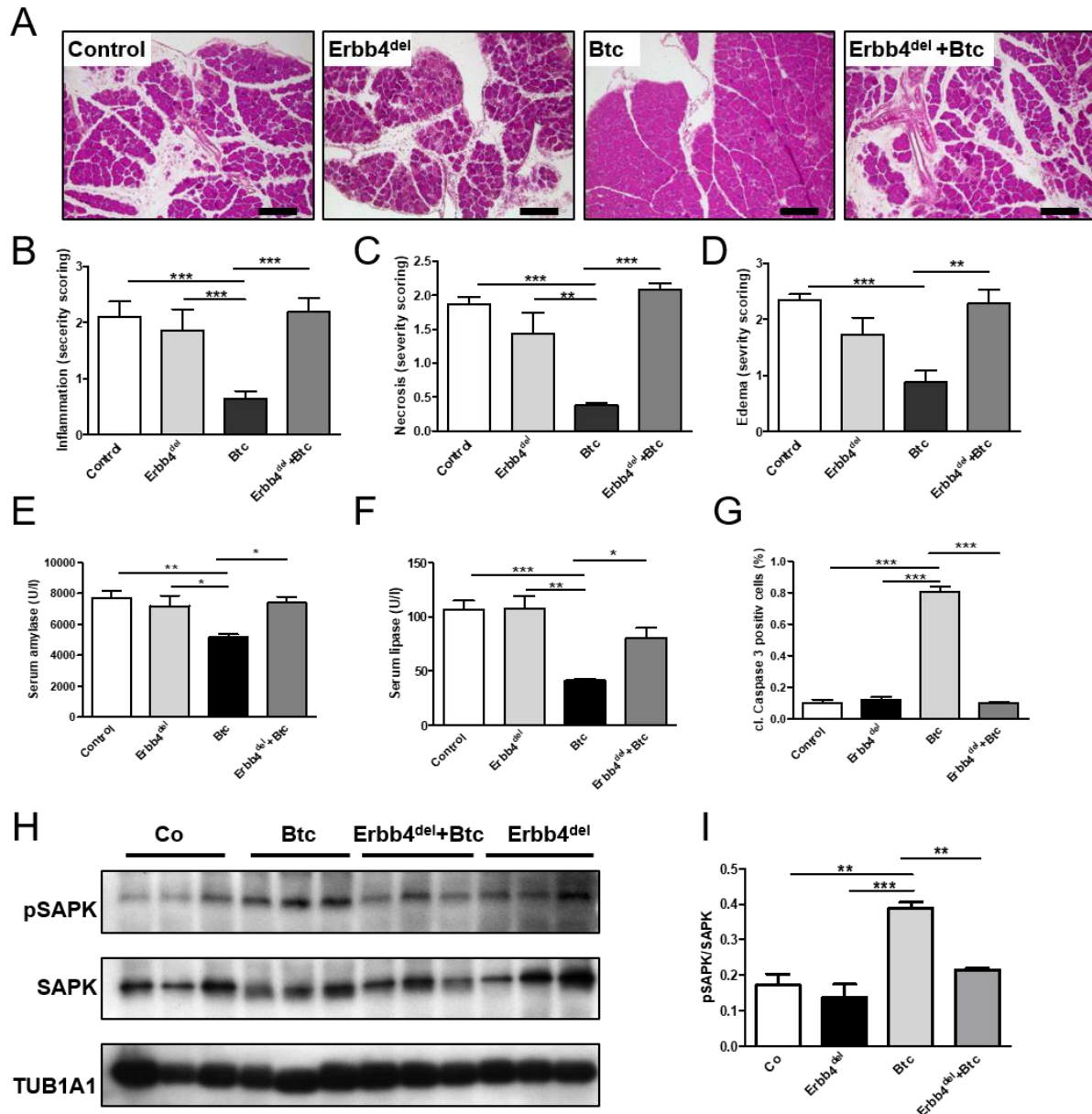


**Figure 2.2: Investigation of Erbb4<sup>del</sup>+Btc mice during caerulein induced AP**

**A** Representative H&E staining of 24-h-lasting AP in 12 weeks old male mice. Scale bars represent 200  $\mu$ m. Only Btc mice show less severe **B** inflammation, **C** necrosis, and **D** edema in histological scores 24 hours after caerulein injection compared to control, Erbb4<sup>del</sup>, and Erbb4<sup>del</sup>+Btc mice. During 24 h caerulein-AP **E** serum amylase and **F** lipase levels were only significantly reduced in Btc mice compared to control, Erbb4<sup>del</sup>, and Erbb4<sup>del</sup>+Btc animals. **G** Quantitative evaluation revealed a significantly higher number of cleaved caspase-3-positive cells in the pancreas of Btc animals compared to control, Erbb4<sup>del</sup>, and Erbb4<sup>del</sup>+Btc mice. **H** Western blot analysis of phospho-SAPK and SAPK 3 hours after an induced caerulein-AP. TUBA1A was used as a loading control. **I** Densitometric analysis revealed a significantly increased level of phospho-SAPK in BTC mice only. Data in **B-G**; **I** are presented as mean+SEM, and were analyzed by ANOVA followed by Tukey's post hoc test. \*P<0.05; \*\*P<0.01, \*\*\*P<0.001.

To confirm that our results are not associated with a caerulein-specific mechanism we employed L-arginine as a second AP-model. Consistent with our data so far, *ErbB4<sup>fl/fl</sup>;Ptf1a<sup>Cre/+</sup>;Btc<sup>tg/+</sup>* mice showed no differences in the histological scoring of the necrotic area, edema, and infiltration of the pancreas compared with *ErbB4<sup>fl/fl</sup>;Ptf1a<sup>Cre/+</sup>* and control mice (Figure 2.3 A-D). Again, only in pancreata of *Btc* mice, we observed less necrosis, edema, and infiltration compared to the other three groups (Figure 2.3 A-D). The increase in serum amylase levels in *Btc* mice at 24 h, 48 h, and 72 h was significantly less pronounced compared to the other three groups (Figure 2.3 E). In addition, we detected only minor pancreatitis-associated lung inflammations in *Btc* mice compared to the other three groups, which all developed lung inflammation 72h after L-arginine pancreatitis (Figure 2.3 F,G). Although ERBB4, per se, does not play a role in AP, we could demonstrate with two independent models of AP induction that the BTC mediated protection against AP is ERBB4-dependent.

#### **2.3.4.4 THE ERBB RECEPTORS AND BTC ARE EXPRESSED IN NORMAL PANCREAS (NP) AND IN CHRONIC PANCREATITIS (CP)**

To evaluate the expression of the ERBB receptors and BTC in the pancreas and to investigate whether the receptors and BTC are expressed during pancreatitis, we performed immunohistochemistry stainings (Suppl. Fig. S 2.2). Due to the inaccessibility of human AP samples and due to the relationship of the two diseases, we performed our investigations in CP. All receptors and BTC were expressed in NP and CP. EGFR and ERBB4 were predominantly expressed in acinar cells, but not in the ducts of NP. ERBB2 and ERBB3 were expressed in both, acinar and duct cells of NP. BTC staining was most prominent in the islets of Langerhans, but also detected in the acinar and duct cells. In CP, EGFR was expressed in all acinar cells and reactive ductal structures, but not in normal duct cells. ERBB2 was detected in acinar cells and strongly in normal and reactive ducts. ERBB3 distribution was similar to NP. ERBB4 was irregularly distributed in acinar cells in NP but, in CP very consistently in ductal structures. BTC distribution in CP was similar to NP.

#### **2.3.4.5 MICROARRAYS REVEALED SEVERAL UPREGULATED GENES ENCODING ECM PROTEINS IN THE PANCREAS OF BTC MICE DURING AP**

To identify regulated genes that could mechanistically explain the protection of BTC against AP we investigated the pancreatic transcriptome of *Btc* mice and control littermates using microarrays. 1009 genes were up-regulated in control animals with AP and 649 genes were up-regulated in *Btc* mice with AP, and 492 of these up-regulated genes are matching in both AP-groups. Both groups with AP share 728 down-regulated genes, and 350 genes were exclusively down-regulated in *Btc* animals with AP. The full microarray data set was uploaded at NCBI Gene Expression Omnibus and has the data accession number GSE121038. Several

of the most abundantly up-regulated genes during AP in Btc mice (the top 20 regulated genes are shown in Suppl. Fig. S 2.3 A) encode proteins of the ECM or for enzymes organizing the

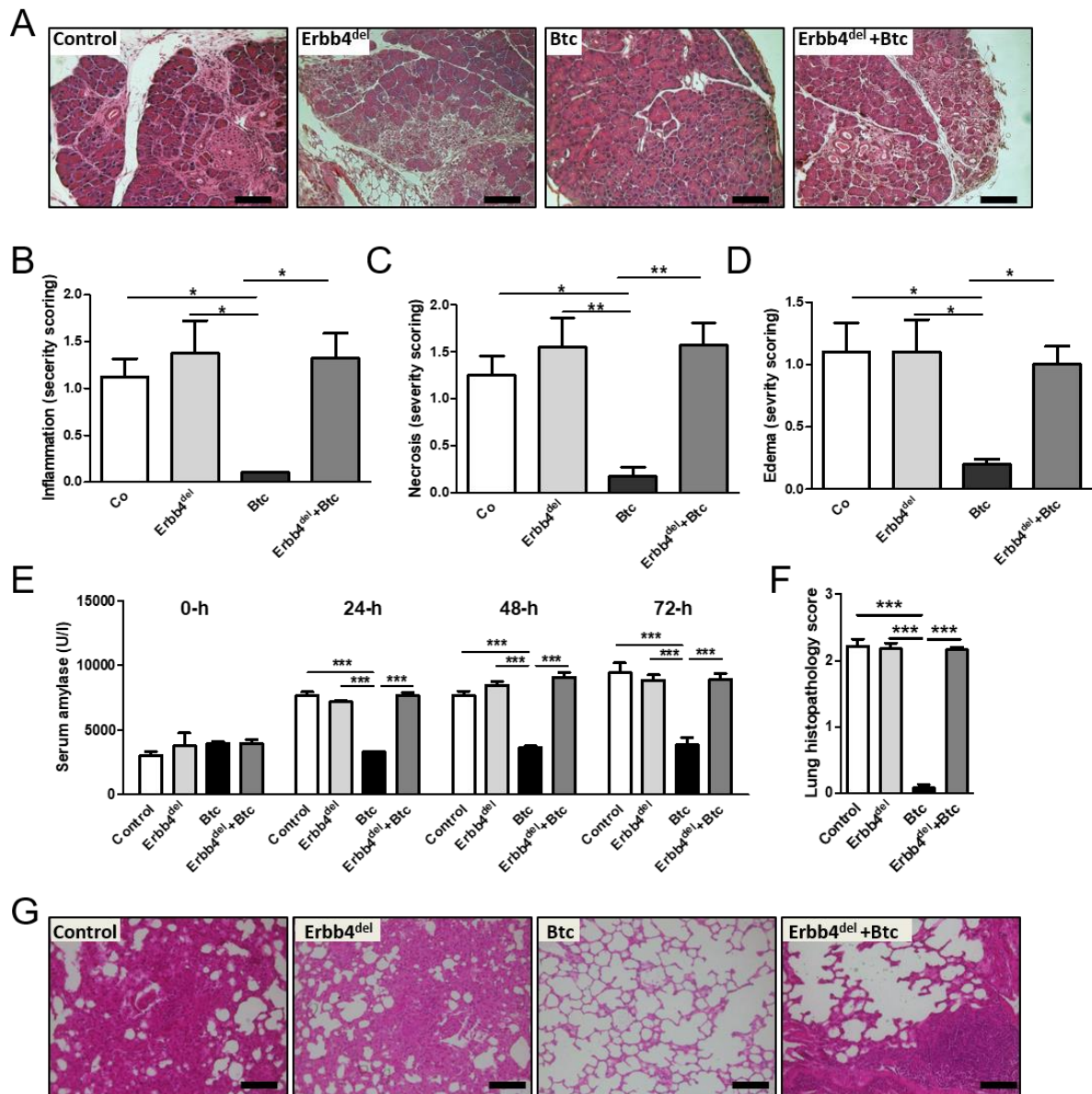


**Figure 2.3: The protective effect of BTC is also lost in Erbb4<sup>del</sup>+Btc mice during L-arginine pancreatitis**  
**A** H&E-stained histological sections revealed less pronounced tissue necrosis, edema, and infiltration in the pancreas of Btc mice as compared Erbb4<sup>del</sup>+Btc, Erbb4<sup>del</sup>, and control animals. Scale bars represent 200  $\mu$ m. Histological scoring revealed that the increase severity score of **B** inflammatory cell infiltration, **C** acinar necrosis, and **D** edema was significantly less prominent in the pancreas of Btc mice as compared to the three other groups. **E** The increase in serum amylase levels in Btc mice at 24 h, 48 h, and 72 h was significantly less pronounced as compared to Erbb4<sup>del</sup>+Btc, Erbb4<sup>del</sup> and control mice. Data in **A-D** are at 72 h after L-arginine administration. **F** Lung histology score after 72h L-arginine pancreatitis. **G** H&E stainings revealed no lung inflammation of Btc mice as compared Erbb4<sup>del</sup>+Btc, Erbb4<sup>del</sup>, and control animals. Scale bars represent 100  $\mu$ m. Data (**B-F**) are presented as mean+SEM, and were analyzed by ANOVA followed by Tukey's post hoc test. \* $P$ <0.05; \*\* $P$ <0.01, \*\*\* $P$ <0.001.

ECM. The mRNA expression profiles were confirmed for 15 of the most interesting genes by quantitative RT-PCR in animals after 3h-AP (Suppl. Fig. S 2.3 B).

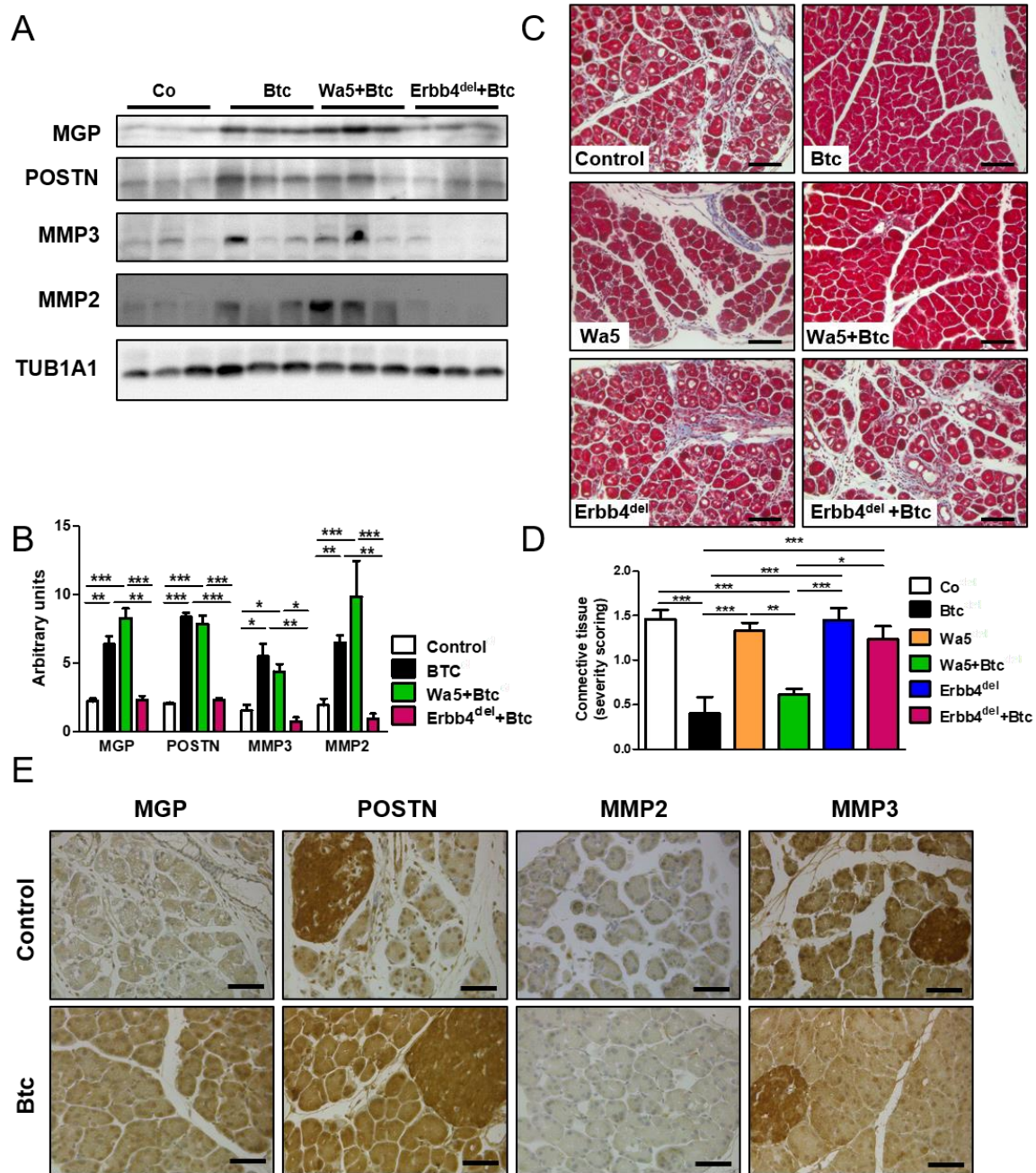


**Figure 2.4: Analysis of ECM**

**A** Western blot revealed increased levels of MGP, POSTIN, MMP2, and MMP3 in Btc and Btc+Wa5 mice, compared to control and Erbb4<sup>del</sup>+Btc mice with 24h-AP. TUB1A1 was used as a loading control. **B** Densitometric analysis of Western Blots revealed significantly increased levels of MGP, POSTN, MMP3, and MMP2 in Btc and Wa5+Btc mice. **C** Representative pictures of Masson's-Trichrome-Stain stainings. Scale bars represent 100µm. **D** Histological score demonstrates significantly reduced levels of connective tissue in Btc and Btc+Wa5 mice, compared to control, Wa5, Erbb4<sup>del</sup>, and Erbb4<sup>del</sup>+Btc mice with 24h AP (n=6/group). **E** Immunohistochemistry stainings of MGP, POSTN, MMP3, and MMP2 in Btc and control mice with 24h AP. Scale bars represent 50µm. Data (**B,D**) are presented as means+SEM, and were analyzed by ANOVA followed by Tukey's post hoc test. \*P<0.05; \*\*P<0.01, \*\*\*P<0.001.

#### 2.3.4.6 BTC INCREASES ECM REMODELING PROTEINS IN AN ERBB4-DEPENDENT MANNER

Next, we investigated whether changes in the most interesting transcripts up-regulated in Btc transgenic animals with and without AP are present at the protein level. Since we know that ERBB4 mediates the protective effect of BTC in AP, we analyzed *Erbb4*<sup>fl/fl</sup>; *Ptf1a*<sup>Cre/+</sup>; *Btc*<sup>tg/+</sup> mice

in more detail. Four of the up-regulated transcripts (*Mgp*, *Postn*, *Mmp2*, *Mmp3*) were validated to be significantly increased at protein level in Btc mice and Wa5+Btc animals with 3h-AP, but not in control animals and *ErbB4<sup>fl/fl</sup>;Ptf1a<sup>Cre/+</sup>;Btc<sup>tg/+</sup>* mice (Figure 2.4 A,B). The fact that these proteins are increased only in mice without AP-phenotype (Btc and Wa5+Btc) and not in *ErbB4<sup>fl/fl</sup>;Ptf1a<sup>Cre/+</sup>;Btc<sup>tg/+</sup>* mice, indicates that these proteins could be part of the BTC-induced protection mechanism.

An increased amount of connective tissue and ECM is often associated with a higher severity of AP. To determine the amount of connective tissue, sections from animals with a 24-h-caerulein-induced AP were stained by Masson's-Trichrome-Stain (Figure 2.4 C). A histological score revealed that the amount of stained connective tissue was clearly lower in Btc and Wa5+Btc mice compared to controls (*Egfr<sup>Wa5/+</sup>*, *ErbB4<sup>fl/fl</sup>;Ptf1a<sup>Cre/+</sup>*, and *ErbB4<sup>fl/fl</sup>;Ptf1a<sup>Cre/+</sup>;Btc<sup>tg/+</sup>* mice) with AP (Figure 2.4 D). Immunohistochemistry stainings revealed that Btc mice express much more MGP and POSTN in their acinar cells compared to control animals during AP (Figure 2.4 E). MMP2 and MMP3 are also expressed in the acinar cells, but IHC showed no obvious differences between both groups. POSTN and MMP3 are highly expressed in the islets of Langerhans. These results show that Btc mice have less ECM and increased amounts of ECM modifier as MMP2, MMP3, POSTIN, and MGP, which could play an important role in the AP protection mechanism of BTC.

#### **2.3.4.7 BTC INCREASES INTRAMEMBRANE PROTEOLYSIS OF ERBB4**

To assess BTC-induced ERBB4 activity in the exocrine pancreas and to investigate whether the receptor plays a role in the progression and severity of pancreatitis, we investigated ERBB4 phosphorylation. Increased ERBB4 phosphorylation was detected in the pancreas of Btc transgenic mice, while the AP status did not seem to influence phosphorylation (Figure 2.5 A). It is known that full-length ERBB4 and also the ICD of ERBB4 can migrate into the nucleus, where both proteins are able to act as transcriptional regulators. RT-PCR analysis revealed that the cleavable JM-a form and both CYT variants (Figure 2.5 B) are expressed in the pancreas. In a next step, we performed a cell fractionation of pancreas of AP-induced Btc and control mice. The fraction purity was analyzed by reference proteins: H3F3A (nucleus), GAPDH (cytosol), and ERBB2 (membrane) (Figure 2.5 E). Western blot analysis of ERBB4 and densitometric evaluations revealed significantly increased ERBB4 in the nucleus fraction of Btc mice compared to controls, and we also found enriched levels of ERBB4-ICD in the nucleus and cytosol in Btc animals with AP (Figure 2.5 C,D).

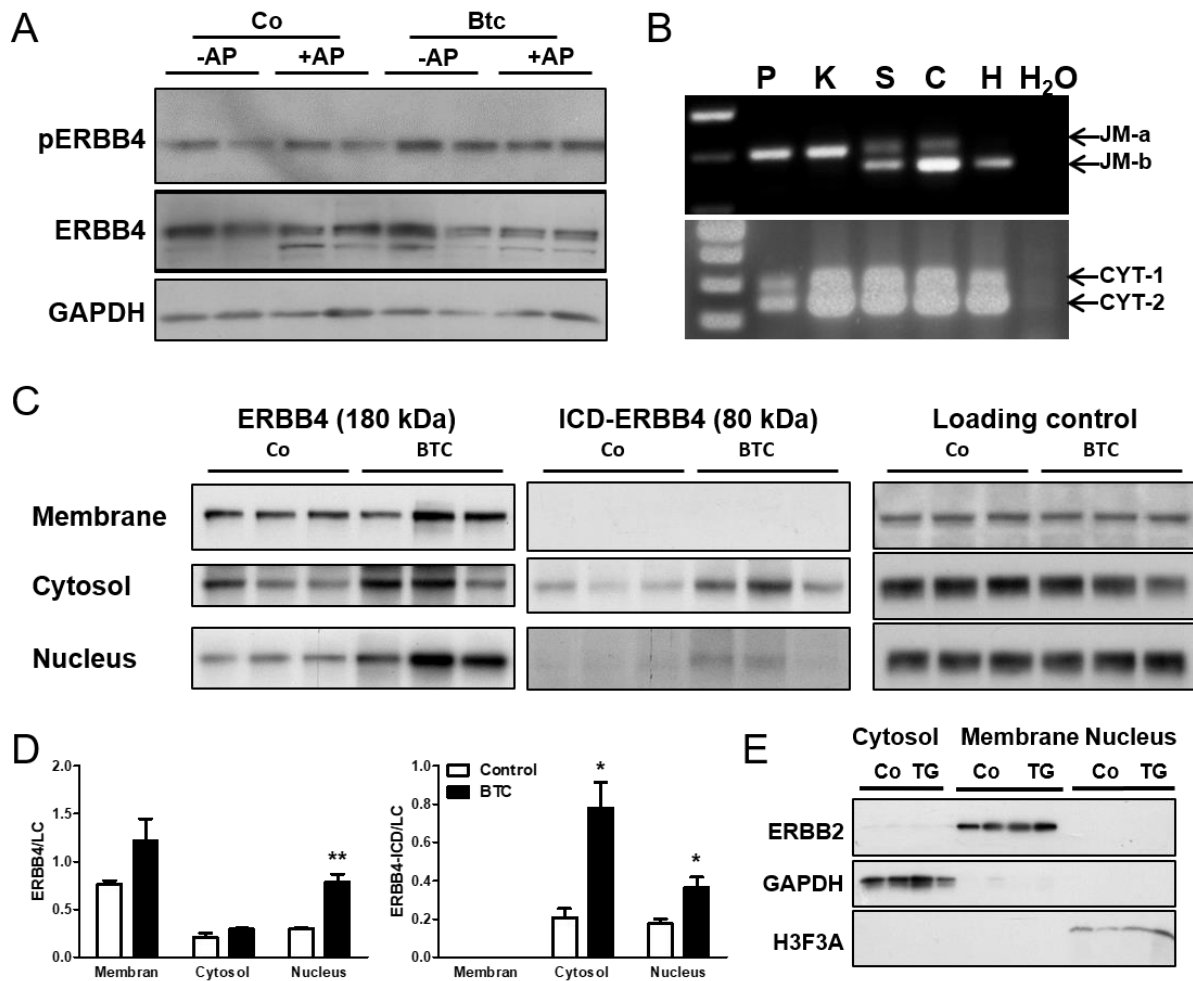


**Figure 2.5: Btc transgenic animals revealed increased levels of the ERBB4-ICD**

**A** Western blot analysis of phospho-ERBB4 and total ERBB4 in the pancreas of control and Btc mice with and without AP. GAPDH was used as a loading control. **B** RT-PCR showed that the JM-a isoform and both CYT isoforms of ERBB4 are expressed in the murine pancreas. P: Pancreas, K: kidney, S: spinal cord, C: cerebellum, H: heart. **C** ERBB4 and the ICD of ERBB4 were detected by Western blot in all three fractions of the pancreas after a 3 h caerulein-induced pancreatitis in BTC and control mice. ERBB2 (membrane), GAPDH (cytosol), and H3F3A (nuclei) were chosen as reference proteins. **D** Densitometric analysis revealed significantly more ERBB4 in the nuclei of Btc mice compared with control animals, and significantly increased levels of the ICD in the cytosol and nuclei of BTC animals. \* $P < 0.05$ ; \*\*  $P < 0.01$ . **E** Western blot analysis confirmed the purity of the fractionated proteins. ERBB2 is mainly expressed in the membrane-fraction, GAPDH only in the cytosol-fraction, and H3F3A exclusively in the nuclei-fraction.

### 2.3.5 DISCUSSION

In a previous study, we showed that transgenic mice overexpressing the EGFR ligand BTC consistently failed to develop caerulein-induced and L-arginine-induced AP<sup>160</sup>. Before BTC can be considered as a therapeutic agent against AP, the mechanism behind its protective effects needs to be clarified. With this in mind we deleted both ERBB receptors that can be directly activated by BTC (EGFR and ERBB4) pancreas-specifically. Interestingly, while EGFR is dispensable for the development and homeostasis of the exocrine pancreas, it is an important proto-oncoprotein for tumor initiation<sup>155,156</sup>. Our data clearly indicate that EGFR does not mediate the protective effect against AP, as this effect is fully maintained in BTC;*Egfr*<sup>+/*Wa5*</sup> mice. The fact that EGFR seems to be dispensable for the homeostasis of the exocrine pancreas indicates that EGFR is not the preferred ERBB receptor of BTC in this tissue.

In light of these findings, we focused our investigations on the second autonomous ERBB receptor and binding partner of BTC, ERBB4. We used a pancreas-specific ERBB4 knockout model<sup>172</sup> for further investigations of BTC mediated effects in the pancreas. Btc transgenic mice lost their protection against AP in the ERBB4 receptor knockout background, strongly indicating that the protective effect is mediated by ERBB4. We revealed previously, that the protective effect of BTC was associated with increased apoptosis and SAPK signaling<sup>160</sup>. In this work, we verified that this effect was also mediated by the ERBB4 receptor, since cleaved Caspase-3 levels were decreased and SAPK was less activated than in BTC mice. This indicates a role for ERBB4 as a driver of apoptosis. Previous studies in human breast cancer have also shown a significance of ERBB4 mediated SAPK activation, resulting in the delay of mitotic progression<sup>177</sup>. Therefore, the activation of SAPK via ERBB4 signaling could represent an interesting druggable target during AP.

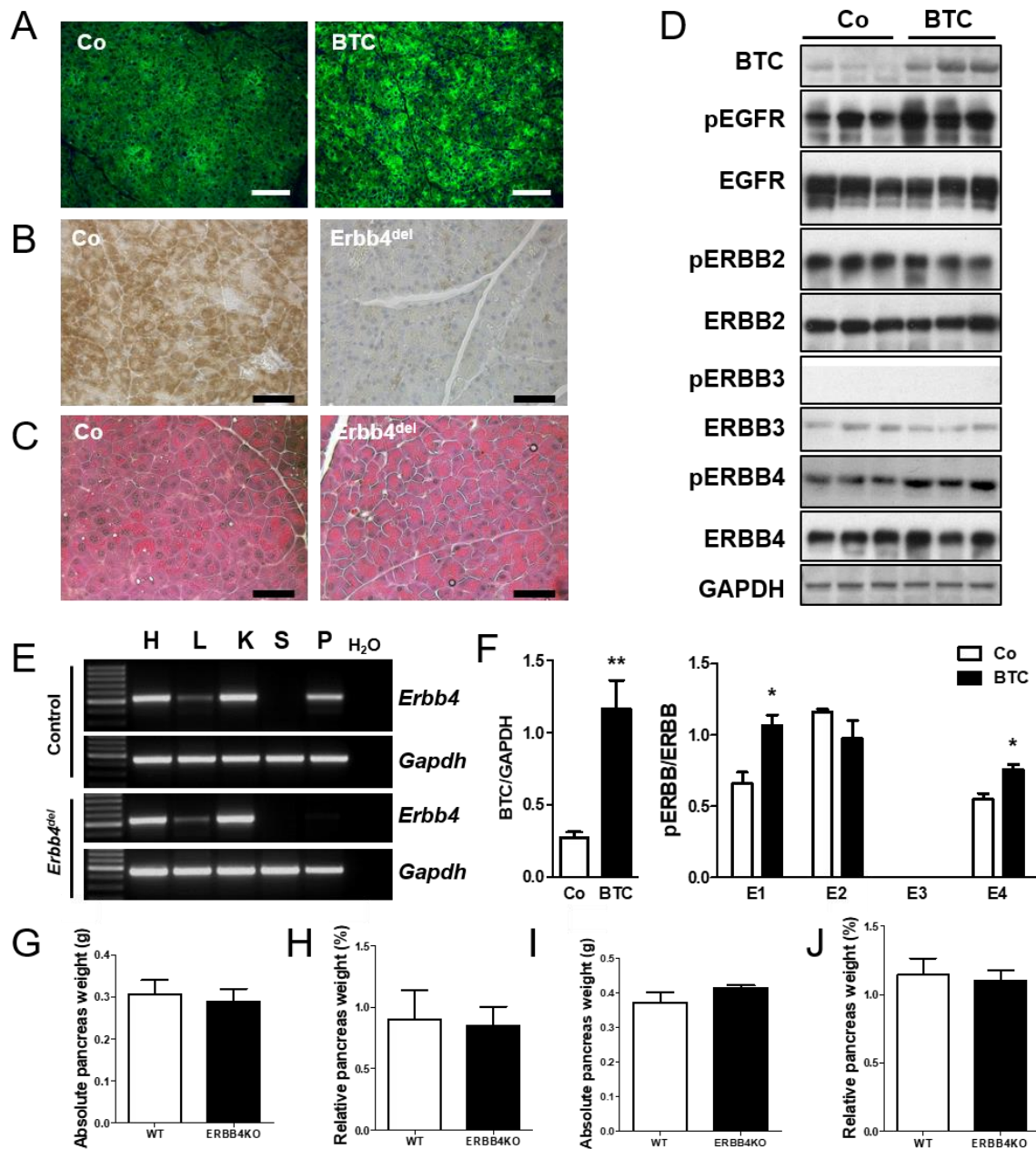
In addition to ligand-induced phosphorylation, ERBB4 can also undergo RIP to release its ICD into the cytosol and the nucleus, where it can act as transcriptional co-activator. We revealed significantly enhanced cytosolic and nuclear ICD presence in Btc transgenic animals concluding that BTC induces the ICD release, which has previously only been reported for the ligand NRG1<sup>178</sup>. In the nucleus, the ERBB4 ICD could bind to interaction partners, as YAP and MDM2<sup>168,178</sup>, and hence, serve as transcriptional co-regulator, enhancing the transcription of the ECM proteins MGP, POSTN, MMP2 and MMP3, we found to be upregulated on mRNA and protein levels in Btc and Wa5+Btc mice, but not in *ErbB4*<sup>fl/fl</sup>; *Ptf1a*<sup>Cre/+</sup>; *Btc*<sup>tg/+</sup> mice upon AP induction, thereby altering the microenvironment and providing a favorable setting for AP protection.

MGP and POSTN are proteins of the ECM<sup>179,180</sup> and MMP2<sup>181</sup> and MMP3<sup>182</sup> are modulators of the ECM, able to prevent fibrosis. ECM remodeling is an important mechanism for cell differentiation and tissue homeostasis, but a deregulation can result in the development of

fibrosis and carcinogenesis<sup>183</sup> and fibrosis has been associated with AP, previously<sup>144,145</sup>. MMPs and collagens are often increased in different tumors and the ECM can play a role in cancer initiation and progression. MMP2 and MMP3 are increasingly expressed by BTC overexpression, possibly in order to prevent early fibrosis, thereby contributing to the protection against AP. The up-regulated ECM proteins, POSTN and MGP, also seem to have a positive effect on AP and is in line with previous findings. POSTN knockout mice showed significantly decreased regeneration after caerulein induced AP, suggesting that POSTN is essential for the recovery of the exocrine pancreas in AP<sup>184</sup>. MGP correlated negatively with pro-inflammatory cytokines and acute phase proteins during AP in humans, and low levels of MGP correlated with a more severe inflammation<sup>185</sup>. A current study demonstrated that MGP is associated with a reduced cytokine production in T-cells and MGP reduces the clinical and histopathological severity of colonic inflammation in murine experimental colitis<sup>186</sup>. MGP, like other Gla-rich proteins, can act as an anti-inflammatory agent in monocytes and macrophages, also during chronic inflammation<sup>187</sup>. We propose that BTC overexpression in AP induces anti-inflammatory and pro-regenerative proteins by the activation of the ERBB4-ICD which alters transcriptional regulation of these targets.

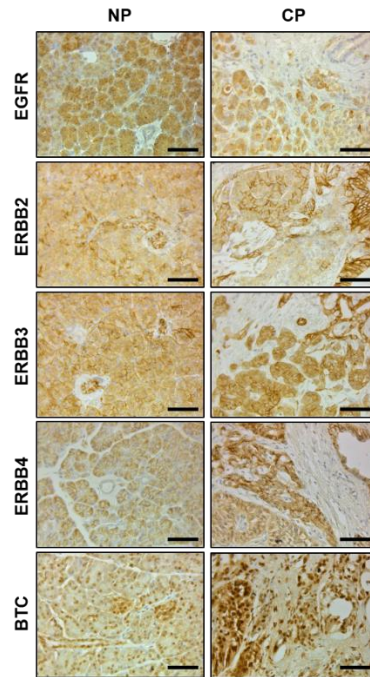
In summary, our report revealed that BTC protects the pancreas against AP through ERBB4. This is achieved possibly by SAPK signaling and subsequent caspase-3 activation, thereby increasing the apoptotic rate and by ICD trafficking with subsequent alteration of the transcriptome, favoring the expression of the anti-inflammatory and pro-regenerative proteins MGP, POSTN, MMP2, and MMP3. We identified the ERBB4 receptor as a promising druggable target to control AP; as a transmembrane receptor, ERBB4 represents an amenable therapeutic target. However, caution must be taken, since cellular responses are distinct and given in a ligand-dependent manner. Other ERBB4 ligands than BTC might bear unfavorable roles for the pancreas, such as HBEGF which leads to metaplastic duct proliferation when overexpressed. Our study rather suggests that the growth factor BTC, or synthetic analogs, could be used as a drug to treat AP or to support conventional AP treatment. In particular, because the overexpression of BTC does not show an adverse phenotype in the pancreas of mice, suggesting only low or even no side-effects, when locally administered.

## 2.3.6 SUPPLEMENTARY FIGURES



### Suppl. Fig. S 2.1: BTC and ERBB receptor expression

**A** Immunofluorescence staining for BTC in the pancreas of transgenic and control mice. **B** Immunohistochemical staining for ERBB4 in the pancreas of *ErbB4<sup>fl/fl</sup>; Ptf1a<sup>Cre/+</sup>* and control mice and **D** H&E staining. Scale bars in **A** represent 200  $\mu$ m and in **B,C** 100  $\mu$ m. **D** Western blot analysis of BTC expression and ERBB expression and phosphorylation of pancreas from transgenic and control animals with 3h-AP. GAPDH was used as reference protein. **E** RT-PCR of several organs from *ErbB4<sup>fl/fl</sup>; Ptf1a<sup>Cre/+</sup>* mice and control mice. *Gapdh* was used as reference gene. **F** Densitometrical analysis of Western blots. **G** Absolute and **H** relative pancreas weight of female *ErbB4<sup>fl/fl</sup>; Ptf1a<sup>Cre/+</sup>* and control animals and of **I,J** male mice showed no differences between genotypes. Data in **F-J** are presented as mean+SEM and were analyzed by Student's t-test. \*P<0.05, P<0.01.



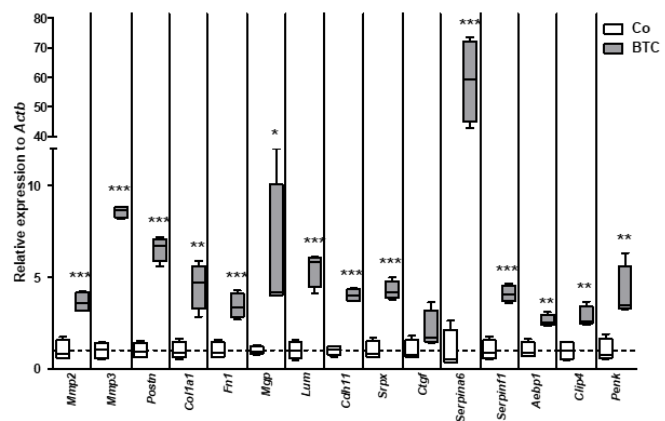
**Suppl. Fig. S 2.2: ERBB receptor and BTC expression in normal pancreas (NP) and human chronic pancreatitis (CP)**

Immunohistochemistry of NP and CP revealed, in NP, EGFR and ERBB4 were expressed in acinar cells, and not in the ducts, while in CP, both were additionally expressed in reactive ductal structures. ERBB2 expression was found in ducts and centroacinar cells and ERBB3 was detected in acinar cells and ducts in NP and BTC expression predominated the islets of Langerhans. In CP, ERBB2 was predominantly expressed in ductal structures. ERBB3 and BTC expression in CP was similar to NP. Scale bars: 50  $\mu$ m.

**A**

	Gene	P-Value		Gene	P-Value
1	Serpina6	0.0000	11	Srm4	0.0065
2	GM6370	0.0000	12	Postn	0.0065
3	Gm46	0.0000	13	Lum	0.0086
4	Mgp	0.0003	14	Ctgf	0.0103
5	Fetub	0.0003	15	Mmp3	0.0103
6	Lamc3	0.0003	16	Fibin	0.0103
7	Serpinf1	0.0010	17	Prx	0.0159
8	Mmp2	0.0029	18	Gif	0.0239
9	Penk	0.0029	19	Lama2	0.0261
10	Srxp	0.0029	20	Cdh11	0.0261

**B**



**Suppl. Fig. S 2.3: Changes in ECM remodeling proteins are associated with the AP-protective effect of BTC**

**A** The 20 most abundantly up-regulated transcripts of *Btc* mice with 3h AP compared with control littermates. For total RNA isolation the pancreas samples were freshly preserved in RNAlater solution. First, the pancreas was perfused by injection of 1 ml RNAlater. Then the perfused pancreas was incubated in 5 ml RNAlater at 4°C for 24h and subsequently frozen at -80 °C until further processing. The microarray analyses were performed with the Agilent SurePrint G3 Mouse GE 8x60K Microarray (G4852A; AMADID 028005) as previously described<sup>188</sup>. The RNA integrity values ranged from 7 to 9 and processed signals were filtered based on “Is well above background” flags, where two samples out of each experimental group must be above the background signal. Differentially abundant genes were determined using the limma<sup>189</sup> package from BioConductor with a FDR  $\leq$  0.05 and at least a 2-fold change (log fold-change  $\geq$  1). The full microarray data set was uploaded at NCBI Gene Expression Omnibus and has the data accession number GSE121038. **B** RT-PCR of transcripts from *Btc* mice compared to control animals during 3h AP. Data in **B** are related to a number of: n= 4 males/group; age: 4 months, and were analyzed by Student's t-test. \*P<0.05; \*\*P<0.01, \*\*\*P<0.001.

## 2.3.7 SUPPLEMENTARY TABLES

Suppl. Table S 2.1: Antibodies employed for Western blots analysis and immunohistochemistry and their dilutions

<b>Western blot</b>			
<b>Antigen</b>	<b>Antibody</b>	<b>Host</b>	<b>Dilution</b>
BTC	R&D Systems, Minneapolis, MN, USA #AF1025	goat	1:500
ERBB4	Cell Signaling, Boston, MA, USA, #4795	rabbit	1:1000
p-ERBB4 (Tyr 1284)	Cell Signaling, #4757	rabbit	1:1000
SAPK	Cell Signaling, #9252	rabbit	1:1000
p-SAPK	Cell Signaling, #9251	rabbit	1:2000
MGP	LifeSpan BioSciences, Seattle, WA, USA, #LS-C341793-100	rabbit	1:1000
POSTN	LifeSpan BioSciences, #LS-C150337	rabbit	1:1000
MMP2	Santa Cruz Biotechnology, #13594 (2C1)	mouse	1:500
MMP3	Santa Cruz Biotechnology, #6839 (C-19)	goat	1:500
ERBB2	Santa Cruz Biotechnology, Dallas, TX, USA #284 (C-18)	rabbit	1:500
H3F3A	Cell Signaling, #9717	rabbit	1:1000
TUB1A1	Cell Signaling, # 2125	rabbit	1:5000
GAPDH	Cell Signaling, #2118	rabbit	1:5000
Goat $\alpha$ Rabbit	Cell Signaling, #7074	goat	1:2500
Rabbit $\alpha$ Mouse	Cell Signaling, #7076	rabbit	1:2000
Donkey $\alpha$ Goat	R&D Systems, #HAF109	donkey	1:2000

## Immunohistochemistry

Antigen	Antibody	Host	Dilution
ERBB4	Santa Cruz Biotechnology, #SC-283	rabbit	1:100
cl. Caspase 3	Cell Signaling, #9664	rabbit	1:100
Ki67	DAKO, #M7249, Hamburg, Germany	rat	1:200
EGFR	R&D Systems, #AF231	goat	1:800
ERBB2	Cell Signaling, #4290	rabbit	1:800
ERBB3	Cell Signaling, #12708	rabbit	1:500
ERBB4	Proteintech, Manchester, UK, #19943-1-AP	rabbit	1:500
BTC	R&D Systems, #AF261NA	goat	1:300
MGP	Proteintech, #10734-1-AP	rabbit	1:200
POSTN	Proteintech, #19899-1-AP	rabbit	1:200
MMP2	Santa Cruz Biotechnology, #13594 (2C1)	mouse	1:200
MMP3	Santa Cruz Biotechnology, #6839 (C-19)	goat	1:200
Rabbit $\alpha$ Goat	DAKO, #E0466	rabbit	1:200
Goat $\alpha$ Rabbit	DAKO, #E0432	goat	1:200
Goat $\alpha$ mouse	DAKO, #E0433	goat	1:200

Suppl. Table S 2.2: Primers and probes employed for RT-PCR

Gene	Forward Primer 5'-3'	Reverse Primer 5'-3'	Probe 5'-3'
<i>Mmp2</i>	TAACCTGGATGCCGTCGT	TTCAGGTAATAAGCACCCCTTGAA	GGTGGTGG
<i>Mmp3</i>	TGCAGCTCTACTTTGTTCTTTGA	AGAGATTTGCGCCAAAAGTG	CCGGGGAG

<i>Postn</i>	TGAGATAAAATATACCAGGATTTCCA	TCTTCTTGCAGGTGTGTCTTT	TTCCACA
<i>Col1a1</i>	AGCAGGTTACCTACTCTGTCC	CTTGCCCCATTCATTTGTCT	ATGGCTGC
<i>Fn1</i>	CGGAGAGAGTGCCCCTACTA	CGATATTGGTGAATCGCAGA	CCTCCTCC
<i>Mgp</i>	TCACGAAAGCATGGAGTCCT	GCTGAGGGGACATAAAGGTG	CAACAGGA
<i>Lum</i>	CAGCAACATTCCGGATGAG	TCATTGTGAGATAAACGCAGGT	CTGGGCTG
<i>Cdh11</i>	ACTGCCTGGCTCAACATCTC	CTGGGACTTTGGTTTCCTGA	GCAGCAGA
<i>Srpx</i>	CCGAAAGGGCTATGAGCTT	AGGGTAGGACATCGCTTCTG	AGCTGGGA
<i>Ctgf</i>	TGACCTGGAGGAAAACATTAAGA	AGCCCTGTATGTCTTCACACTG	CTGGCTGT
<i>Serpina6</i>	CCACCAAAGACACTCCCTTG	GGTGTACAGGAGGGCCATT	CTGCTGCC
<i>Serpinf1</i>	GGACTCTGATCTCAACTGCAAG	AAGTTCTGGGTCACGGTCAG	CTTCTCC
<i>Aebp1</i>	GGAGAAAAACAAGGACCACAAA	ATCCAATAGGTGGGCACT	GGGTGAGG
<i>Clip4</i>	AGGAGCCGTGAAAACCTTG	GATCTGCCCTTTGTCATTCC	AGCTGGGA
<i>Penk</i>	CCCAGGCGACATCAATTT	GCAGGTCTCCCAGATTTTGA	CACATTGG
<i>Actb</i>	CGTGAAAAGATGACCCAGATCA	CACAGCCTGGATGGCTACGT	TTGAGACC TTCAACACC CCAGCCA
<i>ErbB4</i>	CAGCAGTACCGAGCCTTGCG	CAGAGTCATGTTGGAAGGCC	
<i>Jm-ErbB4</i>	AGATGGACTCCTCACATGCC	GGGCTCACCAGCTCTGTC'	
<i>Cyt-ErbB4</i>	AGAATCTCTTGATGAAGAGG	CCATTACAGCAGGAGTCATCA	
<i>Gapdh</i>	TCATCAACGGGAAGCCCATCAC	AGACTCCACGACATACTCAGCACCG	

## 2.4 CONCLUSIONS & OUTLOOK

AP is a common disease with rising incidence, almost always leading to hospitalization due to persistent, severe pain and eventually becoming life-threatening with a mortality of up to 50% in severe AP. Causes for AP are diverse, the major reasons being gall stones and alcohol abuse. The former leads to duct obstruction and increasing pressure on acinar cells which leads to the blockage of zymogens secretion into the lumen of the duct, whereas alcohol acts as a toxin on the exocrine pancreas. Both causes lead to pathological processes, involving ER-stress, disturbed  $Ca^{2+}$  signaling, mitochondrial dysfunction and premature trypsinogen activation resulting in apoptosis, necrosis and auto-digestion. Treatment of AP is only symptomatic and primarily includes analgesics, rehydration to preserve tissue and to prevent hypovolemia and lastly, a proper nutrition strategy, also for pain relief. But each of these attempts still requires concerted handling to prevent a more severe course of the disease or the occurrence of complications for the patient. In addition, none of these options target pathophysiological processes during development or progression of AP. Currently, clinical trials are ongoing using therapies, e.g. targeting  $Ca^{2+}$  channels, and the results are urgently awaited. Frequently, AP occurs more than once. This recurrent AP (RAP) affects approximately one in five patients (with an increased risk for smokers and alcohol consumers), eventually leading to chronic pancreatitis. Furthermore, pancreatic insufficiency belongs to the devastating long-term consequences of AP and every third survivor will end up with *diabetes mellitus*, altogether decreasing quality of life tremendously and underlining the urgent need for an innovative, and particularly, for a pancreas-preserving treatment.

The ERBB system has been partially investigated in AP research. It was revealed that EGF administration in AP mouse models had protective effects on the AP course and that EGFR expression also played a slightly protective role. Both ameliorated the outcome of AP but could not prevent it. A previous study from our lab revealed BTC to have a protective effect on AP, which was much more pronounced than in studies using EGF. *Btc* tg mice were subject to caerulein- and L-arginine-inducible AP whereas AP development in these mice was inhibited compared to wildtype mice. Crossing these mice into a kinase-dead EGFR background could not reverse this phenotype, thus, the BTC-mediated protection was suggested to be independent of EGFR. Instead, increased SAPK signaling is activated.

In this study, we investigated the role of ERBB4 in BTC-mediated protection against AP using caerulein-inducible and L-arginine-inducible AP mouse models. *Btc* tg mice were completely protected from AP development. We found that all ERBB receptors, except for ERBB3 were activated in AP in mice and BTC overexpression enhanced the receptor phosphorylation of EGFR and ERBB4. The loss of ERBB4 in AP of wildtype mice had no effect on the course of

AP, neither had the loss of EGFR, as previously described. The expression of a kinase-dead EGFR in *Btc* tg mice had no effect on AP. But the pancreas-specific loss of ERBB4 resulted in the complete loss of AP protection, revealing ERBB4 as the mediator of the BTC-induced prevention of AP. In *Btc* tg mice lacking ERBB4, serum lipase, amylase and histological scoring of necrosis, apoptosis and edema changed back to the AP conditions as they were observed in wildtype mice. Further, the amount of fibrosis in ERBB4-depleted *Btc* tg mice was similar to control mice upon AP induction, while it was decreased in BTC transgenic AP induced mice. Microarray and quantitative PCR analyses revealed transcriptome changes in *Btc* tg mice compared to wildtype mice. The most upregulated transcripts derived from genes involved in extracellular matrix (ECM)-dynamics, *Mgp*, *Postn*, *Mmp2* and *Mmp3*. The expression of these anti-inflammatory and pro-regenerative proteins was also proven to be different in ERBB4-depleted *Btc* tg mice from single *Btc* tg mice. This verifies that the expression of these genes is ERBB4-dependent. We detected RIP of ERBB4 and subsequent trafficking of its ICD into the cytosol and nucleus. Since the ERBB4 ICD also acts as a transcriptional co-regulator, we suggested that ERBB4 might be involved in the differentially regulated transcription of these ECM proteins, which have shown to be increased in expression in *Btc* tg mice. This mechanism could lead to an altered composition of the pancreatic microenvironment, which is resistant to AP development. MMP2 and MMP3 possibly prevent early fibrogenesis, while POSTN might activate early processes of regeneration and MGP inhibits a strong inflammatory response in AP upon BTC-mediated ERBB4 ICD signaling. A second consequence of BTC overexpression was the enhanced activation of SAPK in AP, which was associated with an increased apoptosis-rate, both of which were not observed in the ERBB4 depleted background. This indicates that ERBB4 is associated with apoptosis regulation.

These data present BTC and ERBB4 as promising targets in AP therapy. However, since probably all ERBB-signaling is strongly ligand-dependent, caution should be taken about choosing ERBB4 as a therapeutic target. The overexpression of the EGFR/ERBB4 ligand HBEGF rather results in metaplastic duct proliferation, which could be triggered by ERBB4. BTC might be the better target for AP treatment. However, also BTC as therapeutic option should be considered carefully. Systemic treatment is rather adverse, since BTC transgenic mice have numerous health issues and since the administration of growth factors might generally increase the risk of tumor development. But BTC overexpression had no effects on the exocrine pancreas, thus, making a locally administered therapy attractive. Further studies must be carried out to investigate the complete mechanism of BTC-mediated protection against AP, to find therapeutic targets, which are possibly less difficult to target.

## **2.5 BRIDGE**

While chronic pancreatitis is established to be a risk factor for pancreatic cancer, there is rising evidence, that AP can also be correlated with an increased risk of developing pancreatic cancer<sup>190,191</sup>. One population-based, age- and sex-matched cohort study revealed that while within two years after the diagnosis of AP, the risk of developing pancreatic cancer was the highest. The chance to develop cancer decreased over time, however, after five and ten years, respectively, the risk was still twice as high compared to patients without AP<sup>192</sup>. Furthermore, patients who had AP have a chance of recurrence and recurrent APs, in turn, can develop into chronic pancreatitis, which emphasizes the association of AP and pancreatic cancer<sup>126</sup>. Since BTC ameliorated the outcome of AP drastically, we wondered whether BTC might also be beneficial in pancreatic cancer.

## **3 BTC IN PANCREATIC CANCER**

### **3.1 INTRODUCTION**

#### **3.1.1 PANCREATIC CANCER**

##### **3.1.1.1 NUMBERS & FACTS: A SURVEY**

PDAC is a malignant tumor of glandular origin arising from the ductal epithelium of the pancreas. It is the most common type of pancreatic cancer (and herein referred to as PDAC, pancreatic ductal adenocarcinoma or pancreatic cancer), followed by neuroendocrine tumors (5%)<sup>193</sup> and acinar cell carcinoma (1-2% of exocrine tumors)<sup>194</sup>. With death cases reaching almost the incidences of approximately 460.000 globally, per year, PDAC is one of the deadliest cancers, worldwide. In Europe, North America and Australia/New Zealand, these rates are even three- to four-fold higher and researchers expect them to remain stable or even to increase in the near future. While we observe declining rates for breast cancer as the current third leading cause of cancer-related deaths in Europe, PDAC is projected to belong to the top three cancer killers after lung and colon cancer in the near future in the European Union and even to be in second place in the USA by the year 2030<sup>195-197</sup>. But why do mortality rates remain stable despite so many years of increasing advances of insights into the basic principles of PDAC? With a 5-year-survival of 8% (after combining all tumor stages) PDAC has the worst survival of all cancers<sup>198</sup>. Reasons for that can be found in the late clinical presentation due to the late onset of symptoms, the spread of metastases at the time of clinical presentation and the lack of early detection due to the poor availability of specific biomarkers<sup>199</sup>. Furthermore, amongst solid tumors, PDAC has the highest amount of stroma impeding therapeutics delivery to the cells of interest in order to be effective<sup>200</sup>. Moreover, the dense fibrotic tissue is further supported by hypovascularization which even worsens drug availability and penetration<sup>201,202</sup>. Another hallmark of PDAC is genomic instability which leads to the rapid development of resistance to targeted therapies<sup>203</sup>.

##### **3.1.1.2 DEVELOPMENT & PROGRESSION OF PDAC**

Preceding the development to a carcinoma in situ, the pancreas undergoes a few preneoplastic changes. In part, prior to the onset of premalignant lesions, acinar cells transdifferentiate into duct cells (acinar-ductal-metaplasia (ADM)) (Figure 3.1, asterisks)<sup>204</sup>. The pancreatic epithelium develops into three different major types of neoplastic precursor lesions, such as pancreatic intraepithelial neoplasia (PanIN), mucinous cystic neoplasia (MCN) and intraductal papillary mucinous neoplasia (IPMN), all of which have the potential to progress into invasive carcinoma<sup>205</sup>, however, the former are the most common and best studied lesions and will be the predominant lesions in the underlying work. PanIN are microscopic flat or papillary lesions,

smaller than 0.5 centimeters (cm), with a columnar epithelium expressing differing amounts of mucins and presenting with differing degrees of cellular, nuclear and architectural atypia<sup>205</sup>. PanIN develop through sequential stages of preneoplastic progression from low-grade lesions including PanIN1(A/B) and PanIN2 to the high-grade lesion PanIN3, the latter being highly associated with the progression to invasive carcinoma. Histologically, these lesions are described as follows:

**PanIN1A/B:** While normal ducts present with a cuboidal epithelium and basally based nuclei (Figure 3.1, arrows), PanIN1A/B present with a flat columnar epithelium (Figure 3.1, white arrowheads) with basally located small round or oval nuclei and abundant supranuclear mucin. PanIN1B are identical to 1A with the exception that 1B has a papillary, pseudostratified epithelium (Figure 3.1, black arrowheads).

**PanIN2:** These lesions are predominantly papillary with nuclear atypia, such as hyperchromatism, nuclear crowding or/and loss of polarity. Regular mitoses can be observed rarely (Figure 3.1, dotted line).

**PanIN3 (carcinoma in situ):** These lesions are papillary. Budding off of epithelial cell clusters into the lumen is frequently observed. PanIN3 present with luminal necrosis. Dystrophic goblet cells with nuclei oriented towards the lumen can be detected and mitoses may occur more frequently and are atypical. Nuclear atypia are more prominent than in PanIN2 lesions and nucleoli are enlarged (Figure 3.1, dotted line).

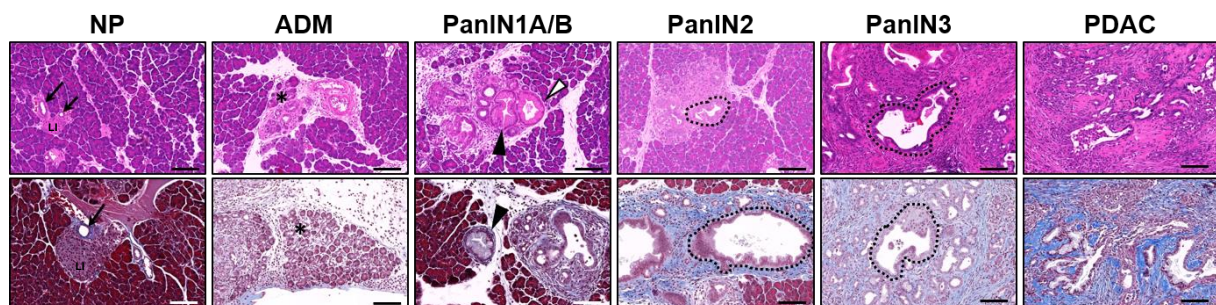


**Figure 3.1: Development and progression of (pre)neoplastic lesions prior to PDAC development**

H&E (upper panels) and Masson's trichrome stainings (lower panels) of murine pancreatic sections. Normal pancreas (NP) composed of predominantly acinar tissue, islets of Langerhans (LI) and normal ducts (arrows), ADM; acinar-ductal metaplasia (asterisks): Acinar cells transform into ductal structures, frequently accompanied by fibrosis, PanIN1A/B; the ductal epithelium becomes columnar, nuclei are still at the basal site of the cell. PanIN1A present with a flat epithelium (white arrowhead), PanIN1B depict a papillary structure (black arrowheads), PanIN2; papillary lesions with loss of polarity in some cells (demarcated line), PanIN3; Papillary lesions with the complete loss of polarity, and budding off of epithelial cell clusters into the lumen and luminal necrosis but with an intact basal membrane (demarcated line), PDAC; carcinoma with cancer cells disrupting the basal membrane of the lesion and migrating into the surrounding desmoplastic tissue.

The carcinoma *in situ* (or PanIN3) is marked by an intact basal membrane that surrounds the epithelial tumor cells (Figure 3.1)<sup>206,207</sup>. During further progression, genetic and epigenetic changes allow a few epithelial cells to acquire mesenchymal features (epithelial-to-mesenchymal transition, EMT) in order to disrupt the basement membrane and to become

invasive, the first crucial step of a cascade of events required for metastatic dissemination. Once, the cancer cells have reached the stromal compartment, they migrate through the stroma and proceed to intravasation, subsequent circulation through the blood stream, extravasation and finally, the formation of micro-metastases and colony formation at the target site<sup>208</sup>, preferably at liver, peritoneum and lungs<sup>209</sup>. EMT is facilitated by the destruction of adherens junctions between cells, of cell-ECM contacts mediated by integrins and by the loss of E-cadherin (CDH1) and concomitant upregulation of N-cadherin (CDH2)<sup>208</sup>. Once, the tumor has metastasized, the patient is inevitably sentenced to death. Systemic treatment by chemotherapy certainly does not only target the primary tumor, but also metastatic lesions, however, investigations suggest that metastases are similarly resistant to drug delivery as to the primary tumor due to a similar desmoplastic environment making it challenging to control metastatic burden in PDAC<sup>201</sup>. Genetically, metastases are clones of the primary tumor and do not display a specific genomic imprint<sup>210</sup>.

#### **3.1.1.3 MICROENVIRONMENT**

A hallmark of PDAC is the microenvironment of the tumor cells. The cancer cells are surrounded by an excessive desmoplastic reaction which provides an environment that comprises predominantly activated pancreatic stellate cells (PSC) secreting and storing extracellular matrix (ECM) and immune cells ensuring an inflammatory reaction<sup>200,201</sup>. PSCs are quiescent under physiological conditions and are only activated upon injury and inflammation of the pancreas, or by cytokine and growth factor stimulation. Once activated, they acquire myofibroblast-like characteristics, which is marked by the expression of the PSC-specific marker alpha-smooth muscle actin (ACTA2). PSCs change their morphology, start to proliferate and migrate, secrete ECM and maintain an excessive cross-talk with the ECM. These characteristics make them one of the key players of PDAC<sup>211,212</sup>. They also communicate with the cancer cells in order to propagate their invasion by remodeling the dense tumor stroma<sup>213</sup>. These pro-tumorigenic properties made them a promising target in the search for PDAC treatment, however, surprisingly, the depletion of PSCs or PSC-driven pathways in pancreatic cancer resulted in increased invasiveness and in a worse prognosis of PDAC in quite a few *in vivo* studies<sup>214</sup>, suggesting a protective response of PSCs upon tumor development and indicating a rather ambivalent role of PSCs. Whether this is due to differential epigenetic regulation, different responses to microenvironmental cues or due to different sub-populations within the PSCs has to be determined. PSCs deserve a lot more attention and caution since their role(s) in PDAC development still have to be revealed.

#### **3.1.1.4 GENOMIC LANDSCAPE OF PANCREATIC CANCER**

Over 90% of all PDAC patients present a point mutation in the *KRAS* gene<sup>215-218</sup>, predominantly resulting in the replacement of amino acid 12 or, less frequently, of codon 13

or 61 in the resulting protein sequence<sup>219</sup>. Regarding codon 12, numerous sequencing studies revealed that in 41% to 48% of all cases, glycine is replaced by an aspartic acid (KRAS<sup>G12D</sup>), more variably, in 11% to 33% glycine is substituted by valine (KRAS<sup>G12V</sup>), in 15% to 20% by arginine (KRAS<sup>G12R</sup>) and the remaining mutations in codon 12 are the substitution of glycine by alanine (Ala), cysteine (Cys) or Ser<sup>220-222</sup>. KRAS mutations are the initiating mutations in PDAC tumorigenesis as they are the first mutations to be detected already in low grade PanIN<sup>30</sup>. These mutations do not lead to the immediate development of neoplastic cells. Instead, there is a long latency period until cells harboring mutated KRAS transform into invasive carcinoma, and also, the penetrance is below 100%, meaning that not all cells develop invasiveness. In fact, further mutations are required to proceed to higher dysplastic lesions. The further progression to the PanIN2 stage is permitted by the loss of tumor suppressor cyclin-dependent kinase inhibitor 2A (*CDKN2A*). The further loss of tumor suppressor (*TP53*) and Mothers Against Decapentaplegic Homolog 4 (*SMAD4*) is observed only in high grade lesions and in invasive carcinoma. Additionally, genomic instability by telomere shortening is another hallmark that is observed already in over 90% of low grade PanIN and which deteriorates with the grade of lesions. Other genomic aberrations are copy number alterations, as well as chromothripsis, a phenomenon by which up to thousands of chaotic chromosomal rearrangements occur in a single event<sup>223</sup>.

### **3.1.1.5 KRAS**

KRAS is one of the RAS family proteins. RAS proteins are G-proteins cycling between a guanine-diphosphate (GDP) and guanine-triphosphate (GTP) bound state determining the activity of the binary molecular switch. They possess a weak intrinsic GTPase activity capable of hydrolysing GTP, thereby switching into the inactive state which is strongly stimulated by GTPase activating enzymes (GAPs). Upon the interaction with guanine nucleotide exchange factors (GEFs), GTP is loaded back onto the RAS protein providing it with the capability to interact with further intracellular signaling molecules. Oncogenic mutations, such as frequently detected in the *KRAS* gene in PDAC, impair the intrinsic GTPase function, as well as the interaction with GTPases which results in the permanent loading of GTP and thus, in a constitutively active RAS protein<sup>219,224</sup>. Oncogenic KRAS is responsible for enhanced proliferation, suppression of apoptosis, a dysregulated metabolism, a reorganized microenvironment, evasion of the immune response and enhanced metastatic spread in pancreatic cancer<sup>225</sup>. The three major pathways by which KRAS signaling is transduced in PDAC, are the canonical rapidly accelerated fibrosarcoma (RAF)/MEK/MAPK and the PI3K, 3-phosphoinositide-dependent protein kinase-1 (PDK1)/ protein kinase-B (PKB/AKT) pathways and the RalGEFs pathway<sup>226</sup>.

### 3.1.1.6 THERAPY

#### SYSTEMIC THERAPY

Due to the late diagnosis, only 15-20% of all pancreatic cancer cases are local, and thus, eligible to surgical resection<sup>227</sup> improving the 5-year-survival up to 12-19%<sup>228-230</sup>. Those and all remaining patients who suffer from locally advanced or metastatic pancreatic cancer, are treated with either adjuvant or neoadjuvant systemic therapy, respectively<sup>227</sup>. More than 20 years ago, gemcitabine monotherapy was regarded as the standard-of-care treatment for pancreatic cancer. Today, FOLFIRINOX, and still, gemcitabine are the two standard-of-care therapies for good performance status patients, while gemcitabine is almost exclusively administered in combination with nab-paclitaxel<sup>231</sup>. Gemcitabine is a synthetic fluoridated nucleoside prodrug. It is incorporated into the DNA as a masquerade cytosine, thereby eluding the repair mechanisms of the cell and inhibiting the replication process<sup>232</sup>. Nab-paclitaxel (albumin-bound paclitaxel) is an anti-mitotic drug which stabilizes microtubule formation through binding and therefore disrupting microtubule-spindle dynamics during mitosis resulting in apoptotic cell death<sup>233</sup>. The combination of those two drugs prolonged the median survival of the patients by almost two months (8.5 vs. 6.7 months), the 1-year-survival by almost 60% (35% vs. 22%) and the 2-year-survival by 100% (9% vs. 4%) compared to the administration of gemcitabine alone. Furthermore, the progression-free survival and the response rate were significantly improved<sup>234</sup>. FOLFIRINOX is a combinatorial therapy of folinic acid (vitamin B derivative), 5-fluoruracil (5-FU, pyrimidine analog), irinotecan (topoisomerase inhibitor) and oxaliplatin (platinum-based DNA-crosslinker). 5-FU inhibits the thymidylate synthase (TS) resulting in the lack of (for DNA replication essential) deoxythymidine triphosphate and also in the incorporation of TS metabolites into RNA and DNA<sup>235</sup>. A study comparing FOLFIRINOX combination therapy to gemcitabine monotherapy revealed that FOLFIRINOX treatment prolonged the median survival by 4.3 months (11.1 vs. 6.8 months), more than doubled the 1-year-survival (48.4% vs. 20.6%) and tripled the 18-month-survival (18.6% vs. 6%). However, the improvements of FOLFIRINOX are accompanied by a higher incidence of adverse events which must be considered for every single patient when weighing up the right chemotherapy<sup>236</sup>.

#### TARGETED THERAPY

Targeted therapies aim to battle the culprit on a molecular level very specifically. The tumor is attacked where it develops and ideally, the side effects are reduced. A few oncogenes involved in the pathogenesis of PDAC development are known and have already been targeted in clinical trials, such as EGFR, ERBB2, vascular endothelial growth factor/receptor (VEGF/VEGFR), platelet derived growth factor receptor (PDGFR), BRAF, RAS, PI3K, MEK1/2, poly (ADP-Ribose) polymerase 1 (PARP1), sonic hedgehog (SHH) and more. Some of these

seem to be promising targets<sup>231</sup>. In the following, therapies targeting members of the ERBB family are summarized.

EGFR is frequently overexpressed in human pancreatic cancers<sup>237-239</sup> and EGFR expression levels correlate with a poor prognosis, fast progression or aggressiveness of pancreatic cancer<sup>237,240,241</sup>. So, EGFR has been an attractive target in search of a therapeutic agent. There are two ways to inhibit the RTK, in particular, either with monoclonal antibodies (mABs) or small molecule inhibitors. The two most prominent and promising mABs which progressed to clinical trials were Cetuximab and Panitumumab. Both bind to the extracellular domain of EGFR, thereby competing with the ligand, inhibiting receptor dimerization and activation, and instead, inducing receptor internalization. Cetuximab additionally induces immune responses in the host potentiating its anti-tumorigenic effect<sup>242</sup>. Another way to inhibit EGFR activity effectively is achieved by a small molecule, named erlotinib. It competes with ATP for the ATP-binding site of the tyrosine kinase domain of the receptor in a reversible manner resulting in the inhibition of autophosphorylation and thus, activation of the same<sup>243</sup>.

The expression levels of ERBB2 in PDAC vary from low and modest to high. However, most of the investigations are consistent with the finding that ERBB2 overexpression is rather observed in premalignant lesions than in invasive carcinomas<sup>238,240,244-248</sup>. These findings were sufficient to target the receptor with the mAB trastuzumab, hitherto successfully used for the treatment of metastatic breast and gastric cancer<sup>249</sup>.

However, several meta-analyses revealed that targeted therapies in PDAC have no benefit over conventional mono-chemotherapies<sup>250,251</sup>. Although erlotinib treatment combined with gemcitabine leads to a significantly (but marginally) increased overall survival, it has no clinical relevance<sup>252</sup>. Also, trastuzumab had either no or only negligibly beneficial effects on the overall or progression-free survival in combination with chemotherapy compared to conventional monotherapies<sup>253,254</sup>. So still, after more than 20 years of intense research and after the enormous advances in pancreatic cancer research, systematic treatment with toxic chemotherapy is the standard-of-care therapy for patients.

### **3.1.2 THE ERBB FAMILY IN PANCREATIC CANCER**

There is an urgent need to overcome the limited understanding of the biology of EGFR signaling since so many therapeutic approaches failed to target EGFR and EGFR signaling. This includes the understanding of the complete ERBB family and their designated ligands instead of one single member of the family. The ERBB receptors and ligands play crucial roles in pancreatic cancer, however, certainly, there is still much in the hidden which will be

discovered in the future. In the following, it is summarized what is known about the ERBB network in PDAC, beginning with the ligands.

### **3.1.2.1 THE LIGANDS**

#### *GROUP I LIGANDS*

The overexpression of TGFA in the pancreas of mice results in ADM, which is accompanied by a fibrotic response and which can further progress into malignant carcinoma<sup>147</sup>. TGFA was verified to be responsible for early events in PDAC development, since primary murine acinar cells undergo ADM in 3-D tissue culture after TGFA stimulation<sup>255</sup>. According to the Human Protein Atlas (pathology atlas) database, high TGFA mRNA levels are considered as a bad prognostic factor in PDAC patients<sup>256</sup>. Amphiregulin (AREG) overexpression leads to a different response in the pancreas. Compared to TGFA, no fibrosis and no complex tubular formation is observed, however, AREG induces increased proliferation of duct cells, exclusively, leaving acinar cells untouched<sup>149</sup>. Other studies found AREG to be involved in the PDAC outcome. In one study, AREG was expressed in more than 50% of PDAC samples and its expression was correlated with a poor prognosis<sup>257</sup>. High AREG expression levels in PDAC were associated with the hetero-dimerization of EGFR with ERBB3, resulting in enhanced ERK and AKT signaling<sup>258</sup>. The Human Protein Atlas (pathology atlas) database also suggests to treat AREG as a bad prognostic marker in pancreatic cancer, since high mRNA levels significantly coincided with a shorter survival in PDAC patients<sup>256</sup>. EGF is overexpressed in pancreatic cancer compared to normal pancreatic tissue<sup>259</sup> and EGF co-expression together with its designated receptor EGFR is associated with increased tumor aggressiveness<sup>260</sup>. Taken together, for all growth-factors uniquely binding EGFR applies that their expression together with a concomitant expression of the EGF receptor in pancreatic cancer is related to a poor prognosis<sup>261</sup>.

#### *GROUP II LIGANDS*

However, the remaining ligands of the ERBB family also play a role in PDAC. Starting with another, according to the Human Protein Atlas database (pathology atlas)<sup>256</sup> unfavourable prognostic marker, EREG. EREG is overexpressed in human PDAC as well as in human pancreatic cancer cell lines (hPaCaCells) where it carries out growth-stimulatory effects after further exogenic EREG stimulation<sup>262</sup>. One study revealed that a down-regulation of MUCIN4 (MUC4), a transmembrane protein upregulated in premalignant lesions, in pancreatic cancer and hPaCaCells, and which was shown to be involved in the pathogenesis of PDAC, inhibits tumorigenicity and metastasis of pancreatic cancer cells. This observation coincided with the down-regulation of EREG<sup>263</sup>, also assigning a tumorigenic role to EREG. HBEGF was found to be expressed in early lesions of human pancreatic cancer<sup>264</sup>. It also promoted KRAS driven

oncogenesis in a genetically engineered mouse model (GEMM) and the stimulation of wildtype murine acinar cells in three-dimensional (3-D) cell culture resulted in ADM<sup>265</sup>, indicating that HBEGF is involved in the carcinogenesis of the exocrine pancreas.

#### *GROUP III/IV LIGANDS*

Another ERBB ligand family, the NRGs, which activate ERBB3 and ERBB4, also play a role in PDAC. NRG1 was found to be detected in 75% of the cancer cells and in 90% of metastatic lesions of human pancreatic cancer tissues. Stimulatory experiments with NRG1 on pancreatic cancer cell lines resulted in growth stimulatory and growth inhibitory outcomes which was in part explained by receptor availability of ERBB2 and ERBB3 (particularly by the ratio of ERBB2/ERBB3) and by the availability of NRG1 splice forms. While NRG $\beta$ 1 acted as a mitogen, NRG $\alpha$ 1 attenuated the growth of the cell lines. The same study observed a decreased survival for patients with high NRG $\beta$ 1 levels (not significant), while there was no difference for patients with high NRG $\alpha$ 1 levels<sup>266</sup> indicating that NRG $\beta$ 1, but not NRG $\alpha$ 1 might play a tumor-promoting role in PDAC. Another study found NRG1 expression over 50% of pancreatic cancer specimen promoting tumor growth by activating the ERBB3 receptor<sup>267,268</sup>. Interestingly, very recently, fusions of the NRG1 gene were found in 100% of PDAC patients with wildtype KRAS alleles<sup>269</sup>, indicating aberrant ERBB signaling in order to evade constitutive KRAS activation. So far, NRG1 seems to be the only NRG ligand that was revealed to play a role in PDAC<sup>270</sup>.

#### *BTC*

*BTC* (Group II ligand) mRNA was expressed in many pancreatic cancer cell lines and in 90% of human pancreatic cancers. There was a 7.5-fold *BTC* expression in human PDAC tissues compared to the levels detected in normal pancreas. This increase was due to high *BTC* mRNA levels in the duct-like cancer cells. Also, *BTC* mRNA expression was inducible by EGF and HBEGF stimulation in one cancer cell line indicating a cross-induction mechanism for *BTC* by those two EGFR and EGFR/ERBB4 ligands, respectively<sup>271</sup>. Further, *BTC* is a potent mitogen which was shown by stimulation experiments in human pancreatic cancer cells and also *in vivo* by a cell line inoculated mouse model. *BTC* can also regulate its expression through an auto-induction mechanism in pancreatic cancer cells<sup>272</sup>. All these features make *BTC* appear to be involved in pancreatic cancer development or progression, however, after the year 2000, no further investigations of the role of *BTC* in PDAC were carried out. Another characteristic of *BTC* is its ability to trans-differentiate various cell types into insulin-producing cells<sup>103</sup>. Trans-differentiation plays a crucial role in PDAC development, and the ERBB ligands TGFA and HBEGF are known to be involved in ADM. With the trans-differentiation potential of *BTC*, it might also be implicated in ADM and thus, PDAC development.

### 3.1.2.2 THE RECEPTORS

#### EGFR

EGFR is highly expressed in human PDAC. Its pharmacological, as well as its genomic depletion resulted in the inhibition of tumor initiation in mice with pancreas-specific oncogenic KRAS<sup>G12D</sup> or KRAS<sup>G12V</sup>. This was, in the KRAS<sup>G12D</sup> model, attributed to a decreased activation of the MAPK pathway<sup>156,273</sup>. But since EGFR is upstream of KRAS, and MAPK is a downstream target of KRAS, how can EGFR manage to regulate a downstream target of a constitutively active KRAS molecule? The same groups reported that a depletion of the tumor suppressor *TP53*, KRAS-induced oncogenesis is possible, albeit with reduced efficiency indicating that EGFR plays an essential role during tumorigenesis in KRAS driven GEMMs in a *TP53* depleted background<sup>156,273</sup>. Pharmacological inhibition of EGFR in the clinic by erlotinib in combination with gemcitabine only provided marginal benefit in a subset of patients compared to gemcitabine mono-treatment<sup>252</sup>. This suggests that in late stages, the cancer cells possibly escape EGFR dependency. This theory would also be in line with the observation that the loss of differentiation in pancreatic cancers correlated with the decrease of EGFR expression and that human PDAC cell lines with a quasi-mesenchymal subtype were more resistant to erlotinib treatment than cell lines with a classical (milder) phenotype<sup>204,273,274</sup>. However, it has been shown very recently, that EGFR inhibition in combination with the inhibition of one of its downstream targets, CRAF, led to the prevention of premalignant lesions development, to the regression of advanced PDAC in a GEMM and to the inhibition of the proliferation of tumor cells in a patient-derived xenograft (PDX) model<sup>275</sup>. It will be very interesting, whether combinatorial therapies targeting EGFR and CRAF will progress to clinical trials in the near future.

#### ERBB2

While EGFR is highly important for KRAS induced oncogenesis, the role of ERBB2 in pancreatic cancer is less well understood. There are studies showing the expression of ERBB2 mRNA in 100% of PDAC samples with increased (but not significant) ERBB2 expression compared to normal pancreatic tissue<sup>266</sup>. On the other hand, there are studies finding variable, but rather low frequencies of ERBB2 overexpression in PDAC ranging from 2% to 29%, in part due to the amplification of the gene locus. Mutations in the *ERBB2* gene indicating aberrant signaling were not found<sup>276</sup>. A meta-analysis considering six investigations performed by FISH analyses revealed that *ERBB2* gene amplification did not correlate with clinical parameters of pancreatic cancer<sup>277</sup>. However, another study correlated ERBB2 overexpression in 25% of PDAC samples with an aggressive phenotype<sup>278</sup>. Targeting the ERBB2 receptor in clinical trials was also disappointing. However, a recent study revealed that targeting ERBB2 in a PDAC xenograft model with a combination of trastuzumab and a

homemade murine ERBB2-specific mAB was more effective than targeting EGFR with an equivalent mAB combination, although expression levels of ERBB2 were 15-fold lower than EGFR levels<sup>279</sup>. This indicates that ERBB2 might play a less apparent but still, a highly important role. These contradictory findings show that more effort has to be put into the investigation of ERBB2 involvement in PDAC development and progression.

### *ERBB3*

*ERBB3* was expressed in 100% of PDAC samples with a statistically significant increase in mRNA abundance<sup>266</sup>. *ERBB3* was also elevated in more than 50% of PDAC tissues compared to normal pancreas, which was not due to gene amplification. This was associated with advanced tumor stages and shorter survival of the patients<sup>162</sup>. Another study found *ERBB3* to be expressed in many hPaCaCells and in 90% of PDAC samples which was not correlated with the outcome of the disease<sup>280</sup>. But the inhibition of *ERBB3* by miRNA decreased the proliferation and migration of cancer cells by down-regulating AKT and MAPK signaling, thereby also allocating *ERBB3* a role in pancreatic cancer<sup>277</sup>.

Promising experiments revealed that the dual targeting of the hetero-dimer ERBB2/ERBB3 (both with different abundance) with two monoclonal antibodies resulted in pronounced anti-tumor effects in hPaCaCells and xenograft models. In particular, the therapy delayed tumor growth of xenografts arising from cells harbouring KRAS mutations, and which are poorly sensitive to erlotinib treatment<sup>281</sup>.

### *ERBB4*

One of the few studies about *ERBB4* in PDAC revealed weak to moderate *ERBB4* mRNA levels in normal pancreas and in 83% of PDAC samples, detected by real-time (RT)-PCR and immunohistochemistry (IHC). However, *ERBB4* levels were significantly decreased in non-metastatic PDAC compared to tumors that had already spread into lymph nodes or built distant metastases and also compared to normal pancreas. But no correlation between *ERBB4* levels and the survival of the patients could be observed<sup>282</sup>. Only two years later, it was published that *ERBB4* expression in pancreatic cancer was exclusively found in non-metastatic tumors<sup>278</sup>, which is the exact opposite. Other detected *ERBB4* mRNA in 64% of PDAC specimen but with a significant decrease in *ERBB4* abundance compared to normal pancreas. They also detected very low or no levels of *ERBB4* in common human pancreatic cancer cell lines<sup>266</sup> also indicating a rather favourable role for *ERBB4* in PDAC. Other investigations suggested a context-specific role for *ERBB4* in PDAC which can either be tumor suppressive or oncogenic. Mill *et al.* observed that a mutant, constitutively active, *ERBB4* homo-dimer was able to inhibit colony formation in a human pancreatic cell line, while the stimulation of wildtype *ERBB4* with NRG1B was not. However, they have linked ectopic

ERBB4 expression to enhanced anchorage-independent growth induced by NRG1B stimulation in MIAPaCa cells, which was in turn reduced by the inhibition of ERBB4 kinase activity<sup>283</sup>. As also observable in other tumors than the pancreas, ERBB4 seems to play a controversial role in tumorigenesis. It provides features to either act as a tumor suppressor or as tumor driver, and thus, the function of ERBB4 in pancreatic cancer still has to be revealed.

### **3.2 AIM OF THE STUDY**

Almost all ligands of the ERBB family are associated with pancreatic cancer development or progression. Most of them were found to be overexpressed in human PDAC, as well as in hPaCaCells and an increased expression often goes along with an unfavourable prognosis for patients. However, functional studies revealed that every ligand has a unique role in PDAC. While the overexpression of TGFA and HBEGF induced fibrosis and ADM, AREG transgenic mice showed an increased duct proliferation. NRG1 had a dual role, dependent on the presence of its splice isoforms and BTC was a potent mitogen but further information is missing. Certainly, many basic mechanisms have been revealed by the investigation of ERBB ligands, but there are still gaps of knowledge, e.g. which receptors mediate these ligand-induced processes? Beyond the designated receptors of the ligands, further receptors can be activated by hetero-dimerization of the ERBBs. This factor should not be underestimated, in particular, because targeting of only one receptor in a hetero-dimer might not be as efficient as targeting both partners. Furthermore, not all ligands of the family, which were found to be expressed or overexpressed in PDAC specimen were profoundly investigated in animal models.

The expression levels of the ERBB receptors in pancreatic cancer are controversial. Only EGFR was frequently overexpressed, which consistently, coincided with a poor outcome for the patient. Targeting EGFR, however, resulted in disappointing outcomes. ERBB2 overexpression was observed less frequently in PDAC and also to rather low to moderate levels. ERBB3 expression, on the other hand is frequently expressed or overexpressed in PDAC. The prognostic value of the abundance of both receptors, ERBB2 and ERBB3, remains controversial. However, targeting of ERBB2 in combination with EGFR or ERBB3 in hPaCaCells or xenograft models enhances anti-tumor effects, independently of ERBB2 expression levels. ERBB4 expression is rather decreased in human PDAC, but functional studies revealed ambivalent roles for this outlier of the ERBB family. Responses to erlotinib treatment (an EGFR-inhibitor) in patients are independent of the pancreatic EGFR expression levels. In pre-clinical studies, it was also observed that the response rate to ERBB2-targeted combination therapies was not dependent on the ERBB2 expression levels of the responders. ERBB4 also carries out a role that is possibly not correlated to ERBB4 expression levels in

PDAC. In conclusion, it is crucial to investigate the activity of the receptors, rather than just the abundance. Increasing evidence shifts treatment options to combinatorial instead of mono-therapies. Presumably, a wide range of information on pancreatic cancer is still hidden inside the complex ERBB network. With the following study, we will stimulate the ERBB family in mice by applying a ligand with binding affinities for both, EGFR and ERBB4. Beyond receptor expression levels, we will investigate the ERBB receptor activation and the activation of corresponding pathways with the aim to reveal the roles of the ERBB receptors in PDAC development, progression and survival.

### **3.3 STUDY: UNRAVELING THE ERBB NETWORK UPON BETACELLULIN SIGNALING IN PANCREATIC DUCTAL ADENOCARCINOMA IN MICE**

Kathrin Hedegger,<sup>1</sup> Hana Algül,<sup>2</sup> Marina Lesina,<sup>2</sup> Andreas Blutke,<sup>3</sup> Roland M. Schmid,<sup>2</sup>  
Marlon R. Schneider,<sup>1</sup> and Maik Dahlhoff <sup>1\*</sup>

<sup>1</sup>Institute of Molecular Animal Breeding and Biotechnology, Gene Center of the LMU Munich, Germany

<sup>2</sup>Second Department of Internal Medicine, Klinikum rechts der Isar, Technical University of Munich, Germany

<sup>3</sup>Research Unit Analytical Pathology, Helmholtz Zentrum München, Neuherberg, Germany

This project was in parts presented at a podium talk at '*CSHL Meeting: Mechanisms & Models of Cancer*' in Cold Spring Harbor, New York, USA with the title '*Unraveling the ERBB network upon betacellulin signaling in pancreatic ductal adenocarcinoma in mice*' in August, 2018 and in form of a poster talk at the '*39. Jahrestagung des Deutschen Pankreasclubs e.V.*' in Goettingen, Germany in February, 2019.

*Addendum:* This manuscript is in the submission process in a revised version (October, 2019).

### 3.3.1 ABSTRACT

#### Background & Aims

Pancreatic ductal adenocarcinoma (PDAC) will soon belong to the top three cancer killers. The only approved targeted therapy targets the epidermal growth factor receptor (EGFR). Although EGFR is a crucial player in PDAC development, EGFR therapy is rather disappointing. In this study we evaluated the role of the EGFR ligand betacellulin (BTC) in PDAC.

#### Methods

With CRISPR/Cas9 technology we generated a BTC knockout mouse model and a transgenic overexpression model. Both models were crossed with a tumor mouse model for PDAC (*Ptf1a<sup>Cre/+</sup>;KRAS<sup>G12D/+</sup>*). To investigate the ERBB receptors, we deleted each receptor pancreas-specific by using the *Cre-loxP* system.

#### Results

*B<sup>-/-</sup>*KC mice have decelerated PDAC development, associated with decreased EGFR activation. BKC mice developed severe PDAC with a poor survival rate. The dramatically increased BTC-mediated tumor burden is EGFR-dependent, but also ERBB4 and ERBB2 are involved in PDAC development. A depletion of EGFR, ERBB2 or ERBB4 improves the survival rate of BTC-mediated PDAC significantly.

#### Conclusions

A deletion of BTC reduces the tumor burden and BTC overexpression accelerates PDAC development in *KRAS<sup>G12D</sup>* mice, involving EGFR-, ERBB2- and ERBB4-signaling.

### 3.3.2 INTRODUCTION

With a 5-year-survival rate of 8% the pancreatic ductal adenocarcinoma (PDAC) is worldwide one of the deadliest cancers. While mortality rates are declining for many cancers due to early detection and improved treatment, rates for PDAC are still rising<sup>198</sup> promoting PDAC to the top three cancer killers, within the next decade<sup>197</sup>. The standard of care treatment is surgical resection and adjuvant chemotherapy. FOLFIRINOX or gemcitabine in combination with nab-paclitaxel provided the most promising results<sup>203</sup>. However, they do not differentiate between cancerous and normal cells, and as systemic therapies are often associated with unacceptable side effects. There is an urgent need to find customized therapies targeting aberrantly regulated molecules in PDAC. Over 95% of PDAC patients harbor an activating point mutation in the Kirsten rat sarcoma viral oncogene homolog (*KRAS*) gene<sup>284</sup>. Being detected in over 90% of pancreatic intraepithelial neoplasia (PanIN), *KRAS*<sup>G12D</sup> is the initiating mutation in PDAC. However, the progression of PanIN into invasive PDAC comes along with the subsequent loss of the tumor suppressors *CDKN2A*, *TP53* and *SMAD4*<sup>223</sup>. Attempts to target aberrant *KRAS* in PDAC were promising in cell and animal models. However, they rather ended disappointing in clinical trials<sup>285</sup> and so, numerous downstream effectors of *KRAS* are in the focus of ongoing trials. A striking finding was made, when Ardito *et al.* and Navas *et al.* revealed that the epidermal growth factor receptor (EGFR), acting upstream of *KRAS*, was required for oncogenic *KRAS*-driven PDAC tumorigenesis in mice, but only in a *TP53* stable background<sup>156,273</sup>. Indeed, EGFR is the only molecule approved for targeted PDAC therapy in the clinic, although with marginal improvement in survival with only a small subset of patients responding. Surprisingly, the response rate to erlotinib in PDAC patients is independent of the pancreatic EGFR expression status<sup>252</sup>. Thus, many questions concerning EGFR signaling in PDAC remain to be addressed. EGFR is one of four members of the complex family of the ERBB receptors. Together with ERBB2 (HER2, neu), ERBB3 (HER3) and ERBB4 (HER4), EGFR belongs to the receptor tyrosine kinases (RTK). The ERBB receptors homo- or hetero-dimerize after ligand-dependent activation in order to induce cellular responses like proliferation, migration, apoptosis, differentiation and adhesion<sup>9</sup> and with 28 possible receptor combinations (including spliced receptors) and eleven ligands, the family is able to induce 611 different active receptor/ligand combinations<sup>24</sup>. ERBB ligands like epidermal growth factor (EGF)<sup>259,260</sup>, transforming growth factor alpha (TGFA)<sup>147,255</sup>, amphiregulin (AREG)<sup>149,257</sup>, heparin-binding EGF-like growth factor (HBEGF)<sup>264,265</sup> and epiregulin (EREG)<sup>262,263</sup> have been associated with PDAC. While all of them bind EGFR, the latter two also bind ERBB4 indicating that EGFR might not be the only candidate to mediate their effects in PDAC. Another EGFR- and ERBB4-binding ligand, betacellulin (BTC) has also been implicated in PDAC. *BTC* mRNA was not only detected in human pancreatic cancer cell

lines (hPaCaCells) and elevated in human PDAC tissues<sup>271</sup>, BTC was also revealed to be a potent mitogen in human pancreatic cancer cell lines<sup>272</sup> but it is not known through which receptor BTC signaling occurred. This is particularly interesting, since its designated receptor ERBB4 plays controversial roles in PDAC development and progression<sup>266,282,283</sup>. The role of ERBB4 seems to be context-dependent, in particular, probably due to its - in contrast to its ERBB relatives - exceptional nature to signal in a splice-form dependent manner affecting either its cytoplasmic (CYT-1, CYT-2) or juxtamembrane region (JM-a, JM-b) or in form of its soluble intracellular domain (ICD80) after undergoing regulated intramembrane proteolysis (RIP)<sup>286</sup>. There is an urgent need to unravel the complex ERBB system in pancreatic cancer to understand not only the role of EGFR better, but also to show the potential significance of its relatives in order to establish more effectively targeted therapies when it comes to anti-EGFR treatment. To investigate BTC in pancreatic cancer, we generated a BTC knockout mouse model (*Btc*<sup>-/-</sup>) and overexpressed BTC in a transgenic mouse model (*Btc*). Both models were crossed in a PDAC mouse model and additionally to include the receptor mediation we deleted pancreas-specific EGFR, ERBB2, or ERBB4. Survival rate was recorded, pancreata were characterized histologically and were investigated on molecular level to evaluate the role of BTC and the ERBB receptors.

### 3.3.3 METHODS

Mice carrying floxed *Egfr*<sup>fl/fl</sup> (*Egfr*<sup>tm1Dwt</sup>)<sup>287</sup>, *Erb2*<sup>fl/fl</sup><sup>288</sup>, *Erb4*<sup>fl/fl</sup> (*B6;129-Erb4*<sup>tm1Fej/Mmucd</sup>)<sup>171</sup>, *Kras*<sup>G12D/+</sup> (*B6.129S4-Kras*<sup>tm4Tyj/J</sup>)<sup>289</sup> alleles or expressing cre recombinase under the pancreas specific transcription factor 1 alpha (*Ptf1a*-Cre) (*Ptf1a*<sup>tm1(cre)Hnak</sup>)<sup>172</sup> promoter have been described previously. Transgenic mouse lines overexpressing BTC ubiquitously under the control of the chicken-beta-actin gene promoter (*Btc*<sup>tg/+</sup>) have been described, elsewhere<sup>169</sup>. We cross mated *Btc*<sup>tg/+</sup>;*Ptf1a*<sup>Cre/+</sup>;*Kras*<sup>G12D/+</sup> (herein referred as BKC) mice and *Btc*<sup>tg/+</sup>;*Ptf1a*<sup>Cre/+</sup>;*Kras*<sup>G12D/+</sup>;*Egfr*<sup>fl/fl</sup>, and *Btc*<sup>tg/+</sup>;*Ptf1a*<sup>Cre/+</sup>;*Kras*<sup>G12D/+</sup>;*Erb2*<sup>fl/fl</sup> and *Btc*<sup>tg/+</sup>;*Ptf1a*<sup>Cre/+</sup>;*Kras*<sup>G12D/+</sup>;*Erb4*<sup>fl/fl</sup> mice (herein referred to as EGFR KO;BKC, ERBB2 KO;BKC and ERBB4 KO;BKC, respectively) to delete the designated ERBB receptor pancreas-specific using the Cre-loxP-system. Mice were maintained in the C57BL/6N background and housed under specific pathogen-free conditions in the closed barrier facility of the Gene Center Munich at 23°C, 50% humidity and with a 12-h light/dark cycle (lights on at 7 AM). They had free access to water and a standard rodent diet (V1534, Ssniff, Soest, Germany). All animal experiments were approved by the author's institutional committee on animal care and carried out in accordance with the German Animal Protection Law with permission from the responsible veterinary authority. Mice were weighed weekly until the age of 6 months and afterwards still weekly or every two weeks. Mice were sacrificed at the

designated time points or, for survival analysis, were left alive and redeemed as soon as they became moribund.

### **3.3.3.1 GENERATION OF *BTC* KNOCKOUT MICE (*BTC*<sup>-/-</sup>)**

For CRISPR/Cas assisted *Btc* gene disruption using a single guide RNA (sgRNA) specific for exon 2 sequence 5'-GTCTTGCAATTCTCCACTGTG-3', a corresponding oligonucleotide was cloned into the pEX-A-U6-gRNA vector as described previously<sup>290</sup>. Cas9 mRNA and sgRNA were *in vitro* transcribed by using the Ambion Maxiscript SP6 kit (Thermo Fisher Scientific). C57BL/6N zygotes were injected with Cas9 mRNA (50 ng/μl) and sgRNA (100 ng/μl) and embryos were transferred into recipient NMRI mice. Potential founders were identified by PCR using the following primers: sense primer: 5'-GCTTACATGACTTCTAGCCATG-3', antisense primer: 5'-GCTAATCATGGAGGCACAGAAA-3'. Based on the detected mutations, a *PfiI*M restriction fragment length polymorphism assay was established, yielding fragments of 210 bp and 290 bp for wild-type *Btc* and a single fragment of 500 bp for the mutated *Btc* sequence. Two founder animals with the same frameshift mutation were identified (Suppl. Fig. S 3.1).

### **3.3.3.2 REVERSE TRANSCRIPTASE-PCR**

RNA was extracted from different organs with TRIZOL reagent (Invitrogen, Darmstadt, Germany) and 3 μg RNA were reverse-transcribed in a final volume of 30 μL using RevertAid reverse transcriptase (Thermo Scientific, Schwerte, Germany) according to the manufacturer's instructions. To show the qualitative mRNA expression of the *Btc*-KOs, reverse transcription-PCR (RT-PCR) was performed by using reagents from Qiagen (Hilden, Germany). The final reaction volume was 20 μl, and cycle conditions were 94°C for 5 min followed by 35 cycles of 94°C for 1 min, 58°C for 1 min, and 72°C for 1 min using the following primers: forward: 5'-GTTCTGGGTGACACTGGAGC-3', reverse: 5'-CCTTTCTCACAGATGCAGGAG-3'. The amplicon was digested by *PfiI*M (NEB, Frankfurt, Germany) for 90 min at 37°C and subject to agarose electrophoresis to reveal the mutation side. *Gapdh* was used as reference mRNA and amplified with the following primers: forward: 5'-GTGGAAGGGCTCATGACCAC-3', reverse: 5'-GCCACAGCCTTGGCAGCA-3'.

### **3.3.3.3 PANCREAS PREPARATION**

Mice were sacrificed by cervical dislocation at the age of 8 weeks, 12 months or when moribund. The pancreas was isolated, blotted dry and weighed to the nearest milligram. Parts of the head, tail and central part of the pancreas were dissected, pooled, frozen on dry ice and stored at -80°C. The remaining tissue was incubated in 4% para-formaldehyde (PFA, in phosphate-buffered saline, PBS, pH 7.4) overnight and embedded in paraffin. From mice sacrificed at the age of 1 week, the whole pancreas was either frozen on dry ice, or immediately homogenized in total in RLT buffer (Qiagen), freshly supplemented with 1%

beta-mercaptoethanol (BME, Roth, Karlsruhe, Germany) and shock-frozen in liquid nitrogen for RNA isolation, or incubated as a whole in 4% PFA overnight and embedded in paraffin.

#### **3.3.3.4 IMMUNOHISTOCHEMISTRY**

Immunohistochemistry (IHC) was performed detecting murine (m) mBTC, mTGFA, mAREG, mEREG, mACTA2, mEGFR, cleaved Caspase 3 and human (h) hBTC, hEGFR, hERBB2, hERBB3, hERBB4 on PFA-fixed, paraffin-embedded pancreatic tissue. For all immunostainings, the slides were boiled in a pressure-cooker for 15 minutes (min) in 10 mM sodium citrate buffer pH 6.0 or EDTA pH 9, blocked in 3% H<sub>2</sub>O<sub>2</sub> for 30 min and in 5% of the appropriate serum for another 30 min. The primary antibody was incubated over night at 4°C. After washing in PBS the slides were incubated with the appropriate secondary antibody for one hour at room temperature and the signal was amplified using Vectastain® ABC HRP kit (Vector, Burlingame, CA, USA) for 30 min at room temperature. As chromogen, ImmPACT™ DAB peroxidase substrate kit (Vector) was used and the sections were counterstained with hematoxylin (Roth) for 3 min. A list of primary and secondary antibodies with the corresponding dilutions is provided in Suppl. Table S 3.1.

#### **3.3.3.5 HEMATOXYLIN AND EOSIN (H&E) AND MASSON'S TRICHROME STAINING**

H&E and Masson's trichrome stainings were performed on PFA-fixed, paraffin-embedded sections of the pancreas using standard protocols.

#### **3.3.3.6 QUANTIFICATION OF REACTIVE TISSUE IN PANCREATA**

PFA-fixed, paraffin-embedded pancreas was serially sectioned and four sections per pancreas, each taken after every 10<sup>th</sup> section, H&E stained and evaluated under the light microscope by two researchers, independently. Pictures covering the total pancreas area were taken with a 100x magnification lens using a Leica DFC425C digital camera (Leica Microsystems, Wetzlar, Germany). The ratio of the measured area of reactive tissue, consisting of fibrosis, inflammation, pre-neoplastic lesions and scattered lymph nodes was recorded with LAS software version 3.8.0 (Leica Microsystems) and calculated to the measured whole pancreatic area of the section for each animal (n=4). Data were analyzed by Student's *t*-test and plotted as column bar plots in GraphPad Prism (GraphPad Prism version 5.0 for Windows, GraphPad Software, San Diego, CA, USA).

#### **3.3.3.7 RAS ACTIVITY ASSAY**

To evaluate RAS activity in the pancreata, the Active Ras Detection Kit (Cell Signaling) was used according to the manufacturer's instructions. In brief, dissected, frozen pancreas was homogenized in lysis/binding/wash buffer, freshly supplemented with phenylmethanesulfonyl fluoride, and 500 mg of the lysate were incubated with the GST-Raf1-Ras binding domain for one hour at 4° C, washed and eluted under denaturing conditions and object to an SDS-gel

electrophoresis using Mini-PROTEAN® TGX Stain-Free™ Precast Gels (BIORAD, Hercules, California, USA) and subsequent Western blot analysis detecting mRAS. Total protein was quantified using Image Lab 6.0.1 (Bio-Rad) and the amount of active RAS was referenced to total protein and plotted in GraphPad Prism. Data were analyzed by Student's *t*-test.

#### **3.3.3.8 CO-IMMUNOPRECIPITATION**

Pancreata were homogenized in a TRIS-based buffer (50 mM Tris, 150 mM NaCl, 1% NP40, 10% glycerol, 1M EDTA; freshly supplemented with protease and phosphatase inhibitors) and 350 µg of protein has been subject to immunoprecipitation targeting EGFR. For this, the lysate was incubated with 1 µg of EGFR antibody (Santa Cruz, SC-03) or 1 µg of normal IgG antibody (R&D Systems) at 4° C overnight and incubated with 50 µl of protein A magnetic beads (Cell Signaling) for 30 min at room temperature. After washing the precipitate was eluted under denaturing conditions and applied to a Western blot detecting ERBB2 (Santa Cruz, SC-284), ERBB3 (Santa Cruz, SC-285) and EGFR as control.

#### **3.3.3.9 HISTOPATHOLOGICAL GRADING**

The pancreatic sections were analyzed by two researchers, independently, in a blinded fashion. The area of acinar cells, ADM, PanIN1-3, PDAC and fibrosis was determined by point counting in five randomly selected areas of H&E and Masson's trichrome stained sections of four mice using established histomorphological criteria<sup>205-207</sup>. For this, a grid of crosses was laid over stained sections using a netScope viewer software of the (Net-Base Software GmbH, Freiburg, Germany) and crosses hitting the appropriate structure were counted and calculated to the sum of crosses hitting the area of the pancreas. Data were analyzed by 2-way-ANOVA and plotted as column bar plots in GraphPad Prism.

#### **3.3.3.10 WESTERN BLOT ANALYSIS**

Pancreas of animals was homogenized in Laemmli-extraction buffer as described previously<sup>175</sup>. Protein samples with equal concentrations were electrophoresed on 10% polyacrylamide-sodium dodecyl sulfate gels and blotted to PVDF-membranes (GE Healthcare, Munich, Germany). The membranes were blocked with 5% milk and incubated with the primary antibodies overnight at 4°C. After washing, the membranes were incubated in the appropriate horseradish peroxidase-conjugated secondary antibody. Immunoreactive bands were visualized by chemiluminescence with an ECL kit (GE Healthcare or Thermo Scientific). Antibodies and dilutions are supplied in Suppl. Table S 3.2. Densitometrical analyses were performed with ImageJ 1.52a and plotted in GraphPad Prism (GraphPad Prism version 5.0).

#### **3.3.3.11 REAL-TIME-PCR**

RNA was extracted from shock-frozen pancreatic tissues with RNeasy kit (Qiagen) and cDNA was synthesized using RevertAid reverse transcriptase (Thermo Scientific) according to the

manufacturer's instructions. Quantitative mRNA expression analysis was performed by quantitative real-time RT-PCR (qRT-PCR) using the StepOne™ Real Time PCR-Systems (Applied Biosystems™, Waltham, Massachusetts, USA). 1 µL of cDNA in final reaction volume of 10 µl were used and the final primer concentration was 0.5 µM. Cycle conditions were 50 °C for 2 min, followed by 95 °C for 2 min followed by 40 cycles of 95 °C for 15 s, 60 °C for 15 sec, and 72 °C for 1 min. For Quantification the threshold cycle ( $C_T$ ) number was used. We performed no-template control and no-RT control assays, which produced negligible signals with  $C_T$  values that were greater than 35. Experiments were performed in duplicates or triplicates for each sample. Primers used for qPCR are listed in Suppl. Table S 3.3. Transcript copy numbers were normalized to ribosomal protein L30 (*Rpl30*).

### **3.3.3.12 CELL CULTURE AND STIMULATION EXPERIMENTS**

PANC-1 and BxPC-3 cells were purchased from CLS (Cell lines service, Eppelheim, Germany) four months before the experiments were performed. All human permanent cell lines in the CLS cell bank have been authenticated by using the STR DNA profiling analysis. Mycoplasma testing will be done every 6 months for all cultured cells using a mycoplasma detection kit (PlasmoTest, InvivoGen, Toulouse, France). Both cancer cell lines were maintained at 37 °C and 5% CO<sub>2</sub>. PANC-1 cells were cultured in Dulbecco's Modified Eagle Medium (DMEM, Merck), BxPC-3 cells in Roswell Park Memorial Institute 1640 medium (RPMI, Merck), both supplemented with 10% fetal bovine serum (FBS, Merck) and 1% Penicillin/Streptomycin (Merck). At a confluence of 90%, cells were starved overnight (1% FBS) and stimulated the next day with 50 ng/ml of recombinant human BTC (rhBTC, R&D Systems #261-CE) for 5 and 15 min. Cells were then lysed in a TRIS-based buffer (50 mM Tris, 150 mM NaCl, 1% NP40, 10% glycerol, 1M EDTA; freshly supplemented with protease and phosphatase inhibitors (Roche)) and subject to Western blot analysis detecting phosphorylation and total expression of the ERBB receptors.

### **3.3.3.13 3-D PRIMARY CELL CULTURE**

For acini isolation 3-week-old wildtype mice were dissected, pancreata were washed twice in sterile ice-cold PBS and immediately minced and digested twice in collagenase P solution (Hanks Balanced Salt Solution (HBSS, Sigma, Taufkirchen, Germany), 5% FBS, 0.2 mg/mL soybean trypsin inhibitor (STI, Sigma), 0.2 mg/mL Collagenase P (Roche, Penzberg, Germany) at 37 °C for 10 min. The pancreatic tissue was gently pressed and washed through a 100 µm cell strainer and incubated in red blood cell lysis buffer (Roth) for 10 min at 37°C. The acini recovered for 1 hour in 3D-culture medium (RPMI 1640, 1% FBS, 1% Penicillin/Streptomycin, 001 mg/ml STI, 1 µg/ml dexamethasone (Sigma)). Prior cell seeding, the culture dishes were coated with a gel of rat tail collagen I (Invitrogen, Carlsbad, California, USA) and RPMI medium, supplemented with NaHCO<sub>3</sub> to adjust the pH for at least 1 hour at

37°C. For seeding, the cell suspension was mixed with the collagen I coating gel in a ratio 1:3, gently placed into the coated dishes and solidified for 1 hour at 37 °C, 5% CO<sub>2</sub>. The matrix was then coated with warm 3D culture medium and stimulated or left untreated. This is a modified protocol of Qu *et al.*<sup>291</sup>. For stimulation experiments, 3D culture medium was supplemented with rhBTC or rhTGFA or left untreated and investigated under a light microscope at days 0, 4 and 5 after treatment. The number of transdifferentiated cells was estimated by two researchers, independently.

### **3.3.3.14 STATISTICS**

Data are presented as means±SEM and compared by two-tailed unpaired Student's *t*-test, and in the case of more than two groups by analysis of variance (ANOVA) and Tukey's multiple comparison test. All data were analyzed with GraphPad Prism (GraphPad Prism version 5.0 for Windows, GraphPad Software, San Diego, CA, USA). *P*-values<0.05 were considered statistically significant.

## **3.3.4 RESULTS**

### **3.3.4.1 THE LACK OF BTC IN KC MICE RESULTS IN A DECREASE OF TUMOR BURDEN AND DECREASED EGFR PHOSPHORYLATION.**

To evaluate the function of BTC in PDAC we generated a BTC knockout mouse (BTC<sup>-/-</sup>) by CRISPR/Cas9 technology. Two founder animals with monoallelic insertions of 1 bp were identified. The insertion of 1 bp leads to a shift in the reading frame in *Btc* exon 2. The mutant *Btc* transcripts encode 27 amino acids (aa) of the extracellular BTC domain, followed by 31 aa missense sequence and a premature termination codon after 58 aa (Suppl. Fig. S 3.1 A). BTC<sup>-/-</sup> mice were viable and showed no macroscopic phenotype, and bred in a Mendelian ratio (data not shown). RT-PCR analysis confirmed the mutated Exon2 of the *Btc* gene (Suppl. Fig. S 3.1 B) and an IHC confirmed the loss of BTC (Suppl. Fig. S 3.1 D). Crossed into the KC background B<sup>-/-</sup>KC mice showed at the age of eight weeks and twelve months no differences in body and relative pancreas weight were detected (Suppl. Fig. S 3.1 C). All B<sup>-/-</sup>KC animals were still vital at the time of dissection at 12 months while KC mice started deceasing already with seven months (Figure 3.2 A). Reactive tissue area of the pancreas (fibrosis, inflammation, ADM,) were determined at the age of eight weeks (Figure 3.2 B,C) revealing a 10-fold decrease in the amount of reactive tissue in B<sup>-/-</sup>KC mice compared to KC mice indicating a decelerated PDAC development. In pancreata of 12-month-old mice, we revealed decreased PDAC progression upon BTC depletion. More low-grade lesions and significantly less invasive carcinoma were identified compared to age-matched KC mice (Figure 3.2 F,G). Western blot analysis revealed reduced EGFR expression and phosphorylation in pancreata of 8-week-old and 12-month-old B<sup>-/-</sup>KC mice compared to age-matched KC mice (Figure 3.2 H,I). These data

indicate that the depletion of BTC attenuates tumor initiation and progression by downregulating EGFR signaling and resulting in a prolonged survival.

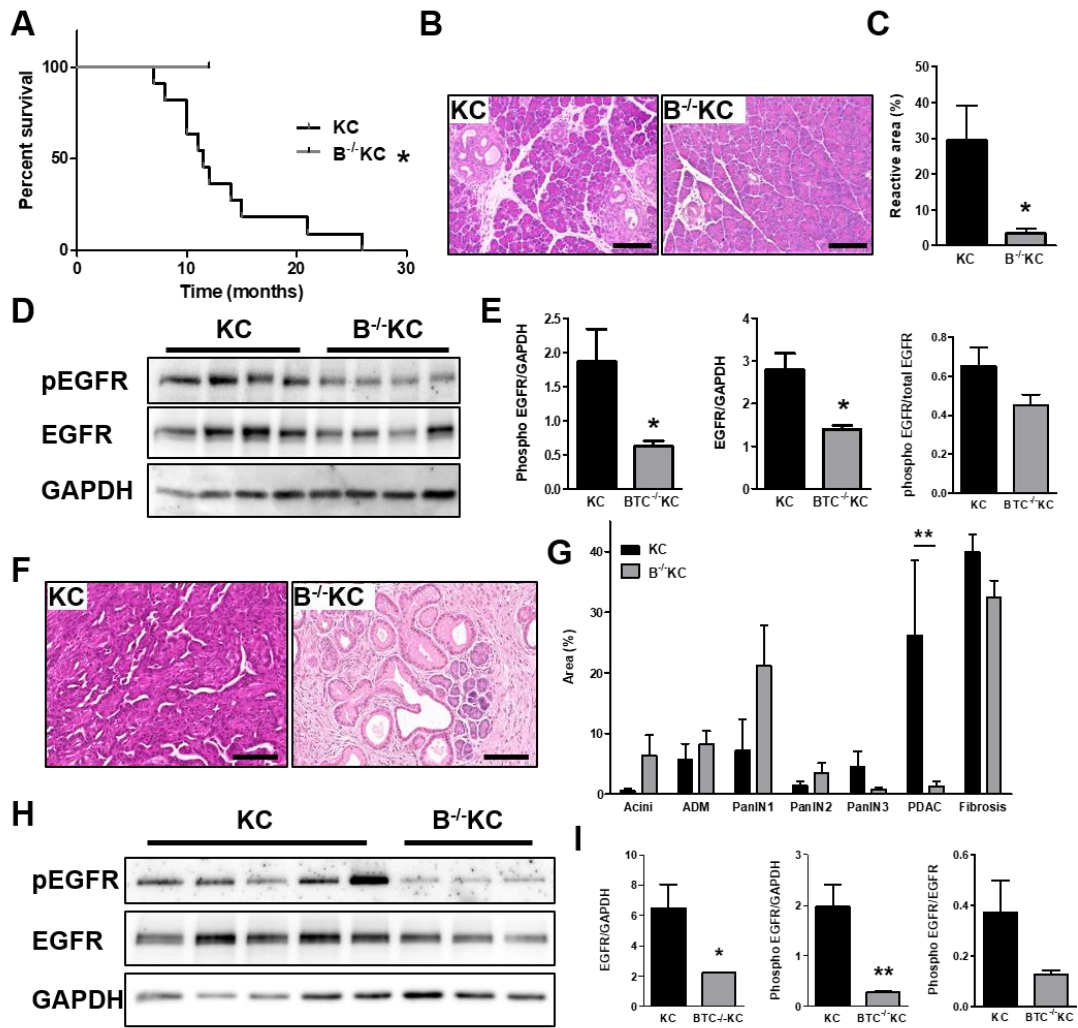


**Figure 3.2: Characterization of B<sup>-/-</sup>KC mice**

**A** Kaplan-Meier-Curve demonstrating the survival of KC and BKC mice. **B** Representative H&E stainings of pancreata of 8-week-old B<sup>-/-</sup>KC mice compared to age-matched KC littermates. **C** Morphometric analysis of reactive tissue in the pancreas of B<sup>-/-</sup>KC (3,8%) and (KC 31,8%) mice. Data were analyzed by Student's *t*-test. **D** Western blot analysis and **E** corresponding densitometrical analyses showing EGFR expression and phosphorylation in pancreata of 8-week-old B<sup>-/-</sup>KC mice compared to age-matched KC pancreata. GAPDH served as reference protein. **F** Representative H&E stainings with **G** histopathological grading of pancreata of 12-month-old mice. **H** Western blot and **I** densitometrical analysis of pancreata of 12-month-old mice showing EGFR expression and phosphorylation in B<sup>-/-</sup>KC mice compared to KC mice. Scale bars: 100 µm. All data were generated as means±SEM. \**P*<0.05, \*\**P*<0.01.

### 3.3.4.2 BTC IS EXPRESSED IN HUMAN PDAC SAMPLES, IN HUMAN PDAC CELL LINES AND IN PANCREATA OF KC MICE.

By IHC, BTC was detected predominantly in the islets of Langerhans and in ducts and acini of human normal pancreas (NP) (Figure 3.3 A). In human PDAC samples (6/6) BTC was identified in PanIN and the adjacent stroma (Figure 3.3 A), and Western blot analysis revealed BTC expression in 5/6 human hPaCaCells (Figure 3.3 B). These data indicate a role for BTC in PDAC development. Since BTC has binding affinities for EGFR and ERBB4 and is also able

to indirectly activate the other ERBB receptors, we evaluated the phosphorylation status of all ERBB receptors upon BTC stimulation in two hPaCaCells. Stimulation of PANC-1 and BxPC-3 cells with 50 ng/ml hBTC activated all receptors at 5 and 15 min, while ERBB3 was constitutively activated, basally, in both cell lines (Figure 3.3 D). In addition, we detected all ERBB receptors by immunostaining in human PDAC (Suppl. Fig. S 3.2). These data indicate that the ERBB system is involved in human PDAC. The pancreata of KC mice revealed a strong positive immunostaining for endogenous BTC expression in low- and high grade PanIN in 5/6 samples (Figure 3.3 D).

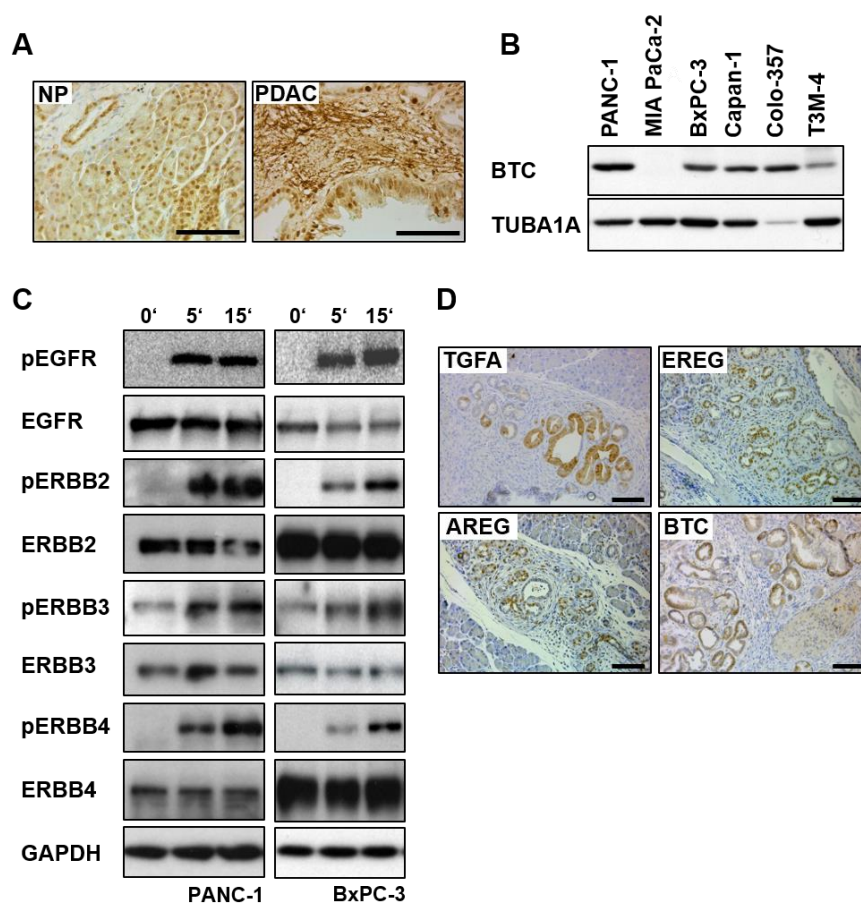


**Figure 3.3: BTC is expressed in human PDAC samples, in human PDAC cell lines and in pancreata of KC mice.**

**A** Immunohistochemistry staining against BTC in human normal pancreas (NP) and in human pancreatic cancer specimen. **B** Western blot analysis of BTC expression in 5/6 human pancreatic cancer cell lines. TUBA1A served as a reference protein. **C** PANC-1 (left panel) and BxPC-3 (right panel) were stimulated with BTC for 5 and 15 minutes. Western blot analysis shows ERBB receptor expression and phosphorylation. GAPDH served as reference protein. **D** Immunohistochemistry stainings against BTC, TGFA, AREG, and EREG in PanIN of KC mice. Scale bars: 100  $\mu$ m.

### **3.3.4.3 THE OVEREXPRESSION OF BTC IN KC MICE LEAD TO EARLY ONSET OF PDAC AND HIGH MORTALITY.**

To investigate how BTC could influence PDAC, we overexpressed BTC in a murine PDAC model. We crossed ubiquitously overexpressing BTC mice<sup>117</sup> into the KC background

(*Ptf1a<sup>cre/+</sup>;Kras<sup>G12D/+</sup>;Btc<sup>tg/+</sup>*, herein referred to as BKC mice). BKC mice developed cachexia after six weeks and lost up to 25% of their body weight within the following two weeks (Figure 3.4 A). The major cohort of BKC mice (13/18) died at 2 months (median survival: 2.75 months), whereas KC mice had a median survival of 11 months (Figure 3.4 B). Up to the age of eight weeks, the relative pancreas weight of BKC mice was unchanged compared to the pancreas of KC mice, but at the age of 12 months the relative pancreas weight was significantly reduced in BKC mice (Figure 3.4 C). H&E stainings of the pancreata of 1-week-old mice of both groups appeared normal (Figure 3.4 D). Already at the age of four weeks up to two thirds of the BKC pancreata were interfused by inflammation, fibrosis, ADM and low-grade PanIN (Figure 3.4 D), while these structural abnormalities were hardly observed in age-matched KC pancreata (Figure 3.4 D). At the age of eight weeks, still more than 70% of the pancreata looked normal in KC mice (Figure 3.4 D). However, pancreata of age-matched BKC mice were completely replaced by low- and high-grade PanIN and invasive carcinoma and a massive amount of desmoplasia (Figure 3.4 D,F). Desmoplasia were indicated by alpha-smooth-muscle-actin (ACTA2) staining (Figure 3.4 E), detecting activated pancreatic stellate cells. A Masson's trichrome staining revealed a massive amount of collagen fibers (Figure 3.4 F) in BKC animals compared to age matched KC mice (Figure 3.4 F). 75% of KC mice developed high grade PanIN and carcinoma during their lifetime (Figure 3.4 D), while 100% of BKC mice had developed carcinomas already at the age of eight weeks. BTC overexpression in the KC mouse leads to a very early onset of PDAC, cachexia and to a drastic increase in mortality.

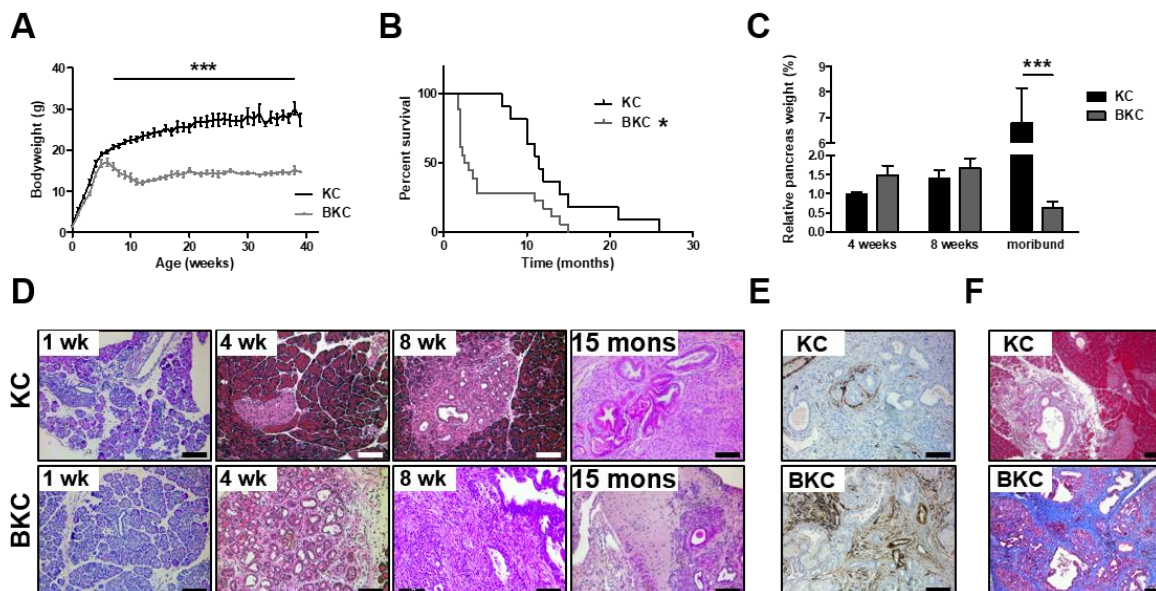


**Figure 3.4: BTC induces adverse events in KC mice**

**A** Body weight curve of BKC mice compared to KC littermates. Data were analyzed by 2-way-ANOVA. **B** Kaplan-Meier-Curve depicting the survival of BKC mice (median survival: 2,75 months) compared to KC mice (median survival: 11 months). Data were analyzed using a Log-rank test. **C** Relative pancreas weights of BKC mice at the ages of four and eight weeks and twelve months compared to age-matched KC mice. Data were analyzed by 1-way-ANOVA and Tukey's multiple comparison test. **D** H&E staining of pancreata of 1-week-old; 4-week-old;

8-week-old and mice at the age of 15 months. **E** Representative immuno-staining of ACTA2 in pancreata of 8-week-old KC and BKC mice to reveal the amount of activated stellate cells. **F** Masson's Trichrome staining of pancreata of 8-week-old KC and BKC mice depicting connective tissue in BKC mice. Scale bars: 100  $\mu$ m. All data were generated as means $\pm$ SEM. \* $P$ <0.05, \*\*\* $P$ <0.001.

#### **3.3.4.4 BTC ACTIVATES THE ERBB RECEPTORS, ENHANCES RAS ACTIVITY AND INDUCES ADM.**

BTC is able to bind both autonomous receptors, EGFR and ERBB4, and due to receptor hetero-dimerization, BTC also activates ERBB2 or ERBB3. We investigated the ERBB receptor phosphorylation by Western blot analysis upon BTC overexpression in KC mice at the age of one week, an appropriate time point, since pancreatic tissues were still normal and, most importantly, had a similar cellular composition. BTC overexpression in KC mice resulted in the activation of EGFR, ERBB2 and ERBB4. ERBB3 was not phosphorylated in both groups. ERBB expression levels were similar in both groups (Figure 3.5 A,B). To evaluate the receptor dimerization behavior upon BTC activation, we performed co-immunoprecipitations. In BKC mice EGFR bound ERBB2, but not ERBB3. KC mice had much less EGFR/ERBB2 dimers even though, when the reduced amount of pulled-down EGFR protein was considered. Due to the high heterogeneity in pancreata of BKC mice at the age of eight weeks, we compared tumors of 8-week-old BKC mice with tumors of 12-month-old KC mice presenting a similar tumor burden. The amount of EGFR/ERBB2 dimers in KC pancreata was again lower compared to BKC mice (Figure 3.5 C). ERBB3 did not bind to EGFR in any condition. There are several ways for BTC to accelerate PDAC development. KRAS<sup>G12D</sup> is the initiating mutation in PDAC but the latency for tumor development is very long and often, other stimuli are necessary to induce RAS dependent transformation of normal tissue<sup>292-294</sup>. We assumed that BTC could be a driver of RAS activity to accelerate tumor development. A RAS activity assay of pancreata of 8-week-old KC mice and BKC mice revealed that BKC mice harbor a significantly higher amount (3-fold) of active RAS compared to KC mice (Figure 3.5 D,E). To investigate which receptors transmit BTC induced RAS activation, we studied RAS activity in the pancreata of BKC mice with either EGFR (E1 KO;BKC), ERBB2 (E2 KO;BKC) or ERBB4 (E4 KO;BKC) depleted. We revealed that BTC-mediated RAS activity was exclusively transmitted by EGFR (Figure 3.5 F). Also crucial for PDAC is ADM development. Since it is known that BTC regulates (trans-) differentiation<sup>106-110</sup>, we assumed that BTC might be involved in trans-differentiating acinar to duct cells, thereby accelerating the onset of PDAC. We isolated wildtype murine acinar cells, embedded them into a 3-D collagen matrix and stimulated with BTC or TGFA, for 5 days (Figure 3.5 G). While wildtype cell clusters did not show signs of transformation, the majority of BTC stimulated cells transformed into a duct-like shape, as observed in TGFA treated cells (data not shown). Through specific signaling cascades or in a tissue-dependent manner, ERBB4 is able to synthesize four different splice isoforms. We hypothesized that BTC might be able to induce alternative splicing in the Erbb4

gene causing splice-form-dependent signaling in the KC pancreas. However, we revealed by real-time PCR that BTC had no significant influence on *ErbB4* splicing in pancreata of KC mice (Figure 3.5 H).

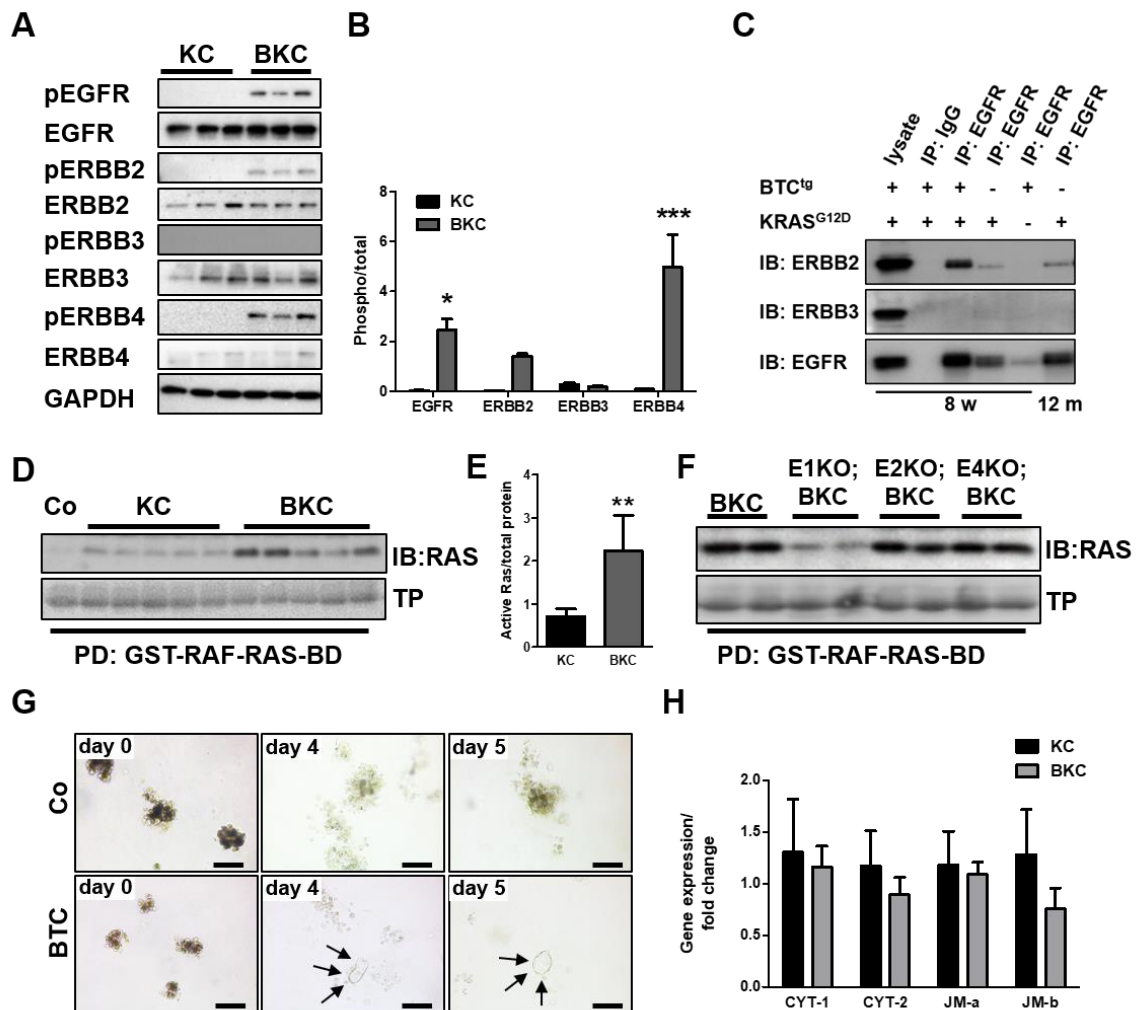


**Figure 3.5: BTC activates the ERBB receptors, enhances RAS activity and induces ADM**

**A** Western blot and **B** corresponding densitometrical analysis showing the phosphorylation of EGFR, ERBB2, ERBB3 and ERBB4 in pancreata of 1-week-old BKC mice compared to age-matched KC mice. GAPDH served as reference protein. Data were analyzed by 2-way-ANOVA with Bonferroni post-test. **C** Co-immunoprecipitation of EGFR and indicated receptors in lysates of pancreata of mice with different genotypes (indicated with a + or – above the IBs) at the age of 8 weeks (w) and of KC mice at the age of 12 months (m). **D** RAS activity assay with **E** corresponding densitometrical analysis illustrating the abundance of active RAS protein in pancreata of KC mice upon BTC overexpression. Total protein (TP) served as reference. Data were analyzed with a Student's *t*-test. **F** RAS activity assay comparing pancreata of BKC mice with pancreata of BKC mice lacking either EGFR (E1KO;BKC), ERBB2 (E2KO;BKC) or ERBB4 (E4KO;BKC). **G** 3-D primary tissue culture of acinar cells of 3-week-old wildtype mice, treated with BTC compared to untreated cells (Co). Scale bars: 100  $\mu$ m. **H** Real-time PCR targeting ERBB4 splice forms in 1-week-old BKC and KC mice. PD, pull down, IB, immunoblot, GST-RAF-RAS-BD, glutathione-S-transferase-RAF-RAS-binding domain, arrows indicate ductal structures. All data were generated as means  $\pm$  SEM. \**P*<0.05, \*\**P*<0.01, \*\*\**P*<0.001.

### 3.3.4.5 ERBB2 AND ERBB4 AFFECT THE TUMOR BURDEN IN BKC MICE.

BTC signaling is mediated by EGFR enhancing RAS activity, but in order to reveal, whether ERBB2 and ERBB4 are involved in BTC-mediated PDAC, we knocked out ERBB2 or ERBB4 individually. The lack of ERBB2 or ERBB4 in the BKC mouse (E2 KO;BKC and E4 KO;BKC,

respectively) showed different effects. While all groups grew similar until week six after birth, E2 KO;BKC mice had significantly reduced body weight compared to BKC mice and E4 KO;BKC mice showed a significantly increased body weight compared to BKC littermates (Figure 3.6 A), predicting a better outcome for mice with an ERBB4 depletion. Indeed, the Kaplan-Meier curve depicts, with a median survival of 15 months the longest survival in E4 KO;BKC mice, but also, E2 KO;BKC mice present with a median survival of 12,5 months a significantly prolonged survival compared to BKC mice (median survival: 2.75 months) (Figure 3.6 B), indicating oncogenic functions for both receptors. The relative pancreatic weight of E2 KO;BKC mice was decreased compared to that of BKC mice at the age of eight weeks ( $P=0,059$ ) (Figure 3.6 C, left panel) and was similarly lower in moribund mice (Figure 3.6 C, right panel). The H&E (Figure 3.6 D, left panel) and Masson's trichrome (Figure 3.6 D, right panel) staining of E4 KO;BKC pancreata revealed a penetration of cancer cells similar to BKC mice, presenting with fibrosis, PanIN and carcinoma, while the lack of ERBB2 rather resembled a picture of atypical flat lesions mixed with ADM and low grade PanIN, with the same amount of fibrosis compared to BKC pancreata, but with a decreased penetration of (pre-)neoplastic tissue, since acinar tissue was frequently observed. Western blot analysis revealed that the loss of ERBB4 induced changes in the ERBB signaling network (Figure 3.6 E,F). The lack of ERBB4 resulted in a significantly decreased EGFR and ERBB2 phosphorylation, and it induced enhanced ERBB3 activation. Further, the lack of ERBB4, resulted in a significant downregulation of MAPK and SAPK signaling. In 1-week-old mice, EGFR activation was significantly enhanced in E4 KO;BKC pancreata, also MAPK activation was increased (Suppl. Fig. S 3.3 A,B). Compared to the knockout of ERBB4, the lack of ERBB2 only resulted in significantly decreased SAPK signaling and in decreased EGFR phosphorylation ( $P=0.055$ ). But no compensation of other ERBB receptors was observed (Suppl. Fig. S 3.4 A,B). Despite decreased SAPK signaling acinar cells of ERBB2 KO;BKC mice demonstrated cleaved caspase-3 positivity in immunostainings (Suppl. Fig. S 3.4 C).

#### **3.3.4.6 THE LOSS OF EGFR ALMOST RESCUES THE BTC-MEDIATED PHENOTYPE IN 8-WEEK-OLD KC MICE COMPLETELY.**

We deleted EGFR pancreas-specifically and revealed that EGFR depleted BKC mice (EGFR KO;BKC) had increased body weights indicating a better physical condition at the age of two and twelve months (Figure 3.7 A, left panel). 100% of EGFR KO;BKC mice were still vital at the time of dissection (12 months) indicating a drastically prolonged survival compared to BKC mice (data not shown). Their pancreas weights were significantly decreased in 8-week-old and increased in 12-month-old mice compared to BKC mice (Figure 3.7 A, right panel) implying a better condition. Histology analysis revealed a predominantly normal pancreas in EGFR KO;BKC mice, albeit with multiple foci presenting ADM (H&E, Figure 3.7 B), but with a

complete lack of fibrosis, shown by Masson's trichrome staining to pancreata of BKC mice (Figure 3.7 B). ADM in 8-week-old mice did not occur due to incomplete homologous recombination of the EGFR locus, as observed in Ardito *et al.* and Navas *et al.*<sup>156,273</sup>, as verified in the negative immunostaining targeting EGFR (Figure 3.7 E). However, ADM were positive for ERBB2, ERBB3 and ERBB4 (Figure 3.7 E). Interestingly, Western blot analysis revealed that the lack of EGFR comes along with a decrease in phosphorylation and expression of ERBB2, ERBB3 and full length ERBB4 (Figure 3.7 C,D). However, we revealed that the ICD of ERBB4 was highly phosphorylated in the pancreata of EGFR KO;BKC mice compared to BKC mice indicating compensational ERBB4 signaling for ADM development upon the loss of EGFR (Figure 3.7 C,D).

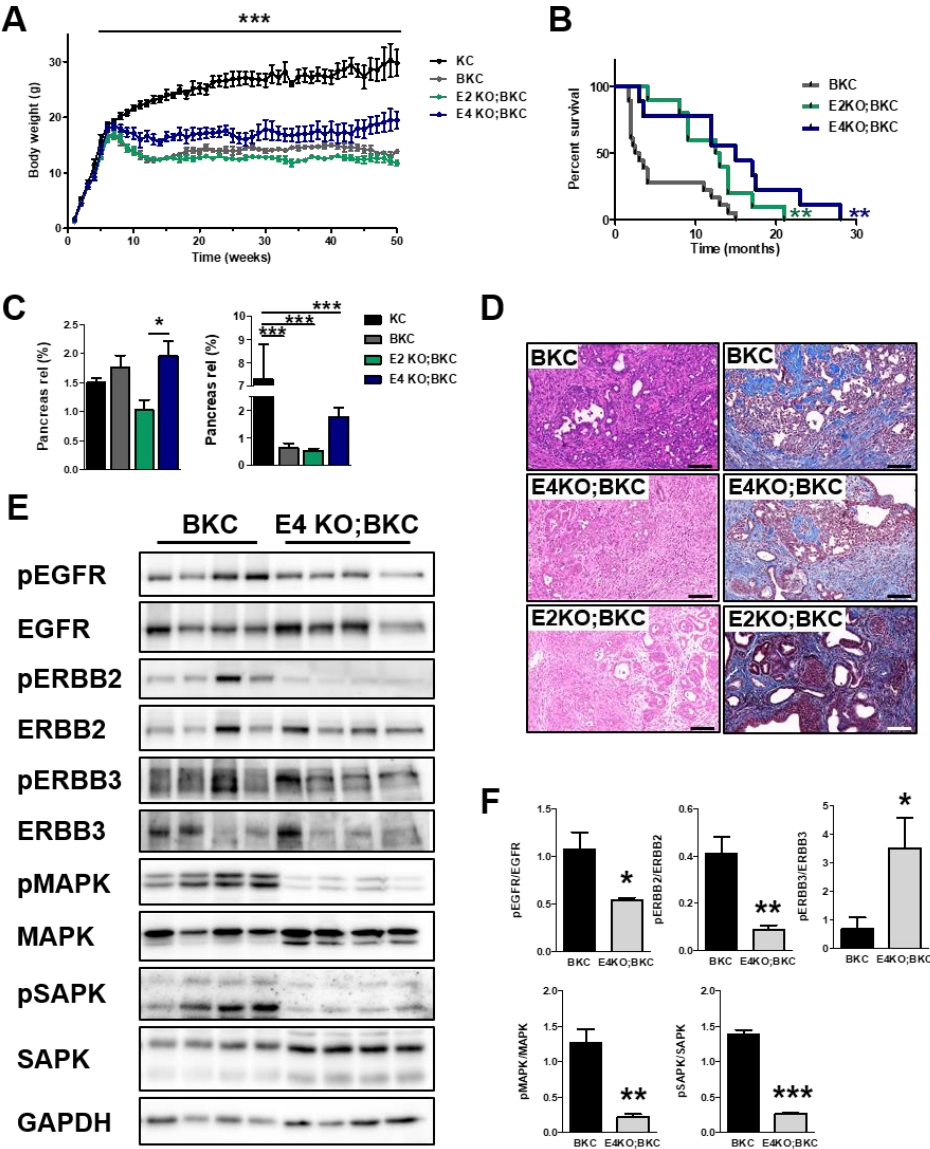


**Figure 3.6: ERBB2 and ERBB4 affect the tumor burden in BKC mice**  
**A** Body weight curves all groups. Data were analyzed by 2-way-ANOVA. **B** Kaplan-Meier-Curve depicting the survival of E2 KO;BKC mice (median survival: 12.5 months) and E4 KO;BKC mice (median survival: 15 months)

compared to BKC mice (median survival: 2,75 months). Data were analyzed using a Log-rank test. **C** Relative pancreatic weight of all groups of 8-week-old mice (left panel) and of 12-months-old mice (right panel) compared to E2 KO;BKC, E4 KO;BKC and KC mice. Data were analyzed by ANOVA and Tukey's multiple comparison tests. **D** Histology of BKC mice compared to E2KO;BKC and E4KO;BKC mice at 8 weeks represented by H&E (left panel) and Masson's trichrome staining (right panel). **E** Western blot analysis with **F** corresponding densitometrical analysis comparing pancreata of 8-week-old BKC mice to E4KO;BKC littermates. Data were analyzed by ANOVA and Tukey's multiple comparison tests. \* $P < 0.05$ , \*\* $P < 0.01$ , \*\*\* $P < 0.001$ . Scale bars: 100  $\mu\text{m}$ .

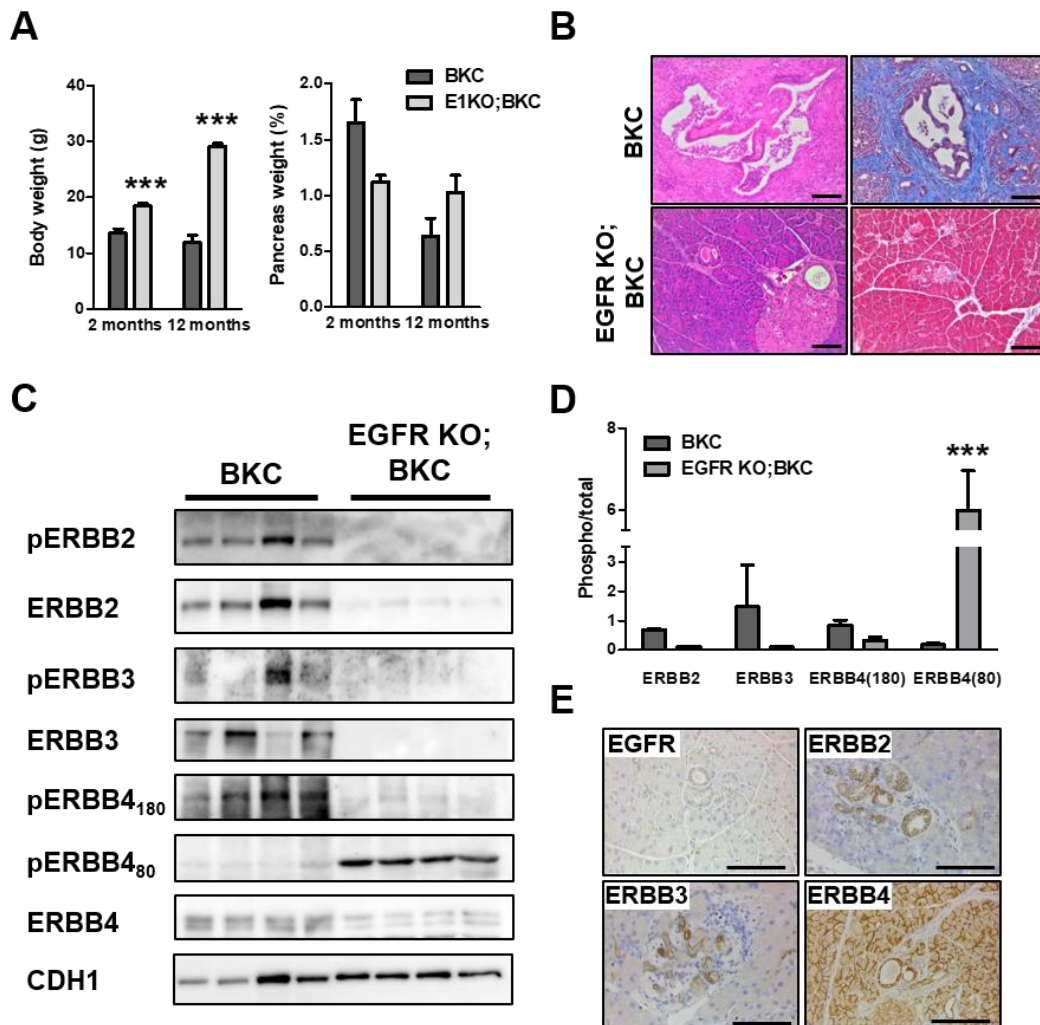


**Figure 3.7: The lack of EGFR in BKC mice revealed major changes in body weight, histology and in ERBB signaling**

**A** Body and relative pancreas weights of EGFR KO;BKC mice compared to BKC mice. Data were analyzed by ANOVA and Tukey's multiple comparison test. **B** Representative H&E (left panel) and Masson's trichrome (right panel) stainings of pancreata of BKC mice and EGFR KO;BKC mice. **C** Western blot analysis and **D** corresponding densitometrical analysis showing the phosphorylation and expression of ERBB2, ERBB3 and full length ERBB4, and the phosphorylation of the ICD of ERBB4. CDH1 served as reference protein. Data were analyzed by ANOVA and Tukey's multiple comparison test. **E** Immunohistochemistry stainings against EGFR, ERBB2, ERBB3 and ERBB4 of pancreas samples of 8-week-old EGFR KO;BKC mice. Scale bars: 100  $\mu\text{m}$ . \*\*\* $P < 0.001$ .

### 3.3.5 DISCUSSION

PDAC belongs to the deadliest malignancies, worldwide<sup>198</sup>. EGFR is crucial for the development of oncogenic KRAS-induced PDAC development<sup>156,273</sup>. However, targeting EGFR is only marginally beneficial with a small subset of patients responding to EGFR-targeted therapy<sup>252</sup>. Since EGFR is only one family member of four RTKs, either working autonomously or as partner of ERBB2, ERBB3 or ERBB4, we assumed that the remaining ERBB receptors had been underestimated in recent years and could also play an important role in PDAC. In particular, because ERBB ligands, specific for ERBB4, have been implicated in PDAC development or progression. To estimate the power of ERBB ligands in PDAC, we deleted BTC (specific for EGFR and ERBB4) in the KC mouse model (B<sup>-/-</sup>KC) and revealed that the initiation and progression of PDAC was decelerated. A 100% rate of viable B<sup>-/-</sup>KC mice at the age of 12 months also suggests increased survival rates. The benefits of BTC deletion might stem from decreased EGFR expression and phosphorylation levels, which we observed in B<sup>-/-</sup>KC pancreata during all investigated ages. To our knowledge, we are the first group, which deleted an ERBB ligand in PDAC. It is intriguing to observe that the deletion of only one ERBB ligand can be powerful enough to modulate EGFR regulation and PDAC progression, in particular, because in human and in murine PDAC, almost all seven EGFR ligands are expressed abundantly and could, compensate the loss of one single ligand. We provide evidence that BTC is functionally involved in murine PDAC, since its loss affects the KC mouse so powerful and since it is also expressed in human PDAC, hPaCaCells and in PanIN of all our investigated KC mice. In hPaCaCells, it activates all receptors of the family. At the age of eight weeks, BKC pancreata presented PDAC and desmoplasia and BKC mice displayed a decrease in the median survival of almost nine months compared to KC mice. This is a drastic phenotype, when compared to the overexpression of the EGFR ligand TGFA presenting IPMN-like lesions, and showing only low-grade lesions at eight weeks with a higher median survival<sup>295</sup> as BKC mice. HBEGF overexpression in KC pancreata revealed a complete replacement of the normal pancreatic tissue by low-grade lesions PanIN3 and PDAC, already at the age of two weeks<sup>265</sup>. In the latter study the soluble form of HBEGF was overexpressed, which might lead to a more drastic outcome than by using full-length. However, there is enough evidence to state that BTC is implicated in PDAC as a tumor promoting factor. BTC activates EGFR and ERBB4 and it activates ERBB2, at least by hetero-dimerization with EGFR, implying that ERBB2 and ERBB4 also play a role in BTC-mediated PDAC. KC mice have a long latency to develop tumors and although all pancreatic cells are equipped with mutated KRAS, only a subset of cells develops lesions and, at low frequency, invasive PDAC<sup>292</sup>. Studies suggest that the additional loss of tumor suppressors<sup>296</sup> or that other secondary events, *i.e.* pancreatitis<sup>293</sup> or incidences increasing KRAS<sup>G12D</sup> activity above a certain threshold<sup>294</sup>, are required to initiate

tumorigenesis. BTC could be such a factor enhancing RAS activation, mediated by EGFR and thereby possibly accelerating the onset and progression of PDAC. ERBB2 and ERBB4 are not involved in RAS activation, indicating that only EGFR homo-dimers. It is not surprising that EGFR is a crucial player in KRAS-mediated oncogenesis, since it was shown that mice do not developed PDAC in an *EGFR* depleted background<sup>156,273</sup>. EGFR is crucial for acinar cells to trans-differentiate into duct cells. The EGFR ligands TGFA and HBEGF have been implicated in this process, previously<sup>147,265</sup>. BTC has a differentiation potential in many other cell types<sup>106-110</sup> and we found that BTC is also able to transdifferentiate wildtype acinar cells into duct cells. However, BTC transgenic mice never developed ADM at any age. BTC is not an oncoprotein per se, it effects only as trigger for tumorigenesis.

While the importance of EGFR in PDAC is established in the field, the role for ERBB2 and ERBB4 are discussed controversially. *ERBB2* mRNA was reported to be expressed in 100% of PDAC samples with increased protein expression compared to normal pancreas<sup>266</sup>. A different study published overexpression of ERBB2 in PDAC only at low frequencies<sup>276</sup>. Although *ERBB2* amplification was not associated with the outcome of PDAC in a meta-analysis<sup>297</sup>, another study correlated the overexpression of ERBB2 with an aggressive phenotype<sup>278</sup>. However, to our knowledge, no functional studies regarding ERBB2 in PDAC exist, and attempts to targeting ERBB2 were rather disappointing<sup>253</sup>. The deletion of *ErbB2* in BKC mice resulted in a significantly prolonged survival, which can be explained by decelerated PDAC development, observed in the histopathology sections of the pancreata. Since ERBB2 hetero-dimerizes with EGFR, and therefore might have a function in PDAC, it is not surprising that ERBB2 depletion has a beneficial effect in BKC mice. The delay in PDAC progression might be explained by a decrease in EGFR and SAPK signaling. SAPK activity was decreased in ERBB2 depleted BKC mice, but it cannot be associated with decreased apoptosis, since cleaved caspase-3 positivity rather indicated enhanced apoptosis compared to BKC mice. Possibly, decreased SAPK signaling results in transcriptional regulation rather than in the regulation of apoptosis. The ambivalence of ERBB4 in PDAC, as in many other cancers, has emerged from studies stating tumor suppressive functions for the receptor, in that ERBB4 expression was low in PDAC tissues and hPaCaCells<sup>266</sup> and decreased in non-metastatic tumors<sup>282</sup>. Other studies showed that a constitutively active ERBB4 homo-dimer mutant inhibited colony formation in a pancreatic cancer cell line<sup>283</sup>. Other investigations rather classified ERBB4 as an oncogene, after revealing enhanced anchorage-independent growth of hPaCaCells by the stimulation of ectopic ERBB4 expression<sup>283</sup>. We also attribute ERBB4 an oncogenic function, since its knockout prolonged the survival of BKC mice enormously. The majority of pancreata of BKC mice lacking ERBB4 showed a similar histopathology as BKC mice, displaying with high-grade PanIN and carcinoma, which is not in line with the

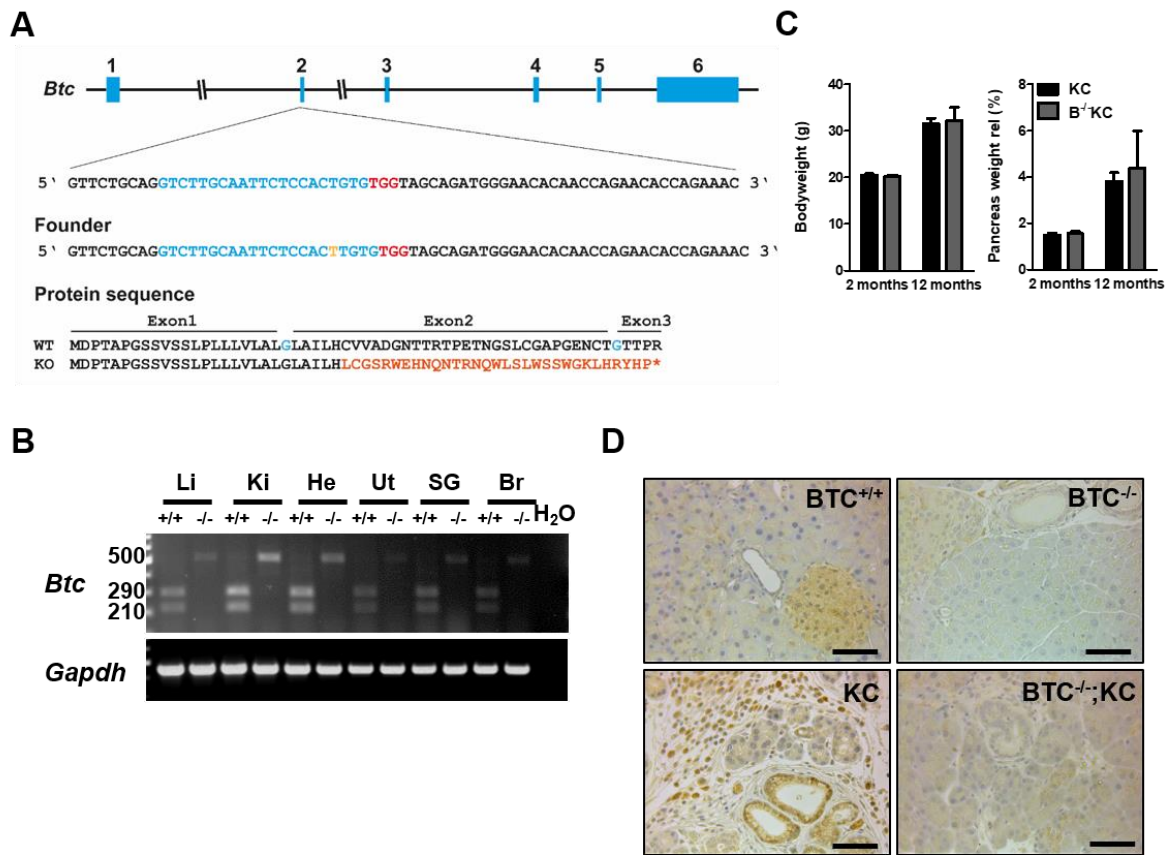
survival outcome. ERBB4 depleted BKC mice revealed decreased EGFR activity, MAPK and SAPK signalling. Decreased MAPK activation is not simply explained by decreased EGFR signaling, since this pathway was not affected by the loss of ERBB2 (also displaying decreased EGFR activity,  $P=0.055$ ). Thus, these changes must be specific to ERBB4 depletion. Considering that ERBB4 KO;BKC mice did not show a reduction in RAS activity, it is surprising that they show reduced MAPK signaling, which acts downstream of RAS. Without ERBB4 signaling, RAS might change the selection of downstream targets. The reduction in MAPK signaling might result in a reduced transcription activity of its target genes, thereby acting in an anti-tumorigenic way. In Western blots of 1-week-old mice, we detected enhanced EGFR and MAPK activity in ERBB4-depleted BKC mice indicating that EGFR/MAPK are involved in PDAC induction, but may EGFR/MAPK are not as important for PDAC progression. This supports the thesis of EGFR dependency in KC mice, but the compensatory mechanism also indicates a role for ERBB4 in PDAC initiation, too. It also suggests the causality of EGFR and MAPK activity in an ERBB4-dependent manner. Possibly, MAPK signaling is preferably regulated by EGFR/ERBB4 hetero-dimers, independently of ERBB2. Although EGFR signaling was decreased, no histopathologic changes were detected. Increased ERBB3 activation possibly compensates, in part, the loss of EGFR signaling. ERBB4 individuality results on the one hand from its capability to produce splice forms that affect ERBB4 signaling, on the other hand, ERBB4 can act through its cytosolic domain<sup>286</sup> (ICD). Both events were not observed in BKC mice.

The deletion of *Egfr* resulted in the almost complete reversion of the BKC phenotype. Pancreatic and body weights recovered and the histological landscape appeared almost normally. However, in 8-week-old BKC mice lacking EGFR, ADM lesions were observed multi-focally, which were verified to be EGFR negative, but ERBB2, ERBB3 and ERBB4 positive, indicating that, when the family is challenged, other receptors possibly take over to induce ADM. Interestingly, the lack of EGFR was accompanied by the downregulation of ERBB2, ERBB3 and full length ERBB4, but it induced ERBB4 ICD signaling indicating a compensatory mechanism upon the loss of EGFR. The ERBB4 ICD is possibly responsible for ADM development in EGFR depleted BKC mice, since all remaining receptors, which were expressed in ADM lesions were less phosphorylated. These findings are in line with a study that associated BTC with resistance to EGFR treatment in breast cancer cell lines<sup>115</sup>. The treatment with tyrosine kinase inhibitors led to acute BTC expression, induction of ERBB2/ERBB4 dimers and ERBB4 cleavage, thereby evading EGFR inhibition and reactivating of EGFR mediated signaling cascades. This is partially in line with our results regarding ERBB4 activation and ERBB4 RIP upon BTC activation in an EGFR depleted PDAC mouse model. This compensational mechanism of the ERBB family could possibly play a role

in the resistance of an EGFR inhibitor therapy in PDAC patients, and in attenuated PDAC development in EGFR/TP53-depleted KC mice<sup>156,273</sup>.

We have shown that the depletion of BTC ameliorates the outcome of PDAC and, appropriately, that BTC overexpression deteriorates PDAC prognosis in KC mice. BTC involves not only EGFR activation, it also uses their partners in crime to induce accelerated PDAC development and progression. BTC enhances RAS activity, thereby potentially transforming acinar to duct cells. The beneficial loss of ERBB2 and ERBB4 implies that both receptors are potent oncogenes in PDAC. Especially, enhanced ERBB4 ICD activation upon EGFR depletion points to a compensatory behavior of the ERBB family emphasizing their role as co-targets in combinatorial EGFR-targeted therapies. Our data promotes the results of Momeny *et al.* who revealed the pan-ERBB inhibitor dacomitinib to exhibit stronger anti-tumor effects than conventional single-receptor targeting of PDAC cells<sup>298</sup>. We suggest, that targeting the whole ERBB family, rather than a single receptor, might be promising for future custom PDAC therapy development.

### 3.3.6 SUPPLEMENTARY FIGURES



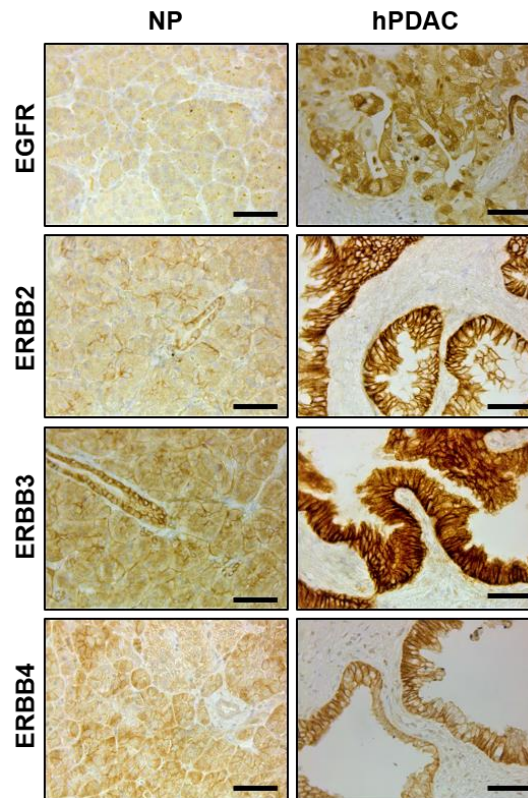
#### Suppl. Fig. S 3.1: Generation and verification of the BTC knockout mouse

**A** Partial DNA sequence of *Btc* exon 2. The sgRNA binding site is indicated in blue, the protospacer adjacent motif (PAM) in red. Insertions (orange) of 1 bp lead a shift of reading frame. Partial amino acid (aa) sequences encoded by the WT and mutant *Btc* alleles. WT BTC aa sequence in black (aa coded by adjacent non-symmetrical exons in blue), missense aa sequence in red, and the premature termination codon as asterisk. WT=wildtype. KO=knockout.

**B** Verification of the frame shift by reverse-transcriptase PCR of Li (liver), Ki (kidney), He (heart), UT (uterus), SG (salivary gland), Br (brain) after the restriction of the 500 bp amplicon with PfiMI into fragments of 290 and 210 bp, respectively. The successful cleavage by PfiMI indicates wildtype *Btc* (*Btc*<sup>+/+</sup>), while the lack of cleavage indicates the successful frame shift introduced by CRISPR/Cas9 and hence the BTC knockout (*Btc*<sup>-/-</sup>). H<sub>2</sub>O served as negative control, *Gapdh* as control PCR.

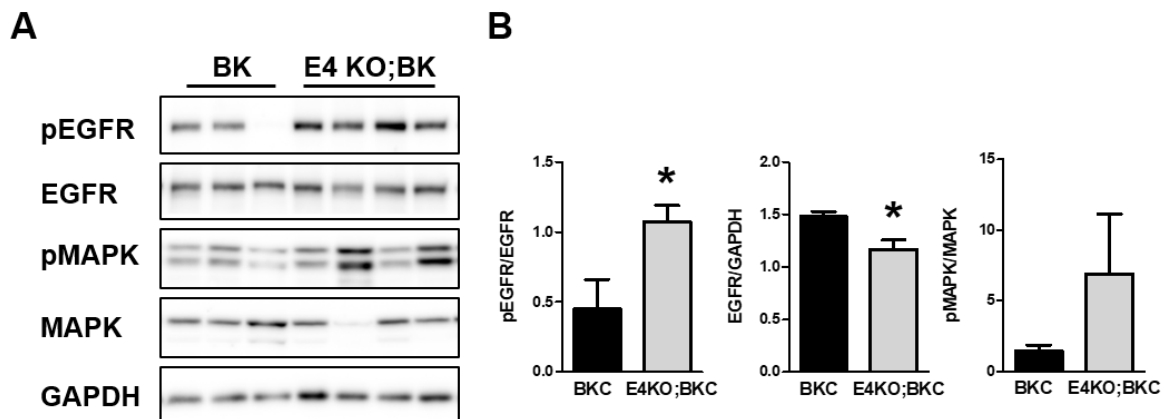
**C** The crossing of *BTC*<sup>-/-</sup> mice into the KC background showed no change of body or pancreatic weights at the ages of 8 weeks or 12 months, respectively.

**D** Immunohistochemistry targeting BTC in the pancreas of wildtype mice (*BTC*<sup>+/+</sup>) marking the islets of Langerhans and the cell membrane of acinar cells, *BTC* knockout mice (*BTC*<sup>-/-</sup>) presenting no signal for BTC staining. KC mice express BTC in premalignant lesions and *BTC*<sup>-/-</sup>;KC mice are immuno-negative for BTC. Scale bars: 100 μm.



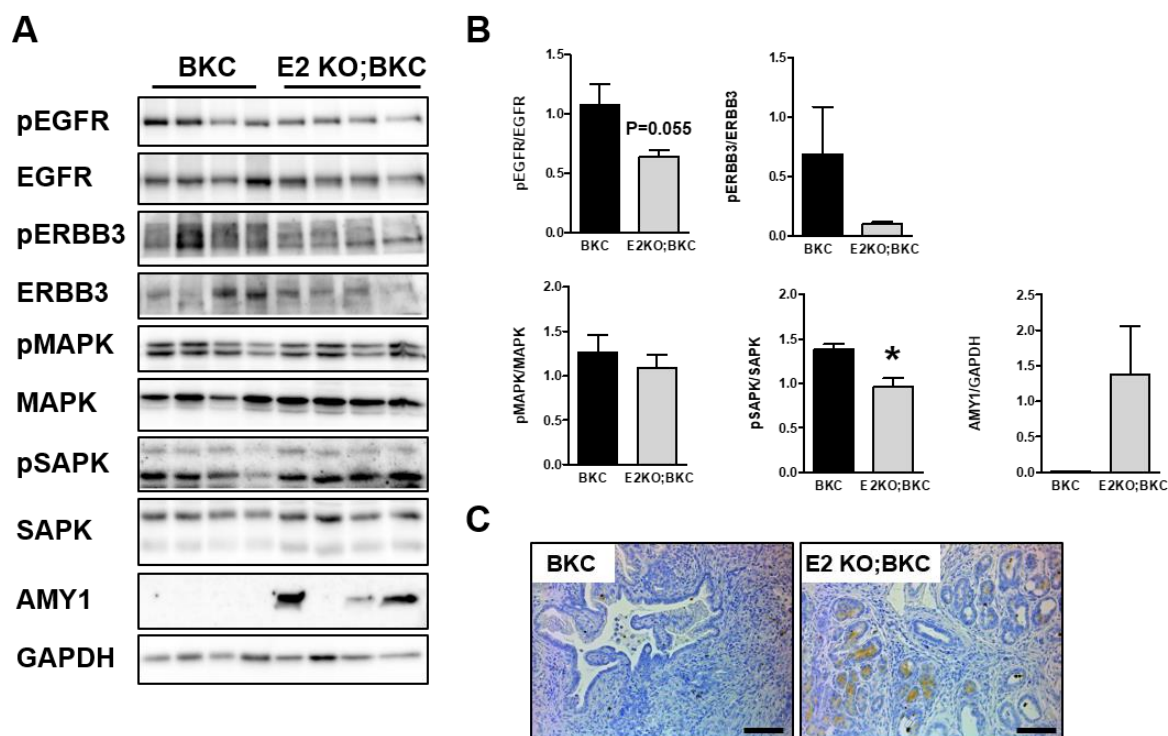
**Suppl. Fig. S 3.2: ERBB receptors in normal pancreas (NP) and in human PDAC (hPDAC)**

Immunohistochemistry in NP and PDAC reveals the expression of all ERBB receptors in PanIN of human PDAC. Scale bars: 50  $\mu$ m.



**Suppl. Fig. S 3.3: Activation of EGFR in pancreata of 1-week-old mice**

**A** Western blot and **B** corresponding densitometrical analyses of pancreata of 1-week-old ERBB4 KO;BKC mice depict enhanced EGFR activation and decreased EGFR expression compared to age-matched BKC mice. GAPDH served as reference protein. Data were analyzed by Student's *t*-test, \**P*<0.05.



**Suppl. Fig. S 3.4: Change of BKC pancreata upon ERBB2 depletion in 8-week-old mice**

**A** Western blots and **B** corresponding densitometrical analyses of BKC pancreata compared to E2 KO;BKC pancreata revealed significantly decreased SAPK activation. Data were analyzed by Student's *t*-test, \**P*<0.05. **C** IHC detecting cleaved caspase 3 in pancreata of BKC mice lacking ERBB2 compared to BKC mice, demonstrates the activation of apoptosis in acinar clusters upon the loss of ERBB2. Scale bars: 100  $\mu$ m.

### 3.3.7 SUPPLEMENTARY TABLES

**Suppl. Table S 3.1: Antibodies employed for IHC**

Antigen	Antibody	Host	Dilution
mBTC	R&D Systems, Minneapolis, MN, USA #AF1025	Goat	1:500
hBTC	R&D Systems, AF261NA	Goat	1:300
TGFA	Merck, Darmstadt, Germany, GF10	Mouse	5 $\mu$ g/ml
AREG	R&D Systems, MAB989	Mouse	5 $\mu$ g/ml
EREG	R&D Systems, AF1068	Goat	5 $\mu$ g/ml
ACTA2	Proteintech, Manchester, UK, #14395-1- AP	Rabbit	1:200
mEGFR	R&D Systems, AG1280	Goat	5 $\mu$ g/ml

<b>hEGFR</b>	R&D Sytems #AF231	Goat	1:800
<b>hERBB2</b>	Cell Signaling #4250	Rabbit	1:800
<b>hERBB3</b>	Cell Signaling #12708	Rabbit	1:500
<b>hERBB4</b>	Proteintech #19941-1-AP	Rabbit	1:400
<b>Cleaved Caspase 3</b>	Cell Signaling #9661	Rabbit	1:200
<b>Donkey <math>\alpha</math> Goat</b>	R&D Systems, #HAF109	Donkey	1:200
<b>SignalStain® Boost IHC Detection Reagent</b>	Cell Signaling #8114		Ready to use

**Suppl. Table S 3.2: Antibodies employed for Western blot**

All antibodies from Cell Signaling and mBTC (R&D) were diluted in 5% BSA in TBS-T, while all Santa Cruz antibodies were diluted in 5% milk in TBS-T.

<b>Antigen</b>	<b>Antibody</b>	<b>Host</b>	<b>Dilution</b>
<b>p-EGFR (Tyr1068)</b>	Cell Signaling, Boston, USA #3777	Rabbit	1:1000
<b>p-ERBB2 (Tyr877)</b>	Cell Signaling #2241	Rabbit	1:1000
<b>p-ERBB3 (Tyr1289)</b>	Cell Signaling #4791	Rabbit	1:1000
<b>p-ERBB4 (Tyr 1258)</b>	Abcam, Camebridge, UK ab76132	Rabbit	1:1000
<b>EGFR</b>	Santa Cruz, Heidelberg, Germany #03	Rabbit	1:500
<b>ERBB2</b>	Santa Cruz #284	Rabbit	1:500
<b>ERBB3</b>	Santa Cruz #285	Rabbit	1:500
<b>ERBB4</b>	Santa Cruz #283	Rabbit	1:500
<b>p-SAPK</b>	Cell Signaling #9251	Rabbit	1:1000
<b>SAPK</b>	Cell Signaling #9252	Rabbit	1:1000
<b>p-p44/42 MAPK (Thr202/Tyr204)</b>	Cell Signaling #4370	Rabbit	1:1000
<b>p44/42 MAPK</b>	Cell Signaling #9102	Rabbit	1:1000

<b>CDH1</b>	Cell Signaling #14472	Mouse	1:1000
<b>mRAS</b>	Cell Signaling #8832	Mouse	1:200
<b>mBTC</b>	R&D Systems #AF1025	Goat	1:2000
<b>TUBA1A</b>	Cell Signaling, # 2125	Rabbit	1:5000
<b>GAPDH</b>	Cell Signaling, #2118	Rabbit	1:5000
<b>Goat α Rabbit</b>	Cell Signaling, #7074	Goat	1:2500
<b>Rabbit α Mouse</b>	Cell Signaling, #7076	Rabbit	1:2000

Suppl. Table S 3.3: Primers employed for real time-PCR

<b>Gene</b>	<b>Primer type</b>	<b>Primer sequence</b>
<b><i>ERBB4 JM-a</i></b>	Forward Primer	5'- GTGTAACGGTCCCCTAGTC -3'
	Reverse Primer	5'- GCCATGATCACCAGGATGAAG -3'
<b><i>ERBB4 JM-b</i></b>	Forward Primer	5'- CATTGAAGACTGCATCGGCCT -3'
	Reverse Primer	5'- GCCATGATCACCAGGATGAAG -3'
<b><i>ERBB4 CYT-1</i></b>	Forward Primer	5'- GTGAAATTGGACACAGCCCTCC -3'
	Reverse Primer	5'- GGAGTCATCAAACATCTCAGCC -3'
<b><i>ERBB4 CYT-2</i></b>	Forward Primer	5'- GACTCCAATAGGAATCAGTTTGTG -3'
	Reverse Primer	5'- GGAGTCATCAAACATCTCAGCC -3'
<b><i>GAPDH</i></b>	Forward Primer	5'- GTGGAAGGGCTCATGACCAC -3'
	Reverse Primer	5'- GCCCACAGCCTTGGCAGCA -3'
<b><i>RPL30</i></b>	Forward Primer	5'- AACAACTGTCCAGCTTTGAGG -3'
	Reverse Primer	5'- GCATACTCTGTAGTATTTTCCACACG -3'

### 3.4 CONCLUSIONS & OUTLOOK

PDAC is expected to become the 3<sup>rd</sup> leading cause of cancer deaths in the near future. Although striking findings have been made during the past 20 years, treatment has improved only marginally during that period. The initializing events of PDAC development were elucidated, the mutations resulting in PanIN development and aberrant signaling were revealed. This yielded in promising targets for treatment options and in numerous clinical trials. However, so far, none of these options provided significant benefit in the clinic. Due to the onset of symptoms only in late stages of the disease and the lack of early markers, PDAC is a disease with a high mortality, barely giving clinicians the chance to attempt treatment. In the majority of cases, at the time of clinical presentation, patients are in an advanced and metastatic disease stage and frequently, only palliative treatment can be provided. With only 8%, the 5-year survival rate is the worst of all cancers. And rates are even worse for locally advanced or overall advanced stage patients. The only attempt for a cure described so far is resection of the pancreas, which can only be applied to 15-20% of the affected patients, thereby increasing their 5-year-survival up to 19%. Besides resection, the standard-of-care therapy is systemic chemotherapy. For targeted therapy, EGFR has been the most promising target, since it is frequently overexpressed in PDAC and associated with a poor outcome for the patient. Also, the depletion of EGFR prevented the development of pancreatic cancer in PDAC mouse models, highlighting the disease's dependency on EGFR. The inhibition of EGFR by the small molecule erlotinib in combination with gemcitabine therapy significantly increased the survival of PDAC patients compared to gemcitabine mono-therapy, albeit with only marginal relevance in the clinic. In pre-clinical and clinical trials, PDAC cancer cells commonly evade EGFR dependency but the underlying mechanisms are still not understood. Publications on the involvement of the remaining ERBB receptors of the family are controversial. The PDAC research community currently does not agree on the prognostic value of ERBB2 expression, while ERBB3 is consistently associated with poor outcome for the patient and ERBB4 is mostly expressed at low levels in human PDAC. However, functional studies of ERBB4 attribute an ambivalent role to this receptor. ERBB ligands present a different case, since the majority of them is frequently expressed or overexpressed in pancreatic cancer and, especially TGFA and HBEGF seem to be deeply involved in PDAC development. However, many gaps remain about the participation of each receptor in these processes. The approach of this work aimed to investigate the receptor system more closely in a PDAC mouse model. The approach should reveal the involvement of family members, other than EGFR, which were possibly underestimated due to low expression levels or contradictory findings.

We revealed a major role of BTC on PDAC development by the depletion of the ligand by CRISPR/Cas9 technology in a PDAC mouse model (*Ptf1a*<sup>cre/+</sup>; KKRAS<sup>G12D/+</sup>, herein referred to

as KC mice). KC mice harbor a constitutive activation of KRAS via mutation, specifically in the pancreas due to Cre-loxP technology using the pancreas-specific promoter *Ptf1a*. KC mice lacking BTC presented attenuated PDAC development. This event might be associated with the decreased EGFR phosphorylation and expression upon BTC depletion in KC mice, observed in early and late stages of PDAC development. To analyze BTC function in PDAC and which receptors are involved, we crossed *Btc* tg mice with KC mice. KC mice generally display a long latency and an incomplete penetrance to develop pancreatic adenocarcinoma. *Btc*<sup>tg/+</sup>; *Ptf1a*<sup>cre/+</sup>; *Kras*<sup>G12D/+</sup> mice (herein referred to as BKC mice) express BTC ubiquitously. Although being only specific for EGFR and ERBB4, BTC induced a complex activation of the ERBB system and resulted in the hetero-dimerization of ERBB2, at least with EGFR. While ERBB3 activation was not observed in BKC mice, it could be stimulated by BTC in human cells. EGFR, ERBB2 and ERBB4 activation was discovered in both models. The majority of BKC mice died at eight weeks with a median survival of 2.75 months, which is approximately nine months less compared to the median survival of KC mice. Pancreata of BKC mice were completely replaced by desmoplastic tissue and PDAC, which started as early as after one week of age. We revealed BTC to be able to induce ADM in 3-D primary cell culture of wildtype acinar cells. ADM is a crucial step in pancreatic carcinogenesis, which is initiated by oncogenic KRAS. However, in the PDAC community, it is generally suggested that an additional trigger is required for comprehensive oncogenic KRAS activation in the pancreas. Our investigations revealed that BTC enhanced RAS activation, thereby possibly shifting RAS activity above a certain threshold, in order to induce ADM. In pancreata of BKC mice with a pancreas-specific deletion of the EGFR receptor (using the Cre-loxP system), we observed that the enhanced RAS activation was exclusively mediated by EGFR. BKC mice lacking ERBB2 or ERBB4 (ERBB2 KO;BKC and ERBB4 KO;BKC, respectively) did not show any changes in RAS activation compared to BKC mice. However, RAS activity does not seem to be the only crucial function by which BTC accelerated PDAC development. The pancreas-specific KO of ERBB2 and ERBB4 in BKC mice significantly prolonged the survival (ERBB2 KO;BKC median survival: 12.5 months, ERBB4 KO;BKC median survival: 15 months), which could be explained, in part in ERBB2 KO;BKC mice, by attenuated PDAC progression. The grade of PDAC and the degree of replacement of acinar tissue in ERBB4 KO;BKC mice was similar to BKC mice. The lack of each receptor resulted in reduced EGFR activation, and the lack of ERBB4 in BKC mice also led to reduced MAPK and SAPK signaling, which has to be specific to EGFR/ERBB4 hetero-dimers, since it was not observed in ERBB2 KO;BKC animals. Additionally, ERBB2 activation was decreased in ERBB4 KO;BKC mice. The depletion of EGFR revealed the most prominent alteration of the BKC phenotype. The pancreata of these mice presented predominantly normal, but they displayed ADM multi-focally, which were positive for ERBB2, ERBB3 and ERBB4 immuno-stainings. In these mice, Western blot

analyses revealed that the lack of EGFR was accompanied by the decreased phosphorylation and expression of ERBB2, ERBB3 and full-length ERBB4. However, the ICD of ERBB4 was highly phosphorylated, indicating a compensatory mechanism of ERBB4 signaling upon EGFR depletion.

Manipulating the activity of the ERBB family in a PDAC mouse model points to an oncogenic role for ERBB2 and ERBB4, which might not be obvious at first. In particular, ERBB2 and ERBB4 affect the survival either by influencing PDAC progression or intracellular signaling. Though EGFR has the most dominant pathogenic effect, it is not exclusively responsible for the phenotype. ADM development possibly by ICD signaling of ERBB4, despite EGFR depletion, highlights the importance of the remaining ERBB family members, in particular, considering EGFR targeted therapies or the development of resistance to EGFR treatment. A recent study about the pan-inhibition of the ERBB family, rather than one single receptor in human PDAC cells revealed promising results. This and our data suggest that PDAC treatment should involve all ERBB receptors and not be focused on EGFR alone. The broader inhibition spectrum might have the advantage of decreased medication doses and thereby possibly of a reduction of side effects in the clinic. Many clinical trials are underway, mostly targeting intracellular signaling molecules. However, based on the redundancy and complexity of these signaling pathways, the inhibition of single molecules is ineffective in interrupting these pathways and extracellular signals are still successfully transmitted into a cellular response. This is also true for targeting of EGFR. Hence, the combinatorial inhibition of a certain signaling molecule and its up- or downstream target is favored by researchers, today. Using this approach, promising results have recently been presented including EGFR combinatorial therapies. Yet, the influence of the remaining receptors ERBB2, ERBB3 and ERBB4 should not be underestimated. Still, they might be part of a redundant signaling cascade and possibly provide an alternative signaling route within the EGFR axis.

## 4 SUPPLEMENTARY PROJECT

During the studies of my PhD, I was involved in an additional project, which resulted in a manuscript, which was re-submitted to the journal '*International Journal of Obesity*' in July 2019. *Addendum*: This manuscript was accepted for publication in a revised version in October 2019 at '*International Journal of Obesity*'.

I presented this project in form of a podium talk at the '*European Association for the studies of diabetes*' with the title '*Maternal and paternal pre-conceptual overweight results in different sex-specific transcriptome changes of blastocysts and spermatozoa sncRNAs*' in Munich in September, 2016, and in form of a podium talk at the '*50. Jahrestagung Physiologie und Pathologie der Fortpflanzung*' with the title '*Peri-conceptual overweight in male and female mice causes sex-specific transcriptome changes in blastocysts which could result from differentially expressed sncRNA in spermatozoa of obese males*' in Munich in February, 2017.

### 4.1 CONCLUSIONS

Adverse environmental effects before and during pregnancy, e.g. stress, under- or overnutrition or *diabetes mellitus* can cause epigenetic changes in the developing embryo, which can, in turn, lead to a permanent dysregulation of tissues or organs and manifest as diseases in the adult offspring. With an increase of obesity by 150 million adults within the last decade to over 650 million obese adults and 125 million obese children, obesity is a globally rising problem. The rates for overweight are even higher. Reasons for this may not exclusively be attributed to lifestyle changes. Evidence is rising that the susceptibility of becoming obese is inherited epigenetically. Prior to this study, our lab investigated the offspring of peri-conceptionally obese female mice and found differences in the phenotypes of the adult male and female offspring compared to the offspring of lean mothers. This indicated that maternal epigenetic programming of the offspring is sex-specific. However, there was increasing evidence that the father's nutrition and disease history also had an influence on the

health of the offspring, but no sex-specific differences were reported, yet. Also unknown was, how and at which time point of embryonic development these epigenetic changes, provided by both parents, act on the embryo. In the early blastocyst of mice (3.5 *days post coitum*), both strands of parental DNA of the embryo are being de-methylated and embryonic gene activation begins, starting with *de novo* methylation. We assumed this period to be an ideal time window for epigenetic changes to occur.

In this study, we investigated the transcriptome of blastocysts derived from either peri-conceptionally obese mothers or fathers using microarray analyses and sorted the blastocysts sex-specifically by real-time PCR. The blastocyst transcriptome was compared to the transcriptome of blastocysts which derived from lean parents. We observed that obesity of the mother led to changes in the blastocyst transcriptome, which were predominantly affecting male blastocysts (92 differently abundant transcripts (DAT)) and of which the major change was an increase of DATs. Only four DATs were down-regulated in female blastocysts. Obesity of the father, however, resulted in exclusively increased DATs in male blastocysts and in predominantly decreased DATs in female blastocysts. The datasets of DATs of obese mothers and obese fathers showed a considerable overlap. These data revealed that an obesogenic exposure to both parents leads to transcriptome changes in the early embryo, which were more pronounced in male than in female blastocysts. And while in male blastocysts, DATs were predominantly upregulated, in female embryos, DATs were predominantly downregulated. The presence of RNA in sperm is reported controversially, but there is evidence rising that small non-coding RNA (sncRNA) might be carried in the sperm and inherited to the next generation, or even trans-generationally. We performed Next Generation Sequencing (NGS) on small RNAs of the sperm of obese mice and we revealed nine microRNAs (miRNAs) to be more abundant than in the sperm of lean mice. By NGS we detected targets of these miRNAs in oocytes of lean mice, and revealed that 75% of the decreased DATs could possibly have been targeted by these nine miRNAs of obese fathers. During the course of our study, an increasing number of studies was published, all with evidence on different kinds of RNA in the sperm of mice, which act on the epigenome of the embryo but their mechanisms still need to be determined. Our findings demonstrate that epigenetic changes affecting the transcriptome the embryo are sex-specific and that they occur before embryo implantation *in utero*. Sperm small RNA are possibly inducing these changes. These data shed light on the importance of the contribution of both parents, that obesity can alter the embryo significantly in a sex-dependent manner, thereby laying the basis for future diseases of the offspring.

## **4.2 SEX-SPECIFIC PROGRAMMING EFFECTS OF PARENTAL OBESITY IN PRE-IMPLANTATION EMBRYONIC DEVELOPMENT**

Kathrin Hedegger<sup>1</sup>, Julia Philippou-Massier<sup>2</sup>, Stefan Krebs<sup>2</sup>, Helmut Blum<sup>2</sup>, Stefan Kunzelmann<sup>3</sup>, Klaus Förstemann<sup>3</sup>, Martina Gimpfl<sup>4</sup>, Adelbert A. Roscher<sup>4</sup>, Regina Ensenauer<sup>4,5</sup>, Eckhard Wolf<sup>1,2,6</sup>, Maik Dahlhoff<sup>1\*</sup>

<sup>1</sup> Institute of Molecular Animal Breeding and Biotechnology, Gene Center, Ludwig-Maximilians-Universität München, Feodor-Lynen-Strasse 25, 81377 Munich, Germany

<sup>2</sup> Laboratory for Functional Genome Analysis (LAFUGA), Gene Center, Ludwig-Maximilians-Universität München, Feodor-Lynen-Strasse 25, 81377 Munich, Germany

<sup>3</sup> Department of Biochemistry, Gene Center, Ludwig-Maximilians-Universität München, Feodor-Lynen-Strasse 25, 81377 Munich, Germany

<sup>4</sup> Research Center, Dr. von Hauner Children's Hospital, Ludwig-Maximilians-Universität München, Lindwurmstrasse 4, 80337 Munich, Germany

<sup>5</sup> Experimental Pediatrics and Metabolism, Department of General Pediatrics, Neonatology and Pediatric Cardiology, University Children's Hospital, Heinrich Heine University Düsseldorf, Moorenstrasse 5, 40225 Düsseldorf, Germany

<sup>6</sup> German Center for Diabetes Research (DZD), Helmholtz Zentrum München, Ingolstädter Landstr. 1, 85764 Neuherberg, Germany

### **4.2.1 ABSTRACT**

Obesity is a global rising problem with epidemiological dimension. Obese parents can have programming effects on their offspring leading to obesity and associated diseases in later life. This constitutes a vicious circle. Epidemiological data and studies in rodents demonstrated differential programming effects in male and female offspring, but the timing of their developmental origin is not known. This study investigated if sex-specific programming effects of parental obesity can already be detected in the pre-implantation period. Diet induced obese male or female mice were mated with normal-weight partners and blastocysts were recovered. Gene expression profiling revealed sex-specific responses of the blastocyst transcriptome to maternal and paternal obesity. The changes in the transcriptome of male blastocysts were more pronounced than those of female blastocysts, with a stronger impact of paternal than of maternal obesity. The sperm of obese mice revealed an increased abundance of several miRNAs compared to lean mice. Our study indicates that sex-specific programming effects of parental obesity already start in the pre-implantation period and reveals specific alterations of the sperm miRNA profile as mechanistic link to programming effects of paternal obesity.

## 4.2.2 INTRODUCTION

Epidemiological studies revealed that, during pregnancy, maternal environmental factors, like diseases, stress, body composition and lifestyle can have developmental programming effects and cause diseases in later life of the offspring, e.g. obesity, type 2 diabetes and cardiovascular diseases<sup>299,300</sup>. Developmental programming results in altered gene expression caused by epigenetic changes, such as histone modifications<sup>301</sup>, methylation of CpG islands<sup>302</sup> or small non-coding RNAs (sncRNA)<sup>303</sup> *in utero*. A sensitive time window for programming is the *de novo* methylation of the genome at the early blastocyst stage<sup>304</sup>. We and other groups demonstrated that peri-conceptional overnutrition in female mice induces sex-specific programming of long-term health risks in the offspring<sup>305-310</sup>. Male offspring showed increased weight gain, while female offspring gained less body fat compared to sex-matched offspring from normal-weight mothers<sup>310</sup>. In addition, paternal programming effects have been demonstrated as a consequence of an altered small RNA profile in their sperm<sup>303</sup>, which - after fertilization of oocytes - can influence gene expression of the early embryo. In our current study, we investigated whether pre-conceptional maternal or paternal obesity affects the embryonic transcriptome already at the blastocyst stage and if such changes are different between male and female embryos. Our previously established diet induced obesity (DIO) mouse model<sup>310</sup> and lean control mice were used to recover blastocysts as well as oocytes and sperm. Since we observed that maternal obesity has a sex-specific programming effect in the offspring<sup>310</sup>, we sexed the blastocysts before analyzing their transcriptomes. As a potential mechanism of paternal programming effects, we investigated sncRNAs of sperm of obese vs. lean mice and matched them to their predicted target mRNAs in oocytes of lean and obese female mice.

## 4.2.3 MATERIALS AND METHODS

See details in *Supplementary Materials and Methods (4.2.4)*.

### 4.2.3.1 ANIMALS

All procedures were performed in accordance with the Committee on Animal Health and Care of the state of Upper Bavaria (Regierung von Oberbayern, Germany; permission Az. 55.2.1.54-2532-51-12) and according to the German Animal Welfare Act and Directive 2010/63/EU on the protection of animals used for scientific purposes. NMRI mice (RjHan:NMRI) were purchased from Janvier (Le Genest St Isle, France). For a period of nine weeks, cohorts of three-week-old mice were fed a modified D12492 high-fat, high-calorie diet (HFD) (E15741-34; ssniff, Soest, Germany), or received a control diet to D12492 (CD) (ssniff) (Suppl. Table S 4.5). At the age of twelve weeks, mice were killed to recover sperm or oocytes, or mated. Three types of mating were set up (n = 7 per mating type): i) obese male × lean female (M<sub>Ob</sub>×F<sub>Co</sub>);

ii) lean male × obese female ( $M_{Co} \times F_{Ob}$ ); and lean male × lean female ( $M_{Co} \times F_{Co}$ ) (Suppl. Fig. S 4.1 A-E). At day 3.5 post coitum, female mice were sacrificed and blastocysts were isolated in M2 medium.

#### **4.2.3.2 SEXING OF BLASTOCYSTS AND MICROARRAY ANALYSIS**

Blastocysts were sexed by quantitative RT-PCR analysis of *Slc25a5* (X-chromosome specific) and *Ddx3y* (Y-chromosome specific) expression (Suppl. Fig. S 4.1 F,G). For holistic gene expression analysis the lysate of three sex matched blastocysts from one mother were pooled and analyzed on an Affymetrix GeneChip™ (Thermo Fisher Scientific) according to the manufacturer's instructions. Four replicates of blastocyst pools were analyzed for each parental group ( $M_{Ob} \times F_{Co}$ ,  $M_{Co} \times F_{Ob}$ ,  $M_{Co} \times F_{Co}$ ); in total: 24 microarrays.

#### **4.2.3.3 TRANSCRIPTOME ANALYSIS OF SPERM AND OOCYTES**

For transcriptome analysis the sperm of eight obese and eight lean mice, and oocyte pools (pools of 4 oocytes per dam) of six obese and six lean mice were investigated. RNA-sequencing libraries were generated using the tagmentation technology of the NexteraXT Kit (Illumina) following the manufacturer's instructions.

#### **4.2.3.4 STATISTICAL ANALYSIS**

Data was analyzed by Student's *t*-test (unpaired and equal). Data is represented as mean+SD (GRAPHPAD PRISM version 5.0). Microarray data sets were analyzed by Local Pooled Error (LPE) estimation.  $P < 0.05$  was considered significant.

### **4.2.4 SUPPLEMENTARY MATERIALS AND METHODS**

#### **4.2.4.1 ANIMALS AND ENVIRONMENTAL ENRICHMENT**

NMRI mice (RjHan:NMRI) were purchased from Janvier (Le Genest St Isle, France). Mice were maintained under specific pathogen-free conditions in the closed barrier facility of the Gene Center, Munich at 23 °C, 40% humidity, with a 12 h light/dark cycle (lights on at 7 AM) and had access to water and their appropriate diet *ad libitum*. All procedures were performed in accordance with the Committee on Animal Health and Care of the state of Upper Bavaria (Regierung von Oberbayern, Germany; permission Az. 55.2.1.54-2532-51-12) and according to the German Animal Welfare Act and Directive 2010/63/EU on the protection of animals used for scientific purposes.

#### **4.2.4.2 DIET, MATING AND TISSUE REMOVAL**

**For blastocyst analysis:** For a period of nine weeks a three-week-old cohort of seven male (M) and female (F) mice were fed a modified D12492 high-fat, high-calorie diet (HFD) (E15741-34; ssniff, Soest, Germany), and another cohort of 14 male and female animals received a control diet D12492 (CD) (ssniff) (diet composition is shown in (Suppl. Table S 4.5). Body

weight was monitored every week and body fat content was measured weekly by magnetic resonance imaging (Minispec LF50; Bruker, Stuttgart, Germany). At the age of 12 weeks, HFD mice ( $M_{Ob}$ ,  $F_{Ob}$ ) were mated with CD mice ( $M_{Co}$ ,  $F_{Co}$ ) and as control group CD fed animals were mated with each other. During mating all animals were fed the CD and screened for vaginal plugs every morning and evening. At day 3.5 *post coitum* (dpc), female mice were sacrificed by cervical dislocation and blastocysts were isolated in M2 medium. Blastocysts were washed three times in PBS, separately snap frozen in PBS, and stored at -80 °C until used for further analysis.

**For sperm analysis:** 16 three-week-old male mice received either a HFD or a CD for a period of nine weeks prior to sperm isolation. Both *caudae epididymidis* were removed, trimmed free from fat and placed in PBS for sperm swim up. The *caudae epididymidis* were incised at five different spots, enabling the sperm to swim up in 200  $\mu$ l PBS for five minutes. The PBS containing sperm was transferred into an Eppendorf tube containing 1 ml PBS for 10 minutes. Motile sperm swam to the upper phase of the PBS while somatic cells sedimented to the bottom of the tube. The upper 200  $\mu$ l phase PBS, containing the motile sperm, was transferred into a fresh Eppendorf tube containing 700  $\mu$ l QIAzol buffer (QIAGEN, Hilden, Germany), sonicated with a low amplitude (Bioruptor Plus, Diagenode SA, Seraing, Belgium) for five cycles. Each cycle consisted of a pulse of 30 seconds followed by a rest of 90 seconds. Afterwards, the samples were shock frozen in liquid nitrogen and stored at -80 °C.

**For oocyte analysis:** 18 three-week-old female mice received either a HFD or CD, respectively, for a period of nine weeks prior to being mated with vasectomized male mice. During mating, all animals were fed a CD and screened for vaginal plugs every morning and evening. At day 0.5 p.c. female mice were sacrificed by cervical dislocation and oocytes were isolated in M2 medium. Oocytes were washed three times in PBS, separately snap frozen in PBS, and stored at -80 °C until used for further analysis.

#### **4.2.4.3 MICROARRAY ANALYSIS OF SEXED BLASTOCYSTS**

Isolated, single blastocysts were lysed in 10  $\mu$ l buffer using Direct Lysis Kit (NuGEN, Leek, Netherlands) according to the manufacturer's instructions. For blastocyst sexing 1  $\mu$ l lysate was used in a TaqMan Geneexpression Assay using the CellsDirect One-step qRT-PCR Kit (Thermo Fisher Scientific, Darmstadt, Germany) according to the manufacturer's instructions. Blastocysts were sexed by quantitative RT-PCR for the following genes: *Slc25a5* (X-chromosome specific) and *Ddx3y* (Y-chromosome specific). Therefore, the following TaqMan gene expression assays were used: Assay-ID: Mm00846873\_g1 and Assay-ID: Mm00465349\_m1 (Thermo Fisher Scientific). The TaqMan Assay was carried out in a StepOne machine (Thermo Fisher Scientific) in a final volume of 20  $\mu$ l. Assay conditions were:

Holding Stage: 50°C for 15 min, 95°C for 2 min and for the Cycling Stage (with in total 50 cycles): 95°C for 15 sec, 60°C for 45 sec.

For whole-transcriptome gene expression analysis the lysate of three sex-matched blastocysts from one mother were pooled. Per parental group ( $M_{Ob} \times F_{Co}$ ,  $M_{Co} \times F_{Ob}$ ,  $M_{Co} \times F_{Co}$ ) and for each male or female blastocyst pool, four replicates were analyzed, respectively; in total: 24 microarrays. Targets for the microarray analysis were generated using the Ovation One-Direct System (NuGEN) according to the manufacturer's instructions. Briefly, first primer was annealed to the lysate followed by first and second strand cDNA synthesis. Purified cDNA was amplified using the SPIA technology (NuGEN). Before amplified targets were purified post-SPIA modification was completed. 4  $\mu$ g of purified target cDNA was fragmented and Biotin-labeled using the FL-modul (NuGEN) according to the manufacturer's instructions. Afterwards the quality of the fragmented and labeled samples were controlled by using the Agilent 2100 Bioanalyzer. 1.5  $\mu$ g of fragmented and labeled sample was hybridized on an Affymetrix GeneChip™ (Thermo Fisher Scientific) using the respective Hybridization, Wash and Stain Kit (Thermo Fisher Scientific) according to the manufacturer's instructions. After 17 (+/- 1) hours of hybridization the microarrays were read out on the Affymetrix Fluidics Station. The full blastocyst transcriptome data set was uploaded at NCBI Gene Expression Omnibus and has the data accession number GSE133767.

#### **4.2.4.4 QUANTITATIVE RT-PCR**

Total RNA was isolated with TRIZOL reagent (Invitrogen, Darmstadt, Germany) and 1  $\mu$ g of RNA samples were reverse-transcribed in a final volume of 20  $\mu$ l using RevertAid Reverse Transcriptase (Thermo Fisher Scientific) according to the manufacturer's instructions. Quantitative RT-PCR was carried out in a LightCycler®480 (Roche, Mannheim, Germany) using the primers (0.5  $\mu$ M) listed in Suppl. Table S 4.4, 1  $\mu$ l cDNA, 0.2  $\mu$ M probe (Universal ProbeLibrary Set, Roche), and the LightCycler® 480 Probes Master Mix (Roche) in a final volume of 10  $\mu$ l. Cycle conditions were 95°C for 5 min for the first cycle, followed by 45 cycles at 95°C for 10 s, 60°C for 15 s, and 72°C for 1 s. Transcript copy numbers were normalized to beta-actin (*Actb*) mRNA copies. The  $\Delta$ Ct value of the sample was determined by subtracting the average Ct value of the target gene from the average Ct value of the *Actb* gene. For each primer pair we performed no-template control and no-RT control assays, which produced negligible signals that were usually greater than 40 in Ct value. All experiments were performed in duplicates. All primers and probes are listed in Suppl. Table S 4.4.

#### **4.2.4.5 RNA ISOLATION OF MOUSE SPERM**

Total RNA was extracted from purified sperm using the miRNeasy Kit (Qiagen, Hilden, Germany) according to the manufacturer's instructions. In brief, the in QIAzol buffer

shock-frozen sperm samples were thawed on ice and incubated for 5 min at room temperature (RT). Chloroform was added to the homogenate, thoroughly mixed and centrifuged at 4 °C to get separate phases. The aqueous phase was extracted and mixed with 100% ethanol and applied to a silica-based RNeasy spin column to bind total RNA >18nt. A DNase digest was performed for 15 min at RT. The RNA was washed several times and dissolved in RNase-free water. The RNA samples were concentrated and purified by an RNA-bead cleanup with Agencourt® RNAClean® XP Beads (Beckman Coulter, Krefeld, Germany). Total RNA was incubated and bound to magnetic RNAClean® XP Beads in 80% ethanol, washed and eluted in RNase-free water. The RNA concentration was measured by Qubit™ fluorimeter (Thermo Fisher Scientific). RNA quality was investigated by performing a capillary gel electrophoresis using an Agilent RNA 6000 Pico Chip and an Agilent Small RNA Chip on the Agilent 2100 Bioanalyzer according to the manufacturer's instructions.

#### **4.2.4.6 LIBRARY PREPARATION AND SEQUENCING OF SMALL RNAs OF MOUSE SPERM**

A cDNA library was prepared using the NEXTflex™ Small RNA Sequencing Kit v2 (HIS Diagnostics GmbH, Freiburg, Germany) according to the manufacturer's instructions starting with less than 2 µg of total RNA. In brief, the NEXTflex™ 4N adenylated adapter was ligated to the 3'-end of the small RNA prior to the ligation of the adapter to the 5'-end. After reverse transcription of the first strand using universal primers, the product was purified by Agencourt AMPure XP bead clean up (Beckman Coulter) and the second strand was synthesized by PCR amplification using NEXTflex™ Small RNA Barcode Primers – Set A. The PCR products were fragmented on a TBE-PAGE, the gel was stained with SYBR Gold (Invitrogen) and fragments of the size of 150 nucleotides were excised, eluted and purified. The quality of the cDNA was investigated using an Agilent DNA 1000 Chip on the Agilent 2100 Bioanalyzer according to the manufacturer's instructions and sequenced on an Illumina HiSeq1500 machine (single end read, 50 nt). Deep sequencing reads were preprocessed on a Galaxy server<sup>311</sup> hosted by LAFUGA, Gene Center, Munich. The data was demultiplexed using *Illumina Demultiplex* v1.0.0, adapter sequences were removed from the 3' end using *Clip Adaptor Sequence* v1.0.0 (tggaattc, seed 8, mismatch 0, minimum length after clipping 1), random nucleotides at the 5' and 3' end of the reads were trimmed using *FastqFilter* v1.0 (enable trimming T, absolute, 4nt each end) and length selection of the reads was performed using *Filter FASTQ* v1.0.0. Length selected reads were mapped to the mouse genome, to mature miRNAs, hairpins, rRNAs, tRNAs and piRNA cluster (mm9) using Bowtie<sup>312</sup>, (-v0). The abundance of reads mapping to specific features was analyzed using Perl scripts and R v3.2.3. Statistical significance was calculated using the two-sided Mann-Whitney U test and plotted in R. Data is represented as mean ± SD (GRAPHPAD PRISM version 5.0 for Windows, GraphPad Software, San Diego, CA, USA).

#### **4.2.4.7 TRANSCRIPTOME ANALYSIS OF ISOLATED MOUSE SPERM**

For transcriptome analysis 2 ng of isolated RNA were treated with DNaseI (Thermo Scientific). Afterwards, the RNA was used to generate double-stranded cDNA using the Ovation RNA Seq V2 Kit (NuGEN) according to the manufacturer's instructions. The purified cDNA was quantified using the HS DNA Kit (Thermo Fisher Scientific). Samples were measured on Qubit™ fluorimeter (Thermo Fisher Scientific). Sequencing libraries were generated using the Ovation Rapid DR Multiplex System (NuGEN) according to the manufacturer's instructions. Briefly, between 1.4 and 1.8 µg of double-stranded cDNA were fragmented with the M220 Focused ultrasonicator (Covaris, Brighton, UK). On this system the fragment size was programmed to peak at 250 bp. After purification, the concentration of the fragmented cDNA was determined using the HS DNA Kit (Thermo Fisher Scientific). Samples were measured on Qubit™ fluorimeter (Thermo Fisher Scientific). In the following end repair, 250 ng of fragmented and purified cDNA were used. After adapter ligation and final repair, the DNA was purified and amplified. After amplification, the sequencing libraries were purified and quantified using a DNA 1000 Chip on the Agilent 2100 Bioanalyzer according to the manufacturer's instructions and finally sequenced on an Illumina HiSeq1500 machine (single-end read, 100 nt). The sequencing reads were preprocessed on a Galaxy server<sup>311</sup> (hosted by LAFUGA, Gene Center, Munich). The data was demultiplexed using *Illumina Demultiplex* v1.0.0 and adapter sequences were removed from the 3' end using *Clip Adaptor Sequence* v1.0.0 (seed 10, mismatch 0, minimum length after clipping 20). The output was mapped to the mouse genome (mm10). The abundance of reads mapping to the specific feature type (here: exon, minimum alignment quality 0, mode union, paired-end no, strand specificity yes) were analyzed using *HTSeq-count* v1.0.0 and a differential gene expression analysis (CD vs. HFD) based on the negative binomial distribution was performed using *DESeq2*<sup>313</sup> v1.0.19 setting the FDR < 0.05. The full sperm transcriptome data set was uploaded at NCBI Gene Expression Omnibus and has the data accession number GSE133915, and the miRNA data set was uploaded at European Nucleotide Archive and has the data accession number PRJEB33337.

#### **4.2.4.8 TRANSCRIPTOME ANALYSIS OF OOCYTES**

Full-length cDNA of four pooled oocytes was generated using the SMART Seq v4 Ultra Low Input RNA kit for Sequencing (Takara Bio, Mountain View, CA, USA) according to the manufacturer's instructions. The template switching activity of reverse transcriptase to enrich full-length cDNA as well as the addition of defined PCR adapters directly to the ends of the first strand cDNA define the SMART technology. In brief, after lysis, full-length first strand cDNA was generated followed by reverse transcription and long-distance PCR. Finally, the amplified cDNA was purified using Agencourt AMPure XP Beads (Beckman Coulter). The

obtained full-length cDNA was validated using the Qubit™ fluorimeter (Thermo Fisher Scientific).

The RNA-Sequencing libraries were generated using the tagmentation technology of the NexteraXT Kit (Illumina) following the manufacturer's instructions. This technology relies on an engineered transposome to tagment double stranded DNA and tagging it with a universal overhang. In brief, double stranded template DNA is combined with Nextera XT transposome with adapters. After tagmentation to fragments and the addition of adapters, a limited-cycle PCR was performed to add index adapter sequences. Finally, libraries were purified using Agencourt AMPure XP Beads (Beckman Coulter). Libraries were quantified on the Bioanalyzer and finally sequenced on an Illumina HiSeq1500 machine (single end read, 100 nt). The sequencing reads were preprocessed on a Galaxy server<sup>311</sup> (hosted by LAFUGA, Gene Center, Munich). The data was demultiplexed using *Illumina Demultiplex* v1.0.0 and adapter sequences were removed from the 3' end using *Clip Adaptor Sequence* v1.0.0 (seed 10, mismatch 0, minimum length after clipping 20). The output was mapped to the mouse genome (mm10). The abundance of reads mapping to the specific feature type (here: exon, minimum alignment quality 0, mode union, paired-end no, strand specificity yes) were analyzed using *HTSeq-count* v1.0.0 and a differential gene expression analysis (CD vs. HFD) based on the negative binominal distribution was performed using *DESeq*<sup>313</sup> v1.0.19 setting the FDR < 0.05. The full oocyte transcriptome data set was uploaded at NCBI Gene Expression Omnibus and has the data accession number GSE133914.

#### **4.2.4.9 STATISTICAL ANALYSIS**

Body weight and body fat content were statistically analyzed using PROC MIXED (linear mixed models; SAS release 8.2, SAS Institute, Cary, NC, USA) considering the fixed effects of diet, age, their interaction, and the random effect of animal<sup>310</sup>. qRT-PCR was analyzed by Student's *t*-test (unpaired and equal). Data is represented as mean+SD (GRAPHPAD PRISM version 5.0). Microarray data sets were analyzed by Local Pooled Error (LPE) estimation. *P*<0.05 was considered significant.

## 4.2.5 RESULTS

### 4.2.5.1 PARENTAL OBESITY INFLUENCES GENE EXPRESSION AT THE BLASTOCYST STAGE IN A SEX-SPECIFIC MANNER

Microarrays revealed that in blastocysts of obese fathers ( $M_{Ob}$ ) the transcript abundance of 98 genes was altered compared to control blastocysts. Interestingly, this effect was strongly dependent on the sex of the embryos. In male blastocysts, all differentially abundant transcripts (DATs;  $n = 49$ ) were increased, whereas in female blastocysts the majority of DATs was decreased in abundance (47 down, 2 up), resulting in 217 DATs between male and female blastocysts from obese fathers. In contrast, maternal obesity ( $F_{Ob}$ ) mainly affected the transcriptome of male blastocysts (92 DATs; 79 up, 13 down compared with male control blastocysts), while the transcriptome of female blastocysts was only moderately altered (4 DATs down compared with female control blastocysts) and only 7 DATs were found between male and female blastocysts (Figure 4.1 B; Suppl. Table S 6.1). These results demonstrate, that male and female blastocysts are differently affected by parental obesity. Furthermore, the transcriptome changes induced by paternal or maternal obesity in male blastocysts showed a considerable overlap, while no overlap in DATs was found between male and female blastocysts derived from either obese fathers or mothers (Figure 4.1 C). Microarray results were confirmed for eight genes by quantitative RT-PCR (Suppl. Fig. S 4.2).



#### **4.2.5.2 DIFFERENT MIRNAS AND PIRNAS WERE UP-REGULATED IN THE SPERM OF HFD MICE**

Since there is evidence rising that sncRNAs can be inherited by sperm and that they provide an explanation for specific disease susceptibilities in the offspring<sup>300,303,314</sup>, we investigated the small RNA pattern in sperm of obese males vs. lean controls (Suppl. Fig. S 4.3 A). Next generation sequencing (NGS) revealed 11 small RNAs with significant abundance differences between sperm of M<sub>Ob</sub> mice and M<sub>Co</sub> sperm (Figure 4.2 A). Since miRNAs silence mRNAs, we evaluated if lower expressed transcripts in blastocysts derived from M<sub>Ob</sub> are predicted or validated targets of miRNAs that were up-regulated in their sperm. Indeed, 34 out of 47 down-regulated transcripts in female blastocysts are targets of the identified miRNAs (Suppl. Table S 4.1). On the other hand, we identified 18 target mRNAs of the two significantly down-regulated miRNAs (miR-30a/b) upregulated in male blastocysts derived from obese fathers (Suppl. Table S 4.2). Besides the altered miRNA pattern, we found the products of five piwi-interacting RNAs (piRNAs) of the pachytene loci<sup>315</sup> to be significantly up-regulated and one of the prepachytene gene loci<sup>315</sup> to be down-regulated in the sperm of M<sub>Ob</sub> mice compared with M<sub>Co</sub> sperm (Figure 4.2 B).

#### **4.2.5.3 NGS ANALYSIS REVEALED NUMEROUS SIGNIFICANT CHANGES IN THE TRANSCRIPTOME OF OOCYTES FROM OBESE FEMALES**

We evaluated the transcriptome of oocytes from obese and lean female mice by NGS (Suppl. Fig. S 4.3 B). We identified 442 transcripts with significantly increased and 221 transcripts with significantly decreased abundance in oocytes of F<sub>Ob</sub> compared with F<sub>Co</sub> oocytes (Suppl. Table S 4.3 (with top 20 genes) and Suppl. Table S 6.2 for the complete list). We investigated whether the down-regulated mRNAs of female blastocysts from M<sub>Ob</sub>, potentially serving as targets of the up-regulated miRNAs in the sperm of M<sub>Ob</sub>, were already expressed in the transcriptome of F<sub>Co</sub>-oocytes. We identified 27 mRNAs in the oocyte transcriptome, which match potential targets of the four most up-regulated miRNAs in the sperm of M<sub>Ob</sub> mice (Figure 4.2 C). This analysis confirmed that the mRNA targets of our identified miRNAs in the M<sub>Ob</sub> sperm are expressed in oocytes and were down-regulated in female blastocysts generated by fertilization with M<sub>Ob</sub> sperm.

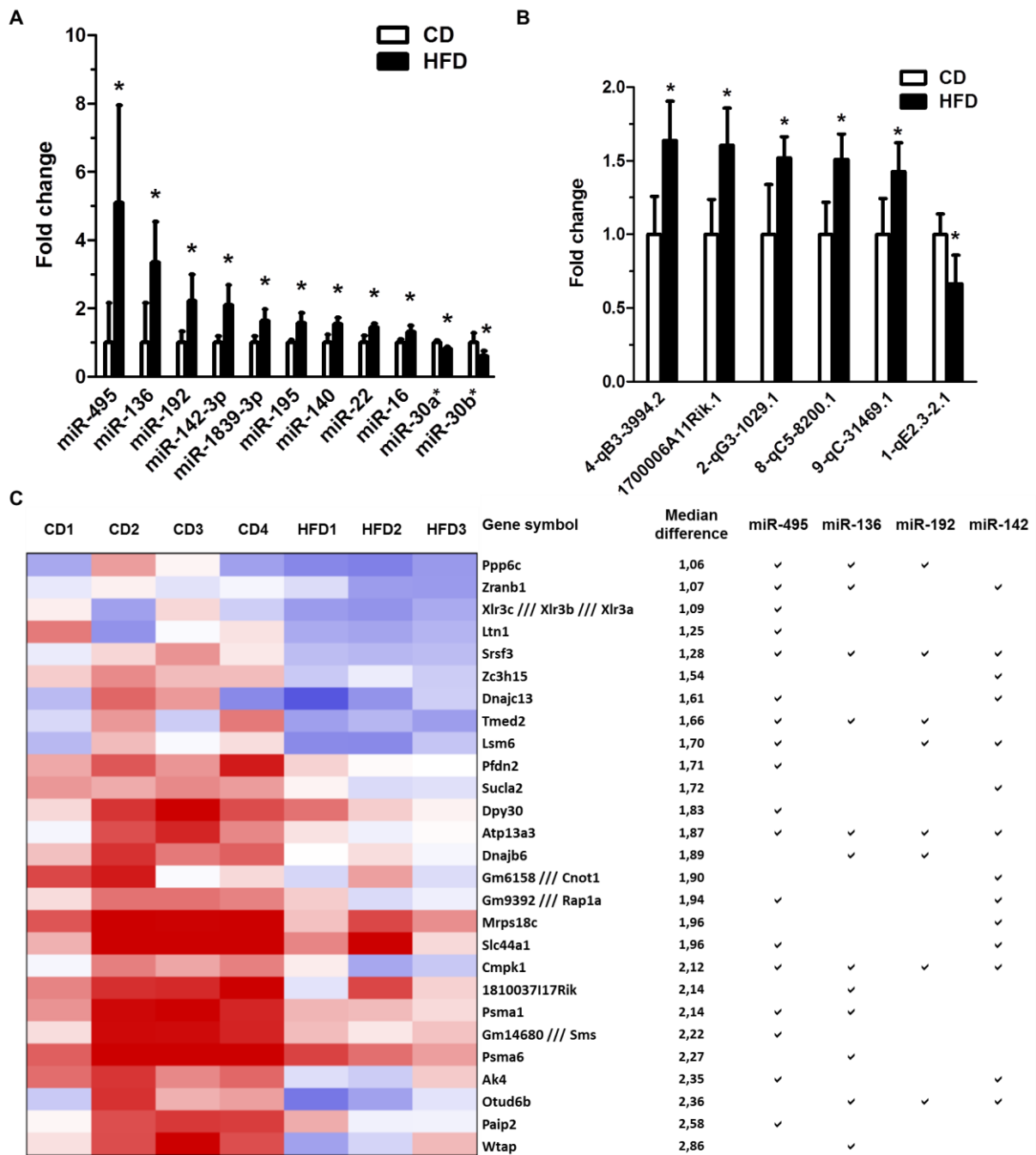


**Figure 4.2: Differential abundance of small RNAs in the sperm of obese ( $M_{Ob}$ ) compared with lean control males ( $M_{Co}$ )**

**A** Significantly regulated miRNAs in the sperm of  $M_{Ob}$  vs.  $M_{Co}$  mice. **B** Significantly regulated piRNAs in the sperm of  $M_{Ob}$  vs.  $M_{Co}$  mice. Significance was calculated using the two-sided Mann-Whitney U-test; \* $P < 0.05$ . **C** Heatmap and matches of the most prominently up-regulated miRNAs in sperm of  $M_{Ob}$  mice and their target mRNAs, which were significantly down-regulated in the transcriptome of blastocysts of  $M_{Ob}$  mice.

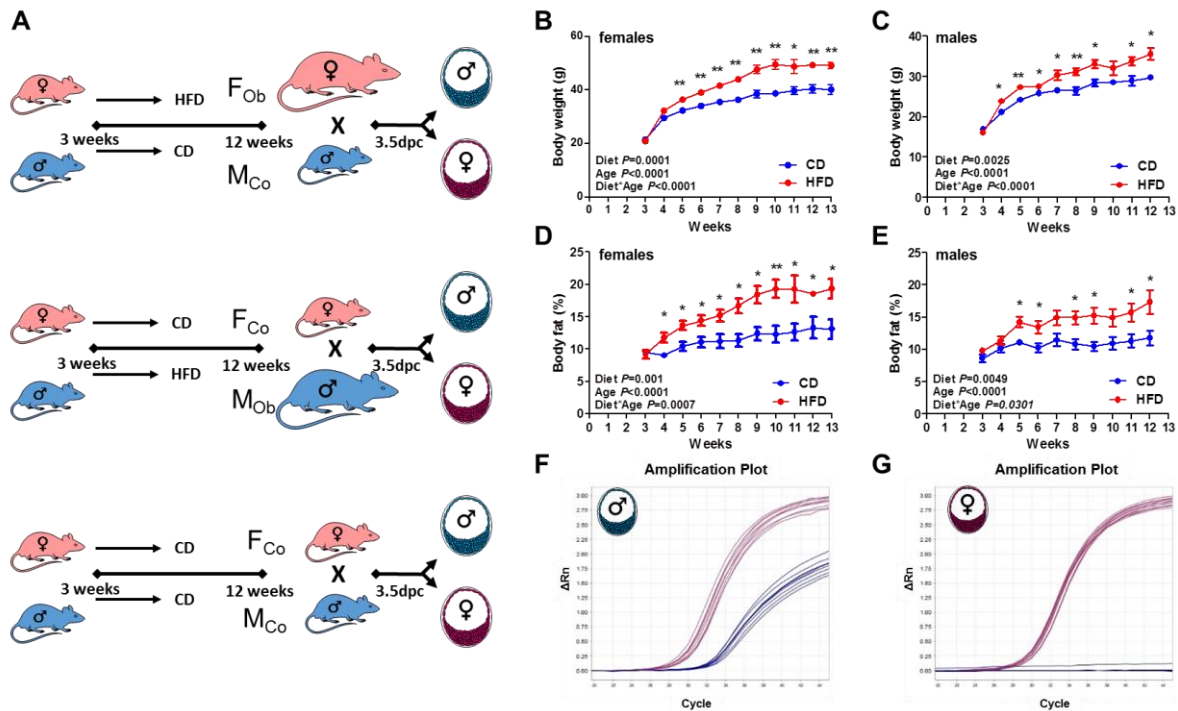
#### 4.2.6 DISCUSSION

Studies verified that the sex plays a fundamental role during the initiation phase of diseases, in particular on the molecular level of mental disorders and metabolic diseases<sup>316</sup>. In our current work, we revealed that male blastocysts of obese females ( $F_{Ob}$ ) have a higher number of transcriptome changes than female blastocysts. This is in line with our previous observation of more marked phenotypic changes (e.g. increased body weight) in male than in female offspring of obese mothers<sup>310</sup>, which was also observed by other studies<sup>305-308,317</sup>. Taken together, these observations suggest that during pre-implantation development male embryos are more susceptible than female embryos to an obesogenic maternal environment and the resulting programming effects may – at least in part – persist into postnatal life.

Interestingly, paternal obesity also resulted in significant transcriptome changes of blastocysts, which were clearly sex-specific. The 49 DATs found in male blastocysts were increased in abundance and overlapped completely with the set of up-regulated DATs in male blastocysts of obese mothers, demonstrating concordant effects of parental obesity on the transcriptome of male blastocysts. In contrast, 47 of 49 DATs in female blastocysts of obese fathers were down-regulated transcripts, demonstrating sex-specific programming of paternal obesity. Recently, several studies showed correlations of paternal obesity with the development of non-communicable diseases in the offspring, suggesting that paternal obesity at conception may impact on the offspring's metabolic health later in life<sup>318,319</sup>. *In vitro* fertilization studies showed that spermatozoa of DIO mice induced the development of increased body weight in the offspring, indicating a function for spermatozoa in epigenetic programming of the offspring<sup>300,319,320</sup>. We showed that obesity causes significant alterations in the RNA profile of mouse sperm, such as increased abundances of nine miRNAs. Interestingly, almost 75% of the down-regulated transcripts in female blastocysts of obese fathers were predicted targets of these nine miRNAs. Differentially regulated piRNAs in mouse sperm could possibly be inherited to the next generation and have an impact on the F2 generation as described previously<sup>321</sup>. Future studies, e.g. with sex-sorted sperm, are required to provide further insights into sex-specific paternal programming effects in pre-implantation embryos. Mechanisms how the sperm RNA code can influence metabolic health of offspring have been reviewed recently<sup>322</sup>.

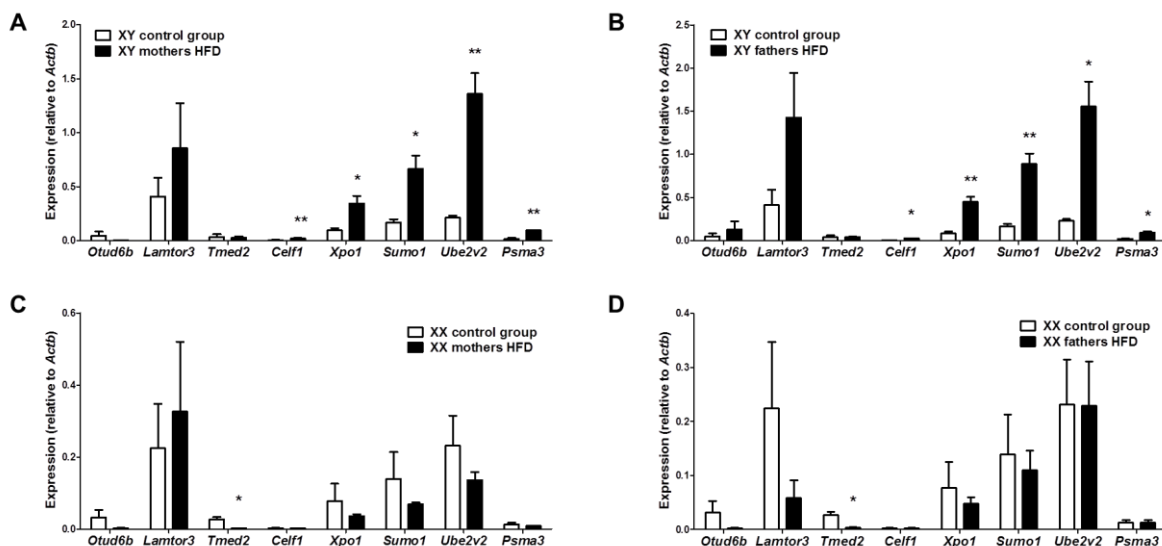
In conclusion, our study revealed differential transcriptome changes in male and female blastocysts associated with maternal or paternal obesity, suggesting the preimplantation period as a critical window for sex-specific developmental programming effects.

## 4.2.7 SUPPLEMENTARY FIGURES



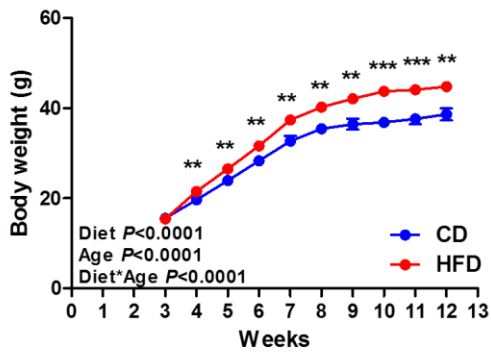
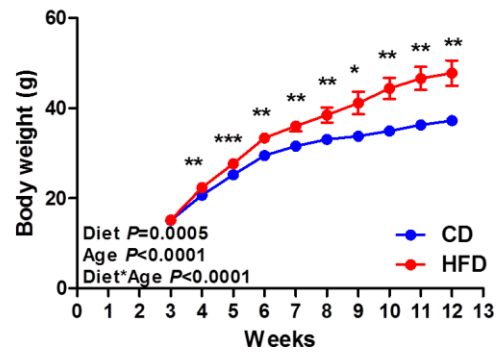
**Suppl. Fig. S 4.1: Experimental design and sexing of blastocysts**

**A** Study design. **B,C** Body weight curve of male **B** and female **C** mice during exposure to HFD and CD.  $n=7$  HFD/7 CD. **D,E** Body fat of **D** male and **E** female mice was measured by magnetic resonance imaging. Data is represented as mean $\pm$ SEM, was analyzed by 2-way ANOVA, and differences between groups were analyzed by Student's t-test (unpaired and unequal). \* $P<0.05$ , \*\* $P<0.01$ . **F,G** Quantification plots of RT-PCR analysis for sex-sorting show X-chromosome linked gene *Slc25a5* (purple) and Y-chromosome linked gene *Ddx3y* (blue) of male f and female g blastocysts.



**Suppl. Fig. S 4.2: Microarrays were confirmed by quantitative RT-PCR of 8 selected genes**

**A** Male blastocysts (XY) of HFD mothers, **B** male blastocysts (XY) of HFD fathers, **C** female blastocysts (XX) of HFD mothers, **D** female blastocysts (XX) of HFD fathers were compared with the CD group. Expression levels are relative to *Actb* expression. Data is represented as mean $\pm$ SEM, and significance was calculated by Student's t-test. \* $P<0.05$ , \*\* $P<0.01$

**A****B****Suppl. Fig. S 4.3: Body weights of donor mice**

**A** Body weight of sperm donors fed a HFD or CD.  $n=8$  HFD/8 CD. **B** Body weight of oocytes donors fed a HFD or CD.  $n=9$  HFD/9 CD. Data is represented as mean $\pm$ SEM, and were analyzed by 2-way ANOVA, and statistical differences between groups were calculated by Student's t-test. \* $P < 0.05$ , \*\* $P < 0.01$ , \*\*\* $P < 0.001$ .

## 4.2.8 SUPPLEMENTARY TABLES

**Suppl. Table S 4.1: Correlation of the down-regulation of transcripts in female blastocysts of M<sub>Ob</sub> with miRNA abundance in sperm of obese mice**

Down-regulated transcripts of female blastocysts derived from obese fathers M<sub>Ob</sub>, which are predicted or validated targets of significantly up-regulated miRNAs in the sperm of obese fathers M<sub>Ob</sub>.

	miR- 1839	miR- 136	miR- 142	miR- 140	miR- 495	miR- 16	miR- 22	miR- 192
<i>Otud6b</i>	✓	✓	✓	✓	✓	✓	✓	✓
<i>Atp13a3</i>		✓	✓		✓	✓	✓	✓
<i>Ak4</i>	✓		✓	✓	✓	✓	✓	
<i>Ppp6c</i>		✓	✓		✓	✓	✓	✓
<i>Cmpk1</i>		✓	✓	✓	✓	✓		✓
<i>Lsm6</i>			✓	✓	✓		✓	✓
<i>Tmed2</i>		✓		✓	✓		✓	✓
<i>Zranb1</i>		✓	✓	✓	✓	✓		
<i>Dnajb6</i>		✓		✓	✓			✓
<i>Slc44a1</i>	✓		✓		✓		✓	
<i>Srsf3</i>		✓	✓		✓			✓
<i>Xlr3b</i>	✓				✓	✓	✓	
<i>Xlr3c</i>	✓				✓	✓	✓	
<i>Cnot1</i>			✓	✓	✓	✓		
<i>Dnajc13</i>			✓	✓	✓			
<i>Nabp1</i>	✓				✓		✓	
<i>Rap1a</i>			✓		✓	✓	✓	
<i>Wtap</i>	✓	✓		✓			✓	
<i>Xlr3a</i>	✓					✓	✓	
<i>Atp6v1c1</i>	✓				✓			
<i>Dpy30</i>					✓		✓	
<i>Gm2016</i>		✓						✓
<i>Ltn1</i>					✓		✓	
<i>Mrps18c</i>			✓				✓	
<i>Paip2</i>					✓	✓	✓	
<i>Sms</i>					✓	✓	✓	
<i>Zc3h15</i>			✓				✓	
<i>Nop56</i>	✓					✓		
<i>Sucla2</i>			✓	✓		✓		
<i>Psm1</i>		✓			✓			

<b><i>Pisma6</i></b>	✓	✓
<b><i>Uxt</i></b>	✓	
<b><i>Pfdn2</i></b>	✓	
<b><i>Fth1</i></b>		✓

**Suppl. Table S 4.2: Correlation of the up-regulation of transcripts in male blastocysts of M<sub>Ob</sub> with miRNA abundance in sperm of obese mice**

Upregulated transcripts in male blastocysts derived from obese fathers and their matches as predicted or validated targets of significantly underrepresented miRNAs found in the sperm of obese mice M<sub>Ob</sub>.

	miR-30a	miR-30b
<b><i>Ube2v2</i></b>	✓	✓
<b><i>Dnajc13</i></b>	✓	✓
<b><i>Ltn1</i></b>	✓	✓
<b><i>Celf1</i></b>	✓	✓
<b><i>Tra2b</i></b>	✓	✓
<b><i>Xpo1</i></b>	✓	✓
<b><i>Purb</i></b>	✓	✓
<b><i>Eif2s1</i></b>	✓	✓
<b><i>Lsm6</i></b>	✓	✓
<b><i>Ttc1</i></b>	✓	✓
<b><i>Prdx2</i></b>	✓	✓
<b><i>Ppp4r2</i></b>	✓	✓
<b><i>Arih2</i></b>	✓	
<b><i>Rbbp6</i></b>	✓	
<b><i>Lamtor3</i></b>	✓	
<b><i>Sumo1</i></b>		✓
<b><i>Myef2</i></b>		✓
<b><i>Calcoco2</i></b>		✓

**Suppl. Table S 4.3: Differentially regulated genes in oocytes of F<sub>Ob</sub> vs. F<sub>Co</sub> mice**

Listed are the top 20 genes, sorted by p-value. For the complete list, please find Suppl. Table S 6.2.

Down-regulated Transcripts				Upregulated transcripts			
<i>Gene</i>	log2- fold Change	<i>p</i> -value	<i>p</i> -adj	<i>Gene</i>	log2- fold Change	<i>p</i> -value	<i>p</i> -adj
<i>Plcl1</i>	-4,36	9,16E-09	8,96E-05	<i>Rpl41</i>	3,44	1,63E-07	3,98E-04
<i>Ung</i>	-1,85	6,19E-08	3,03E-04	<i>Anapc13</i>	3,55	1,51E-07	3,98E-04
<i>Prps2</i>	-3,31	1,63E-06	9,40E-04	<i>2210417A02Rik</i>	2,54	4,14E-07	6,80E-04
<i>4930512B01Rik</i>	-2,31	2,93E-06	1,40E-03	<i>Ndufa11</i>	3,22	4,17E-07	6,80E-04
<i>Sh2d3c</i>	-1,95	3,16E-06	1,40E-03	<i>Timm8b</i>	1,51	1,00E-06	8,65E-04
<i>E2f4</i>	-1,44	7,56E-06	2,39E-03	<i>Sergef</i>	1,71	1,00E-06	8,65E-04
<i>Trim75</i>	-1,72	1,37E-05	3,08E-03	<i>Ndufb8</i>	1,82	1,02E-06	8,65E-04
<i>Ube2s</i>	-1,10	1,42E-05	3,08E-03	<i>Lsm7</i>	1,83	1,06E-06	8,65E-04
<i>Naa40</i>	-1,36	1,91E-05	3,60E-03	<i>Cox6a1</i>	2,93	6,65E-07	8,65E-04
<i>Pla2g15</i>	-1,32	2,21E-05	3,73E-03	<i>Acot13</i>	3,45	7,72E-07	8,65E-04
<i>Myt1</i>	-1,11	2,64E-05	4,10E-03	<i>Uba52</i>	3,04	1,22E-06	9,20E-04
<i>Gm15787</i>	-1,66	2,93E-05	4,21E-03	<i>Rplp2</i>	1,58	1,46E-06	9,40E-04
<i>Pkmyt1</i>	-0,94	3,14E-05	4,39E-03	<i>Znrd1as</i>	2,02	1,62E-06	9,40E-04
<i>Tbc1d10a</i>	-1,02	3,26E-05	4,49E-03	<i>Zfp935</i>	2,25	1,42E-06	9,40E-04
<i>Wasf1</i>	-1,19	4,08E-05	5,09E-03	<i>Ccdc122</i>	1,41	1,87E-06	1,01E-03
<i>Snx9</i>	-1,38	5,42E-05	5,76E-03	<i>Nop10</i>	1,66	2,64E-06	1,36E-03
<i>Sreb2</i>	-2,04	5,84E-05	5,89E-03	<i>Myl6</i>	1,53	3,01E-06	1,40E-03
<i>Ncoa4</i>	-1,55	7,38E-05	6,81E-03	<i>Acbd7</i>	1,72	3,89E-06	1,65E-03
<i>Sh3bgrl2</i>	-1,54	7,64E-05	6,83E-03	<i>Lsm4</i>	2,95	4,08E-06	1,66E-03

<i>Patz1</i>	-1,49	7,75E-05	6,83E-03	<i>Ndufa1</i>	2,95	4,86E-06	1,90E-03
--------------	-------	----------	----------	---------------	------	----------	----------

Suppl. Table S 4.4: Primers and probes employed for quantitative RT-PCR analysis

<b>Gene</b>	<b>Forward Primer</b> 5'-3'	<b>Reverse Primer</b> 5'-3'	<b>Probe</b> 5'-3'
<i>Celf1</i>	CCAAGTGGTACCAATGCTCTC	TCGGTGAAGACCCTGCTG	CATCCAGC
<i>Lamtor3</i>	CTGAACTGCGGGAACACC	GCAGAATCGATCTCCACTCC	GGCTGGAG
<i>Tmed2</i>	TGGACATCGACGTGGAGA	GGACTCCCGGTCTCCTTTA	GGACCAGA
<i>Otud6b</i>	AGAAGGCATCGGAAGGAGA	AGCGTTCTTCATTCCCTGAA	AGGAGCTG
<i>Xpo1</i>	GGAAGTCAACACTTTGATATTCCTC	CCATCAATAAACGGACCTTTG	GGAGACAG
<i>Sumo1</i>	TGCTGATAATCATACTCCGAAAGA	CCCCGTTTGTTCCTGATAAA	GGAGGAAG
<i>Ube2v2</i>	TACAAGGTGGACAGGCATGA	GATGGAGGAGCTTCTGGGTA	GGCCACCA
<i>Psma3</i>	GAAGCAGAGAAATATGCCAAGG	GCAACTGTTACAGAAATGTAA ACCA	CCATCCGC
<i>Actb</i>	CGTGAAAAGATGACCCAGATCA	CACAGCCTGGATGGCTACGT	TTTGAGACC TTCAACACC CCAGCCA

Suppl. Table S 4.5: Composition of provided diets.

<b>Crude Nutrients</b>	<b>High Fat Diet (HFD)</b> %	<b>Control Diet (CD)</b> %
<b>Dry matter</b>	97.1	96.7
<b>Crude protein (N x 6.25)</b>	24.1	24.1
<b>Crude fat</b>	34.0	5.1
<b>Crude fibre</b>	6.0	6.4
<b>Crude ash</b>	6.1	6.2
<b>N free extracts</b>	27.0	54.7
<b>Starch</b>	2.2	26.0
<b>Sugar/Dextrines</b>	22.4	26.1
<b>Energy</b>	24.4 MJ/Kg	15.1 MJ/Kg

## 5 REFERENCES

- 1 Miettinen, P. J. *et al.* Epithelial immaturity and multiorgan failure in mice lacking epidermal growth factor receptor. *Nature* **376**, 337-341, (1995).
- 2 Sibilio, M. & Wagner, E. F. Strain-dependent epithelial defects in mice lacking the EGF receptor. *Science (New York, N.Y.)* **269**, 234-238, (1995).
- 3 Threadgill, D. W. *et al.* Targeted disruption of mouse EGF receptor: effect of genetic background on mutant phenotype. *Science (New York, N.Y.)* **269**, 230-234, (1995).
- 4 Lee, K. F. *et al.* Requirement for neuregulin receptor erbB2 in neural and cardiac development. *Nature* **378**, 394-398, (1995).
- 5 Erickson, S. L. *et al.* ErbB3 is required for normal cerebellar and cardiac development: a comparison with ErbB2-and heregulin-deficient mice. *Development (Cambridge, England)* **124**, 4999-5011, (1997).
- 6 Gassmann, M. *et al.* Aberrant neural and cardiac development in mice lacking the ErbB4 neuregulin receptor. *Nature* **378**, 390-394, (1995).
- 7 Linggi, B. & Carpenter, G. ErbB receptors: new insights on mechanisms and biology. *Trends Cell Biol* **16**, 649-656, (2006).
- 8 Schulze, W. X., Deng, L. & Mann, M. Phosphotyrosine interactome of the ErbB-receptor kinase family. *Molecular systems biology* **1**, 2005.0008, (2005).
- 9 Yarden, Y. & Sliwkowski, M. X. Untangling the ErbB signalling network. *Nat Rev Mol Cell Biol* **2**, 127-137, (2001).
- 10 Graus-Porta, D., Beerli, R. R., Daly, J. M. & Hynes, N. E. ErbB-2, the preferred heterodimerization partner of all ErbB receptors, is a mediator of lateral signaling. *The EMBO journal* **16**, 1647-1655, (1997).
- 11 Tzahar, E. *et al.* A hierarchical network of interreceptor interactions determines signal transduction by Neu differentiation factor/neuregulin and epidermal growth factor. *Molecular and cellular biology* **16**, 5276-5287, (1996).
- 12 Guy, P. M., Platko, J. V., Cantley, L. C., Cerione, R. A. & Carraway, K. L., 3rd. Insect cell-expressed p180erbB3 possesses an impaired tyrosine kinase activity. *Proceedings of the National Academy of Sciences of the United States of America* **91**, 8132-8136, (1994).
- 13 Klapper, L. N. *et al.* The ErbB-2/HER2 oncoprotein of human carcinomas may function solely as a shared coreceptor for multiple stroma-derived growth factors. *Proceedings of the National Academy of Sciences of the United States of America* **96**, 4995-5000, (1999).
- 14 Holbro, T. *et al.* The ErbB2/ErbB3 heterodimer functions as an oncogenic unit: ErbB2 requires ErbB3 to drive breast tumor cell proliferation. *Proceedings of the National Academy of Sciences of the United States of America* **100**, 8933-8938, (2003).
- 15 Lee-Hoeflich, S. T. *et al.* A central role for HER3 in HER2-amplified breast cancer: implications for targeted therapy. *Cancer research* **68**, 5878-5887, (2008).
- 16 Shin, D. H., Jo, J. Y. & Han, J. Y. Dual Targeting of ERBB2/ERBB3 for the Treatment of SLC3A2-NRG1-Mediated Lung Cancer. *Molecular cancer therapeutics* **17**, 2024-2033, (2018).
- 17 Fichter, C. D. *et al.* A new model system identifies epidermal growth factor receptor-human epidermal growth factor receptor 2 (HER2) and HER2-human epidermal growth factor receptor 3 heterodimers as potent inducers of oesophageal epithelial cell invasion. *The Journal of pathology* **243**, 481-495, (2017).
- 18 Shi, Y. *et al.* A novel proximity assay for the detection of proteins and protein complexes: quantitation of HER1 and HER2 total protein expression and homodimerization in formalin-fixed, paraffin-embedded cell lines and breast cancer tissue. *Diagnostic molecular pathology : the American journal of surgical pathology, part B* **18**, 11-21, (2009).

- 19 Huang, W. *et al.* Comparison of central HER2 testing with quantitative total HER2 expression and HER2 homodimer measurements using a novel proximity-based assay. *American journal of clinical pathology* **134**, 303-311, (2010).
- 20 Ghosh, R. *et al.* Trastuzumab has preferential activity against breast cancers driven by HER2 homodimers. *Cancer research* **71**, 1871-1882, (2011).
- 21 Spears, M. *et al.* In situ detection of HER2:HER2 and HER2:HER3 protein-protein interactions demonstrates prognostic significance in early breast cancer. *Breast cancer research and treatment* **132**, 463-470, (2012).
- 22 Olayioye, M. A. *et al.* ErbB-1 and ErbB-2 acquire distinct signaling properties dependent upon their dimerization partner. *Molecular and cellular biology* **18**, 5042-5051, (1998).
- 23 Singh, B., Carpenter, G. & Coffey, R. J. EGF receptor ligands: recent advances. *F1000Research* **5**, (2016).
- 24 Roskoski, R., Jr. The ErbB/HER family of protein-tyrosine kinases and cancer. *Pharmacological research* **79**, 34-74, (2014).
- 25 Soltoff, S. P. & Cantley, L. C. p120cbl is a cytosolic adapter protein that associates with phosphoinositide 3-kinase in response to epidermal growth factor in PC12 and other cells. *The Journal of biological chemistry* **271**, 563-567, (1996).
- 26 Plowman, G. D. *et al.* Ligand-specific activation of HER4/p180erbB4, a fourth member of the epidermal growth factor receptor family. *Proceedings of the National Academy of Sciences of the United States of America* **90**, 1746-1750, (1993).
- 27 Riese, D. J., 2nd *et al.* Betacellulin activates the epidermal growth factor receptor and erbB-4, and induces cellular response patterns distinct from those stimulated by epidermal growth factor or neuregulin-beta. *Oncogene* **12**, 345-353, (1996).
- 28 Beerli, R. R. & Hynes, N. E. Epidermal growth factor-related peptides activate distinct subsets of ErbB receptors and differ in their biological activities. *The Journal of biological chemistry* **271**, 6071-6076, (1996).
- 29 Riese, D. J., 2nd, Komurasaki, T., Plowman, G. D. & Stern, D. F. Activation of ErbB4 by the bifunctional epidermal growth factor family hormone epiregulin is regulated by ErbB2. *The Journal of biological chemistry* **273**, 11288-11294, (1998).
- 30 Komurasaki, T., Toyoda, H., Uchida, D. & Morimoto, S. Epiregulin binds to epidermal growth factor receptor and ErbB-4 and induces tyrosine phosphorylation of epidermal growth factor receptor, ErbB-2, ErbB-3 and ErbB-4. *Oncogene* **15**, 2841-2848, (1997).
- 31 Elenius, K., Paul, S., Allison, G., Sun, J. & Klagsbrun, M. Activation of HER4 by heparin-binding EGF-like growth factor stimulates chemotaxis but not proliferation. *The EMBO journal* **16**, 1268-1278, (1997).
- 32 Culouscou, J. M., Plowman, G. D., Carlton, G. W., Green, J. M. & Shoyab, M. Characterization of a breast cancer cell differentiation factor that specifically activates the HER4/p180erbB4 receptor. *The Journal of biological chemistry* **268**, 18407-18410, (1993).
- 33 Tzahar, E. *et al.* ErbB-3 and ErbB-4 function as the respective low and high affinity receptors of all Neu differentiation factor/hereregulin isoforms. *The Journal of biological chemistry* **269**, 25226-25233, (1994).
- 34 Plowman, G. D. *et al.* Heregulin induces tyrosine phosphorylation of HER4/p180erbB4. *Nature* **366**, 473, (1993).
- 35 Pinkas-Kramarski, R. *et al.* ErbB tyrosine kinases and the two neuregulin families constitute a ligand-receptor network. *Molecular and cellular biology* **18**, 6090-6101, (1998).
- 36 Busfield, S. J. *et al.* Characterization of a neuregulin-related gene, Don-1, that is highly expressed in restricted regions of the cerebellum and hippocampus. *Molecular and cellular biology* **17**, 4007-4014, (1997).
- 37 Carraway, K. L., 3rd *et al.* Neuregulin-2, a new ligand of ErbB3/ErbB4-receptor tyrosine kinases. *Nature* **387**, 512-516, (1997).
- 38 Chang, H., Riese, D. J., 2nd, Gilbert, W., Stern, D. F. & McMahan, U. J. Ligands for ErbB-family receptors encoded by a neuregulin-like gene. *Nature* **387**, 509-512, (1997).

- 39 Zhang, D. *et al.* Neuregulin-3 (NRG3): a novel neural tissue-enriched protein that binds and activates ErbB4. *Proceedings of the National Academy of Sciences of the United States of America* **94**, 9562-9567, (1997).
- 40 Jones, J. T., Akita, R. W. & Sliwkowski, M. X. Binding specificities and affinities of egf domains for ErbB receptors. *FEBS letters* **447**, 227-231, (1999).
- 41 Harari, D. *et al.* Neuregulin-4: a novel growth factor that acts through the ErbB-4 receptor tyrosine kinase. *Oncogene* **18**, 2681-2689, (1999).
- 42 Elenius, K. *et al.* Characterization of a naturally occurring ErbB4 isoform that does not bind or activate phosphatidyl inositol 3-kinase. *Oncogene* **18**, 2607, (1999).
- 43 Jones, F. E., Welte, T., Fu, X. Y. & Stern, D. F. ErbB4 signaling in the mammary gland is required for lobuloalveolar development and Stat5 activation during lactation. *The Journal of cell biology* **147**, 77-88, (1999).
- 44 Williams, C. C. *et al.* The ERBB4/HER4 receptor tyrosine kinase regulates gene expression by functioning as a STAT5A nuclear chaperone. *The Journal of cell biology* **167**, 469-478, (2004).
- 45 Ni, C. Y., Murphy, M. P., Golde, T. E. & Carpenter, G. gamma -Secretase cleavage and nuclear localization of ErbB-4 receptor tyrosine kinase. *Science (New York, N.Y.)* **294**, 2179-2181, (2001).
- 46 Omerovic, J. *et al.* Ligand-regulated association of ErbB-4 to the transcriptional co-activator YAP65 controls transcription at the nuclear level. *Experimental cell research* **294**, 469-479, (2004).
- 47 Komuro, A., Nagai, M., Navin, N. E. & Sudol, M. WW domain-containing protein YAP associates with ErbB-4 and acts as a co-transcriptional activator for the carboxyl-terminal fragment of ErbB-4 that translocates to the nucleus. *The Journal of biological chemistry* **278**, 33334-33341, (2003).
- 48 Linggi, B. & Carpenter, G. ErbB-4 s80 intracellular domain abrogates ETO2-dependent transcriptional repression. *The Journal of biological chemistry* **281**, 25373-25380, (2006).
- 49 Paatero, I. *et al.* Interaction with ErbB4 promotes hypoxia-inducible factor-1alpha signaling. *The Journal of biological chemistry* **287**, 9659-9671, (2012).
- 50 Vecchi, M. & Carpenter, G. Constitutive proteolysis of the ErbB-4 receptor tyrosine kinase by a unique, sequential mechanism. *J Cell Biol* **139**, 995-1003, (1997).
- 51 Rio, C., Buxbaum, J. D., Peschon, J. J. & Corfas, G. Tumor necrosis factor-alpha-converting enzyme is required for cleavage of erbB4/HER4. *The Journal of biological chemistry* **275**, 10379-10387, (2000).
- 52 De Angelis Campos, A. C. *et al.* Epidermal growth factor receptors destined for the nucleus are internalized via a clathrin-dependent pathway. *Biochem Biophys Res Commun* **412**, 341-346, (2011).
- 53 Lin, S. Y. *et al.* Nuclear localization of EGF receptor and its potential new role as a transcription factor. *Nature cell biology* **3**, 802-808, (2001).
- 54 Hsu, S. C. & Hung, M. C. Characterization of a novel tripartite nuclear localization sequence in the EGFR family. *The Journal of biological chemistry* **282**, 10432-10440, (2007).
- 55 Wang, S. C. *et al.* Binding at and transactivation of the COX-2 promoter by nuclear tyrosine kinase receptor ErbB-2. *Cancer Cell* **6**, 251-261, (2004).
- 56 Giri, D. K. *et al.* Endosomal transport of ErbB-2: mechanism for nuclear entry of the cell surface receptor. *Molecular and cellular biology* **25**, 11005-11018, (2005).
- 57 Offterdinger, M., Schofer, C., Weipoltshammer, K. & Grunt, T. W. c-erbB-3: a nuclear protein in mammary epithelial cells. *J Cell Biol* **157**, 929-939, (2002).
- 58 Elenius, K. *et al.* A novel juxtamembrane domain isoform of HER4/ErbB4. Isoform-specific tissue distribution and differential processing in response to phorbol ester. *The Journal of biological chemistry* **272**, 26761-26768, (1997).
- 59 Elenius, K. *et al.* Characterization of a naturally occurring ErbB4 isoform that does not bind or activate phosphatidyl inositol 3-kinase. *Oncogene* **18**, 2607-2615, (1999).

- 60 Sundvall, M. *et al.* Cell death or survival promoted by alternative isoforms of ErbB4. *Molecular biology of the cell* **21**, 4275-4286, (2010).
- 61 Muraoka-Cook, R. S. *et al.* ErbB4 splice variants Cyt1 and Cyt2 differ by 16 amino acids and exert opposing effects on the mammary epithelium in vivo. *Molecular and cellular biology* **29**, 4935-4948, (2009).
- 62 Memon, A. A. *et al.* Expression of HER3, HER4 and their ligand heregulin-4 is associated with better survival in bladder cancer patients. *British journal of cancer* **91**, 2034-2041, (2004).
- 63 Ni, H. *et al.* ErbB4 acts as a suppressor in colitis and its associated carcinoma by negatively regulating cholesterol metabolism. *Carcinogenesis*, (2018).
- 64 Liu, Y. *et al.* ERBB4 acts as a suppressor in the development of hepatocellular carcinoma. *Carcinogenesis* **38**, 465-473, (2017).
- 65 Donoghue, J. F. *et al.* Activation of ERBB4 in Glioblastoma Can Contribute to Increased Tumorigenicity and Influence Therapeutic Response. *Cancers* **10**, (2018).
- 66 Prickett, T. D. *et al.* Analysis of the tyrosine kinome in melanoma reveals recurrent mutations in ERBB4. *Nature genetics* **41**, 1127-1132, (2009).
- 67 Rudloff, U. & Samuels, Y. A growing family: adding mutated Erbb4 as a novel cancer target. *Cell cycle (Georgetown, Tex.)* **9**, 1487-1503, (2010).
- 68 Nielsen, T. O., Poulsen, S. S., Journe, F., Ghanem, G. & Sorensen, B. S. HER4 and its cytoplasmic isoforms are associated with progression-free survival of malignant melanoma. *Melanoma research* **24**, 88-91, (2014).
- 69 Fujiwara, S. *et al.* The localization of HER4 intracellular domain and expression of its alternately-spliced isoforms have prognostic significance in ER+ HER2- breast cancer. *Oncotarget* **5**, 3919-3930, (2014).
- 70 Junttila, T. T. *et al.* Cleavable ErbB4 isoform in estrogen receptor-regulated growth of breast cancer cells. *Cancer research* **65**, 1384-1393, (2005).
- 71 Maatta, J. A. *et al.* Proteolytic cleavage and phosphorylation of a tumor-associated ErbB4 isoform promote ligand-independent survival and cancer cell growth. *Molecular biology of the cell* **17**, 67-79, (2006).
- 72 Tang, C. K. *et al.* Ribozyme-mediated down-regulation of ErbB-4 in estrogen receptor-positive breast cancer cells inhibits proliferation both in vitro and in vivo. *Cancer research* **59**, 5315-5322, (1999).
- 73 Lodge, A. J. *et al.* Type 1 growth factor receptor expression in node positive breast cancer: adverse prognostic significance of c-erbB-4. *Journal of clinical pathology* **56**, 300-304, (2003).
- 74 Zhu, Y. *et al.* Coregulation of estrogen receptor by ERBB4/HER4 establishes a growth-promoting autocrine signal in breast tumor cells. *Cancer research* **66**, 7991-7998, (2006).
- 75 Aqeilan, R. I. *et al.* Association of Wwox with ErbB4 in breast cancer. *Cancer research* **67**, 9330-9336, (2007).
- 76 Naresh, A. *et al.* The ERBB4/HER4 intracellular domain 4ICD is a BH3-only protein promoting apoptosis of breast cancer cells. *Cancer research* **66**, 6412-6420, (2006).
- 77 Kew, T. Y. *et al.* c-erbB-4 protein expression in human breast cancer. *British journal of cancer* **82**, 1163-1170, (2000).
- 78 Tovey, S. M. *et al.* Outcome and human epidermal growth factor receptor (HER) 1-4 status in invasive breast carcinomas with proliferation indices evaluated by bromodeoxyuridine labelling. *Breast Cancer Res* **6**, R246-251, (2004).
- 79 Giubellino, A., Burke, T. R., Jr. & Bottaro, D. P. Grb2 signaling in cell motility and cancer. *Expert opinion on therapeutic targets* **12**, 1021-1033, (2008).
- 80 Tari, A. M. & Lopez-Berestein, G. GRB2: a pivotal protein in signal transduction. *Seminars in oncology* **28**, 142-147, (2001).
- 81 McCubrey, J. A. *et al.* Roles of the Raf/MEK/ERK pathway in cell growth, malignant transformation and drug resistance. *Biochimica et biophysica acta* **1773**, 1263-1284, (2007).

- 82 Roepstorff, K., Grovdal, L., Grandal, M., Lerdrup, M. & van Deurs, B. Endocytic downregulation of ErbB receptors: mechanisms and relevance in cancer. *Histochemistry and cell biology* **129**, 563-578, (2008).
- 83 Bouyain, S., Longo, P. A., Li, S., Ferguson, K. M. & Leahy, D. J. The extracellular region of ErbB4 adopts a tethered conformation in the absence of ligand. *Proceedings of the National Academy of Sciences of the United States of America* **102**, 15024-15029, (2005).
- 84 Blobel, C. P. ADAMs: key components in EGFR signalling and development. *Nat Rev Mol Cell Biol* **6**, 32-43, (2005).
- 85 Sahin, U. *et al.* Distinct roles for ADAM10 and ADAM17 in ectodomain shedding of six EGFR ligands. *J Cell Biol* **164**, 769-779, (2004).
- 86 Roskoski, R., Jr. ErbB/HER protein-tyrosine kinases: Structures and small molecule inhibitors. *Pharmacological research* **87**, 42-59, (2014).
- 87 Macdonald-Obermann, J. L. & Pike, L. J. Different epidermal growth factor (EGF) receptor ligands show distinct kinetics and biased or partial agonism for homodimer and heterodimer formation. *The Journal of biological chemistry* **289**, 26178-26188, (2014).
- 88 Zeng, F. & Harris, R. C. Epidermal growth factor, from gene organization to bedside. *Seminars in cell & developmental biology* **28**, 2-11, (2014).
- 89 Dahlhoff, M., Schafer, M., Wolf, E. & Schneider, M. R. Genetic deletion of the EGFR ligand epigen does not affect mouse embryonic development and tissue homeostasis. *Experimental cell research* **319**, 529-535, (2013).
- 90 Luetteke, N. C. *et al.* Targeted inactivation of the EGF and amphiregulin genes reveals distinct roles for EGF receptor ligands in mouse mammary gland development. *Development (Cambridge, England)* **126**, 2739-2750, (1999).
- 91 Singh, B. & Coffey, R. J. From wavy hair to naked proteins: the role of transforming growth factor alpha in health and disease. *Seminars in cell & developmental biology* **28**, 12-21, (2014).
- 92 Shirasawa, S. *et al.* Dermatitis due to epiregulin deficiency and a critical role of epiregulin in immune-related responses of keratinocyte and macrophage. *Proceedings of the National Academy of Sciences of the United States of America* **101**, 13921-13926, (2004).
- 93 Meyer, D. & Birchmeier, C. Multiple essential functions of neuregulin in development. *Nature* **378**, 386-390, (1995).
- 94 Iwamoto, R. *et al.* Heparin-binding EGF-like growth factor and ErbB signaling is essential for heart function. *Proceedings of the National Academy of Sciences of the United States of America* **100**, 3221-3226, (2003).
- 95 Britto, J. M. *et al.* Generation and characterization of neuregulin-2-deficient mice. *Molecular and cellular biology* **24**, 8221-8226, (2004).
- 96 Yan, L. *et al.* Neuregulin-2 ablation results in dopamine dysregulation and severe behavioral phenotypes relevant to psychiatric disorders. *Molecular psychiatry* **23**, 1233-1243, (2018).
- 97 Hayes, L. N. *et al.* Neuregulin 3 Knockout Mice Exhibit Behaviors Consistent with Psychotic Disorders. *Molecular neuropsychiatry* **2**, 79-87, (2016).
- 98 Paramo, B., Wyatt, S. & Davies, A. M. An essential role for neuregulin-4 in the growth and elaboration of developing neocortical pyramidal dendrites. *Experimental neurology* **302**, 85-92, (2018).
- 99 Nugroho, D. B. *et al.* Neuregulin-4 is an angiogenic factor that is critically involved in the maintenance of adipose tissue vasculature. *Biochem Biophys Res Commun* **503**, 378-384, (2018).
- 100 Shing, Y. *et al.* Betacellulin: a mitogen from pancreatic beta cell tumors. *Science (New York, N.Y.)* **259**, 1604-1607, (1993).
- 101 Schneider, M. R. & Wolf, E. The epidermal growth factor receptor ligands at a glance. *Journal of cellular physiology* **218**, 460-466, (2009).

- 102 Watanabe, T. *et al.* Recombinant human betacellulin. Molecular structure, biological activities, and receptor interaction. *The Journal of biological chemistry* **269**, 9966-9973, (1994).
- 103 Dahlhoff, M., Wolf, E. & Schneider, M. R. The ABC of BTC: Structural properties and biological roles of betacellulin. *Seminars in cell & developmental biology* **28**, 42-48, (2014).
- 104 Roepstorff, K. *et al.* Differential effects of EGFR ligands on endocytic sorting of the receptor. *Traffic (Copenhagen, Denmark)* **10**, 1115-1127, (2009).
- 105 Henriksen, L., Grandal, M. V., Knudsen, S. L., van Deurs, B. & Grovdal, L. M. Internalization mechanisms of the epidermal growth factor receptor after activation with different ligands. *PloS one* **8**, e58148, (2013).
- 106 Mashima, H. *et al.* Betacellulin and activin A coordinately convert amylase-secreting pancreatic AR42J cells into insulin-secreting cells. *J Clin Invest* **97**, 1647-1654, (1996).
- 107 Watada, H. *et al.* PDX-1 induces insulin and glucokinase gene expressions in alphaTC1 clone 6 cells in the presence of betacellulin. *Diabetes* **45**, 1826-1831, (1996).
- 108 Yoshida, S. *et al.* PDX-1 induces differentiation of intestinal epithelioid IEC-6 into insulin-producing cells. *Diabetes* **51**, 2505-2513, (2002).
- 109 Li, W. C., Horb, M. E., Tosh, D. & Slack, J. M. In vitro transdifferentiation of hepatoma cells into functional pancreatic cells. *Mech Dev* **122**, 835-847, (2005).
- 110 Paz, A. H. *et al.* Betacellulin overexpression in mesenchymal stem cells induces insulin secretion in vitro and ameliorates streptozotocin-induced hyperglycemia in rats. *Stem cells and development* **20**, 223-232, (2011).
- 111 Demeterco, C., Beattie, G. M., Dib, S. A., Lopez, A. D. & Hayek, A. A role for activin A and betacellulin in human fetal pancreatic cell differentiation and growth. *The Journal of clinical endocrinology and metabolism* **85**, 3892-3897, (2000).
- 112 Huotari, M. A., Palgi, J. & Otonkoski, T. Growth factor-mediated proliferation and differentiation of insulin-producing INS-1 and RINm5F cells: identification of betacellulin as a novel beta-cell mitogen. *Endocrinology* **139**, 1494-1499, (1998).
- 113 Sundaresan, S., Roberts, P. E., King, K. L., Sliwkowski, M. X. & Mather, J. P. Biological response to ErbB ligands in nontransformed cell lines correlates with a specific pattern of receptor expression. *Endocrinology* **139**, 4756-4764, (1998).
- 114 Olsen, D. A. *et al.* Increased concentrations of growth factors and activation of the EGFR system in breast cancer. *Clinical chemistry and laboratory medicine* **50**, 1809-1818, (2012).
- 115 Kong, A. *et al.* HER2 oncogenic function escapes EGFR tyrosine kinase inhibitors via activation of alternative HER receptors in breast cancer cells. *PloS one* **3**, e2881, (2008).
- 116 Jackson, L. F. *et al.* Defective valvulogenesis in HB-EGF and TACE-null mice is associated with aberrant BMP signaling. *The EMBO journal* **22**, 2704-2716, (2003).
- 117 Schneider, M. R. *et al.* Betacellulin overexpression in transgenic mice causes disproportionate growth, pulmonary hemorrhage syndrome, and complex eye pathology. *Endocrinology* **146**, 5237-5246, (2005).
- 118 Gratao, A. A., Dahlhoff, M., Sinowatz, F., Wolf, E. & Schneider, M. R. Betacellulin overexpression in the mouse ovary leads to MAPK3/MAPK1 hyperactivation and reduces litter size by impairing fertilization. *Biology of reproduction* **78**, 43-52, (2008).
- 119 Dahlhoff, M. *et al.* Betacellulin protects from pancreatitis by activating stress-activated protein kinase. *Gastroenterology* **138**, 1585-1594, 1594 e1581-1583, (2010).
- 120 Lankisch, P. G., Apte, M. & Banks, P. A. Acute pancreatitis. *Lancet (London, England)* **386**, 85-96, (2015).
- 121 Bollen, T. L. Acute pancreatitis: international classification and nomenclature. *Clinical radiology* **71**, 121-133, (2016).
- 122 Peery, A. F. *et al.* Burden of Gastrointestinal, Liver, and Pancreatic Diseases in the United States. *Gastroenterology* **149**, 1731-1741.e1733, (2015).

- 123 Lankisch, P. G., Assmus, C., Maisonneuve, P. & Lowenfels, A. B. Epidemiology of  
pancreatic diseases in Luneburg County. A study in a defined German population.  
*Pancreatology* **2**, 469-477, (2002).
- 124 Hollemans, R. A. *et al.* Pancreatic exocrine insufficiency following acute pancreatitis:  
Systematic review and study level meta-analysis. *Pancreatology* **18**, 253-262, (2018).
- 125 Das, S. L. *et al.* Newly diagnosed diabetes mellitus after acute pancreatitis: a  
systematic review and meta-analysis. *Gut* **63**, 818-831, (2014).
- 126 Lee, P. J. & Papachristou, G. I. New insights into acute pancreatitis. *Nature reviews.  
Gastroenterology & hepatology*, (2019).
- 127 Banks, P. A. *et al.* Classification of acute pancreatitis--2012: revision of the Atlanta  
classification and definitions by international consensus. *Gut* **62**, 102-111, (2013).
- 128 Basurto Ona, X., Rigau Comas, D. & Urrutia, G. Opioids for acute pancreatitis pain.  
*The Cochrane database of systematic reviews*, Cd009179, (2013).
- 129 Huber, W. & Schmid, R. M. Akute Pankreatitis. *Dtsch Arztebl International* **104**, A-1832,  
(2007).
- 130 Mirtallo, J. M. *et al.* International consensus guidelines for nutrition therapy in  
pancreatitis. *JPEN. Journal of parenteral and enteral nutrition* **36**, 284-291, (2012).
- 131 Tse, F. & Yuan, Y. Early routine endoscopic retrograde cholangiopancreatography  
strategy versus early conservative management strategy in acute gallstone  
pancreatitis. *The Cochrane database of systematic reviews*, Cd009779, (2012).
- 132 van Brunschot, S. *et al.* Treatment of necrotizing pancreatitis. *Clinical gastroenterology  
and hepatology : the official clinical practice journal of the American  
Gastroenterological Association* **10**, 1190-1201, (2012).
- 133 Mossner, J. Update lecture: benign diseases of the exocrine pancreas. *Digestive  
diseases (Basel, Switzerland)* **29 Suppl 1**, 9-16, (2011).
- 134 Schroder, M. & Kaufman, R. J. ER stress and the unfolded protein response. *Mutation  
research* **569**, 29-63, (2005).
- 135 Xu, C., Bailly-Maitre, B. & Reed, J. C. Endoplasmic reticulum stress: cell life and death  
decisions. *J Clin Invest* **115**, 2656-2664, (2005).
- 136 Lampel, M. & Kern, H. F. Acute interstitial pancreatitis in the rat induced by excessive  
doses of a pancreatic secretagogue. *Virchows Archiv. A, Pathological anatomy and  
histology* **373**, 97-117, (1977).
- 137 Liu, Q. *et al.* The effect of epidermal growth factor on the septic complications of acute  
pancreatitis. *The Journal of surgical research* **69**, 171-177, (1997).
- 138 Warzecha, Z., Dembinski, A., Konturek, P. C., Ceranowicz, P. & Konturek, S. J.  
Epidermal growth factor protects against pancreatic damage in cerulein-induced  
pancreatitis. *Digestion* **60**, 314-323, (1999).
- 139 Dembinski, A. *et al.* Epidermal growth factor accelerates pancreatic recovery after  
caerulein-induced pancreatitis. *European journal of pharmacology* **398**, 159-168,  
(2000).
- 140 Hu, G. *et al.* Reg4 protects against acinar cell necrosis in experimental pancreatitis.  
*Gut* **60**, 820-828, (2011).
- 141 Ozaki, N. *et al.* Autophagy regulation in pancreatic acinar cells is independent of  
epidermal growth factor receptor signaling. *Biochem Biophys Res Commun* **446**, 224-  
230, (2014).
- 142 Huang, Y. *et al.* Role of Kinase Epidermal Growth Factor Receptor and SRC in the  
Caerulein-Induced Acute Pancreatitis in Mice. *Pancreas* **44**, 152-157, (2015).
- 143 Ebert, M., Friess, H., Buchler, M. W. & Korc, M. Differential distribution of human  
epidermal growth factor receptor family in acute pancreatitis. *Digestive diseases and  
sciences* **40**, 2134-2142, (1995).
- 144 Gu, H. *et al.* Alcohol exacerbates LPS-induced fibrosis in subclinical acute pancreatitis.  
*The American journal of pathology* **183**, 1508-1517, (2013).
- 145 Chan, L. K. *et al.* Epithelial NEMO/IKKgamma limits fibrosis and promotes regeneration  
during pancreatitis. *Gut* **66**, 1995-2007, (2017).

- 146 Sandgren, E. P., Luetkeke, N. C., Palmiter, R. D., Brinster, R. L. & Lee, D. C. Overexpression of TGF alpha in transgenic mice: induction of epithelial hyperplasia, pancreatic metaplasia, and carcinoma of the breast. *Cell* **61**, 1121-1135, (1990).
- 147 Wagner, M., Luhrs, H., Kloppel, G., Adler, G. & Schmid, R. M. Malignant transformation of duct-like cells originating from acini in transforming growth factor transgenic mice. *Gastroenterology* **115**, 1254-1262, (1998).
- 148 Means, A. L. *et al.* Overexpression of heparin-binding EGF-like growth factor in mouse pancreas results in fibrosis and epithelial metaplasia. *Gastroenterology* **124**, 1020-1036, (2003).
- 149 Wagner, M. *et al.* Transgenic overexpression of amphiregulin induces a mitogenic response selectively in pancreatic duct cells. *Gastroenterology* **122**, 1898-1912, (2002).
- 150 Blaine, S. A. *et al.* Epidermal growth factor receptor regulates pancreatic fibrosis. *American journal of physiology. Gastrointestinal and liver physiology* **297**, G434-441, (2009).
- 151 Baron, T. H. & Morgan, D. E. Acute necrotizing pancreatitis. *N. Engl. J. Med* **340**, 1412-1417, (1999).
- 152 Frossard, J. L., Steer, M. L. & Pastor, C. M. Acute pancreatitis. *Lancet* **371**, 143-152, (2008).
- 153 Graber, H. U. *et al.* ErbB-4 mRNA expression is decreased in non-metastatic pancreatic cancer. *Int. J. Cancer* **84**, 24-27, (1999).
- 154 Mill, C. P., Gettinger, K. L. & Riese, D. J. Ligand stimulation of ErbB4 and a constitutively-active ErbB4 mutant result in different biological responses in human pancreatic tumor cell lines. *Exp. Cell Res* **317**, 392-404, (2011).
- 155 Ardito, C. M. *et al.* EGF receptor is required for KRAS-induced pancreatic tumorigenesis. *Cancer Cell* **22**, 304-317, (2012).
- 156 Navas, C. *et al.* EGF Receptor Signaling Is Essential for K-Ras Oncogene-Driven Pancreatic Ductal Adenocarcinoma. *Cancer Cell* **22**, 318-330, (2012).
- 157 Wagner, M., Luhrs, H., Kloppel, G., Adler, G. & Schmid, R. M. Malignant transformation of duct-like cells originating from acini in transforming growth factor transgenic mice. *Gastroenterology* **115**, 1254-1262, (1998).
- 158 Wagner, M. *et al.* Transgenic overexpression of amphiregulin induces a mitogenic response selectively in pancreatic duct cells. *Gastroenterology* **122**, 1898-1912, (2002).
- 159 Means, A. L. *et al.* Overexpression of heparin-binding EGF-like growth factor in mouse pancreas results in fibrosis and epithelial metaplasia. *Gastroenterology* **124**, 1020-1036, (2003).
- 160 Dahlhoff, M. *et al.* Betacellulin protects from pancreatitis by activating stress-activated protein kinase. *Gastroenterology* **138**, 1585-1594, 1594, (2010).
- 161 Standop, J. *et al.* ErbB2 oncogene expression supports the acute pancreatitis-chronic pancreatitis sequence. *Virchows Archiv : an international journal of pathology* **441**, 385-391, (2002).
- 162 Friess, H. *et al.* Enhanced erbB-3 expression in human pancreatic cancer correlates with tumor progression. *Clinical cancer research : an official journal of the American Association for Cancer Research* **1**, 1413-1420, (1995).
- 163 Gilbertson, R. *et al.* Novel ERBB4 juxtamembrane splice variants are frequently expressed in childhood medulloblastoma. *Genes Chromosomes. Cancer* **31**, 288-294, (2001).
- 164 Veikkolainen, V. *et al.* Function of ERBB4 is determined by alternative splicing. *Cell Cycle* **10**, 2647-2657, (2011).
- 165 Zhang, Y. W. *et al.* Presenilin/gamma-secretase-dependent processing of beta-amyloid precursor protein regulates EGF receptor expression. *Proc. Natl. Acad. Sci. U. S. A* **104**, 10613-10618, (2007).
- 166 Lee, H. J. *et al.* Presenilin-dependent gamma-secretase-like intramembrane cleavage of ErbB4. *J. Biol. Chem* **277**, 6318-6323, (2002).

- 167 Komuro, A., Nagai, M., Navin, N. E. & Sudol, M. WW domain-containing protein YAP associates with ErbB-4 and acts as a co-transcriptional activator for the carboxyl-terminal fragment of ErbB-4 that translocates to the nucleus. *J. Biol. Chem* **278**, 33334-33341, (2003).
- 168 Arasada, R. R. & Carpenter, G. Secretase-dependent tyrosine phosphorylation of Mdm2 by the ErbB-4 intracellular domain fragment. *J. Biol. Chem* **280**, 30783-30787, (2005).
- 169 Schneider, M. R. *et al.* Betacellulin Overexpression in Transgenic Mice Causes Disproportionate Growth, Pulmonary Hemorrhage Syndrome, and Complex Eye Pathology. *Endocrinology* **146**, 5237-5246, (2005).
- 170 Lee, D. *et al.* Wa5 is a novel ENU-induced antimorphic allele of the epidermal growth factor receptor. *Mamm. Genome* **15**, 525-536, (2004).
- 171 Long, W. *et al.* Impaired differentiation and lactational failure of Erbb4-deficient mammary glands identify ERBB4 as an obligate mediator of STAT5. *Development* **130**, 5257-5268, (2003).
- 172 Nakhai, H. *et al.* Ptf1a is essential for the differentiation of GABAergic and glycinergic amacrine cells and horizontal cells in the mouse retina. *Development* **134**, 1151-1160, (2007).
- 173 Schmidt, J. *et al.* Histopathologic correlates of serum amylase activity in acute experimental pancreatitis. *Dig. Dis. Sci* **37**, 1426-1433, (1992).
- 174 Vrolyk, V., Schneberger, D., Le, K., Wobeser, B. K. & Singh, B. Mouse model to study pulmonary intravascular macrophage recruitment and lung inflammation in acute necrotizing pancreatitis. *Cell Tissue Res*, (2019).
- 175 Dahlhoff, M., Schafer, M., Muzumdar, S., Rose, C. & Schneider, M. R. ERBB3 is required for tumor promotion in a mouse model of skin carcinogenesis. *Mol. Oncol* **9**, 1825-1833, (2015).
- 176 Hoesl, C., Rohrl, J. M., Schneider, M. R. & Dahlhoff, M. The receptor tyrosine kinase ERBB4 is expressed in skin keratinocytes and influences epidermal proliferation. *Biochimica et biophysica acta. General subjects* **1862**, 958-966, (2018).
- 177 Muraoka-Cook, R. S. *et al.* Heregulin-dependent delay in mitotic progression requires HER4 and BRCA1. *Mol. Cell Biol* **26**, 6412-6424, (2006).
- 178 Haskins, J. W., Nguyen, D. X. & Stern, D. F. Neuregulin 1-activated ERBB4 interacts with YAP to induce Hippo pathway target genes and promote cell migration. *Science signaling* **7**, ra116, (2014).
- 179 Kudo, A. & Kii, I. Periostin function in communication with extracellular matrices. *Journal of cell communication and signaling* **12**, 301-308, (2018).
- 180 Luo, G. *et al.* Spontaneous calcification of arteries and cartilage in mice lacking matrix GLA protein. *Nature* **386**, 78-81, (1997).
- 181 Lekstan, A. *et al.* Concentrations and activities of metalloproteinases 2 and 9 and their inhibitors (TIMPS) in chronic pancreatitis and pancreatic adenocarcinoma. *Journal of physiology and pharmacology : an official journal of the Polish Physiological Society* **63**, 589-599, (2012).
- 182 Bramhall, S. R., Stamp, G. W., Dunn, J., Lemoine, N. R. & Neoptolemos, J. P. Expression of collagenase (MMP2), stromelysin (MMP3) and tissue inhibitor of the metalloproteinases (TIMP1) in pancreatic and ampullary disease. *British journal of cancer* **73**, 972-978, (1996).
- 183 Lopez, J. I., Mouw, J. K. & Weaver, V. M. Biomechanical regulation of cell orientation and fate. *Oncogene* **27**, 6981-6993, (2008).
- 184 Hausmann, S. *et al.* Loss of Periostin Results in Impaired Regeneration and Pancreatic Atrophy after Cerulein-Induced Pancreatitis. *The American journal of pathology* **186**, 24-31, (2016).
- 185 Kusnierz-Cabala, B. *et al.* Serum matrix Gla protein concentrations in patients with mild and severe acute pancreatitis. *Clinical laboratory* **57**, 999-1006, (2011).
- 186 Feng, Y. *et al.* Mesenchymal stromal cells-derived matrix Gla protein contribute to the alleviation of experimental colitis. *Cell death & disease* **9**, 691, (2018).

- 187 Viegas, C. S. B. *et al.* Gla-rich protein function as an anti-inflammatory agent in monocytes/macrophages: Implications for calcification-related chronic inflammatory diseases. *PloS one* **12**, e0177829, (2017).
- 188 Gebhardt, S. *et al.* Exploration of global gene expression changes during the estrous cycle in equine endometrium. *Biology of reproduction* **87**, 136, (2012).
- 189 Ritchie, M. E. *et al.* limma powers differential expression analyses for RNA-sequencing and microarray studies. *Nucleic acids research* **43**, e47, (2015).
- 190 Chung, S. D., Chen, K. Y., Xirasagar, S., Tsai, M. C. & Lin, H. C. More than 9-times increased risk for pancreatic cancer among patients with acute pancreatitis in Chinese population. *Pancreas* **41**, 142-146, (2012).
- 191 Karlson, B. M. *et al.* The risk of pancreatic cancer following pancreatitis: an association due to confounding? *Gastroenterology* **113**, 587-592, (1997).
- 192 Kirkegard, J., Cronin-Fenton, D., Heide-Jorgensen, U. & Mortensen, F. V. Acute Pancreatitis and Pancreatic Cancer Risk: A Nationwide Matched-Cohort Study in Denmark. *Gastroenterology* **154**, 1729-1736, (2018).
- 193 Bartolini, I. *et al.* Current Management of Pancreatic Neuroendocrine Tumors: From Demolitive Surgery to Observation. *Gastroenterology research and practice* **2018**, 9647247, (2018).
- 194 Chaudhary, P. Acinar Cell Carcinoma of the Pancreas: A Literature Review and Update. *The Indian journal of surgery* **77**, 226-231, (2015).
- 195 Bray, F. *et al.* Global cancer statistics 2018: GLOBOCAN estimates of incidence and mortality worldwide for 36 cancers in 185 countries. *CA: a cancer journal for clinicians* **68**, 394-424, (2018).
- 196 Ferlay, J., Partensky, C. & Bray, F. More deaths from pancreatic cancer than breast cancer in the EU by 2017. *Acta Oncologica* **55**, 1158-1160, (2016).
- 197 Rahib, L. *et al.* Projecting cancer incidence and deaths to 2030: the unexpected burden of thyroid, liver, and pancreas cancers in the United States. *Cancer research* **74**, 2913-2921, (2014).
- 198 Siegel, R. L., Miller, K. D. & Jemal, A. Cancer statistics, 2018. *CA: a cancer journal for clinicians* **68**, 7-30, (2018).
- 199 Singhi, A. D., Koay, E. J., Chari, S. T. & Maitra, A. Early Detection of Pancreatic Cancer: Opportunities and Challenges. *Gastroenterology*, (2019).
- 200 Thomas, D. & Radhakrishnan, P. Tumor-stromal crosstalk in pancreatic cancer and tissue fibrosis. *Molecular cancer* **18**, 14, (2019).
- 201 Whatcott, C. J. *et al.* Desmoplasia in Primary Tumors and Metastatic Lesions of Pancreatic Cancer. *Clinical cancer research : an official journal of the American Association for Cancer Research* **21**, 3561-3568, (2015).
- 202 Olive, K. P. *et al.* Inhibition of Hedgehog signaling enhances delivery of chemotherapy in a mouse model of pancreatic cancer. *Science (New York, N.Y.)* **324**, 1457-1461, (2009).
- 203 Aslan, M., Shahbazi, R., Ulubayram, K. & Ozpolat, B. Targeted Therapies for Pancreatic Cancer and Hurdles Ahead. *Anticancer research* **38**, 6591-6606, (2018).
- 204 Perera, Rushika M. & Bardeesy, N. Ready, Set, Go: The EGF Receptor at the Pancreatic Cancer Starting Line. *Cancer Cell* **22**, 281-282, (2012).
- 205 Distler, M., Aust, D., Weitz, J., Pilarsky, C. & Grutzmann, R. Precursor lesions for sporadic pancreatic cancer: PanIN, IPMN, and MCN. *BioMed research international* **2014**, 474905, (2014).
- 206 Hruban, R. H. *et al.* An illustrated consensus on the classification of pancreatic intraepithelial neoplasia and intraductal papillary mucinous neoplasms. *The American journal of surgical pathology* **28**, 977-987, (2004).
- 207 Hruban, R. H. *et al.* Pancreatic intraepithelial neoplasia: a new nomenclature and classification system for pancreatic duct lesions. *The American journal of surgical pathology* **25**, 579-586, (2001).
- 208 Kalluri, R. & Weinberg, R. A. The basics of epithelial-mesenchymal transition. *J Clin Invest* **119**, 1420-1428, (2009).

- 209 Iacobuzio-Donahue, C. A. *et al.* DPC4 Gene Status of the Primary Carcinoma Correlates With Patterns of Failure in Patients With Pancreatic Cancer. **27**, 1806-1813, (2009).
- 210 Giovannetti, E. *et al.* Never let it go: Stopping key mechanisms underlying metastasis to fight pancreatic cancer. *Seminars in Cancer Biology* **44**, 43-59, (2017).
- 211 Vonlaufen, A. *et al.* Pancreatic stellate cells: partners in crime with pancreatic cancer cells. *Cancer research* **68**, 2085-2093, (2008).
- 212 Ferdek, P. E. & Jakubowska, M. A. Biology of pancreatic stellate cells-more than just pancreatic cancer. *Pflugers Archiv : European journal of physiology* **469**, 1039-1050, (2017).
- 213 Schneiderhan, W. *et al.* Pancreatic stellate cells are an important source of MMP-2 in human pancreatic cancer and accelerate tumor progression in a murine xenograft model and CAM assay. *Journal of cell science* **120**, 512-519, (2007).
- 214 Pandol, S. J. & Edderkaoui, M. What are the macrophages and stellate cells doing in pancreatic adenocarcinoma? *Frontiers in physiology* **6**, 125, (2015).
- 215 Jones, S. *et al.* Core signaling pathways in human pancreatic cancers revealed by global genomic analyses. *Science (New York, N.Y.)* **321**, 1801-1806, (2008).
- 216 Hezel, A. F., Kimmelman, A. C., Stanger, B. Z., Bardeesy, N. & Depinho, R. A. Genetics and biology of pancreatic ductal adenocarcinoma. *Genes Dev* **20**, 1218-1249, (2006).
- 217 Biankin, A. V. *et al.* Pancreatic cancer genomes reveal aberrations in axon guidance pathway genes. *Nature* **491**, 399-405, (2012).
- 218 Waddell, N. *et al.* Whole genomes redefine the mutational landscape of pancreatic cancer. *Nature* **518**, 495-501, (2015).
- 219 Karnoub, A. E. & Weinberg, R. A. Ras oncogenes: split personalities. *Nat Rev Mol Cell Biol* **9**, 517-531, (2008).
- 220 Miglio, U. *et al.* KRAS mutational analysis in ductal adenocarcinoma of the pancreas and its clinical significance. *Pathology, research and practice* **210**, 307-311, (2014).
- 221 Cancer Genome Atlas Research Network. Electronic address, a. a. d. h. e. & Cancer Genome Atlas Research, N. Integrated Genomic Characterization of Pancreatic Ductal Adenocarcinoma. *Cancer Cell* **32**, 185-203 e113, (2017).
- 222 Windon, A. L. *et al.* A KRAS wild type mutational status confers a survival advantage in pancreatic ductal adenocarcinoma. *Journal of gastrointestinal oncology* **9**, 1-10, (2018).
- 223 Fischer, C. G. & Wood, L. D. From somatic mutation to early detection: insights from molecular characterization of pancreatic cancer precursor lesions. *The Journal of pathology* **246**, 395-404, (2018).
- 224 di Magliano, M. P. & Logsdon, C. D. Roles for KRAS in Pancreatic Tumor Development and Progression. *Gastroenterology* **144**, 1220-1229, (2013).
- 225 Pylayeva-Gupta, Y., Grabocka, E. & Bar-Sagi, D. RAS oncogenes: weaving a tumorigenic web. *Nature reviews. Cancer* **11**, 761-774, (2011).
- 226 Eser, S., Schnieke, A., Schneider, G. & Saur, D. Oncogenic KRAS signalling in pancreatic cancer. *British journal of cancer* **111**, 817-822, (2014).
- 227 Ryan, D. P., Hong, T. S. & Bardeesy, N. Pancreatic adenocarcinoma. *The New England journal of medicine* **371**, 1039-1049, (2014).
- 228 Ferrone, C. R. *et al.* Pancreatic ductal adenocarcinoma: long-term survival does not equal cure. *Surgery* **152**, S43-49, (2012).
- 229 Han, S. S. *et al.* Analysis of long-term survivors after surgical resection for pancreatic cancer. *Pancreas* **32**, 271-275, (2006).
- 230 Winter, J. M. *et al.* 1423 pancreaticoduodenectomies for pancreatic cancer: A single-institution experience. *Journal of gastrointestinal surgery : official journal of the Society for Surgery of the Alimentary Tract* **10**, 1199-1210; discussion 1210-1191, (2006).
- 231 Chiaravalli, M., Reni, M. & O'Reilly, E. M. Pancreatic ductal adenocarcinoma: State-of-the-art 2017 and new therapeutic strategies. *Cancer treatment reviews* **60**, 32-43, (2017).

- 232 Huang, P., Chubb, S., Hertel, L. W., Grindey, G. B. & Plunkett, W. Action of 2',2'-  
difluorodeoxycytidine on DNA synthesis. *Cancer research* **51**, 6110-6117, (1991).
- 233 Jordan, M. A. & Wilson, L. Microtubules as a target for anticancer drugs. *Nature*  
*reviews. Cancer* **4**, 253-265, (2004).
- 234 Von Hoff, D. D. *et al.* Increased survival in pancreatic cancer with nab-paclitaxel plus  
gemcitabine. *The New England journal of medicine* **369**, 1691-1703, (2013).
- 235 Longley, D. B., Harkin, D. P. & Johnston, P. G. 5-fluorouracil: mechanisms of action  
and clinical strategies. *Nature reviews. Cancer* **3**, 330-338, (2003).
- 236 Conroy, T. *et al.* FOLFIRINOX versus gemcitabine for metastatic pancreatic cancer.  
*The New England journal of medicine* **364**, 1817-1825, (2011).
- 237 Ueda, S. *et al.* The correlation between cytoplasmic overexpression of epidermal  
growth factor receptor and tumor aggressiveness: poor prognosis in patients with  
pancreatic ductal adenocarcinoma. *Pancreas* **29**, e1-8, (2004).
- 238 Dancer, J., Takei, H., Ro, J. Y. & Lowery-Nordberg, M. Coexpression of EGFR and  
HER-2 in pancreatic ductal adenocarcinoma: a comparative study using  
immunohistochemistry correlated with gene amplification by fluorescent in situ  
hybridization. *Oncology reports* **18**, 151-155, (2007).
- 239 Pham, N. A. *et al.* Immunohistochemical analysis of changes in signaling pathway  
activation downstream of growth factor receptors in pancreatic duct cell  
carcinogenesis. *BMC cancer* **8**, 43, (2008).
- 240 Xue, A., Scarlett, C. J., Jackson, C. J., Allen, B. J. & Smith, R. C. Prognostic  
significance of growth factors and the urokinase-type plasminogen activator system in  
pancreatic ductal adenocarcinoma. *Pancreas* **36**, 160-167, (2008).
- 241 Bourghardt Fagman, J. *et al.* EGFR, but not COX-2, protein in resected pancreatic  
ductal adenocarcinoma is associated with poor survival. (2019).
- 242 Yan, L., Hsu, K. & Beckman, R. A. Antibody-based therapy for solid tumors. *Cancer*  
*journal (Sudbury, Mass.)* **14**, 178-183, (2008).
- 243 Grunwald, V. & Hidalgo, M. Developing inhibitors of the epidermal growth factor  
receptor for cancer treatment. *Journal of the National Cancer Institute* **95**, 851-867,  
(2003).
- 244 Day, J. D. *et al.* Immunohistochemical evaluation of HER-2/neu expression in  
pancreatic adenocarcinoma and pancreatic intraepithelial neoplasms. *Human*  
*Pathology* **27**, 119-124, (1996).
- 245 Yamanaka, Y. *et al.* Overexpression of HER2/neu oncogene in human pancreatic  
carcinoma. *Human Pathology* **24**, 1127-1134, (1993).
- 246 Hall, P. A. *et al.* The c-erb B-2 proto-oncogene in human pancreatic cancer. *The*  
*Journal of pathology* **161**, 195-200, (1990).
- 247 Satoh, K. *et al.* An immunohistochemical study of the c-erbB-2 oncogene product in  
intraductal mucin-hypersecreting neoplasms and in ductal cell carcinomas of the  
pancreas. *Cancer* **72**, 51-56, (1993).
- 248 Dugan, M. C. *et al.* HER-2/neu expression in pancreatic adenocarcinoma: relation to  
tumor differentiation and survival. *Pancreas* **14**, 229-236, (1997).
- 249 Figueroa-Magalhães, M. C., Jelovac, D., Connolly, R. M. & Wolff, A. C. Treatment of  
HER2-positive breast cancer. *The Breast* **23**, 128-136, (2014).
- 250 Ciliberto, D. *et al.* Systematic review and meta-analysis on targeted therapy in  
advanced pancreatic cancer. *Pancreatology* **16**, 249-258, (2016).
- 251 Ottaiano, A. *et al.* Gemcitabine mono-therapy versus gemcitabine plus targeted therapy  
in advanced pancreatic cancer: a meta-analysis of randomized phase III trials. *Acta*  
*oncologica (Stockholm, Sweden)* **56**, 377-383, (2017).
- 252 Moore, M. J. *et al.* Erlotinib plus gemcitabine compared with gemcitabine alone in  
patients with advanced pancreatic cancer: a phase III trial of the National Cancer  
Institute of Canada Clinical Trials Group. *Journal of clinical oncology : official journal of*  
*the American Society of Clinical Oncology* **25**, 1960-1966, (2007).

- 253 Harder, J. *et al.* Multicentre phase II trial of trastuzumab and capecitabine in patients with HER2 overexpressing metastatic pancreatic cancer. *British journal of cancer* **106**, 1033, (2012).
- 254 Safran, H. *et al.* Herceptin and gemcitabine for metastatic pancreatic cancers that overexpress HER-2/neu. *Cancer investigation* **22**, 706-712, (2004).
- 255 Means, A. L. *et al.* Pancreatic epithelial plasticity mediated by acinar cell transdifferentiation and generation of nestin-positive intermediates. *Development (Cambridge, England)* **132**, 3767-3776, (2005).
- 256 Uhlen, M. *et al.* A pathology atlas of the human cancer transcriptome. *Science (New York, N.Y.)* **357**, (2017).
- 257 Wang, L. *et al.* Expression of amphiregulin predicts poor outcome in patients with pancreatic ductal adenocarcinoma. **11**, 60, (2016).
- 258 Yotsumoto, F. *et al.* Amphiregulin regulates the activation of ERK and Akt through epidermal growth factor receptor and HER3 signals involved in the progression of pancreatic cancer. *Cancer science* **101**, 2351-2360, (2010).
- 259 Korc, M. *et al.* Overexpression of the epidermal growth factor receptor in human pancreatic cancer is associated with concomitant increases in the levels of epidermal growth factor and transforming growth factor alpha. *J Clin Invest* **90**, 1352-1360, (1992).
- 260 Yamanaka, Y. *et al.* Coexpression of epidermal growth factor receptor and ligands in human pancreatic cancer is associated with enhanced tumor aggressiveness. *Anticancer research* **13**, 565-569, (1993).
- 261 Kleeff, J. *et al.* Pancreatic cancer--new aspects of molecular biology research. *Swiss surgery = Schweizer Chirurgie = Chirurgie suisse = Chirurgia svizzera* **6**, 231-234, (2000).
- 262 Zhu, Z. *et al.* Epiregulin is Up-regulated in pancreatic cancer and stimulates pancreatic cancer cell growth. *Biochem Biophys Res Commun* **273**, 1019-1024, (2000).
- 263 Chaturvedi, P. *et al.* MUC4 mucin potentiates pancreatic tumor cell proliferation, survival, and invasive properties and interferes with its interaction to extracellular matrix proteins. *Molecular cancer research : MCR* **5**, 309-320, (2007).
- 264 Ito, Y. *et al.* Expression of heparin-binding epidermal growth factor-like growth factor in pancreatic adenocarcinoma. *International journal of pancreatology : official journal of the International Association of Pancreatology* **29**, 47-52, (2001).
- 265 Ray, K. C. *et al.* Heparin-binding epidermal growth factor-like growth factor eliminates constraints on activated Kras to promote rapid onset of pancreatic neoplasia. *Oncogene* **33**, 823-831, (2014).
- 266 Kolb, A. *et al.* Expression and differential signaling of heregulins in pancreatic cancer cells. *International journal of cancer* **120**, 514-523, (2007).
- 267 Ogier, C. *et al.* Targeting the NRG1/HER3 pathway in tumor cells and cancer-associated fibroblasts with an anti-neuregulin 1 antibody inhibits tumor growth in pre-clinical models of pancreatic cancer. *Cancer letters* **432**, 227-236, (2018).
- 268 Liles, J. S. *et al.* Targeting ErbB3-mediated stromal-epithelial interactions in pancreatic ductal adenocarcinoma. *British journal of cancer* **105**, 523-533, (2011).
- 269 Heining, C. *et al.* NRG1 Fusions in KRAS Wild-Type Pancreatic Cancer. *Cancer discovery* **8**, 1087-1095, (2018).
- 270 Ocana, A. *et al.* Neuregulin expression in solid tumors: prognostic value and predictive role to anti-HER3 therapies. *Oncotarget* **7**, 45042-45051, (2016).
- 271 Yokoyama, M. *et al.* Betacellulin, a member of the epidermal growth-factor family, is overexpressed in human pancreatic-cancer. *Int J Oncol* **7**, 825-829, (1995).
- 272 Kawaguchi, M. *et al.* Auto-induction and growth stimulatory effect of betacellulin in human pancreatic cancer cells. *Int J Oncol* **16**, 37-41, (2000).
- 273 Ardito, C. M. *et al.* EGF receptor is required for KRAS-induced pancreatic tumorigenesis. *Cancer Cell* **22**, 304-317, (2012).
- 274 Collisson, E. A. *et al.* Subtypes of pancreatic ductal adenocarcinoma and their differing responses to therapy. *Nature Medicine* **17**, 500, (2011).

- 275 Blasco, M. T. *et al.* Complete Regression of Advanced Pancreatic Ductal Adenocarcinomas upon Combined Inhibition of EGFR and C-RAF. *Cancer Cell* **35**, 573-587.e576, (2019).
- 276 Yan, M., Parker, B. A., Schwab, R. & Kurzrock, R. HER2 aberrations in cancer: implications for therapy. *Cancer treatment reviews* **40**, 770-780, (2014).
- 277 Feng, H. *et al.* MicroRNA-148a Suppresses the Proliferation and Migration of Pancreatic Cancer Cells by Down-regulating ErbB3. *Pancreas* **45**, 1263-1271, (2016).
- 278 Thybusch-Bernhardt, A., Beckmann, S. & Juhl, H. Comparative analysis of the EGF-receptor family in pancreatic cancer: expression of HER-4 correlates with a favourable tumor stage. *International journal of surgical investigation* **2**, 393-400, (2001).
- 279 Maron, R. *et al.* Inhibition of a pancreatic cancer model by cooperative pairs of clinically approved and experimental antibodies. *Biochemical and Biophysical Research Communications* **513**, 219-225, (2019).
- 280 Lemoine, N. R. *et al.* The erbB-3 gene in human pancreatic cancer. *The Journal of pathology* **168**, 269-273, (1992).
- 281 Ghasemi, R. *et al.* Dual targeting of ErbB-2/ErbB-3 results in enhanced antitumor activity in preclinical models of pancreatic cancer. *Oncogenesis* **3**, e117, (2014).
- 282 Graber, H. U. *et al.* ErbB-4 mRNA expression is decreased in non-metastatic pancreatic cancer. *International journal of cancer* **84**, 24-27, (1999).
- 283 Mill, C. P., Gettinger, K. L. & Riese, D. J., 2nd. Ligand stimulation of ErbB4 and a constitutively-active ErbB4 mutant result in different biological responses in human pancreatic tumor cell lines. *Experimental cell research* **317**, 392-404, (2011).
- 284 Bryant, K. L., Mancias, J. D., Kimmelman, A. C. & Der, C. J. KRAS: feeding pancreatic cancer proliferation. *Trends in biochemical sciences* **39**, 91-100, (2014).
- 285 Zeitouni, D., Pylayeva-Gupta, Y., Der, C. J. & Bryant, K. L. KRAS Mutant Pancreatic Cancer: No Lone Path to an Effective Treatment. *Cancers* **8**, (2016).
- 286 Carpenter, G. ErbB-4: mechanism of action and biology. *Experimental cell research* **284**, 66-77, (2003).
- 287 Lee, T. C. & Threadgill, D. W. Generation and validation of mice carrying a conditional allele of the epidermal growth factor receptor. *Genesis* **47**, 85-92, (2009).
- 288 Garratt, A. N., Voiculescu, O., Topilko, P., Charnay, P. & Birchmeier, C. A dual role of erbB2 in myelination and in expansion of the schwann cell precursor pool. *J. Cell Biol* **148**, 1035-1046, (2000).
- 289 Jackson, E. L. *et al.* Analysis of lung tumor initiation and progression using conditional expression of oncogenic K-ras. *Genes Dev* **15**, 3243-3248, (2001).
- 290 Dahlhoff, M. *et al.* CRISPR-assisted receptor deletion reveals distinct roles for ERBB2 and ERBB3 in skin keratinocytes. *The FEBS journal* **284**, 3339-3349, (2017).
- 291 Qu, C. & Konieczny, S. F. Pancreatic Acinar Cell 3-Dimensional Culture. *Bio-protocol* **3**, (2013).
- 292 Hingorani, S. R. *et al.* Preinvasive and invasive ductal pancreatic cancer and its early detection in the mouse. *Cancer Cell* **4**, 437-450, (2003).
- 293 Carriere, C., Young, A. L., Gunn, J. R., Longnecker, D. S. & Korc, M. Acute pancreatitis markedly accelerates pancreatic cancer progression in mice expressing oncogenic Kras. *Biochem Biophys Res Commun* **382**, 561-565, (2009).
- 294 Ji, B. *et al.* Ras activity levels control the development of pancreatic diseases. *Gastroenterology* **137**, 1072-1082, 1082.e1071-1076, (2009).
- 295 Siveke, J. T. *et al.* Concomitant Pancreatic Activation of KrasG12D and Tgfa Results in Cystic Papillary Neoplasms Reminiscent of Human IPMN. *Cancer Cell* **12**, 266-279, (2007).
- 296 Hingorani, S. R. *et al.* Trp53R172H and KrasG12D cooperate to promote chromosomal instability and widely metastatic pancreatic ductal adenocarcinoma in mice. *Cancer Cell* **7**, 469-483, (2005).
- 297 Li, X., Zhao, H., Gu, J. & Zheng, L. Prognostic role of HER2 amplification based on fluorescence in situ hybridization (FISH) in pancreatic ductal adenocarcinoma (PDAC): a meta-analysis. *World journal of surgical oncology* **14**, 38, (2016).

- 298 Momeny, M. *et al.* The ERBB receptor inhibitor dacomitinib suppresses proliferation and invasion of pancreatic ductal adenocarcinoma cells. *Cellular oncology (Dordrecht)*, (2019).
- 299 Fleming, T. P. *et al.* Origins of lifetime health around the time of conception: causes and consequences. *Lancet* **391**, 1842-1852, (2018).
- 300 Huypens, P. *et al.* Epigenetic germline inheritance of diet-induced obesity and insulin resistance. *Nature genetics* **48**, 497-499, (2016).
- 301 Sun, C. *et al.* Epigenetic regulation of histone modifications and Gata6 gene expression induced by maternal diet in mouse embryoid bodies in a model of developmental programming. *BMC developmental biology* **15**, 3, (2015).
- 302 Wang, L. *et al.* Programming and inheritance of parental DNA methylomes in mammals. *Cell* **157**, 979-991, (2014).
- 303 Kawano, M., Kawaji, H., Grandjean, V., Kiani, J. & Rassoulzadegan, M. Novel small noncoding RNAs in mouse spermatozoa, zygotes and early embryos. *PloS one* **7**, e44542, (2012).
- 304 Morgan, H. D., Santos, F., Green, K., Dean, W. & Reik, W. Epigenetic reprogramming in mammals. *Hum. Mol. Genet* **14 Spec No 1**, R47-R58, (2005).
- 305 Lecoutre, S. *et al.* Depot- and sex-specific effects of maternal obesity in offspring's adipose tissue. *The Journal of endocrinology* **230**, 39-53, (2016).
- 306 Sun, B. *et al.* Maternal high-fat diet during gestation or suckling differentially affects offspring leptin sensitivity and obesity. *Diabetes* **61**, 2833-2841, (2012).
- 307 Ornellas, F., Mello, V. S., Mandarim-de-Lacerda, C. A. & Aguilá, M. B. Sexual dimorphism in fat distribution and metabolic profile in mice offspring from diet-induced obese mothers. *Life Sci* **93**, 454-463, (2013).
- 308 Masuyama, H. & Hiramatsu, Y. Additive effects of maternal high fat diet during lactation on mouse offspring. *PloS one* **9**, e92805, (2014).
- 309 Gallou-Kabani, C. *et al.* Sex- and diet-specific changes of imprinted gene expression and DNA methylation in mouse placenta under a high-fat diet. *PloS one* **5**, e14398, (2010).
- 310 Dahlhoff, M. *et al.* Peri-conceptual obesogenic exposure induces sex-specific programming of disease susceptibilities in adult mouse offspring. *Biochimica et biophysica acta* **1842**, 304-317, (2014).
- 311 Afgan, E. *et al.* The Galaxy platform for accessible, reproducible and collaborative biomedical analyses: 2016 update. *Nucleic acids research* **44**, W3-w10, (2016).
- 312 Langmead, B., Trapnell, C., Pop, M. & Salzberg, S. L. Ultrafast and memory-efficient alignment of short DNA sequences to the human genome. *Genome Biol* **10**, R25, (2009).
- 313 Love, M. I., Huber, W. & Anders, S. Moderated estimation of fold change and dispersion for RNA-seq data with DESeq2. *Genome biology* **15**, 550, (2014).
- 314 Gapp, K. *et al.* Implication of sperm RNAs in transgenerational inheritance of the effects of early trauma in mice. *Nature neuroscience* **17**, 667-669, (2014).
- 315 Li, X. Z. *et al.* An ancient transcription factor initiates the burst of piRNA production during early meiosis in mouse testes. *Mol Cell* **50**, 67-81, (2013).
- 316 Goldstein, J. M. *et al.* Prenatal stress-immune programming of sex differences in comorbidity of depression and obesity/metabolic syndrome. *Dialogues in clinical neuroscience* **18**, 425-436, (2016).
- 317 Mingrone, G. *et al.* Influence of maternal obesity on insulin sensitivity and secretion in offspring. *Diabetes care* **31**, 1872-1876, (2008).
- 318 Donkin, I. *et al.* Obesity and Bariatric Surgery Drive Epigenetic Variation of Spermatozoa in Humans. *Cell Metab* **23**, 369-378, (2016).
- 319 Copley, J. E. *et al.* Male-lineage transmission of an acquired metabolic phenotype induced by grand-paternal obesity. *Molecular metabolism* **5**, 699-708, (2016).
- 320 Grandjean, V. *et al.* RNA-mediated paternal heredity of diet-induced obesity and metabolic disorders. *Scientific reports* **5**, 18193, (2015).

- 321 Fullston, T. *et al.* Paternal obesity initiates metabolic disturbances in two generations of mice with incomplete penetrance to the F2 generation and alters the transcriptional profile of testis and sperm microRNA content. *FASEB J* **27**, 4226-4243, (2013).
- 322 Zhang, Y., Shi, J., Rassoulzadegan, M., Tuorto, F. & Chen, Q. Sperm RNA code programmes the metabolic health of offspring. *Nature reviews. Endocrinology* **15**, 489-498, (2019).

## 6 APPENDIX

Suppl. Table S 6.1: Differentially regulated transcripts of male (♂) and female (♀) blastocysts of obese females (F<sub>Ob</sub>) or obese males (M<sub>Ob</sub>), respectively, compared to blastocysts of lean mice (F<sub>Co</sub> x M<sub>Co</sub>).

upregulated transcripts (in bold)
downregulated transcripts
♂ blastocysts F <sub>Ob</sub> x M <sub>Co</sub>
<b>1110012L19Rik</b>
<b>1810035L17Rik</b>
<b>4930522L14Rik</b>
<b>Acadm</b>
<b>Ankrd33b</b>
<b>Arih2</b>
<b>Atp13a3</b>
<b>C430048L16Rik</b>
<b>Ccdc90b</b>
<b>Celf1</b>
<b>Cspp1</b>
<b>Ddx6</b>
<b>Dhx9</b>
<b>Dnajc13</b>
<b>Eif2s1</b>
<b>Erh</b>
<b>Etf1</b>
<b>Etohi1</b>
<b>Fabp3</b>
<b>Fam36a /// AI503316</b>
<b>Gas5</b>
<b>Gins1</b>
<b>Gkap1</b>
<b>Gm12191 /// Rpl30</b>
<b>Gm12952 /// Gm14535 /// Llph</b>
<b>Gm14391 /// Gm14326</b>
<b>Gm14410 /// Gm14430 /// Gm2007 /// Gm14434 /// Gm14308 /// Gm4724 /// 0610010B08Rik</b>
<b>Gm14420</b>
<b>Gm14680 /// Sms</b>
<b>Gm3258 /// Supt4h1</b>
<b>Gm6517</b>
<b>Gm6710 /// LOC627901</b>
<b>Gm8300 /// Gm2022 /// Gm5662 /// Gm2016</b>
<b>Gm9392 /// Rap1a</b>
<b>Gm9769 /// LOC100048119 /// Ptges3</b>
<b>Gnai3</b>

<b>Gtf3c6</b>
<b>H3f3a</b>
<b>Hmgn5</b>
<b>Hspd1</b>
<b>Ik</b>
<b>Lamtor3</b>
<b>Lcp1</b>
<b>Lsm6</b>
<b>Ltn1</b>
<b>Med10</b>
<b>Mir669b</b>
<b>Mir680-1</b>
<b>Mir680-3</b>
<b>Mir9-1</b>
<b>Myef2</b>
<b>Nmt2</b>
<b>OTTMUSG00000016609 /// 100043387 /// Gm14430 /// Gm14434 /// Gm2007 /// Gm14308 /// Gm4724 /// 0610010B08Rik</b>
<b>Park7</b>
<b>Pbrm1</b>
<b>Ppp4r2</b>
<b>Psma3</b>
<b>Rab18</b>
<b>Rap1b</b>
<b>Rnu3a</b>
<b>Rpp30</b>
<b>Shcbp1</b>
<b>Smek2</b>
<b>Snora31</b>
<b>Snord47</b>
<b>Snrpd3</b>
<b>St13</b>
<b>Strn3</b>
<b>Sumo1</b>
<b>Terf1</b>
<b>Tmem62</b>
<b>Tra2b</b>
<b>Ttc1</b>
<b>Ube2v2</b>
<b>Vma21</b>
<b>Xlr5b /// Xlr5c /// Xlr5a</b>
<b>Xpo1</b>
<b>Ywhaz</b>
<b>Zdhhc17</b>
<b>2810422O20Rik</b>
<b>BC051665</b>

---

Mir5117

Gm10324

Gm10792 /// Slc12a6

Luc7l3

Prdx2

Purb

Rbbp6

Snord104

Taf1d

Uba3

Wbp5

♂ **blastocysts**

**F<sub>Co</sub> X M<sub>Ob</sub>**

1810035L17Rik

2810422O20Rik

4930522L14Rik

Arih2

C430048L16Rik

Celf1

Cspp1

Dnajc13

Eif2s1

Etohi1

Gas5

Mir5117

Gins1

Gm10324

Gm12191 /// Rpl30

Gm12952 /// Gm14535 /// Lph

Gm14391 /// Gm14326

Gm14410 /// Gm14430 /// Gm2007 /// Gm14434 /// Gm14308 /// Gm4724 /// 0610010B08Rik

Gm14680 /// Sms

Gm3258 /// Supt4h1

Gm6517

Gm6710 /// LOC627901

Gm8300 /// Gm2022 /// Gm5662 /// Gm2016

Gm9769 /// LOC100048119 /// Ptges3

Gtf3c6

Hmgn5

Lamtor3

Lsm6

Ltn1

Mir669b

Mir680-1

Mir680-3

---

**Myef2**

**OTTMUSG00000016609 /// 100043387 /// Gm14430 /// Gm14434 /// Gm2007 /// Gm14308  
/// Gm4724 /// 0610010B08Rik**

**Park7**

**Prdx2**

**Psma3**

**Purb**

**Rbbp6**

**Rnu3a**

**Snora31**

**Snord104**

**Snord47**

**Sumo1**

**Tra2b**

**Ttc1**

**Ube2v2**

**Wbp5**

**Xlr5b /// Xlr5c /// Xlr5a**

**Xpo1**

♀ **blastocysts**

**F<sub>Ob</sub> x M<sub>Co</sub>**

**Otud6b**

**Snord57 /// Nop56**

**Tmed2**

**Gm8300 /// Gm2022 /// Gm5662 /// Gm2016**

♀ **blastocysts**

**F<sub>Co</sub> x M<sub>Ob</sub>**

**Rny3**

**Ppp4r2**

**1700021F05Rik**

**1810037117Rik**

**Ak4**

**Atp13a3**

**Atp6v1c1**

**Calcoco2**

**Cmpk1**

**Dnajb6**

**Dnajc13**

**Dpy30**

**Fth1**

**Gas5**

**Gm12952 /// Gm14535 /// Llph**

**Gm14680 /// Sms**

**Gm3258 /// Supt4h1**

**Gm6158 /// Cnot1**

Gm6851 /// LOC635999 /// Pin4  
Gm8300 /// Gm2022 /// Gm5662 /// Gm2016  
Gm9392 /// Rap1a  
Gpr137b-ps  
Hprt  
LOC100046079 /// Cox5b  
Lsm6  
Ltn1  
Malat1  
Mrps18c  
Obfc2a  
Otud6b  
Paip2  
Park7  
Pfdn2  
Ppp6c  
Psm1  
Psm6  
Scarna17  
Slc44a1  
Snord57 /// Nop56  
Snrpd3  
Srsf3  
Sucla2  
Tceb1  
Tmed2  
Uxt  
Wtap  
Xlr3c /// Xlr3b /// Xlr3a  
Zc3h15  
Zranb1

**F<sub>Co</sub> X M<sub>Co</sub>**

♂ vs. ♀

**Gm8300 /// Gm2022 /// Gm5662 /// Gm2016**  
**Scarna17**  
**Sumo1**  
**Gm14680 /// Sms**  
**Gm3258 /// Supt4h1**  
**Hmgn5**  
**Gm9769 /// LOC100048119 /// Ptges3**  
**Rbbp7**  
**Gm9392 /// Rap1a**  
**Ube2v2**  
**Gas5**

---

**Gtf3c6**

**Snord57 /// Nop56**

**Lsm6**

**Vma21**

**Dnajc13**

*Rnu2-10*

*Nutf2-ps1*

**F<sub>Ob</sub> X M<sub>Co</sub>**

♂ vs. ♀

**Gas5**

**Rab24**

**A630089N07Rik**

**Otud6b**

*Ssbp1*

*Wbp5*

*Xist*

**F<sub>Co</sub> X M<sub>Ob</sub>**

♂ vs. ♀

**Cspp1**

**Terf1**

**Pdcl3**

**Bzw1**

**Arpc2**

*0610007P22Rik*

*0610009B22Rik*

*1600012F09Rik*

*1700021F05Rik*

*1810035L17Rik*

*1810037I17Rik*

*4930522L14Rik*

*4932438A13Rik*

*6720456B07Rik*

*A630089N07Rik*

*A730098P11Rik /// Gm6747 /// Morf41*

*Actr3*

*Ak4*

*Anapc13*

*Ankrd33b*

*Arcn1*

*Arl6ip1*

*Arl6ip4*

*Atp13a3*

*Atp6v0c*

---

---

*BC051665*

*C1qbp*

*C430048L16Rik*

*Calcoco2*

*Calm1 /// Calm3 /// Calm2*

*Cct7*

*Cdc42*

*Cdv3*

*Celf1*

*Cmpk1*

*Cops2*

*Cops6*

*Cox4i1*

*Csde1*

*Csnk2a1*

*Cstb*

*Cycs*

*Ddx5*

*Ddx6*

*Dhx9*

*Dnajb6*

*Dnajc13*

*Dppa4*

*Dpy30*

*Eef1a1*

*Eif1ax*

*Eif2s1*

*Eif2s2*

*Eif3e*

*Etfb*

*Etohi1*

*Fabp3*

*Foxo3*

*Fth1*

*Gapdh*

*Gas5*

*Ghitm*

*Gins1*

*Gm10177 /// Gm11575 /// Gm4184 /// Sec61g*

*Gm10324*

*Gm10639 /// Gsta2 /// Gsta1 /// Gm3776*

*Gm10792 /// Slc12a6*

*Gm12657 /// H3f3a*

*Gm12952 /// Gm14535 /// Llph*

*Gm13139 /// Gm13251 /// 1700029I01Rik*

*Gm13363 /// LOC100044742 /// Ptp4a1*

---

Gm14326 /// Gm6710
Gm14391 /// Gm14326
Gm14410 /// Gm14430 /// Gm2007
Gm14420
Gm15455
Gm19750 /// Ywhah
Gm3258 /// Supt4h1
Gm5093 /// Gm7589 /// Rpl11
Gm5593 /// Ccnb1
Gm6158 /// Cnot1
Gm6594 /// Gm6750 /// Gm9525 /// Hmgn2
Gm6710 /// LOC627901
Gm8300 /// Gm2022 /// Gm5662 /// Gm2016
Gm9769 /// LOC100048119 /// Ptges3
Gnb1
H2afz
H3f3a
Hdac2
Hmgb1
Hnrnp3
Hnrnpu
Hprt
Hsp90b1
Hspd1
Ifrd1
Ik
Jph1
Kif5b
Larp7
LOC100046079 /// Cox5b
LOC100046628 /// Npm1
LOC100642166
LOC631286 /// Acp1
Lsm6
M6pr-ps /// M6pr
Malat1
Mat2a
Mdm4
Med21
Metap1
Mir297b
Mir330 /// Eml2
Mir598
Mir669b
Mir680-1
Mir680-3

---

*Mir692-1*

*Mir9-1*

*Mospd1*

*Mrpl42*

*Mrps14*

*Mrps18c*

*Myef2*

*Myeov2*

*Nasp*

*Ncapg*

*Ncbp2*

*Ndufa4*

*Ndufb6*

*Nfu1*

*Nono*

OTTMUSG00000016609 /// 100043387

*Otud6b*

*Paip2*

*Park7*

*Pfdn2*

*Ppia*

*Ppp1cc*

*Ppp6c*

*Pramel7*

*Prl4a1*

*Psma1*

*Psma3*

*Psma4*

*Psma5*

*Psma6*

*Psmc5*

*Psmd10*

*Ptp4a2*

*Pttg1*

*Purb*

*Pydc3*

*Rad21*

*Rbbp6*

*Rnf4*

*Rnu2-10*

*Rnu3a*

*Rny3*

*Rock2*

*Rpl12*

*Rpl17*

*Rpl21*

---

---

*Rpl30 /// Gm6109 /// Gm7429*

*Rpl32*

*Rps18*

*Rps23*

*Rps25*

*Rps7*

*Sarnp*

*Scarna17*

*Sec61g*

*Senp6*

*Sf3b1*

*Sfpq*

*Slc30a1*

*Slc44a1*

*Snord14c /// Snord14d /// Hspa8*

*Snord47*

*Snrpd1*

*Snrpd3*

*Snx2*

*Sod1*

*Srsf3*

*Stfa1 /// BC117090 /// BC100530*

*Sub1*

*Suc1g2*

*Sumo2*

*Taf1d*

*Tbca*

*Tcea1*

*Tceb1*

*Tcp1*

*Timm23*

*Tpm4*

*Tpt1*

*Tra2b*

*Trmt112*

*Tspan8*

*Txndc9*

*Txnl1*

*Uba3*

*Ube2v2*

*Uqcrb*

*Utp3*

*Vdac2*

*Vdac3*

*Wbp5*

*Wtap*

---

<i>Xpo1</i>
<i>Ywhae</i>
<i>Ywhaz</i>
<i>Zc3h15</i>
<i>Zdhhc17</i>
<i>Zfp534 /// Gm13051</i>
<i>Zfp58 /// A530054K11Rik /// Zfp87</i>
<i>Zfp706</i>

Suppl. Table S 6.2: **Differentially regulated transcripts in oocytes of obese mice compared to oocytes of lean mice.** Listed according to *p*-adj (adjusted *p*-value), starting with the lowest *p*-adj. All genes are significant with a *p*-adj<0.05. Up-regulated genes first, followed by down-regulated genes.

Upregulated genes						
Gene	baseMean	log2Fold Change	lfcSE	stat	<i>p</i> -value	<i>p</i> -adj
Rpl41	164,84	3,44	0,66	5,24	1,63E-07	3,9822E-04
Anapc13	50,32	3,55	0,68	5,25	1,51E-07	3,9822E-04
2210417A02Rik	29,62	2,54	0,50	5,06	4,14E-07	6,7980E-04
Ndufa11	391,96	3,22	0,64	5,06	4,17E-07	6,7980E-04
Timm8b	2960,41	1,51	0,31	4,89	1,00E-06	8,6522E-04
Sergef	88,38	1,71	0,35	4,89	1,00E-06	8,6522E-04
Ndufb8	1045,11	1,82	0,37	4,89	1,02E-06	8,6522E-04
Lsm7	846,58	1,83	0,37	4,88	1,06E-06	8,6522E-04
Cox6a1	385,75	2,93	0,59	4,97	6,65E-07	8,6522E-04
Acot13	157,91	3,45	0,70	4,94	7,72E-07	8,6522E-04
Uba52	79,85	3,04	0,63	4,85	1,22E-06	9,2036E-04
Rplp2	625,08	1,58	0,33	4,82	1,46E-06	9,4015E-04
Znr1as	51,76	2,02	0,42	4,80	1,62E-06	9,4015E-04
Zfp935	22,71	2,25	0,47	4,82	1,42E-06	9,4015E-04
Ccdc122	812,47	1,41	0,30	4,77	1,87E-06	1,0139E-03
Nop10	641,58	1,66	0,35	4,70	2,64E-06	1,3588E-03
Myl6	337,54	1,53	0,33	4,67	3,01E-06	1,4004E-03
Acbd7	239,01	1,72	0,37	4,62	3,89E-06	1,6536E-03
Lsm4	33,25	2,95	0,64	4,61	4,08E-06	1,6622E-03
Ndufa1	299,37	2,95	0,65	4,57	4,86E-06	1,9023E-03
Tma7	409,33	1,49	0,33	4,55	5,39E-06	2,0264E-03
Rpl37	842,19	1,67	0,37	4,51	6,36E-06	2,2430E-03
Hrsp12	147,01	1,99	0,44	4,51	6,49E-06	2,2430E-03
Pop5	136,95	2,86	0,63	4,50	6,65E-06	2,2430E-03
Myeov2	2719,50	1,49	0,33	4,49	7,19E-06	2,3461E-03
Ndufa4	1739,21	1,88	0,42	4,46	8,33E-06	2,5456E-03
Rwdd1	635,44	1,20	0,27	4,43	9,27E-06	2,7491E-03
Cenpw	647,44	1,07	0,24	4,41	1,03E-05	2,8801E-03
Rplp1	113,89	2,82	0,64	4,41	1,03E-05	2,8801E-03

Gm13826	1772,41	1,46	0,33	4,38	1,16E-05	3,0560E-03
Cycs	931,28	1,65	0,38	4,36	1,28E-05	3,0560E-03
Eef1e1	564,53	1,96	0,45	4,36	1,29E-05	3,0560E-03
Cox14	464,54	2,08	0,48	4,37	1,22E-05	3,0560E-03
1700021F05Rik	107,32	2,13	0,49	4,37	1,23E-05	3,0560E-03
Dynlrb1	572,76	2,51	0,58	4,36	1,31E-05	3,0560E-03
Wwtr1	57,85	2,57	0,59	4,37	1,25E-05	3,0560E-03
Atp6v0e	1126,85	1,44	0,33	4,34	1,41E-05	3,0842E-03
Ndufa3	93,40	2,51	0,58	4,33	1,47E-05	3,1259E-03
Polr2f	1705,99	1,27	0,29	4,33	1,50E-05	3,1298E-03
Gm10745	107,26	1,44	0,33	4,32	1,59E-05	3,2308E-03
Pcbd2	344,41	2,18	0,51	4,30	1,74E-05	3,4707E-03
Gm561	119,43	1,46	0,34	4,29	1,82E-05	3,5078E-03
Polr2j	2617,42	1,64	0,38	4,28	1,83E-05	3,5078E-03
1700018B24Rik	1590,64	1,53	0,36	4,26	2,01E-05	3,7018E-03
Gm2694	345,83	1,80	0,42	4,25	2,16E-05	3,7335E-03
Clec2f	73,80	1,92	0,45	4,25	2,12E-05	3,7335E-03
2010107E04Rik	772,62	2,02	0,48	4,26	2,07E-05	3,7335E-03
Cox6b1	278,87	2,03	0,48	4,24	2,20E-05	3,7335E-03
Psmb2	1598,21	1,76	0,41	4,24	2,28E-05	3,7798E-03
Rit2	104,30	1,18	0,28	4,20	2,62E-05	4,1034E-03
Pcif1	451,61	1,25	0,30	4,21	2,57E-05	4,1034E-03
Rpl23	94,58	2,48	0,59	4,21	2,52E-05	4,1034E-03
Taf1d	600,70	1,10	0,26	4,18	2,87E-05	4,2129E-03
Cpb2	330,61	1,42	0,34	4,18	2,90E-05	4,2129E-03
Pate4	52,86	2,30	0,55	4,18	2,87E-05	4,2129E-03
Paip2	1120,96	2,70	0,65	4,18	2,88E-05	4,2129E-03
Ccdc28b	94,89	2,62	0,63	4,17	3,08E-05	4,3623E-03
Myoc	390,89	1,82	0,44	4,13	3,61E-05	4,8996E-03
Calm2	1293,77	2,38	0,58	4,13	3,68E-05	4,9369E-03
Snrpd1	6952,84	1,11	0,27	4,12	3,81E-05	5,0020E-03
Ttc1	1209,02	1,48	0,36	4,12	3,83E-05	5,0020E-03
4930592A05Rik	15,42	2,71	0,66	4,11	3,92E-05	5,0505E-03
1110001J03Rik	608,31	1,31	0,32	4,09	4,23E-05	5,0851E-03
2610524H06Rik	373,79	1,32	0,32	4,08	4,49E-05	5,0851E-03
Mycbp	748,49	1,32	0,32	4,08	4,57E-05	5,0851E-03
Tbca	1076,73	1,40	0,34	4,08	4,41E-05	5,0851E-03
Rbx1	7651,66	1,50	0,37	4,08	4,55E-05	5,0851E-03
C530044C16Rik	46,14	1,57	0,38	4,09	4,41E-05	5,0851E-03
Tasp1	57,62	1,61	0,39	4,10	4,21E-05	5,0851E-03
Hmgn2	250,17	2,07	0,51	4,08	4,55E-05	5,0851E-03
Ndufb3	154,27	2,25	0,55	4,09	4,26E-05	5,0851E-03
Tm2d1	438,65	2,36	0,58	4,10	4,07E-05	5,0851E-03
Uqcr11	277,32	3,17	0,78	4,08	4,44E-05	5,0851E-03

Rpl11	159,81	2,12	0,52	4,06	5,00E-05	5,5019E-03
Gm5	167,22	2,51	0,62	4,05	5,19E-05	5,6380E-03
Dynll1	677,54	2,41	0,60	4,04	5,27E-05	5,6684E-03
Ndufab1	379,82	1,21	0,30	4,02	5,89E-05	5,8853E-03
Sec62	3000,44	1,24	0,31	4,02	5,85E-05	5,8853E-03
3110009E18Rik	1140,95	1,30	0,32	4,02	5,78E-05	5,8853E-03
Dctpp1	138,45	1,91	0,47	4,02	5,78E-05	5,8853E-03
Sec61g	86,61	2,18	0,54	4,02	5,76E-05	5,8853E-03
Snx3	222,82	1,97	0,49	4,00	6,37E-05	6,2940E-03
0610040F04Rik	358,88	1,65	0,41	3,99	6,50E-05	6,3622E-03
Cox7a2	1078,32	1,60	0,40	3,99	6,60E-05	6,3958E-03
Apoe	45,47	1,80	0,45	3,98	6,96E-05	6,6458E-03
Ugt2b38	41,51	2,04	0,51	3,98	7,00E-05	6,6458E-03
Rpl37a	88,71	1,56	0,39	3,96	7,37E-05	6,8119E-03
Aig1	769,30	1,79	0,45	3,97	7,31E-05	6,8119E-03
Lsm3	884,57	2,00	0,51	3,95	7,68E-05	6,8289E-03
Ube2c	519,02	2,40	0,61	3,95	7,69E-05	6,8289E-03
0610009B22Rik	247,79	2,61	0,66	3,95	7,74E-05	6,8289E-03
AU019823	1147,83	0,99	0,25	3,92	8,71E-05	7,4772E-03
Chchd1	124,41	1,98	0,51	3,91	9,10E-05	7,6666E-03
Gm16497	1020,80	2,04	0,52	3,91	9,13E-05	7,6666E-03
Serpinb12	116,40	2,34	0,60	3,91	9,17E-05	7,6666E-03
Nedd8	704,27	1,80	0,46	3,90	9,74E-05	8,0725E-03
Mrps31	230,33	2,41	0,62	3,90	9,82E-05	8,0730E-03
Cox6b2	1464,29	1,45	0,37	3,89	0,000100283	8,1089E-03
Ltc4s	243,53	2,09	0,54	3,89	0,000100278	8,1089E-03
1700034K08Rik	118,06	1,40	0,36	3,89	0,000101128	8,1101E-03
Hypk	5733,39	1,38	0,36	3,88	0,000102492	8,1259E-03
Nsmce2	3751,51	1,02	0,26	3,87	0,000110908	8,4389E-03
Rpain	220,38	1,23	0,32	3,87	0,000110278	8,4389E-03
Mrps33	844,15	1,60	0,41	3,87	0,000109577	8,4389E-03
Mien1	52,02	2,47	0,64	3,86	0,000111265	8,4389E-03
Gabrr3	339,41	1,25	0,33	3,86	0,000114903	8,4814E-03
Lactb2	275,07	1,27	0,33	3,86	0,000115293	8,4814E-03
4931429P17Rik	90,80	1,47	0,38	3,86	0,000113637	8,4814E-03
Coa3	218,92	1,16	0,30	3,85	0,000116898	8,5353E-03
Uchl4	85,42	1,65	0,43	3,85	0,000119147	8,5841E-03
Spcs1	606,58	1,93	0,50	3,84	0,000121568	8,6477E-03
Tceb1	2785,40	2,15	0,56	3,83	0,000125917	8,8631E-03
Dbi	1203,08	1,05	0,28	3,82	0,000133982	9,3439E-03
7420461P10Rik	1205,95	1,75	0,46	3,81	0,00013948	9,5770E-03
Cnih4	449,07	1,99	0,52	3,80	0,000146182	9,9323E-03
Cadps	33,12	2,91	0,77	3,79	0,000149134	1,0063E-02
Cox6c	897,89	1,52	0,40	3,79	0,000151756	1,0144E-02

Ube2t	1555,83	2,48	0,65	3,79	0,000152405	1,0144E-02
Gm1673	44,37	1,89	0,50	3,78	0,000155198	1,0224E-02
Mlip	22,57	1,92	0,51	3,77	0,000163854	1,0478E-02
Plac8	3362,55	1,14	0,30	3,76	0,000172376	1,0797E-02
Gm20741	24,92	2,08	0,55	3,76	0,000172042	1,0797E-02
Ostc	527,07	1,05	0,28	3,75	0,000178717	1,0929E-02
Polr2i	498,86	1,85	0,49	3,75	0,000177856	1,0929E-02
Igflr1	15,80	2,41	0,65	3,74	0,000182496	1,1090E-02
Tnni3	31,19	2,76	0,74	3,74	0,000185142	1,1182E-02
Ubl5	4029,76	1,25	0,33	3,74	0,000186715	1,1207E-02
Ndufaf2	1257,44	1,23	0,33	3,72	0,000197205	1,1379E-02
A630095E13Rik	1038,29	1,38	0,37	3,72	0,000195817	1,1379E-02
Atox1	277,87	1,68	0,45	3,72	0,000195319	1,1379E-02
Rps28	48,93	1,74	0,47	3,72	0,000197361	1,1379E-02
Srp19	1238,13	0,99	0,27	3,72	0,000201892	1,1514E-02
Nmt1	442,26	1,36	0,37	3,71	0,00020425	1,1514E-02
Glr5	777,77	2,03	0,55	3,71	0,00020353	1,1514E-02
Dera	53,06	2,08	0,56	3,71	0,000206985	1,1553E-02
Rps27l	8076,57	1,34	0,36	3,70	0,000217925	1,2046E-02
B2m	294,92	1,29	0,35	3,69	0,000226582	1,2307E-02
Creb1	22,73	1,60	0,43	3,68	0,000231453	1,2307E-02
Rpl32	256,45	1,85	0,50	3,68	0,000229222	1,2307E-02
Rps24	112,43	1,94	0,53	3,68	0,000230655	1,2307E-02
R3hdml	84,71	2,04	0,55	3,69	0,000228087	1,2307E-02
Eny2	15328,76	1,31	0,35	3,68	0,000233339	1,2340E-02
Minos1	1379,51	1,19	0,32	3,67	0,000239092	1,2577E-02
Haus1	124,61	2,02	0,55	3,67	0,000242681	1,2697E-02
Sar1a	553,45	1,36	0,37	3,67	0,000247073	1,2813E-02
Sub1	26404,62	1,38	0,38	3,66	0,000250268	1,2813E-02
Dad1	648,64	1,69	0,46	3,66	0,000255608	1,2813E-02
Mnd1	135,96	2,01	0,55	3,66	0,000247694	1,2813E-02
Szrd1	100,06	2,37	0,65	3,65	0,000258216	1,2824E-02
Hscb	669,46	1,21	0,33	3,65	0,000265727	1,3131E-02
5730522E02Rik	14,59	1,72	0,47	3,64	0,000270349	1,3225E-02
A630077J23Rik	12,65	2,93	0,81	3,64	0,000277045	1,3419E-02
Dll3	151,66	1,27	0,35	3,63	0,000278575	1,3427E-02
Spata24	23,38	2,54	0,70	3,63	0,000280579	1,3457E-02
1300002E11Rik	325,39	1,90	0,52	3,63	0,000285209	1,3612E-02
Banf1	1631,96	1,13	0,31	3,63	0,000288303	1,3693E-02
Rbm8a	303,76	1,92	0,53	3,62	0,000294693	1,3862E-02
Gstk1	41,03	2,53	0,70	3,62	0,000293429	1,3862E-02
Krt12	606,51	1,32	0,37	3,62	0,000297275	1,3916E-02
Setd4	1032,45	1,94	0,54	3,62	0,000298692	1,3916E-02
Mrpl34	274,28	1,67	0,46	3,61	0,000302187	1,4012E-02

Sp3os	76,91	1,48	0,41	3,61	0,000311953	1,4206E-02
Mtus2	1797,42	1,56	0,43	3,60	0,000317976	1,4206E-02
Rps14	373,91	1,57	0,44	3,60	0,000313874	1,4206E-02
Cops5	327,67	1,57	0,44	3,60	0,000317231	1,4206E-02
Gc	23,90	2,03	0,56	3,61	0,000311027	1,4206E-02
Lage3	91,15	2,19	0,61	3,60	0,000313626	1,4206E-02
Uqcrh	914,68	1,88	0,52	3,59	0,000329647	1,4483E-02
Krtcap2	54,40	2,04	0,57	3,59	0,000330805	1,4483E-02
Spcs3	19,25	2,56	0,71	3,59	0,000331582	1,4483E-02
Mrpl57	395,81	1,45	0,41	3,58	0,000340848	1,4627E-02
Uqcr10	306,80	2,00	0,56	3,59	0,000336885	1,4627E-02
Atpif1	405,53	2,41	0,67	3,58	0,000339939	1,4627E-02
Gm973	141,07	1,49	0,42	3,58	0,000346559	1,4799E-02
Rps10	82,16	1,86	0,52	3,58	0,000347895	1,4799E-02
Lamtor5	492,81	1,98	0,55	3,58	0,000349652	1,4810E-02
Mrps21	289,90	1,60	0,45	3,57	0,000356668	1,4977E-02
Pam16	536,26	1,60	0,45	3,57	0,000361985	1,5135E-02
Cdk15	252,23	1,33	0,37	3,56	0,000369453	1,5320E-02
Rpl35a	67,04	2,34	0,66	3,56	0,000369535	1,5320E-02
Mrpl20	33,34	1,79	0,50	3,56	0,000377726	1,5564E-02
Pafah1b3	82,27	2,15	0,61	3,55	0,000389156	1,5931E-02
Prdx4	11,69	2,68	0,76	3,54	0,000394507	1,6083E-02
C87198	171,66	1,06	0,30	3,54	0,000398438	1,6109E-02
Ddit3	81,93	2,27	0,64	3,54	0,000397657	1,6109E-02
Timm8a2	316,55	0,92	0,26	3,54	0,000403421	1,6243E-02
BC068281	43,51	1,42	0,40	3,53	0,000409947	1,6438E-02
Med6	680,17	1,46	0,41	3,53	0,000412853	1,6487E-02
Eif3k	512,31	1,85	0,53	3,52	0,000432532	1,7133E-02
Romo1	1722,57	1,22	0,35	3,51	0,000450378	1,7480E-02
Mrps16	275,03	1,25	0,36	3,51	0,000453794	1,7480E-02
Cetn2	398,01	1,87	0,53	3,51	0,000450837	1,7480E-02
Sec11c	355,78	2,07	0,59	3,51	0,00044694	1,7480E-02
Fcgbp	97,41	2,19	0,62	3,51	0,000450356	1,7480E-02
Nsa2	390,44	0,76	0,22	3,50	0,000461712	1,7551E-02
Ndufa6	352,90	1,70	0,49	3,50	0,000469227	1,7657E-02
Mrpl42	343,00	1,63	0,47	3,50	0,000472587	1,7716E-02
Mettl18	31,57	2,08	0,59	3,49	0,000482586	1,7817E-02
Prcp	27,83	2,10	0,60	3,49	0,000481898	1,7817E-02
Ms4a6d	175,19	2,17	0,62	3,49	0,000484734	1,7829E-02
Idnk	43,72	2,09	0,60	3,49	0,000490135	1,7961E-02
Rrh	80,39	1,63	0,47	3,48	0,000502449	1,8286E-02
Emc6	530,20	1,62	0,47	3,48	0,000505504	1,8291E-02
Pgbd5	21,90	1,96	0,56	3,48	0,000506621	1,8291E-02
Oosp2	1827,64	1,56	0,45	3,47	0,000516917	1,8594E-02

Rgs10	406,49	1,54	0,45	3,47	0,000529144	1,8910E-02
Rapsn	33,06	1,98	0,57	3,47	0,000529586	1,8910E-02
Med21	2229,21	0,99	0,29	3,46	0,000537801	1,8986E-02
Map3k6	1404,52	1,64	0,48	3,46	0,000541403	1,8986E-02
Tmem251	214,69	2,03	0,59	3,46	0,000540617	1,8986E-02
Malsu1	52,79	2,43	0,70	3,46	0,000535894	1,8986E-02
Lbp	40,02	1,58	0,46	3,46	0,000548507	1,9166E-02
Stra13	1524,51	1,16	0,33	3,45	0,000550861	1,9180E-02
Psm6	556,45	1,79	0,52	3,45	0,000560992	1,9464E-02
Ppil6	57,80	1,20	0,35	3,45	0,00056601	1,9549E-02
2310036O22Rik	218,53	1,59	0,46	3,45	0,000567456	1,9549E-02
Mrps14	3023,28	1,12	0,32	3,45	0,000570438	1,9583E-02
Rpl36a	47,88	2,39	0,69	3,44	0,000573894	1,9633E-02
Lsm8	199,11	1,03	0,30	3,44	0,000585651	1,9767E-02
Tma16	233,24	1,07	0,31	3,44	0,000587011	1,9767E-02
Rpp21	308,27	1,75	0,51	3,44	0,000581811	1,9767E-02
Hspe1	653,69	1,12	0,33	3,43	0,000594582	1,9855E-02
Fabp5	1624,95	1,24	0,36	3,43	0,000594073	1,9855E-02
Rps20	45,85	2,41	0,70	3,42	0,000629462	2,0806E-02
Sfta2	65,91	2,02	0,59	3,41	0,000638226	2,1025E-02
Snrpg	2454,04	1,28	0,38	3,41	0,000647563	2,1194E-02
Mrpl1	150,66	1,70	0,50	3,41	0,00064769	2,1194E-02
Synj2bp	176,74	0,89	0,26	3,41	0,000654672	2,1260E-02
Klhl14	105,03	1,19	0,35	3,40	0,000675176	2,1643E-02
Atp5k	231,75	1,85	0,54	3,40	0,000681328	2,1643E-02
Cdc123	347,54	1,29	0,38	3,39	0,000692222	2,1684E-02
Manf	354,80	2,14	0,63	3,39	0,000689157	2,1684E-02
Ppih	854,06	0,87	0,26	3,39	0,000702391	2,1747E-02
Skp1a	11201,91	1,44	0,42	3,38	0,000716112	2,2033E-02
Smim11	3869,91	1,19	0,35	3,38	0,000730477	2,2132E-02
Batf3	57,33	1,77	0,52	3,38	0,000731919	2,2132E-02
LOC101056136	18,10	1,80	0,53	3,38	0,000724516	2,2132E-02
Coq4	15,48	2,51	0,74	3,38	0,000732915	2,2132E-02
Snrpf	2081,33	1,12	0,33	3,38	0,000736018	2,2141E-02
Pgm3	41,59	1,53	0,45	3,37	0,000740101	2,2144E-02
Tmem258	488,09	1,36	0,40	3,37	0,000745918	2,2250E-02
Txndc9	1622,69	1,90	0,57	3,36	0,000789069	2,3324E-02
Gm9999	20,53	2,33	0,70	3,35	0,000793896	2,3329E-02
Ptrhd1	171,08	1,62	0,48	3,35	0,000818688	2,3911E-02
Gm2382	658,93	1,08	0,32	3,34	0,000831796	2,4073E-02
C130060K24Rik	150,98	1,54	0,46	3,34	0,000842915	2,4073E-02
2410021H03Rik	197,77	1,61	0,48	3,34	0,000835471	2,4073E-02
2210011C24Rik	15,07	1,90	0,57	3,34	0,00084395	2,4073E-02
Acn9	62,27	1,99	0,59	3,34	0,000828097	2,4073E-02

Haus7	78,28	2,24	0,67	3,34	0,000842852	2,4073E-02
H3f3a	419,54	1,52	0,45	3,33	0,000856307	2,4150E-02
2610203C22Rik	20,73	2,00	0,60	3,33	0,000856508	2,4150E-02
Gabarapl2	168,49	0,81	0,24	3,33	0,000878363	2,4695E-02
Rps21	81,73	1,83	0,55	3,33	0,00088239	2,4737E-02
Asf1a	13914,50	0,95	0,29	3,31	0,000925428	2,5114E-02
Atp5c1	1002,21	0,97	0,29	3,32	0,000916085	2,5114E-02
Erh	768,45	1,01	0,30	3,32	0,000911741	2,5114E-02
Snrpe	5732,10	1,08	0,33	3,31	0,00091999	2,5114E-02
Gas5	194,47	1,13	0,34	3,31	0,000922656	2,5114E-02
Npm2	5330,73	1,18	0,36	3,31	0,000930828	2,5114E-02
Rgs1	49,55	1,47	0,44	3,31	0,000919476	2,5114E-02
Tyw5	253,65	0,83	0,25	3,30	0,00095319	2,5574E-02
Nme1	95,16	1,63	0,49	3,30	0,000954053	2,5574E-02
Sesn3	66,60	1,26	0,38	3,30	0,000963625	2,5690E-02
Pdrg1	794,77	1,40	0,42	3,30	0,000963189	2,5690E-02
Pdcd5	402,88	1,79	0,54	3,30	0,000968389	2,5747E-02
Eif1ax	711,57	2,14	0,65	3,30	0,000976209	2,5884E-02
Gas8	27,64	2,21	0,67	3,29	0,001002235	2,6431E-02
Miox	1375,43	1,45	0,44	3,29	0,001013329	2,6592E-02
Shfm1	485,51	1,71	0,52	3,29	0,001014834	2,6592E-02
Ndufa12	52,70	2,33	0,71	3,29	0,001016507	2,6592E-02
4921524J17Rik	3165,70	0,91	0,28	3,28	0,001046733	2,6601E-02
Cetn3	1950,87	0,96	0,29	3,27	0,001056784	2,6601E-02
Rpp30	173,94	1,03	0,32	3,27	0,001057618	2,6601E-02
2810403D21Rik	372,05	1,09	0,33	3,28	0,001051382	2,6601E-02
Dctn3	383,67	1,10	0,34	3,28	0,0010272	2,6601E-02
Mrps24	155,22	1,89	0,58	3,28	0,001029905	2,6601E-02
Ssr2	54,34	2,02	0,62	3,28	0,001049149	2,6601E-02
Ccdc124	57,26	2,03	0,62	3,28	0,001022516	2,6601E-02
Etfb	62,82	2,18	0,66	3,28	0,001025715	2,6601E-02
Ndufa13	255,51	1,28	0,39	3,27	0,00106571	2,6736E-02
Sptlc2	415,79	1,16	0,36	3,27	0,001078066	2,6976E-02
B4galt4	684,43	1,48	0,45	3,27	0,001081028	2,6982E-02
Trappc1	836,47	1,10	0,34	3,27	0,001085802	2,7032E-02
Slc9a3r2	30,59	2,01	0,61	3,26	0,001098683	2,7214E-02
Cyb5	575,26	2,23	0,68	3,26	0,00110273	2,7245E-02
Gng5	1035,37	1,06	0,33	3,26	0,001113025	2,7361E-02
Psma4	703,66	0,99	0,31	3,25	0,001151754	2,8172E-02
Cnpy2	38,14	2,46	0,76	3,24	0,00117932	2,8631E-02
Gfra4	130,41	1,65	0,51	3,24	0,00119436	2,8925E-02
Ndufb6	1326,59	1,37	0,42	3,24	0,001200374	2,8999E-02
Trappc6a	121,69	1,38	0,43	3,23	0,001227269	2,9358E-02
Pfdn1	612,37	1,25	0,39	3,23	0,001242633	2,9653E-02

Rpf2	94,35	2,02	0,63	3,23	0,001247419	2,9669E-02
Sdhd	164,64	1,85	0,57	3,22	0,00126678	2,9938E-02
Prorsd1	68,47	1,07	0,33	3,22	0,001285952	2,9962E-02
2010012O05Rik	82,76	1,14	0,35	3,22	0,001286174	2,9962E-02
Gstm5	1694,89	1,54	0,48	3,22	0,00128385	2,9962E-02
Rps12	61,39	1,73	0,54	3,22	0,001283822	2,9962E-02
Ost4	107,02	2,08	0,65	3,22	0,001298387	3,0103E-02
Zp4-ps	26,90	1,77	0,55	3,22	0,001303682	3,0154E-02
Ppap2a	1241,84	1,06	0,33	3,21	0,001315492	3,0284E-02
Polr1d	404,00	1,44	0,45	3,21	0,001313507	3,0284E-02
Mrpl54	78,73	1,82	0,57	3,21	0,001340578	3,0503E-02
Zcchc9	241,73	1,03	0,32	3,20	0,001364169	3,0683E-02
3110045C21Rik	64,90	1,71	0,54	3,20	0,00135706	3,0683E-02
Itgb3bp	21,51	2,14	0,67	3,20	0,001358521	3,0683E-02
Ifitm3	1605,38	1,03	0,32	3,20	0,001377135	3,0814E-02
Crcp	33,96	1,90	0,59	3,20	0,001379462	3,0814E-02
Cisd1	548,82	1,91	0,60	3,20	0,001378966	3,0814E-02
Mif	89,21	1,92	0,60	3,20	0,001387321	3,0919E-02
Men1	16,00	2,19	0,69	3,19	0,001416054	3,1484E-02
Rab3b	435,32	2,04	0,64	3,19	0,001422732	3,1493E-02
Rasl2-9	47,34	1,69	0,53	3,18	0,001460036	3,1744E-02
2610034M16Rik	462,21	1,58	0,50	3,18	0,001489282	3,2237E-02
Mrpl32	929,31	1,23	0,39	3,18	0,001496062	3,2312E-02
B230118H07Rik	132,13	1,40	0,44	3,17	0,001521144	3,2354E-02
4933408N05Rik	178,40	1,48	0,47	3,17	0,001510682	3,2354E-02
Acyp1	24,83	2,27	0,72	3,17	0,001519778	3,2354E-02
Rin3	560,02	0,98	0,31	3,17	0,001535944	3,2598E-02
Defb50	16,04	2,08	0,66	3,17	0,001540232	3,2618E-02
Ift52	73,56	1,36	0,43	3,15	0,001607711	3,3828E-02
Gm5083	107,80	1,11	0,35	3,15	0,001613947	3,3843E-02
Ccl25	19,00	2,25	0,71	3,15	0,001618841	3,3843E-02
Hmga2-ps1	39,73	1,83	0,58	3,15	0,001644244	3,4228E-02
Ccdc38	1671,50	0,96	0,31	3,14	0,001665744	3,4428E-02
Capns1	23,66	2,23	0,71	3,14	0,001667934	3,4428E-02
Tcstv3	107,62	1,53	0,49	3,14	0,001677508	3,4481E-02
Slco1a5	57,56	1,56	0,50	3,14	0,001675079	3,4481E-02
Fen1	15,96	2,37	0,76	3,14	0,001707445	3,4949E-02
Psm3	263,52	1,55	0,49	3,14	0,001717317	3,5038E-02
Ii10rb	64,75	1,90	0,61	3,13	0,001726097	3,5038E-02
Prim1	113,54	1,75	0,56	3,13	0,001733594	3,5117E-02
Trappc6b	314,95	1,27	0,41	3,12	0,001794122	3,5881E-02
Cmc1	758,32	1,28	0,41	3,12	0,001781472	3,5881E-02
Mocs2	319,72	1,55	0,50	3,12	0,001786591	3,5881E-02
Wfdc15a	49,10	1,58	0,51	3,12	0,001796988	3,5881E-02

Mrpl15	61,53	1,69	0,54	3,12	0,00179596	3,5881E-02
Pfdn4	9379,32	0,96	0,31	3,12	0,001809385	3,5942E-02
Mrps17	362,33	1,63	0,52	3,12	0,001808222	3,5942E-02
Cenpp	270,05	1,18	0,38	3,12	0,001820607	3,5986E-02
Med31	3707,32	0,92	0,30	3,11	0,001848973	3,6181E-02
Gm19299	861,29	0,99	0,32	3,12	0,001839431	3,6181E-02
Ccnb1ip1	50,77	1,98	0,63	3,11	0,001842826	3,6181E-02
Tekt4	131,49	2,01	0,64	3,11	0,001845401	3,6181E-02
Pxmp2	162,45	1,28	0,41	3,11	0,001854747	3,6221E-02
Cir1	680,57	0,91	0,29	3,11	0,001872606	3,6301E-02
E330011O21Rik	1676,71	1,03	0,33	3,11	0,001868629	3,6301E-02
Calm1	30078,35	1,08	0,35	3,11	0,001863023	3,6301E-02
Naip1	77,69	2,01	0,65	3,11	0,001873646	3,6301E-02
Tceb2	44,94	2,21	0,71	3,11	0,001879511	3,6342E-02
Ndufb2	818,63	1,40	0,45	3,11	0,001887139	3,6368E-02
Tmem29	335,80	1,94	0,62	3,10	0,001908846	3,6477E-02
4930500J02Rik	401,12	0,95	0,30	3,10	0,001920182	3,6622E-02
Sdhaf2	124,68	1,65	0,53	3,10	0,001932012	3,6747E-02
Tctex1d2	68,14	1,67	0,54	3,10	0,001935692	3,6747E-02
4933407G14Rik	35,61	1,27	0,41	3,10	0,001944772	3,6804E-02
Srek1ip1	2266,39	1,22	0,40	3,09	0,001975366	3,7188E-02
Hspb11	92,96	1,64	0,53	3,09	0,001973514	3,7188E-02
Snupn	268,00	1,79	0,58	3,09	0,001976493	3,7188E-02
4930524B15Rik	418,49	1,10	0,36	3,09	0,002034721	3,7704E-02
Gnb5	72,30	1,27	0,41	3,09	0,002027297	3,7704E-02
4930404A10Rik	41,87	1,90	0,62	3,09	0,002022528	3,7704E-02
Mrpl18	1881,07	0,88	0,29	3,08	0,00205703	3,8045E-02
Tusc2	29,37	1,98	0,64	3,08	0,002087594	3,8465E-02
N4bp2l2	1307,45	0,76	0,25	3,08	0,002101047	3,8640E-02
Lamtor1	270,36	1,48	0,48	3,07	0,002113732	3,8801E-02
Mtcp1	1367,15	0,94	0,31	3,07	0,002149101	3,9286E-02
Atraid	133,38	1,49	0,48	3,07	0,002152208	3,9286E-02
1110008L16Rik	90,07	1,57	0,51	3,07	0,002166308	3,9470E-02
Son	3553,26	1,06	0,35	3,06	0,002203097	3,9760E-02
Hpd	19,47	2,10	0,69	3,06	0,002203045	3,9760E-02
Gm11548	69,69	0,99	0,32	3,06	0,002212551	3,9793E-02
Gpx1	398,84	1,05	0,35	3,04	0,002344349	4,1933E-02
1700048M11Rik	28,53	1,25	0,41	3,04	0,002372207	4,1977E-02
Apoo	205,89	1,39	0,46	3,04	0,002376379	4,1977E-02
Nudt2	91,32	1,69	0,55	3,04	0,002352986	4,1977E-02
Otub2	137,96	1,73	0,57	3,04	0,002376883	4,1977E-02
Flad1	116,04	1,69	0,56	3,04	0,002390063	4,2058E-02
2410004B18Rik	460,54	0,80	0,26	3,04	0,002400913	4,2173E-02
Mlf1	197,97	0,93	0,31	3,03	0,002456502	4,2919E-02

Rora	1717,96	0,78	0,26	3,03	0,002462098	4,2940E-02
Rnasek	209,74	1,69	0,56	3,03	0,002470352	4,3007E-02
Fmnl3	110,83	1,50	0,50	3,03	0,00247787	4,3056E-02
Pyurf	126,85	2,01	0,66	3,03	0,002481964	4,3056E-02
Apip	1024,00	0,90	0,30	3,02	0,002500376	4,3146E-02
Gstm6	20,88	2,08	0,69	3,02	0,00249424	4,3146E-02
1810037117Rik	2158,37	1,28	0,43	3,02	0,002536162	4,3610E-02
Med28	5017,95	1,24	0,41	3,01	0,002577297	4,4027E-02
Gskip	45,98	1,30	0,43	3,01	0,002578426	4,4027E-02
Epc1	565,41	0,66	0,22	3,01	0,002618453	4,4247E-02
Zfand6	2651,89	0,71	0,24	3,01	0,002612777	4,4247E-02
Rpl39l	389,99	1,53	0,51	3,01	0,00261603	4,4247E-02
Larp1b	19,53	1,68	0,56	3,01	0,002600825	4,4247E-02
Rps4l	111,86	1,76	0,59	3,01	0,002603152	4,4247E-02
Omt2a	53052,73	1,09	0,36	3,01	0,0026289	4,4347E-02
Amz2	135,26	1,47	0,49	3,01	0,002645657	4,4426E-02
2310009A05Rik	13,75	1,83	0,61	3,01	0,002654545	4,4426E-02
Lemd1	11,38	2,41	0,80	3,00	0,002656302	4,4426E-02
Sar1b	755,32	1,18	0,39	3,00	0,002673021	4,4620E-02
Al463170	54,89	1,72	0,57	3,00	0,002677004	4,4620E-02
Ccdc104	330,83	0,81	0,27	3,00	0,002699634	4,4920E-02
Vdac2	487,80	1,01	0,34	3,00	0,002735081	4,5022E-02
Polr2g	4239,98	1,07	0,36	3,00	0,002728419	4,5022E-02
2210013O21Rik	148,49	1,18	0,39	3,00	0,002738123	4,5022E-02
Mrps28	178,00	1,51	0,51	3,00	0,002739091	4,5022E-02
Lsm6	325,98	1,81	0,60	3,00	0,002717718	4,5022E-02
Dynlt1b	41,17	2,01	0,67	3,00	0,002725584	4,5022E-02
Chst7	621,19	1,28	0,43	2,99	0,002762337	4,5109E-02
Pdlim2	75,47	1,91	0,64	2,99	0,002779687	4,5109E-02
Sec61b	1487,20	0,86	0,29	2,99	0,002823375	4,5617E-02
Timm17b	68,22	1,61	0,54	2,99	0,002825395	4,5617E-02
Commd1	550,38	1,50	0,50	2,99	0,002831866	4,5646E-02
Dnajc19	388,20	0,99	0,33	2,98	0,002860663	4,5958E-02
Nhp211	730,06	0,99	0,33	2,98	0,002856346	4,5958E-02
2810408I11Rik	3486,52	1,08	0,36	2,98	0,002871977	4,6065E-02
Magoh	8666,62	1,03	0,35	2,98	0,002894444	4,6349E-02
Esrra	151,78	1,17	0,39	2,97	0,002954515	4,6499E-02
Gm3219	50,08	1,24	0,42	2,97	0,002947936	4,6499E-02
Cenpq	916,30	1,27	0,43	2,97	0,002959638	4,6499E-02
Sptssb	128,38	1,49	0,50	2,97	0,002945271	4,6499E-02
Tnrc6b	1468,70	0,94	0,32	2,97	0,002993265	4,6779E-02
MacroD2	1763,44	0,96	0,32	2,97	0,003006464	4,6779E-02
Tmc5	86,03	1,29	0,43	2,97	0,003007363	4,6779E-02
Pdcl3	620,00	1,38	0,46	2,97	0,002991137	4,6779E-02

1600002D24Rik	154,36	1,72	0,58	2,97	0,003021429	4,6919E-02
Cand2	58,08	1,66	0,56	2,96	0,003038838	4,7044E-02
Ruvbl1	278,74	1,10	0,37	2,96	0,003048979	4,7052E-02
Nrn1l	708,58	1,21	0,41	2,96	0,003066445	4,7247E-02
Commd6	565,27	0,94	0,32	2,96	0,003075291	4,7309E-02
6430710C18Rik	1123,24	1,09	0,37	2,96	0,003109498	4,7748E-02
Snhg6	19,26	1,57	0,53	2,96	0,003125439	4,7748E-02
Il2ra	16,85	1,65	0,56	2,95	0,003128221	4,7748E-02
Sfr1	8582,03	0,75	0,25	2,95	0,003146771	4,7955E-02
Tex26	416,01	1,41	0,48	2,95	0,00317435	4,8033E-02
Gm19705	22,79	1,77	0,60	2,94	0,003247447	4,8806E-02
Kera	185,58	1,15	0,39	2,94	0,003322267	4,9442E-02
Cd96	31,21	2,08	0,71	2,94	0,003325132	4,9442E-02
Txndc17	374,76	0,89	0,30	2,94	0,003330471	4,9447E-02
Auh	3497,71	0,69	0,24	2,93	0,003350538	4,9594E-02
Gtf2a2	5059,77	0,96	0,33	2,93	0,003365772	4,9669E-02
Ptplad2	174,67	1,22	0,42	2,93	0,003362722	4,9669E-02

#### Downregulated genes

Gene	baseMean	log2Fold Change	lfcSE	stat	p-value	p-adj
Picl1	25,73	-4,36	0,76	-5,75	9,16E-09	8,96E-05
Ung	521,53	-1,85	0,34	-5,41	6,19E-08	3,03E-04
Prps2	73,38	-3,31	0,69	-4,79	1,63E-06	9,40E-04
4930512B01Rik	48,53	-2,31	0,49	-4,68	2,93E-06	1,40E-03
Sh2d3c	619,50	-1,95	0,42	-4,66	3,16E-06	1,40E-03
E2f4	1960,77	-1,44	0,32	-4,48	7,56E-06	2,39E-03
Trim75	3780,23	-1,72	0,40	-4,35	1,37E-05	3,08E-03
Ube2s	734,60	-1,10	0,25	-4,34	1,42E-05	3,08E-03
Naa40	1172,22	-1,36	0,32	-4,28	1,91E-05	3,60E-03
Pla2g15	264,54	-1,32	0,31	-4,24	2,21E-05	3,73E-03
Myt1	183,74	-1,11	0,26	-4,20	2,64E-05	4,10E-03
Gm15787	40,78	-1,66	0,40	-4,18	2,93E-05	4,21E-03
Pkmyt1	453,81	-0,94	0,23	-4,16	3,14E-05	4,39E-03
Tbc1d10a	153,28	-1,02	0,25	-4,15	3,26E-05	4,49E-03
Wasf1	239,80	-1,19	0,29	-4,10	4,08E-05	5,09E-03
Snx9	1506,12	-1,38	0,34	-4,04	5,42E-05	5,76E-03
Srebf2	30,11	-2,04	0,51	-4,02	5,84E-05	5,89E-03
Ncoa4	991,96	-1,55	0,39	-3,96	7,38E-05	6,81E-03
Sh3bgrl2	586,28	-1,54	0,39	-3,96	7,64E-05	6,83E-03
Patz1	278,52	-1,49	0,38	-3,95	7,75E-05	6,83E-03
Zbtb24	223,82	-1,38	0,35	-3,94	8,27E-05	7,23E-03
Gpr3	532,01	-1,31	0,33	-3,93	8,50E-05	7,36E-03
Cstf1	402,83	-1,50	0,39	-3,88	0,000103313	8,13E-03

Traf4	650,91	-1,11	0,29	-3,88	0,000103817	8,13E-03
Actn4	611,55	-1,42	0,37	-3,86	0,000115098	8,48E-03
Kat7	1234,67	-1,31	0,34	-3,85	0,000119321	8,58E-03
Api5	1114,30	-1,56	0,41	-3,84	0,000121972	8,65E-03
Nedd1	3047,63	-1,36	0,36	-3,82	0,000134658	9,34E-03
Arrdc2	1679,09	-1,24	0,32	-3,81	0,000139975	9,58E-03
Scml2	1126,63	-1,36	0,36	-3,78	0,000155703	1,02E-02
Kif20a	1760,49	-1,28	0,34	-3,78	0,000157253	1,03E-02
Trafd1	622,92	-1,27	0,34	-3,77	0,000160571	1,04E-02
Lypd3	63,59	-2,43	0,64	-3,77	0,000162238	1,04E-02
Hace1	202,14	-1,40	0,37	-3,76	0,000169584	1,08E-02
Smad5	104,91	-1,16	0,31	-3,76	0,000173251	1,08E-02
Wdr1	983,83	-1,24	0,33	-3,75	0,00017853	1,09E-02
Klhl24	117,26	-1,44	0,38	-3,73	0,000189262	1,13E-02
Dtx2	1727,09	-1,63	0,44	-3,73	0,000192122	1,14E-02
Tex19.1	1309,80	-1,38	0,37	-3,72	0,000197713	1,14E-02
Fa2h	437,17	-1,53	0,41	-3,71	0,000204767	1,15E-02
Abcf2	1365,83	-1,14	0,31	-3,71	0,000207822	1,16E-02
Elmo1	22,82	-2,18	0,59	-3,69	0,000223543	1,23E-02
Nupl1	343,14	-1,42	0,38	-3,69	0,000225749	1,23E-02
Mynn	1185,69	-1,37	0,37	-3,66	0,000256687	1,28E-02
Nlrp9a	5597,04	-1,34	0,37	-3,66	0,000254641	1,28E-02
Rnf14	3798,00	-1,19	0,33	-3,66	0,000254844	1,28E-02
Fpgs	2684,81	-1,12	0,31	-3,66	0,000252966	1,28E-02
Dab2	572,15	-1,03	0,28	-3,66	0,000249954	1,28E-02
Dlg1	437,02	-1,11	0,30	-3,64	0,000269487	1,32E-02
Ube3c	342,11	-1,12	0,31	-3,64	0,000272783	1,33E-02
Ttc17	168,12	-1,51	0,42	-3,61	0,000304022	1,40E-02
Ppp2r1b	275,70	-1,34	0,37	-3,60	0,000316596	1,42E-02
A230046K03Rik	163,78	-1,48	0,41	-3,60	0,000321447	1,43E-02
Nlrp4b	3435,08	-1,03	0,29	-3,59	0,000329713	1,45E-02
Klhl13	509,77	-1,09	0,30	-3,58	0,000340663	1,46E-02
Raf1	3931,52	-1,34	0,38	-3,57	0,000354732	1,50E-02
Far1	1031,92	-1,24	0,35	-3,55	0,000378602	1,56E-02
Abhd4	2013,78	-1,20	0,34	-3,53	0,000417779	1,66E-02
Tpst2	29,28	-1,65	0,47	-3,52	0,000439479	1,73E-02
Cdt1	574,25	-0,90	0,26	-3,51	0,000452622	1,75E-02
Slc25a40	155,07	-1,09	0,31	-3,51	0,000455967	1,75E-02
Phf1	1525,46	-1,01	0,29	-3,50	0,000459147	1,75E-02
Ptpr	1713,93	-0,85	0,24	-3,50	0,000462814	1,76E-02
Ect2	1483,72	-1,29	0,37	-3,50	0,000465384	1,76E-02
BC005764	62,19	-1,81	0,52	-3,49	0,000474748	1,77E-02
Pygo2	68,84	-1,64	0,47	-3,49	0,00048143	1,78E-02
Champ1	744,95	-1,03	0,30	-3,48	0,000502739	1,83E-02

Zfp964	72,76	-1,43	0,41	-3,46	0,000537801	1,90E-02
Nup107	1113,38	-1,21	0,35	-3,44	0,000587915	1,98E-02
Itsn2	2745,66	-1,03	0,30	-3,44	0,00058554	1,98E-02
Itgb1	256,08	-1,05	0,31	-3,43	0,000605167	2,01E-02
Rbm38	1690,57	-1,21	0,35	-3,42	0,000620218	2,06E-02
Fstl5	705,58	-1,66	0,49	-3,41	0,000658413	2,13E-02
Piga	790,45	-1,25	0,37	-3,41	0,000656997	2,13E-02
Plekhg1	631,89	-0,87	0,26	-3,41	0,000657844	2,13E-02
Mcm4	1620,92	-1,46	0,43	-3,40	0,000681124	2,16E-02
Cdc42se2	14528,54	-1,25	0,37	-3,40	0,000674108	2,16E-02
Rnf185	3877,49	-1,12	0,33	-3,40	0,000677439	2,16E-02
Zfp735	2262,21	-1,35	0,40	-3,40	0,000683912	2,17E-02
Reep1	71,45	-2,17	0,64	-3,39	0,000694299	2,17E-02
Exoc2	30,73	-1,99	0,59	-3,39	0,000695922	2,17E-02
Ints4	306,19	-1,20	0,35	-3,39	0,000692966	2,17E-02
Tada3	266,19	-0,96	0,28	-3,39	0,000702287	2,17E-02
Cse1l	177,95	-1,42	0,42	-3,39	0,000710272	2,19E-02
Stk38	731,79	-1,14	0,34	-3,38	0,000720913	2,21E-02
Aqp9	478,79	-1,16	0,34	-3,38	0,000730275	2,21E-02
Hsf1	1171,76	-1,25	0,37	-3,38	0,000737744	2,21E-02
Inpp5e	32,70	-1,61	0,48	-3,36	0,000775344	2,30E-02
Zbtb33	227,55	-1,07	0,32	-3,36	0,000776722	2,30E-02
Lrrc8b	664,57	-1,36	0,41	-3,35	0,000794006	2,33E-02
Parp12	9336,38	-1,05	0,32	-3,35	0,000818624	2,39E-02
Trove2	39,66	-1,37	0,41	-3,34	0,000838452	2,41E-02
Gtpbp10	300,82	-1,10	0,33	-3,34	0,000840271	2,41E-02
Lamp2	153,66	-1,70	0,51	-3,33	0,000856003	2,42E-02
Khdrbs1	112,58	-1,10	0,33	-3,34	0,000852733	2,42E-02
Thsd7b	67,54	-1,66	0,50	-3,32	0,000885688	2,48E-02
Pde3a	85,60	-1,42	0,43	-3,32	0,000907898	2,51E-02
Kbtbd8	6651,41	-1,39	0,42	-3,31	0,000923781	2,51E-02
Zbtb41	288,38	-1,21	0,36	-3,32	0,000904017	2,51E-02
Usp9x	1061,22	-1,13	0,34	-3,31	0,000931748	2,51E-02
Taf6	822,91	-1,07	0,32	-3,31	0,000927886	2,51E-02
Usp21	929,27	-0,96	0,29	-3,31	0,000919239	2,51E-02
Myo5b	1783,97	-0,94	0,29	-3,29	0,000999441	2,64E-02
Flcn	1147,44	-1,18	0,36	-3,28	0,001053742	2,66E-02
Calu	481,44	-1,16	0,35	-3,28	0,001033395	2,66E-02
Stat3	532,92	-1,12	0,34	-3,28	0,001049408	2,66E-02
Rrm1	438,88	-1,10	0,34	-3,28	0,001037125	2,66E-02
Klhl8	5063,03	-0,97	0,30	-3,28	0,001039889	2,66E-02
Sytl4	2553,14	-0,88	0,27	-3,28	0,001033356	2,66E-02
Add3	598,88	-1,36	0,42	-3,27	0,001088839	2,70E-02
Gsk3a	131,43	-1,03	0,32	-3,26	0,001107366	2,73E-02

Ddi2	197,68	-1,75	0,54	-3,26	0,001130553	2,77E-02
Aph1b	81,71	-1,62	0,50	-3,25	0,001155721	2,82E-02
Dhx32	1242,19	-0,97	0,30	-3,25	0,001160514	2,82E-02
Ctps	3639,78	-1,04	0,32	-3,24	0,001206032	2,91E-02
Ptbp1	980,94	-1,13	0,35	-3,24	0,001209993	2,91E-02
Scarb1	412,26	-0,88	0,27	-3,23	0,001225613	2,94E-02
Bzw1	709,88	-0,98	0,30	-3,23	0,00124933	2,97E-02
Hiat1	640,92	-1,34	0,42	-3,23	0,001253281	2,97E-02
Till5	184,86	-1,31	0,41	-3,22	0,001278767	3,00E-02
Ctdspl2	818,96	-1,08	0,34	-3,22	0,001283162	3,00E-02
Gas2l3	638,57	-1,13	0,35	-3,22	0,001291261	3,00E-02
4833439L19Rik	241,78	-1,14	0,35	-3,21	0,001325711	3,04E-02
Tfdp1	1083,88	-0,94	0,29	-3,21	0,001323916	3,04E-02
Vps35	1914,87	-1,05	0,33	-3,21	0,001336318	3,05E-02
Mcm7	707,74	-0,88	0,28	-3,21	0,001339819	3,05E-02
Papss1	419,28	-1,01	0,31	-3,21	0,001348698	3,06E-02
Smyd4	59,52	-1,27	0,40	-3,20	0,001362547	3,07E-02
Zfp60	1708,07	-1,29	0,41	-3,19	0,001419092	3,15E-02
Dmxl2	303,21	-0,99	0,31	-3,19	0,001426638	3,15E-02
Polk	174,66	-1,47	0,46	-3,19	0,001441841	3,17E-02
Gyk	1791,24	-1,01	0,32	-3,19	0,00144203	3,17E-02
Ythdf3	2675,81	-1,08	0,34	-3,18	0,00145537	3,17E-02
Tnpo1	812,48	-1,01	0,32	-3,18	0,001452305	3,17E-02
Nlrp4a	6380,84	-1,00	0,31	-3,18	0,001459126	3,17E-02
Haus5	349,23	-0,93	0,29	-3,18	0,001447985	3,17E-02
Gjb2	29,57	-1,91	0,60	-3,18	0,001486013	3,22E-02
Xpo6	269,33	-1,55	0,49	-3,17	0,001520387	3,24E-02
Ipo11	41,77	-1,52	0,48	-3,17	0,001520976	3,24E-02
Skp2	288,96	-1,29	0,41	-3,17	0,001503622	3,24E-02
Fam126b	1177,49	-1,06	0,33	-3,17	0,001513271	3,24E-02
Scyl2	1047,02	-1,12	0,35	-3,16	0,001554249	3,28E-02
Pcid2	2357,34	-1,05	0,33	-3,16	0,001587903	3,35E-02
Dis3l2	63,39	-1,06	0,34	-3,15	0,0016179	3,38E-02
Pola2	446,68	-0,90	0,29	-3,15	0,001624541	3,39E-02
Arhgap19	185,58	-1,28	0,41	-3,15	0,00165958	3,44E-02
Fpgt	593,74	-1,12	0,36	-3,14	0,00166344	3,44E-02
Inpp5a	247,15	-0,82	0,26	-3,14	0,001697761	3,48E-02
Gm13242	58,49	-1,18	0,38	-3,13	0,001725077	3,50E-02
Cul4b	2813,80	-0,82	0,26	-3,13	0,001722532	3,50E-02
Fbxl5	3309,32	-1,10	0,35	-3,13	0,001759712	3,56E-02
Cttnbp2	164,79	-1,11	0,35	-3,12	0,001791274	3,59E-02
Cbl	35,55	-1,49	0,48	-3,12	0,001811039	3,59E-02
Trim11	535,28	-0,98	0,31	-3,12	0,001819949	3,60E-02
Zfp942	750,41	-1,23	0,40	-3,12	0,001837848	3,62E-02

Ndufs1	95,60	-1,18	0,38	-3,11	0,001888459	3,64E-02
Med15	1310,53	-1,15	0,37	-3,11	0,001893707	3,64E-02
Pacsin2	2047,06	-1,01	0,32	-3,11	0,001895726	3,64E-02
Zfp235	194,25	-1,34	0,43	-3,10	0,001902825	3,64E-02
Cdc23	785,07	-0,76	0,25	-3,10	0,001938032	3,67E-02
Ust	120,66	-1,69	0,55	-3,09	0,001992543	3,74E-02
Adck3	13,12	-2,01	0,65	-3,09	0,002017537	3,77E-02
Wdr35	11,72	-1,80	0,58	-3,09	0,002011956	3,77E-02
Prps1l3	173,94	-1,13	0,36	-3,09	0,002025864	3,77E-02
Zfand2a	804,83	-1,11	0,36	-3,09	0,002031163	3,77E-02
Hspa9	2277,58	-0,86	0,28	-3,08	0,002070611	3,82E-02
Fbxo18	676,67	-0,97	0,32	-3,07	0,002126377	3,90E-02
Otogl	42,02	-1,89	0,62	-3,06	0,002178307	3,95E-02
Prkcb	38,55	-1,73	0,57	-3,06	0,00217824	3,95E-02
Kcnip4	82,35	-1,17	0,38	-3,06	0,002199374	3,98E-02
Tgfbr3	211,83	-1,09	0,35	-3,06	0,002206642	3,98E-02
Mark2	1363,98	-1,35	0,44	-3,06	0,002244488	4,03E-02
Ncstn	714,36	-1,53	0,50	-3,05	0,002285339	4,10E-02
Gm4944	48,64	-1,49	0,49	-3,04	0,002371177	4,20E-02
Ubqln1	4458,79	-1,11	0,36	-3,04	0,002365666	4,20E-02
Cry1	2535,49	-1,08	0,35	-3,04	0,00236112	4,20E-02
Birc3	10023,94	-0,97	0,32	-3,04	0,002389359	4,21E-02
Lrp2bp	59,24	-1,11	0,37	-3,03	0,002407809	4,22E-02
Kif23	7111,11	-1,04	0,34	-3,03	0,002451693	4,29E-02
Trim37	410,51	-1,06	0,35	-3,02	0,002497272	4,31E-02
Mcm10	331,39	-0,88	0,29	-3,02	0,002511898	4,33E-02
Cmtr2	548,16	-1,26	0,42	-3,02	0,002566937	4,40E-02
Nlgn1	277,01	-0,95	0,32	-3,01	0,002572858	4,40E-02
Tjap1	330,34	-0,99	0,33	-3,01	0,002611841	4,42E-02
Zfp616	2081,74	-1,23	0,41	-3,01	0,002649374	4,44E-02
Zfp74	239,48	-0,88	0,29	-3,01	0,002652699	4,44E-02
Hps3	54,44	-1,27	0,42	-2,99	0,002744479	4,50E-02
Gpatch1	566,51	-1,00	0,33	-2,99	0,002747123	4,50E-02
Gm15941	491,00	-0,99	0,33	-3,00	0,002716769	4,50E-02
Stard7	2323,70	-0,72	0,24	-2,99	0,002754808	4,51E-02
Foxj2	40,07	-1,73	0,58	-2,99	0,002777968	4,51E-02
Zfp750	747,75	-1,03	0,34	-2,99	0,002774316	4,51E-02
Asun	655,32	-0,82	0,28	-2,99	0,002780115	4,51E-02
Pde4a	62,21	-1,37	0,46	-2,99	0,002802948	4,54E-02
Nlrp4f	14444,10	-0,99	0,33	-2,98	0,002906133	4,64E-02
Acbd5	774,17	-0,85	0,29	-2,98	0,002906357	4,64E-02
Exoc1	1483,66	-1,05	0,35	-2,98	0,00292798	4,65E-02
Kdm7a	2114,01	-1,04	0,35	-2,97	0,002933188	4,65E-02
Sh2b3	75,82	-1,02	0,34	-2,98	0,002920669	4,65E-02

Mtmt14	2775,72	-0,83	0,28	-2,97	0,002937988	4,65E-02
Dcaf8	1881,60	-0,79	0,27	-2,97	0,002930771	4,65E-02
Fbxo43	2449,07	-0,79	0,27	-2,97	0,00296084	4,65E-02
Pggt1b	390,43	-1,06	0,36	-2,97	0,003002899	4,68E-02
Hsd1l	193,61	-0,96	0,32	-2,97	0,003005912	4,68E-02
Nlrp4g	4591,44	-1,01	0,34	-2,97	0,003025925	4,69E-02
Ehd3	66,09	-1,26	0,43	-2,96	0,003047728	4,71E-02
Ampd3	691,68	-1,50	0,51	-2,96	0,003124021	4,77E-02
Slain1os	92,97	-1,12	0,38	-2,96	0,003125805	4,77E-02
Phtf2	1514,50	-1,10	0,37	-2,95	0,003151601	4,80E-02
Pspc1	19,25	-1,51	0,51	-2,95	0,003176371	4,80E-02
Fam118a	2201,15	-0,99	0,34	-2,95	0,003174924	4,80E-02
Mcm2	919,97	-0,89	0,30	-2,95	0,003167951	4,80E-02
1700017B05Rik	134,41	-1,45	0,49	-2,95	0,003187706	4,81E-02
Csde1	2026,30	-1,01	0,34	-2,94	0,003232403	4,87E-02
Cs	1922,75	-0,93	0,31	-2,94	0,003244774	4,88E-02
Tug1	169,60	-1,27	0,43	-2,94	0,003264094	4,90E-02
Atf2	6031,51	-1,06	0,36	-2,94	0,003298633	4,94E-02
Gpcpd1	1113,79	-1,00	0,34	-2,94	0,003305129	4,94E-02
Slc7a6os	1197,28	-0,77	0,26	-2,94	0,003303365	4,94E-02
6330409D20Rik	13,51	-1,69	0,58	-2,94	0,00331328	4,94E-02
Klhl15	97,65	-1,03	0,35	-2,93	0,003343395	4,96E-02